ULTRASOUND IMAGING OF SYNOVITIS: RELATIONSHIP TO PATHOBIOLOGY AND RESPONSE TO THERAPY

Kelly, Stephen Gerard

ULTRASOUND IMAGING OF SYNOVITIS: RELATIONSHIP TO PATHOBIOLOGY AND RESPONSE TO THERAPY

Stephen Gerard Kelly

A thesis submitted for the degree of Doctor of Philosophy at Queen Mary University of London School of Medicine and Dentistry

Submitted: April 2013

Abstract

Ultrasound (US) imaging has made significant progress over the past 20 years in relation to its role in inflammatory arthritis, and in particular, Rheumatoid Arthritis. Modern US machines provide crisp, detailed images of superficial anatomical structures which has facilitated the uptake of US imaging as an important assessment tool within the Rheumatology department. Diagnostic and prognostic information can now assist clinicians decisions with the goal of improving patient treatment and subsequent outcome. In addition, 3D US imaging has recently been suggested as an additional imaging modality with potential benefits in the assessment of inflammatory arthritis. Recent work has focused on providing a reliable, responsive US joint count which can be assimilated into routine care as well as providing a platform for clinical research. Thus, my ***first aim*** was to show that a defined limited US data set, including 2D and 3D imaging, shows acceptable reliability. I demonstrate that both imaging modalities are reliable in terms of reading and image acquisition when restricted to a limited US data set. My ***second aim***, was to demonstrate that a limited US data set is responsive. Using both a physiological and pharmacological trigger, I demonstrate that both 2D and 3D imaging are responsive and that combining US endpoints with DAS28 (Disease Activity Score - 28) increased the effect size and identifies treatment effects early.

Despite notable advances in musculoskeletal US research, there is still need for better understanding of the pathophysiological correlates of ultrasound imaging. Therefore my ***final aim*** was to examine the relationship of Power Doppler Signal (PDS) and gray-scale synovial thickening with histological features of synovitis at a single joint level and with an extended joint US data set. I firstly show that the harvesting of synovial tissue, using a minimally invasive US-guided biopsy technique, is safe and well tolerated by patients and that the quality of tissue and RNA extracted is good. Using this tissue collection method, I demonstrate a good correlation of US and histological parameters of synovitis (specifically CD68+ sub-lining macrophages)

at a single joint level, in both an early and established RA cohort. This relationship is maintained if the US assessment is extended to a discrete US joint data set. Furthermore, within the knee joint I demonstrated that PDS correlates well with synovial tissue expression of inflammatory mediators of neoangiogenesis and histological assessment of synovial vascular area.

Declaration

I declare that the following thesis has been composed by myself, that it embodies the results of my own special work, and that it does not include work forming part of a thesis presented successfully for a degree at this or any other university.

Stephen Gerard Kelly

Acknowledgements

Firstly, I would like to thank Professor Costantino Pitzalis for convincing me of the merits of undertaking this PhD. His support and encouragement throughout this period have been invaluable. I count myself fortunate to have had the opportunity to work in such a stimulating environment and received the opportunities to develop under his mentorship as both colleague and friend.

I would also like to thank Professor Peter Taylor who, as my second supervisor, was a reliable source of advice and direction. He kindly facilitated my involvement in the study described in Chapter 5.

I would like to thank my colleagues, Dr. Fran Humby and Dr. Michele Bombardieri for their support, insight and good humor over the past few years. Their contribution to all the translational work described in this thesis has been important both in the conception and execution of these projects. In addition, I would like to thank Dr. Oscar Epis who initially provided training in ultrasound guided synovial biopsy techniques which was critical to much of the work described. I would also like to thank Dr. Matt Seymour who worked as a collaborator with me on Chapter 1 and 5.

I would like to thank all of the staff at Experimental Medicine and Rheumatology and in particular Dr. Becki Hands for her help in processing and scoring all of the biopsy samples and Dr. Alessandra Marrelli who contributed significantly to the laboratory aspect to Chapter 6. Our clinical team deserve thanks and specifically Dr. Nora Ng, Dr. Maria Di Cicco, and Celia Breston RGN for their help in data collection and day to day supervision of patients participating in many of the studies described within the thesis. I would also like to thank the Consultant body at Barts Health, Rheumatology department for their support in developing an effective Early Arthritis Clinic which allowed recruitment to these projects.

Finally, I would like to thank my wife, Lucy, for graciously allowing me to take time out of training to undertake this period of research and for her support and encouragement throughout this time which has been unwavering. I would also like to

thank my three children - Emily, Tristan and Elise, for providing both ample distraction and inspiration in equal measures. Lastly, this thesis is dedicated to my mother and father who have always supported my education and development in every way that they possibly could.

Thank you Mum and Dad.

Contents

List of Figures

List of Tables

Abbreviations

3D - three dimensional

ACPA - anti-citrullinated peptide/protein antibodies

ACR - American college of rheumatology

AID - activation induced cytidine deaminase

Ang - angiopoietin

Anti-CCP - anti-cyclic citrullinated peptide

CIA - collagen induced arthritis

CK(R) - chemokine receptor

CPJ - cartilage pannus junction

CRP - C reactive protein

CTLA 4-Ig - cytotoxic T lymphocyte associated antigen

DAS - disease activity score

DC - dendritic cell

DMARD - Disease modifying Anti-Rheumatic Drugs

DIA - digital image analysis

DMARD - Disease modifying Anti-Rheumatic Drugs

DS - diffuse score

EAC - Early Arthritis Clinic

ELISA - enzyme linked immunosorbent assay

ELN - ectopic lymphoneogenesis

ESR - erythrocyte sedimentation rate

FDC - follicular dendritic cell

G 1,2,3 - Grade 1,2,3

GC - germinal centre

GS - Grey Scale

HAQ - Health Assessment Questionnaire

H&E - Haematoxylin and Eosin

HEV - high endothelial venule

HIF - Hypoxia inducible factor

HLA -human leukocyte associated antigen

ICC- intra class correlation coefficientIg

H -immunoglobulin heavy chain

IHC- immunohistochemistry

IL (R) - interleukin (receptor)

MIF- macrophage inhibitory factor

MMPs -metalloproteinases

MRI- magnetic resonance imaging

OMERACT - Outcome Measures in Rheumatoid Arthritis Clinical Trials

OPG -osteoprotegerin

PBMC -peripheral blood mononuclear cells

PDS - Power Doppler Signal

PDA - Power Doppler Area

PsA - Psoriatic Arthrtis

pSS -primary Sjogren's syndrome

RA - Rheumatoid arthritis

RAMRIS - Rheumatoid Arthritis MRI scoring system

RANK-L - Receptor activator of nuclear κβ-Ligand

RCTs - Randomised control trials

RF - Rheumatoid factor

RI - Resistance Index

ROI- region of interest

SCID -Severe combined immunodeficiency

SLE -systemic lupus erythematosus

SPP -suprapatellar pouch

STA - Synovial thickness area

STi - Synovial thickness index

TCR -t cell receptor

TGF-β - Transforming Growth Factor - β

Th -T helper cell

Tie - Angiopoietin receptor Tyrosine kinase

TNFa - Tumour necrosis factor α

TLS - Tertiary lymphoid structures

TUI - Topographical ultrasound imaging

UK- United Kingdom

US - Ultrasound

USA- United States of America

VAS - Visual Analogue Scale

VASCi - Vascular index

VGEF -vascular growth endothelial factor

VEGF-R - vascular growth endothelial factor - receptor

1. Introduction

Rheumatoid arthritis (RA) is one of the most important chronic inflammatory disorders in the UK. The diagnosis of RA leads to considerable morbidity and an increased mortality[1] [2]. According to the National Audit Office (2009 - http://www.nao.org.uk/) there are 26,000 new cases of RA each year with 582,000 prevalent cases in England. 45% of these people are of working age and within 1 year of diagnosis 30% are unemployed. RA is characterized by a symmetrical, erosive polyarthritis, resulting from chronic synovitis, and the presence of circulating autoantibodies such as rheumatoid factor (RF) and anti-cyclic citrullinated peptide (ACPA), strongly suggesting an autoimmune pathogenesis[3].

One of the first recorded descriptions of inflammatory arthritis was noted in the Ebers Papyrus, an Egyptian medial text, dated approximately 1500 BC[4]. Post-mortem examinations of Egyptian mummies has also shown evidence of an erosive polyarthritis. This was extensively reported by Sir Grafton Elliot Smith FRCS FRCP, who was the first chair holder of anatomy at the Cairo School of Medicine from 1900-1909[5]. Other societies have made similar description of an RA-like disorder with Charak Samhita from Indian in around 300 – 200 BC describing a condition involving joint pain, swelling with subsequent loss of joint mobility and function. Hippocrates also made some insightful observations regarding different forms of arthritis including gout, osteoarthritis and RA around 400 B.C. It wasn't until the 1st centuary AD that Celsus, the Roman encyclopedist, documented the classic manifestations of joint inflammation (*tumor* - swelling, *rubor* - redness, *calor* - warmth and *dolor* - pain). It is Galen however, who is attributed to adding a fifth tenant of inflammation, *functio laesa* - loss of function. Treatment of joint pain, swelling and warmth in inflammatory arthritis has been our aim as physicians for many centuries. The long term consequences of joint damage and loss of function relating to poorly controlled RA are obvious. Despite this clear relationship for many years the classic pyramidal therapeutic approach to treatment escalation was the norm. Following a

number of seminal publications, a systematic approach to early intervention with frequent monitoring and escalation of therapy has become widely accepted[6-11]. The consequence of this has been the recognition of an important population of patients with early inflammatory arthritis. In parallel, more focus has been given to the assessment and charcterisation of inflammation in these subjects. A focus on disease pathogenesis has resulted in a better understanding of the pathological processes causing joint inflammation with the consequence of targeted therapeutic discoveries, such as anti-TNF[12]. The technological advancements in this time frame have also heralded ultrasound and MRI imaging as potential novel imaging modalities which may contribute to disease activity assessment in addition to already validated tools such as the Disease Activity Score (DAS). This thesis focuses on the role of ultrasound imaging in the assessment of synovitis. I examine its relationship with clinical and histological parameters of Rheumatoid arthritis as well as its responsiveness to physiological and pharmacological induced changes. The over arching aim is to build upon the current existing evidence base for ultrasound imaging and suggest further areas for research and development, with a particular focus on patients with early inflammatory arthritis.

1.1 Early Inflammatory Arthritis

Over the past decade there has been a focus on early Rheumatoid arthritis (RA) which has lead to the formation of Early Arthritis Clinics (EAC) within Rheumatology departments. The development of such clinics is a direct consequence of the proven benefit of early initiation of disease-modifying anti-rheumatic drug (DMARD) therapy[13-15]. Previously, therapeutic intervention in RA was guided by a 'pyramid approach', delaying aggressive therapy until either the patients symptoms warranted escalation or following evidence of joint destruction. We are now aware that patients with inflammatory arthritis, who have early initiation of therapy, do better in terms of function and disease progression than patients with a delayed start [16-18].

There is a wide spectrum of patients who potentially may attend an Early Inflammatory Arthritis Clinic. These will range from true 'undifferentiated arthritis', early RA, Spondyloarthropathies, Connective Tissue Disease (CTD) and sarcoidosis[19]. The table below gives a reflection of the relative proportion of patients attending such a clinic.

Table 1-1: Diagnostic categories seen in an early arthritis clinic

The approximate percentage of different diagnostic categories presenting to an Early Arthritis Clinic over a 2 year period (modified from Visser et.al.[19])

Diagnosis	Percentage
Rheumatoid Arthritis	30
Undifferentiated Arthritis	26
Crystal arthropathy	11
Osteoarthritis	6
Psoriatic Arthritis	5
Sarcoid arthritis	5
Reactive arthritis	3
Connective tissue disorders	3
Spondylarthropathy	4
Other	7

1.1.1 Prognostic algorithms

1.1.2 Clinical variables

There have been a number of studies reporting the basic demographics of patients with early inflammatory arthritis[8-10]. Unfortunately, the definition of early inflammatory arthritis, period of follow up and patient inclusion criteria are inconsistent, thus limiting any conclusions which may be drawn. Earlier studies have tended to include only those patients fulfilling the ACR diagnostic criteria (1987) which provides suitable information pertaining to this specific sub-group of inflammatory arthritis patients but omits a substantial population of undifferentiated inflammatory arthritis suffers. Fulfilling the ACR diagnostic criteria at inception is a marker of poor

prognosis, which makes the analysis of its individual components impossible in such a prospective study[20]. Prospective studies using more general inclusion criteria, such as one or two swollen joints, Rheumatoid factor (RF) positivity and inflammatory symptoms, are more representative of the case load seen by clinicians in their early arthritis clinics. This approach has facilitated the development of prognostic algorithms and predictive frameworks which attempted to clarify the risk of radiological and functional deterioration from the initial clinical presentation[19 21].

Early arthritis studies recruiting undifferentiated arthritis, have shown that a number of patients have a self-limiting course for their arthritis (15-50%) and this tends to be associated with younger age of onset (18-25 years), a short duration of symptoms before presentation and not fulfilling the ACR diagnostic criteria[22-26]. Although the follow up period of these studies varied from 1 to 5 years, those patients who were eventually diagnosed as having a self-limiting disease tended to show improvement much earlier. Tunn et. al. reported 50% of patients in their EAC having a self-limiting disease process, however limiting the inclusion criteria to 6 months of symptom duration[22]. This clearly skews the population of patients with a greater likely hood of having a self-limiting course rather than persistence of symptoms. Perhaps a more useful conclusions drawn from these prospective studies are the Positive and Negative predictive value of the selected variables (PPV / NPV). The Norfolk Arthritis Register showed a Positive predictive value for the above variables in predicting a self-limiting disease course is approximately 63% whilst poor prognostic factors could only provide a 60% and 63% PPV for radiographic progression and functional deterioration (as measured by Health assessment questionnaire – HAQ)[27]. This has been reflected in a number of other similar studies but this degree of accuracy is insufficient to allow these variables to be used to direct therapeutic intervention which is of paramount importance with respects to improving disease outcomes in early Rheumatoid and undifferentiated arthritis[28-30].

1.1.3 Serology

The predictive value of serological markers for RA has also been explored separately from clinical variables in early arthritis populations. The frequency of positive RF or Anti-CCP antibodies has been commented on by a number of studies. RF positivity varies from 20 - 45% in early arthritis populations with Anti-αnti-CCP antibodies being found in 15-38% of patients[31-34].

Ates et al. assessed the diagnostic value of anti-CCPantibodies in patients with early arthritis. Sixty-four adult patients with early arthritis and disease duration of less than 4 months were followed up for 9 months. The combination of anti-CCP and IgM-RF positivity had a very high specificity and positive predictive value (100%) but a rather low sensitivity (33.3%) with respects to an eventual diagnosis of RA[35]. Overall performance of the anti-CCP test alone for the early RA was better than IgM-RF and similar to the combination of anti-CCP and IgM-RF.

Jansen et.al. assessed the predictive value of anti-cyclic citrullinated peptide (anti-CCP) antibodies above conventional variables for progressive erosive in a cohort of patients with early inflammatory oligo- and polyarthritis[36]. Symptom duration was limited to less than 2 years and patients with bacterial, psoriatic, crystal-induced arthritis or spondyloarthropathy excluded. Two hundred and eight-two patients were included with thirty-two percent of the patient's positive for anti-CCP at baseline. Anti-CCP correlated significantly ($p < 0.001$) with a progressive erosive disease after 2 years, but not with a low functional capacity. The positive predictive value (PPV) for radiographic progressive disease was 63%, whilst the negative predictive value (NPV) was 90%. Raza et. al. have also investigated the use of Anti-CCP and rheumatoid factor (RF), alone and in combination, in patients with very early synovitis (symptom duration less than 3 months) and followed up for nearly 18 months[37]. One hundred twenty-four patients were assessed at base line with ninety-six patients followed up longitudinally. The specificity, PPV and sensitivity of this antibody combination for the development of persistent disease-fulfilling classification criteria for RA were 97%, 86%, and 63% respectively.

1.1.4 Composite frameworks

A seminal paper was published by Visser et. al, who followed a similar approach to other prospective early arthritis databases. However, his predefined outcome measures differed significantly[19]. His rational is based upon the premise that making a diagnosis of RA is merely a surrogate marker for what the clinician and patients are really concerned with at presentation. Rheumatoid Arthritis is a heterogeneous disease process with a spectrum of possible clinical outcomes in terms of functional ability and radiographic erosions. Whether a patient will have a persistent, erosive arthritis is a much more pertinent question with the potential, if answered, to guide therapeutic intervention rather than predicting whether their arthritis will ever satisfy a set of classification criteria. In most studies, either the physician's clinical diagnosis or the disease classification according to the 1987 American College of Rheumatology (ACR) classification criteria has been used as the gold standard[38-42]. As a consequence, assessing the same diagnostic tests used in the diagnostic criteria (e.g. early morning stiffness, symmetrical synovitis etc) against this physician defined gold standard leads to circularity and overestimation of the diagnostic properties of such tests. The ideal algorithm would allow patients with predicted poor outcome to be treated more aggressively whilst those with a relatively a benign prognosis could be spared the potential complications of such aggressive therapy.

Five hundred and twenty-four, newly referred patients with early inflammatory arthritis were evaluated and potentially diagnostic determinants obtained at the first visit. The Arthritis outcome was recorded at 2 years' follow up (persistent vs self-limiting, erosive vs non-erosive). Variables from the patient's history, physical examination, blood and imaging were processed by logistic regression analysis. The discriminative ability of the model was expressed as a receiver operating characteristic (ROC) area under the curve (AUC). The predictive variables are shown in table 1 with their odds ratio and score.

Table 1-2: Predictive model of persistent and erosive arthritis

Adapted from Visser et.al. Arthritis and Rheumatism 46,2: 357-365[19]. A prediction model for Persistent and erosive arthritis.

Criterion	Persistent vs Self-limiting arthritis		Erosive vs Non-erosive arthritis given persistence	
	Odds Ratio	Score	Odds Ratio	Score
Symptom duration > 6 weeks but < 6 months > 6 months	 2.49 5.49	 2 3	 0.96 1.44	 0 0
Morning Stiffness > 1hr	1.96	1	1.96	1
Arthritis in 3 or more joint groups	1.73	1	1.73	1
Bilateral MTP compression	1.65	1	3.78	2
IgM-RF	2.99	2	2.99	2
Anti-CCP	4.58	3	4.58	3
Erosions on radiographs	2.75	2	Infinite	Infinite

A score of 8, 9 or 10 provides a probability of persistence of 0.87, 0.92 and 0.95 respectively and a score of 7, 8 and 9 provides a probability of erosive disease of 0.86, 0.92 and 0.95 respectively. This model fares reasonably well and the discriminating ability for erosive versus non-erosive arthritis model was 0.90. The discriminating ability for persistent versus self-limiting arthritis was lower at 0.82 which is insufficient to allow for accurate management decisions to be made with confidence. However, a small proportion of patients will have a high score which would still confer a high probability of erosive disease and thus should precipitate the initiation of aggressive disease modifying therapy at an early stage.

Recently, Van der Helm-Vanmil et. al. attempted a similar exercise on a large cohort of undifferentiated arthritis (570) followup for 1 year[28]. A prediction rule was developed using data from the Leiden Early Arthritis Clinic. The prediction rule consisted of 9 clinical variables: sex, age, localization of symptoms, morning stiffness, the tender joint count, the swollen joint count, the C-reactive protein level, RF positivity, and the presence of anti-cyclic citrullinated peptide antibodies. The clinical end point for this study was the development of Rheumatoid Arthritis which as previously discussed introduces circularity in attempting to evaluate variables which

themselves are required to confirm the clinical endpoint. Despite this one useful aspect to the model developed was that its negative predictive value was 0.97. Given the significant proportion of patients who will ultimately have a self-limiting arthritis this could be a useful model for identifying such patients. Unfortunately this model only attempts to discriminate between Rheumatoid Arthritis and Non-Rheumatoid Arthritis patients. The Non-RA patients do not necessarily all have a benign course and so further work is required to produce a definitive predictive frame work for both self-limiting disease and aggressive persistent erosive disease which can be easily introduced to daily clinical practice.

1.2 Assessment tools in Rheumatoid Arthritis

1.2.1 Disease activity score (DAS)

The DAS score was developed initially form a large prospective cohort of patients. A comprehensive list of variables was identified as relevant factors used by clinicians in making decisions about patients disease activity and treatment. Factor analysis and regression analysis produced a weighted 4 factor score with weighting of individual components. The subsequent development of the EULRA response criteria was based on a large cohort of patients receiving treatment with DMARDS. High and low disease activity were determined by clinical decisions and the DAS assessed in this light (figure 1-1). High disease activity was deemed to be the commencement of DMARDS or lack of DMARD effect. A low disease activity state was declared if the DMARD was stopped because of remission, no change DMARD therapy or not starting DMARDs for at least 1 year. Compared to the ILAR / ACR response criteria the EULRA response criteria showed reproducibility and discriminate ability[43 44].

Figure 1-1: Depiction of DAS score mapped to clinical decision of high and low disease activity.

Mapping of the DAS score to low and high disease activity state as indicated by expert clinical decision. Reproduced from van Gestel, et. al. Arthritis and Rheumatism vol. 39; 1 p34 - 40[45]

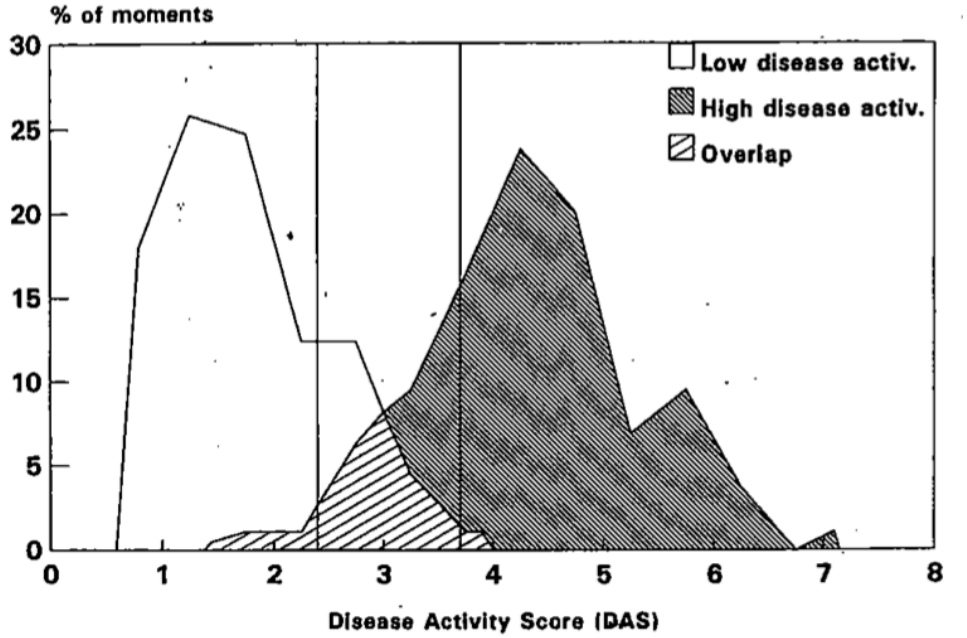

The graph above may be considered dated with the current use of DAS28 as a measure of RA disease activity however it illustrates the significant variation seen in DAS and clinicians interpretation of the patients disease activity. While at a cohort level, a distinction can be made between low and high disease activity based on DAS, there is significant spread of results. A new theme in the literature is clinical and imaging remission in patients with RA. We are aware that some patients with a low DAS28 score may continue to have develop progressive erosive disease. It has been suggested that imaging may help to identify these 'progressors'. From the graph above it is clear that even with a low DAS, a significant number of patients were still deemed sufficiently active and required change in therapy. It may be that imaging is helping us to identify those patients with sub-clinical disease activity (by DAS standards). It remains unclear weather the escalation of these treatment for these patients makes a difference in erosive disease progression.

The EULAR response criteria were subsequently developed using the DAS score providing a further dimension to patients assessment to include change as well as an absolute measure of disease activity[45]. Construct validity was assumed based on the prediction of erosive progression on x-rays and close correlation with the HAQ score. The mean error of the DAS score was 0.6 which underlies the 1.2 change in DAS (2 x error) which is still used to day in assessing response to therapy. The EULAR response criteria developed from this work seems to fair well when compared to the ACR improvement criteria.

Table 1-3: EULAR response criteria for DAS28

EULAR response criteria for DAS28

DAS 28 at endpoint	Improvement of DAS28 from baseline		
	≤ 1.2	>0.6 and ≤ 1.2	≤ 0.6
≤ 3.2	Good		
>3.2 and ≤ 5.1		Moderate	
> 5.1			None

Subsequently, the DAS28 was proposed and a modified but valid clinical assessment tool. The DAS28 was developed in a similar fashion to the DAS44 but with a reduced joint count and different weights to the individual factors[46]. The prospective cohort used to develop the DAS28 was again based on a set of early rheumatoid arthritis patients. Long term follow up of these patients provided the construct validity in terms of erosive disease and HAQ[47]. Since their development the DAS28 has been extensively validated and is currently used in routine care, as well as clinical trials, as an effective tool for measuring disease activity and monitoring response to therapy[48-50].

1.2.2 Health Assessment Questionnaire (HAQ)

The HAQ was first published in 1980 by Stanford Arthritis center[51]. It was the result of work to encapsulate patient reported outcomes in Rheumatoid Arthritis. The original HAQ had a number of dimensions (death, disability, discomfort, iatrogenic, economic) with further subdivision of these categories into subdomains, and further still into components. The disability dimension however has come to be used in isolation as the HAQ-DI.

The HAQ-DI is usually self-ɑdministered, but may also be given face-to-face. The Disability Index consists of eight categories 1) dressing and grooming, 2) arising, 3) eating, 4) walking, 5) hygiene, 6) reach, 7) grip, and 8) common daily activities. For each of these categories, patients report the amount of difficulty they have in performing two or three specific activities. HAQ Disability Index is entirely self-explanatory and easily performed in clinic.

The HAQ-DI has been validated extensively including as a self reported outcome when posted making it a very flexible assessment tool. Construct and criterion validity have been demonstrated as well as responsiveness and reliability[52-56]. It has been correlated with many other self-reported outcome measures including AIMS[57], EuroQuol[58], Depression scales[59 60], Nottingham Health Profile[61], WOMAC score[62] and importantly radiographic progression[63 64]. It is also often included in models of health economics particularly productivity, morbidity, health care utilization due to its correlation with work capacity, occupation and the ability to maintain an independent life within the community[65-67].

The HAQ is also integral to current drug approval processes within the UK. The National Institute for Clinical Excellence (NICE) accepts submissions from the pharmaceutical industry and a decision is made as to the cost of the improvement in quality of life generated. The HAQ plays an important role in assessing the quality of life in a number of models used for submissions[68].

1.2.3 Radiographic assessment

The use of radiographs to examine the damage to joints from synovial inflammation has been a constant feature of clinical practice and therapeutic trials for many years. It has many advantages such as relatively inexpensive, easily performed and images of many joints of both hands and feet can be assessed in one sitting. Two major scoring systems have been used over the past two decades - Larsen score[69] and Sharp score[70]. Lately, most clinical trials use the modified Sharp score as proposed by van der Heijde[71]. This particular score includes the hands and feet: 16 joints of the hands and wrists / 15 joints of the feet scored for erosions, 15 joints of the hands and wrists / 6 joints of the feet scored for loss of joint space. This provides a maximal score of 280 for erosions and 168 for joint space narrowing. The large number of joints scored provides plenty of opportunity to detect change over time.

Scoring of radiographs can be performed in time order or blinded to time order. Whilst chronological reading improves the signal detection of this scoring system it is not usually performed in the setting of clinical trials[72]. Two readers are used in trials with a third reader present as an adjudicator. The averaged score is used between both readers, reducing measurement error although a likely consequence is the concurrent reduction in signal although this is thought to be small in experts[73]. An interesting debate surrounding the relevance of negative radiographic scores is underway. The possibility of 'healing' erosions with negative radiographic scores being seen in the context of clinical trials. Due to the inherent margins of error in the scoring system a small negative result may not be clinically relevant however there is on going work to better understand the relevance at both the cohort and individual level[74 75].

There is good evidence that the radiographic damage correlates with inflammatory activity. Time integrated values for DAS and CRP have been shown to correlate with erosive progression on radiographs[76-78]. In addition, a number of studies have confirmed the relationship between radiological damage scores and function as determined by the HAQ in cross-sectional populations[78-81]. Longitudinal data is

available which suggests that erosive disease is not a linear concept but patients have periods of accelerations. In addition, statistical modeling of a longitudinally followed cohort of patients over a 10 year period, with careful adjustment for disease activity, would suggest that the rate of erosive burden co-determines physical function in addition to the inflammatory load.

New imaging modalities such as ultrasound and MRI have been shown to have more sensitive at detecting erosions of small joints of the hands and wrists[82]. These are therefore attractive imaging alternatives. However, radiographs are reproducible easily administered and have a wealth of validation. Until the other imaging modalities can match this body of work a place remains for radiographs in both clinical practice and trials.

Figure 1-2: Hand radiographs of a patients with RA

Radiographs of the hands and wrist demonstrating erosive disease at the MCP joints and wrists with marked loss of joint space.

1.2.4 MRI

MRI is a sensitive imaging modality and can assess many aspects of inflammation within the Rheumatoid joint including synovial inflammation, erosions, bone edema. There is no ionizing radiation and the multi-planar capabilities provides further

detailed assessment of the region of interest[83 84]. Its incorporation into clinical studies has facilitated further validation as an outcome measure and help refine its use. Despite the significant benefits of MRI, the significant costs associated with the initial purchase of the machine make its utility limited to larger resourced centers. Low field MRI scanners are now becoming available at reduced cost and would appear to be more tolerable for patients. The reduction in the magnet strength does generate noise however newer machines can perform a Short Tau Inversion Recovery (STIR) to improve sensitivity to synovitis in the context of inflammatory arthritis. There is also a time constrain with limited number of joints which can be suitably imaged in a reasonable time frame.

MRI has been validated against synovial histology in both the knee and small joints of the hands (MCPs) demonstrating a clear relationship between post gadolinium enhancement on MRI and macroscopically visualized synovitis. In addition, boney change was shown to be correlated with MRI determined erosions[85 86]. An interesting observation by Brown and colleagues demonstrated that subclinical inflammation seen on MRI but not detected clinically increased the risk of erosive progression on that cohort[87]. Bone marrow edema also seem to be a predictor of erosive disease in RA patients with it representing the only independent predictor of radiographic progression in a number of longitudinal studies[88-90]. Detection of erosions by MRI has also been correlated with CT erosions (accepted 'gold standard') as well as ultrasound in small joints[91 92]. There is certainly greater sensitivity compared to plain radiography in detecting erosions and loss of joint space[91 93]. This has been demonstrated with both high field and low field MRI[94].

Scoring of MRI images in RA has been extensively examined by the OMERACT (Outcome Measures in Rheumatoid Arthritis Clinical Trials) task force with the publication of the RA MRI scoring system (RAMRIS). This score has been validated extensively showing itself to be reliable and sensitive to change following therapeutic intervention[95-97]. The use in this context is potentially a significant step forward in clinical trials. Currently both disease activity assessment and radiographic

progression require a large population of patients with a clinical trial setting. The use of a more sensitive imaging modality may reduce the number of patients need to treat. MRI has been incorporated into a number of clinical trials of both DMARDS and biologic agents with promising results[98-101]. Some work is still to be done with regards to the validation with functional outcome but there are clear advantages associated with this imaging modality[102].

1.3 Ultrasound Imaging

Ultra - from the Latin meaning 'beyond'

Sound - vibrations transmitted through an elastic solid, liquid or gas (also defined as a 'meaningless noise')

1.3.1 Historical Perspective

Echolocation is a method utilized by a variety of animals to pinpoint objects and perceive their environment by means of reflection of ultrasonic sounds. Echolocation used by bats was observed in the early 19th century by Lazzaro Spallanzani, an Italian scientist, who would release blind bats in a room and observe the way they avoided colliding into objects directly in their path. Spallanzani's interpretation of these findings prompted him to describe a 'sixth sense' afforded to bats[103]. The puzzle of the 'sixth sense' was finally solved by Donald Griffin in 1938 who first coined the term "echolocation". Echolocation is widely known to be used by bats, dolphins and whales but many other species such as owls, rodents, seals, and the platypus have been found to use this evolutionary 'sixth sense'. There has also been some evidence that blind humans can use echolocation to aid orientation and mobility[104 105].

The use of ultrasound in a commercial setting can be traced to the sinking of the Titanic when in 1913 when British scientist L.F. Richardson filed a patent to detect icebergs with underwater echo ranging[106]. Following the First World War, C. Chilwosky and P. Langvin, developed the first practical echo ranging in water using the combination of piezoelectric technology and vacuum tube amplifier. Further

developments, towards the end of the Second World War, applied the pulse-echo ranging technology to electromagnetic waves producing the first RADAR (RAdio Detection And Ranging). The subsequent development of real-time scanners in the 1960s and 70s superseded the old static b-mode scanners and heralded an age of miniaturization. In 1981 the Hewlett Packard produced a phased array system which was the forerunner of future systems, having wheels, microprocessors and programmable capabilities which were up-gradable. The late 1990's brought the development of three dimensional (3D) imaging and subsequent arrival of four dimensional (4D – 'real-time 3D') imaging.

1.3.2 Doppler Ultrasound

The Doppler effect (or Doppler shift), was named after Christian Doppler, an Austrian physicist who first described the concept in 1842. The 'Doppler Effect is a change in the frequency of a wave, resulting from motion of the wave source or receiver. This is practically demonstrated by the audible change in frequency heard as a Police siren comes towards you (high frequency sound) and then drops to a lower frequency sound as it moves past and away form you (low frequency sound). Doppler US imaging involves detecting and measuring blood flow[107]. The main reflector within blood tissue is the red blood cell. The Doppler shift (f_{Dop}) can be expressed by the equation below and is dependent on the transmitted frequency (ft) of the acoustic wave, the velocity of moving blood (v), the speed of sound (c) within the tissue and the angle between the sound beam and direction of moving blood (θ).

$$f_{Dop} = \frac{2\, ft\, v\, cos\, \theta}{c}$$

The equation can be rearranged, as below, to express blood velocity. This is the fundamental equation on which the US Doppler image is generated.

$$v = \frac{f_{Dop}\, c}{2\, ft\, cos\, \theta}$$

The angle of insonation 'θ' is estimated by the controller by aligning an indicator on the duplex image along the longitudinal axis of the vessel, also known as 'angle correction'. It is important to note that the cosine of 90° is zero, which has an immediate clinically relevant effect of giving a false impression that no flow can be detected if the ultrasound beam is held perpendicular to the direction of blood flow. This is a product of not being able to detect a Doppler shift. The incorporation of a cosine function into the equation would also suggest that an angle of greater than 60 degrees might produce an inaccurate estimation of the Doppler signal due to the rapid escalation of the cosine function curve above this figure. Therefore, an error in the estimation of the angle of insonation can be greatly multiplied if care is not taken when assessing the selected vascular structure.

Figure 1-3: The Doppler effect

Cartoon of US beam and reflection of transmitted pulse form moving red blood cells. The transducer acts as both transmitter and receiver for the sound wave. The change in the frequency of the wave is calculated and expressed as Doppler signal on the display.

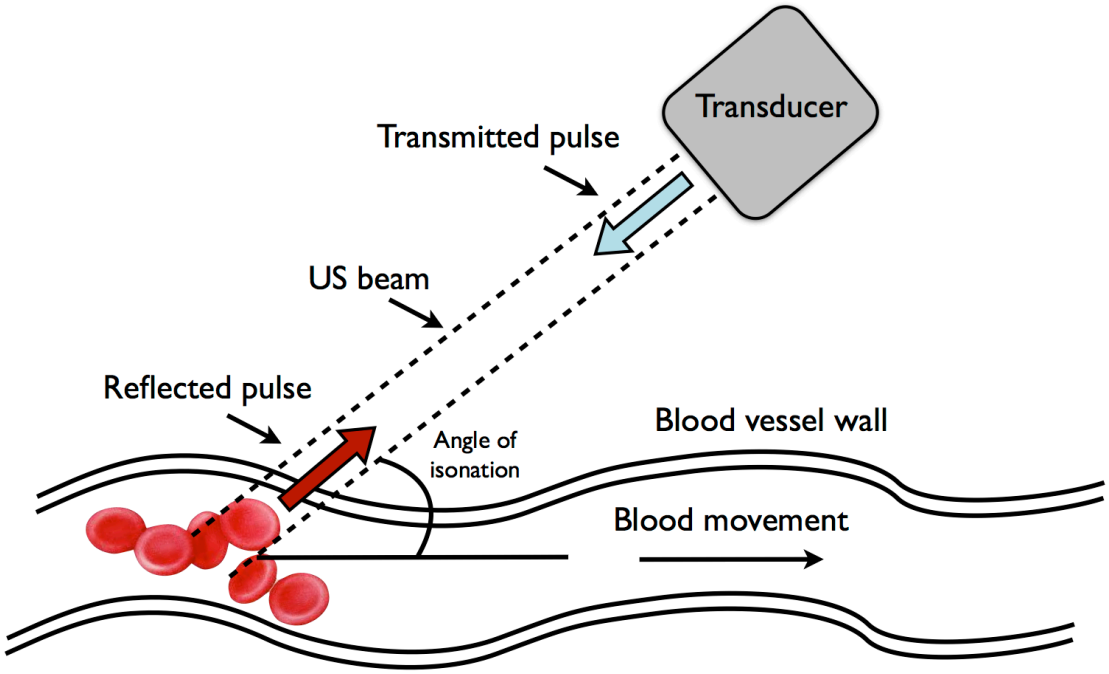

Modern equipment filter out the high amplitude, low-frequency Doppler signals which usually result from tissue movement. This can be due to vessel wall motion or small movement of nearby musculature often under the effects of the vascular impulse especially with respects to major vessels e.g. carotid arteries. These high amplitude, low frequency waves can however be exploited for the purposes of Power Doppler which will be discussed later. There are several forms of Doppler imaging available to the sonographer:

- *Continuous-wave Doppler ultrasonography*
- *Pulsed-wave Doppler ultrasonography*
- *Color Doppler ultrasonography*
- *Duplex ultrasonography*
- *Power Doppler ultrasonography*

Of particular interest to the Rheumatologist is power Doppler which is discussed further below.

1.3.3 Power Doppler

Power Doppler imaging (also known as energy mode Doppler) is a variation on color flow imaging in which the displayed intensity *is not* based on the intensity of the Doppler frequency signal. In Power mode, there is a summation of all of the Doppler shift frequencies and this is represented on the visual display as varying colour intensities of a pixel[108]. This pixel effectively is a measure of the power (or energy) returning from the Doppler shifted signal. Directional information is lost but this modality provides greater sensitivity of Doppler detection at low flow rates. As a result of the addition of Doppler shifted frequencies, a greater signal to noise ratio is reached. This permits for greater receiver gain to be applied across the image with little background interference. However, the greater sensitivity to slow blood flow is achieved with a trade off to noise from mechanical movements from the probe produced by the technician. This balance is favorable provided the gain and PRF are set appropriately. This modality is ideal for imaging blood flow in with small vessels

and in particular the synovium. The use of contrast agents such as Levovist (Schering, Germany) increases the sensitivity of Doppler US, but also implies considerable additional costs, time, and invasiveness to any procedure and has a few potential side-effects[109 110]. The future role of contrast media remains unclear, particularly with the development with B-flow imaging technologies which are more sensitive.

Figure 1-4: US image of an MCP joint showing Power Doppler Signal

2D image of the left second Metacarpal-phalengeal joint, showing synovial hypertrophy and power doppler signal both at the joint articulation and posterior to the metacarpal head.

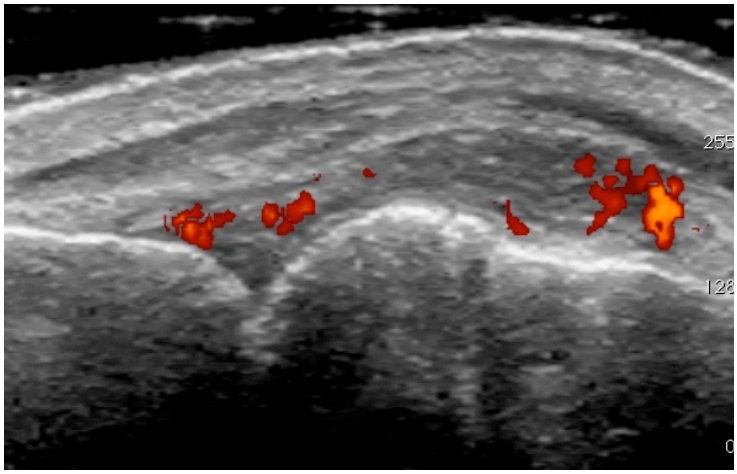

1.3.4 Qualitative and quantitative scoring of Power Doppler Signal

The accurate assessment of PDS is a key component of any clinical study engaging US as a measure of synovitis. There are a number of studies in the literature which have used various methods and these will be briefly discussed below.

Semi-Quantitative score

This is method has been used most frequently to grade PDS in the literature[111-117]. It is relatively quick with reasonable inter-observer variability. Pre-defined criteria may be used or an image atlas used as reference images for scoring[114 118]. This Likert scoring system parallels the semi-quantitative score for MRI images devised and validated by the OMERACT group (Outcome Measures in Rheumatoid Arthritis

Clinical Trials)[119]. This type of scoring can be performed whilst imaging the patient in real time. The draw back is that it artificially divides a continuum of PDS. This type of scale is considered an interval rather than an ordinal as both the order of the elements and the distance between values on the scale provides relevant information to the researcher. As applied to US imaging scoring, there is an inherent weaknesses with a degree of overlap at the extremes of each category and the deviation from the notion that each step along the interval scale represents the same quantified difference i.e. 0 to 1 equates to 2 to 3 in terms of the degree of Doppler signal or synovial thickness increment between each step. Where a small change in US signal is important this tool is likely to be too insensitive. A number of reports have shown this score to detect change and have predictive value both terms of disease flare and erosive outcome in a dedicated joint data set at the cohort level[114 120-124].

Table 1-4: Table of OMERACT B mode and Power Doppler scoring

Proposed OMERACT semi-quantitative score proposed by wakefield et.al. for grey scale and Power Doppler scoring[117].

B Mode	- Grade 0: Normal joint (no synovial hyperthrophy, no joint effusion) - Grade 1: Minimal synovitis (minimal synovial hyperthrophy, with or without minimal joint effusion) - Grade 2: Moderate synovitis (moderate synovial hyperthrophy with or without minimal or moderate joint effusion) - Grade 3: Severe synovitis (severe synovial hypertrophy, with or without severe joint effusion)
Power Doppler	- Grade 0: no vessel in the synovium; - Grade 1: up to 3 single spots signals or 1 confluent spot + up to 2 single spots - Grade 2: vessel signals in less than half of the area of the synovium (< 50%) - Grade 3: vessel signals in more than half of the area of the synovium (> 50%)

Pixel Count / Area

A number of studies have used software to count the number of coloured pixels seen with PDS[125-129]. The measurements depend upon reproducible image collection. Usually, a short video file is recorded of the desired image and this is later frozen at the point of maximum PDS signal which will have a beat to beat variation vary

according to cardiac output. Although this improves upon the observer variability inherent in the semi-quantatative score there remains a degree of variability with judgment being needed as to the maximum signal displayed during the video loop. Using 2D PDS images recorded, only a glimpse of the synovial blood flow can be viewed. There is a significant assumption that this is representative of the overall vascular flow within the joint. This can be in part inferred by histological studies in patients undergoing joint replacements where the PDS was proportional to the vascularity of the synovium specimens[130]. The correlation of the change in PDS, measured by pixel number, with clinical improvement with in the confines of a randomized controlled clinical trial, also supports its validity[131].

Resistance index

This method of assessing vascular flow has been used less frequently[113 132 133]. It requires the ability of the sonographer to accurately image a synovial vessel and, using Duplex US, calculate the resistance index from a standard equation. This gives a relative number which has been shown to change with therapeutic intervention. The significant limitations of this technique are that it is time consuming and ideally a number of vessels should be sampled to gain a representative value for each joint. However, often detecting signal from a single vessel can be extremely challenging. This assessment of vascular flow may be useful in combination with other scoring modalities if extra synovial vessels are to be assessed to compare response to physiological or therapeutic interventions.

1.4 Three Dimensional Ultrasound imaging

Three dimensional (3D) US imaging has been used for some time in the field of Obstetrics but is a relatively tool for musculoskeletal imaging[50 51]. It potentially may provide a solution for the persistent criticism of US variability with respects to image acquisition. Until recently 3D images were generated by free hand movement of the probe over the anatomical site producing variable results. The attachment of a magnetic sensor was required to allow reconstruction of accurate 3D images. The production of a 3D probe which has an in built mechanical motor capable of moving an internal array has significantly improved the quality of images (Figs. 3-H). The

sonographer need only hold the probe still and the internal mechanical engine sweeps across a predetermined angle. The approximate volume of tissue sampled by this probe is 20mm x 20mm x 10mm. This is sufficient to assess the dorsal or palmer surface of a small joint.

Figure 1-5: Cartoon of tilt and freehand 3D US image generation

Representation of A) freehand and B) mechanical tilt 3D volume imaging (cartoons kindly donated by Horst-Peter Johae, General Electric Healthcare).

A **B**

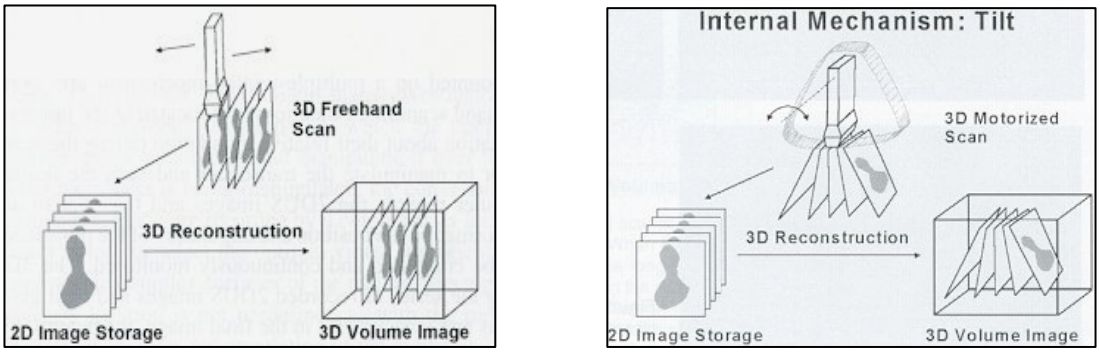

1.4.1 Topographical US imaging (TUI)

Tracking erosive disease in patients with early inflammatory arthritis by US imaging is difficult. Returning to the exact position to assess the same erosion is virtually impossible using 2D reference points. With MRI and CT it is possible to produce topographical images of the joint which allow for repeated imaging of a particular area of interest over time. The capacity to view multiple images, in three planes, through a volume of joint tissue will greatly aid interpretation and scoring of various aspects of synovitis (synovial fluid, thickening and vascularity). The use TUI for this purpose is yet to be investigated.

1.4.2 3D Doppler imaging

The application of 3D technology can be applied equally to Doppler signal as to Grey scale (B-mode) images. The resultant 3D image is effectively a reconstructed angiogram of vascular flow through the block of sampled tissue (Figure 1-5) . Although this is appealing and will undoubtedly give a more representative impression of vascular flow

within the synovium, there are a number of issues which require to be addressed. The sweep of the probe requires approximately six seconds for completion. This allows a number of cardiac cycles to pass with the resultant fluctuation in vascular flow. It may be possible to trigger the scanning process at a specific part of the cardiac cycle or alter the speed of the mechanical sweep to reduce the variation in signal detected. This is a critical aspect of this new technology which will need to be resolved for it to become a convenient and robust method of accessing PDS. The resultant image can once again be scored semi-quantitatively or, with dedicated software, a quantitative calculation of the voxel number (3D pixel). Once again this has not been addressed in the literature.

Figure 1-6: 3D reconstruction of 3D Power Doppler Signal

3D volumetric reconstruction of PD signal within a MCP joint demonstrating digital vessel signal, feeding vessel and synovial doppler signal.

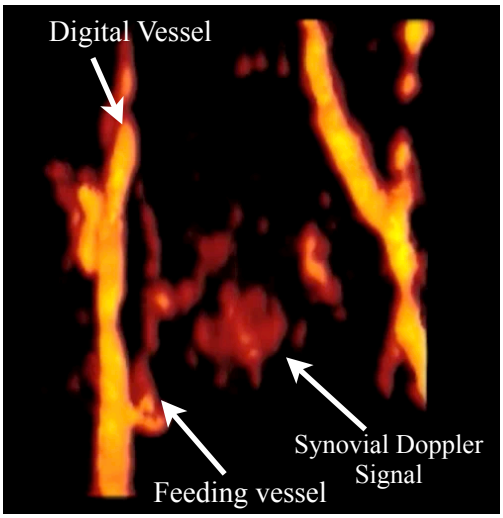

Recently, Naredo has reported a high level of agreement between readers for 3D US. The kappa values for 3D volumetric US were appreciably higher than 2D US in the detection of synovitis / tenosynovitis (0.41 vs. 0.37) and PD signal (0.82 vs 0.45)[134]. She also went on to show that in a cohort of patients receiving Rituximab therapy, 3D volumetric analysis of PD signal was responsive to change. The superior agreement seen with this particular imaging modality may suggest that it has a role to play in the assessment of patients in multi-centered clinical trials although more work is needed to address other aspects of validity[135].

1.5 US assessment in inflammatory arthritis

Musculoskeletal US imaging has emerged as a useful tool in the assessment of inflammatory arthritis. The parallel evolution of the micro-processor, Doppler technology, miniaturization and development of high frequency probes has enabled US to deliver high quality images of small superficial structures such as joints, tendons and ligaments[136]. These developments have permitted its exploitation in the arena of musculoskeletal imaging and in particular inflammatory arthritis. It is non-invasive, relative inexpensive, lacks ionizing radiation and is easily repeatable, making it potentially useful for both diagnosis and monitoring of patient[137]. There has been much work on validating the use of US imaging in the sphere of Rheumatology over the past 20 years. Although this body of work encompasses imaging of tendons, enthesitis, nerves and muscle I will focus principally on the imaging of synovitis in the subsequent sections below.

Clinically evident joint swelling makes a considerable contribution to the ultimate diagnosis of a patient suffering from an inflammatory arthritis. Indeed, the 2010 joint ACR/EULRA classification criteria for RA gives points on a scoring system for the number and distribution of swollen, inflamed joints. US imaging clearly demonstrates the synovial changes which takes place in the small joints of the hands and wrists in patients with Rheumatoid Arthritis with demonstrable increase in synovial thickness, Doppler signal and boney erosions[120 138 139]. Cartilage can also be clearly demonstrated in small and large joints with characteristic ultrasonographic changes demonstrated in crystal arthropathic[140 141]. To this extent MUSK US imaging in inflammatory arthritis has considerable content and face validity.

1.5.1 Ultrasound imaging and synovial histopathology

Criterion validity requires a clear relationship to be established between the imaging modality and a ‘gold standard’ assessment of synovitis, such as histological manifestations of joint inflammation. The two features, most commonly examined in this respect, are synovial vascularity and cellular infiltrates.

Synovial vascularity was investigated by Walther et al., who found a good correlation between histological vascularity and visual grades of PDU signal in the synovium of both knee and hip joints in patients undergoing arthroplasty (r - 0.81 p <0.001)[142]. Schmidt et al. found good agreement between presence of colour Doppler signal and histologically verified pannus tissue in knee joints of RA and osteoarthritis patients undergoing joint replacement surgery[143]. Pannus in this study was histologically defined as 'synovial proliferation with invasive destruction of cartilage and bone'. A study by Fiocco et al. found a significant correlation between B-mode US synovial thickness and the macroscopic grade of synovitis on arthroscopy in arthritic knee joints[144]. The studies by Walther and Schmidt, both used a convenient method for harvesting synovial tissue following ultrasound examination i.e. joint replacement surgery, which has limitations. There is certainly criterion validity with respect to Doppler signal matching synovial vascularity but the presence of secondary OA does limit the relevance of these findings in early inflammatory arthritis. In addition, synovial vessels can be demonstrated histologically in the normal synovial joint, therefore an important question is the relationship of Doppler signal in an earlyinflammatory arthritis cohort and whether this relationship remains fixed following treatment.

Koski et. al. have provided the most extensive assessment to date of ultrasound and cellular changes in synovial histopathology[130]. This study examined the relationship of ultrasound parameters and synovial histological findings in patients undergoing a percutaneous synovial biopsy of the designated joint. Forty-four patients with either monarthritis or polyarthritis were recruited with a majority of knees (25 /44) being biopsied. In this study a robust assessment of the synovial tissue was made with only sections with an intact synovial lining layer being assessed. Seven histological parameters of each specimen was scored (multiplication of synovial lining, villous hypertrophy of the synovial surface, surface fibrin deposition, sub-synovial infiltration of polymorphonuclear leucocytes, sub-synovial infiltration of mononuclear leucocytes, proliferation of blood vessels and fibrosis). Each histopathological and

ultrasound parameter was graded on a semiquantitative scale, with the 7 histological parameters summed to provide an overall score for the biopsied tissue. Grey-scale ultrasound showed synovial proliferation in 39 of 44 (89%) the patients however no significant correlation was found between the degree of synovial proliferation detected with ultrasound, and the overall histopathological score ($r=0.222$, $p=NS$). A positive Doppler signal was detected in 34 of 44 (77%) of the patients and once again no significant correlation was found between the amount of the power Doppler signal in the synovium and the overall histopathological score ($r=0.239$, $p=NS$). The amounts of sub-synovial infiltration of polymorphonuclear leucocytes did correlate with the amount of power Doppler signal (0.328, $p<0.05$). Whilst this study makes a more detailed histological assessment of the synovium there is a lack of homogeneity of patients and joints being sampled. A standarised assessment of each joint was not described but significant differences in doppler sensitivities are likely to have arisen between knee, wrist and tendon PDS assessment. The use of a 8MHz probe may also have diminished the US sensitivity and contributed to the lack of correlation in some parameters. With its acknowledged limitations, this study importantly attempts address the question as to the relevance of grey scale synovitis and Doppler signal. However, the cellular infiltrate may differ significantly depending upon the disease entity being investigated. Krenn et. al. were able to differentiate between RA and non-RA (PsA or Reactive arthritis) synovial samples based on a 9 point scoring system for synovial lining layer hypertrophy, cellular infiltrate and organisation[145 146]. Whilst these features were not mutually exclusive of each other there was signifiant difference in the the population as whole. More recently an MRI based study examining the response of PsA patients to Etanercept showed that CD3 lymphocytes appear to be a superior biomarker of response to therapy rather than CD68 sub-lining macrophages typically seen in RA[147]. Thus the differences in synovial histomorphology and cellular behaviour demonstrated within various arthropathies would suggest caution in attributing a universal relationship, at least with grey scale synovitis, and synovial infiltrate.

1.5.2 The relationship of ultrasound imaging and clinical assessment of disease activity

Another important aspect of validating US imaging in inflammatory arthritis is testing the relationship between existing measures of RA synovitis and disease activity. This is problematic as no 'gold standard' clinical assessment tools exist. The clinical indices of disease activity such as the DAS and ACR were originally validated against long-term patient outcome measures such as the Health Assessment Questionnaire (HAQ) and radiographic erosions[148-151]. In this respect, the ultimate validation of US imaging will have to be against these standards, however given the current adoption of DAS28 as a measure of disease activity routinely used in clinic US imaging needs to be compared with this composite score.

A number of authors have demonstrated a moderate correlation of US assessment and DAS28. Hameed et.al. scored 10 MPC and 10 PIP joints in established RA patients (mean disease duration 11 years) with relatively active disease clinically - mean DAS28 5.1 (range 2.87-7.33)[152]. Both the Grey scale and Doppler scores were correlated as a joint count (binary, absence or presence) and a summed score (0-3 / joint; total score of 0-60). Only a modest correlation was found with the US grey-scale joint summed score ($r = 0.34$; $p=0.01$), however no correlation was found with the summed power Doppler summed score. The components of the DAS 28 also performed poorly with only the tender joint count being correlated significantly to the grey scale joint count ($r = 0.38$; $P = 0.006$). The swollen joint count and VAS failed to show any relationship with any of the US parameters in this study. In keeping with these findings, Salaffi showed that US detected a higher number of joints with US defined synovitis than did clinical examination with an average of 19.1 out of 44 joints being deemed inflamed on US and only an average of 12.6 ($P = 0.01$)[153]. A study by Shio, examined the relationship of US Power Doppler in both knee joints and MCP joints in 10 patients before and after infliximab therapy[132]. A significant correlation was found at baseline with knee joints doppler and the CRP ($P < 0.01$), ESR ($P < 0.01$), and 3 variable DAS28 ($P < 0.05$), but not with the MCP US-

PD scores. Interestingly, none of the US parameters correlated with clinical or biochemical response. A single joint approach to relating US findings to clinical disease activity was also taken by Ellegaard et. al. who use the colour fraction in a single wrist joints to correlate with clinical parameters of disease activity[129]. The colour fraction represents the ratio of colour pixels / synovial area. There was a significant, but small, correlation between the colour fraction and DAS28 ($r = 0.29$; $P < 0.01$), CRP ($r = 0.5$; $P < 0.001$) and ESR ($r = 0.5$; $P < 0.001$) but no correlation with the tender joint count. This finding may suggest the presence of a sentinel joint which may be a useful indicator of overall disease activity.

When a greater number of joints is assessed with US it would appear that the relationship between clinical and US parameters is stronger. In a longitudinal study, Naredo examined 28 joints, corresponding to those assessed for DAS28 scoring, for the presence of PD and graded them on a 0-3 score[154]. The summed PD score correlated with the DAS28 and CRP ($r=0.48$ and $r=0.32$ respectfully) at baseline but not HAQ. At 12 months from follow up the correlation remained with the DAS28 and CRP but also showed a significant correlation with the HAQ score ($r=0.39$). In addition, Kawashiri et. al. correlated PDUS scores of 24 synovial sites with DAS28, simplified disease activity index (SDAI) and clinical disease activity index (CDAI). All positively correlated with the PDUS score as did a number of serum biomarkers such as VEGF and MMP-1. Moreover, using a regressional approach they identified 6 joints which continued to reflect overall clinical activity[155].

Therefore, whilst there is some degree of construct validity with US assessment of synovitis, some discrepancy does exist with the DAS28 clinical assessment of disease activity. Correlations are generally poor / moderate and require an extensive assessment of joints, although moderate correlations are noted with inflammatory markers. Correlations with tender and swollen joint scores are inconsistent. This may suggest that US assessment of disease activity provides additional information to DAS28 alone and as such may supplement clinical disease assessment in specific patients[111 112 156]. The greater sensitivity of US imaging in detecting synovial swelling

has been confirmed by a number of authors[112 157-160]. Sub-clinical inflammatory disease is certainly a well established concept in RA with some suggestion that a stricter level of remission should be applied to patients to include both clinical and imaging remission[161-163]. Wakefiled et. al. described the presence of US synovitis in a cohort of 80 patients that subclinical US synvoitis could be detected in over 30% of clinically non-involved joints. In a follow up study, Brown demonstrated that RA patients in clinical remission, but persistent Power Doppler signal, had an increased chance of having erosive progression on plain x-ray after 12 months follow up[121]. This may not be surprising as DAS28 assessment was developed primarily based on therapeutic decisions to escalate treatment by Rheumatologist in a clinical trial. Therefore it is likely that a spectrum of patients with low DAS28 have on going low grade synovitis which US imaging may be well placed to detect. The integration of DAS and US parameters still requires further work and with particular focus of responsiveness and predictive value.

1.5.3 The relationship of ultrasound imaging and other imaging modalities

The agreement of ultrasound imaging with other imaging modalities provides convergent validity of this technique in the setting of inflammatory arthritis. MRI imaging has been validate in RA both in terms of its predictive value, detection of erosions, its relationship with histologically defined synovitis and detecting change over time[85 91 164-169].

Synovitis

A number of studies have compared US and MRI findings in RA finger joints have shown a high level of agreement with respect to bone erosions and synovitis, as assessed by B-mode (grey scale) and PDS. Specifically, Backhaus et al. found US to be more sensitive than MRI for detection of synovitis in the finger joints with MRI being more sensitive at detecting very small erosions[170]. In a similar study form the same group demonstrated that bursitis, tenosynovitis and erosions in the shoulder

joint were more often detected by MRI and US than conventional radiology techniques[171]. Szkudlarek et al. has shown that the PDS and early MRI enhancement in rheumatoid metacarpophalangeal (MCP) joints were very closely correlated[172]. The sensitivity and specificity of PDS, using MRI as a reference, was 89% and 98% respectively. Similarly, a recently published by Schmidt et. al. demonstrated good correlation between US and low field MRI for MCP and MTP joint synovitis[173].

Despite this encouraging correlation between US and MRI in small joints, when the correlation is examined in large joints such as the shoulder or knee, it would appear that MRI more reliably detects synovitis and erosions[171 174 175].

Tenosynovitis

US appears to be a sensitive method for imaging tendons[176]. Normal tendon ultrasound anatomy shows a densely packed fibrillar pattern of fibres in the longitudinal plane. In tendinosis there is a loss of this pattern, hypoechogenecity and thickening of the tendon and frequently doppler signal demonstrated within its substance. Tenosynovitis, refers to the inflammatory changes seen primarily within the tendon sheath such as fluid accumulation, hypoechoic synovial thickening and Doppler signal[177-179]. It would appear that it is certainly superior to clinical examination but may also has an edge on MRI imaging. In the study by Schmidt et. al. described above, in addition to showing good correlation with synovitis at MTP and MCP joints a superior detection rate of tenosynovitis was noted with US imaging (30 vs 15 patients)[173].

Figure 1-7: Images of normal and inflamed digital flexor tendon

Tendon ultrasound anatomy **A**: normal tendon ultrasound anatomy showing the typical fibrillar structure overlying the MCP joint (volar aspect). **B**: Flexor tenosynovitis demonstrated with Doppler signal, fluid and synovial thickening at the level of the PIP joint (volar aspect).

A

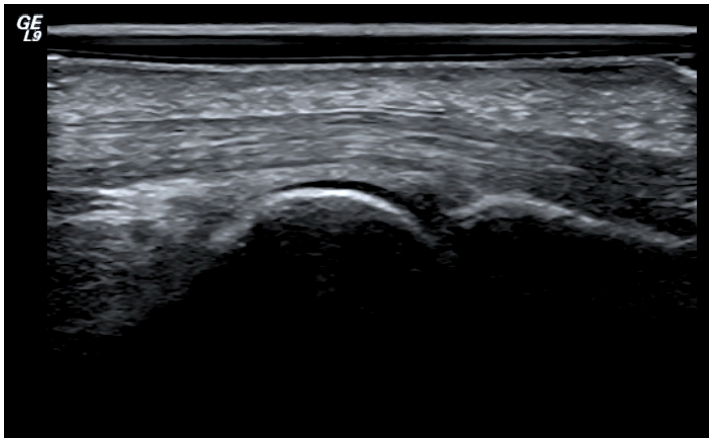

B

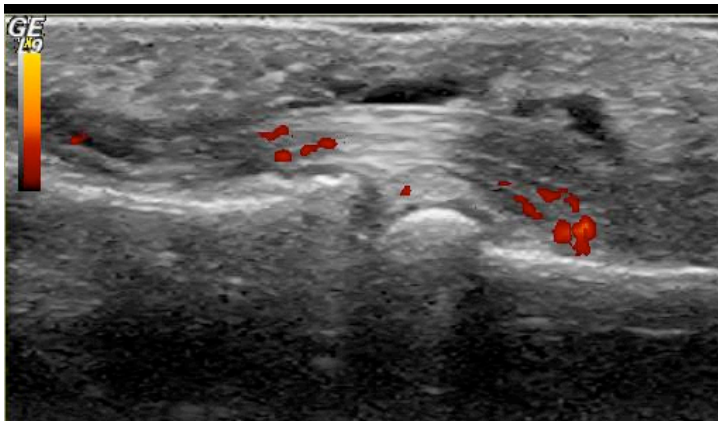

Bone erosions

US technology is capable of imaging bone erosions in the both small and large joints. with one of the first published description of US detected bone erosions was by Fornage in 1988[180]. US determined bone erosions are seen as a break in the cortex of the bone and should traditionally be viewed in two directions (transverse / longitudinal views) before being confirmed[181]. Szkudlarek has suggested a 0-3 score for bone erosions. Bone erosions were defined as changes at the bone surface at the

point adjacent to the joint (0= regular bone surface, 1 = irregularity of the bone cortex in 1 plane only, 2 = formation of a cortical defect seen in 2 planes, 3 = large bone defect creating extensive bone destruction). Whilst this is a helpful step in better characterising bone erosions by US it remains to be seen is such a classification is workable in the clinical or research context. Conceptually, the variation in size of erosions detected in patients with RA would suggest that the interval distance between grade 2 and 3 require further sub-division to facilitate a more sensitive scoring system.

Figure 1-8: longitudinal and transverse images of MCP head erosion.

Bone erosion on the right 2rd Metacarpal head in a patient with seropositive RA **A:** Longitudinal view of MCP showing erosion on the metacarpal head **B:** Transverse view of metacarpal head

A

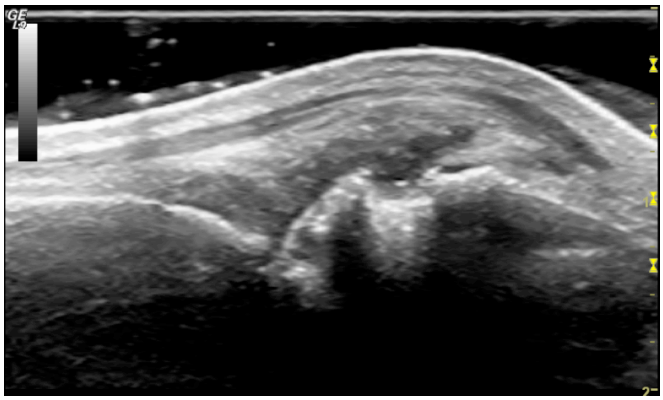

B

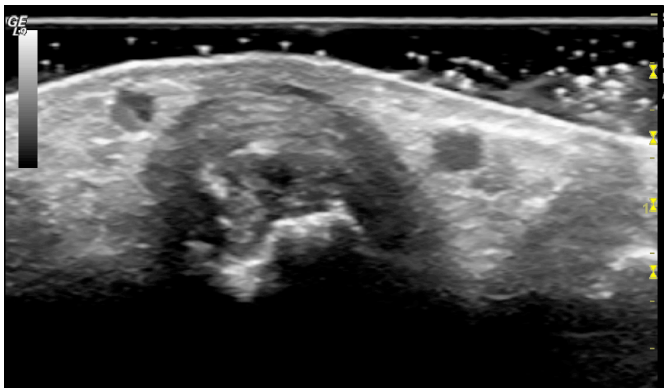

The detection of bone erosions is considered a poor prognosis when see on standard radiographs of the hands and feet[19 182]. There have been a number of studies comparing US imaging, radiography and MRI. US has compared favourably with MRI in detecting bone erosions in finger joints and with a single study suggesting similar detection rates at the shoulder[82 171 183-185]. US imaging is clearly better than plain radiographs at detecting bone erosions with some studies suggesting a 20 – 30% discrepancy in early arthritis patient populations[82 186]. This clearly has significant implications for patients being assessed in an early arthritis clinic.

US bone erosions were followed systematically by Backhaus et al. in 49 patients with various arthritides[170]. Comparisons were made between MRI, US, and radiography of wrist, MCP and PIP joints and after 2 years. Synovitis as detected by MRI and US decreased, whereas the number of bone erosions increased. As previously reported more patients showed erosive progression on US compared with radiography suggesting a higher sensitivity to change. However, it is possible that the inter-observer variability, which was not investigated, was in part contributing to these results. However, Wakefield et. al. has proposed an US score for erosions and shown fair inter-observer agreement and in addition that US detection of erosions in small joints is superior to conventional radiology and comparable to MRI imaging[187]. Others have reported similar findings in hands and feet, however the multi planar advantage inherent with US imaging is limited to the most medial and lateral of the MCP joints (MCP 2+5). Here the ultrasound probe can successfully negotiate the rim of the MCP joint where as at the 3rd - 4th MCP there is limited access to the lateral margins.

In established RA patients, the ability to monitor and track bone erosions in response to therapy can be a useful tool. The development of new erosions is often used as a clinical end point in studies based on plain radiographic imaging. The ability to observe these changes more sensitively may provide a new tool for assessing patient outcomes at an earlier time point. Once again a number of issues

surrounding the reliability of such observations exist, however with new 3D technology these potentially can be addressed[137] (Fig 1-9). The joint surface may be mapped and therefore remove the inherent variability of US imaging using a 2D linear probe with no exact anatomical landmarks to guide probe positioning and image acquisition. A topographical assessment can be performed which may improve inter-reader reliability.

Figure 1-9: Topographical ultrasound image and 3D reconstruction of MCP erosion

3D reconstruction of a metacarpal head showing 2 erosions on the medial and lateral aspect. The topographical image (right hand side) is manipulated to show coronal sections through the metacarpal head. The reference image can be seen on the top right hand corner. A 3D reconstruction of the grey scale image in seen on the left hand image with prominence given to the large erosions on the medial aspect of the joint.

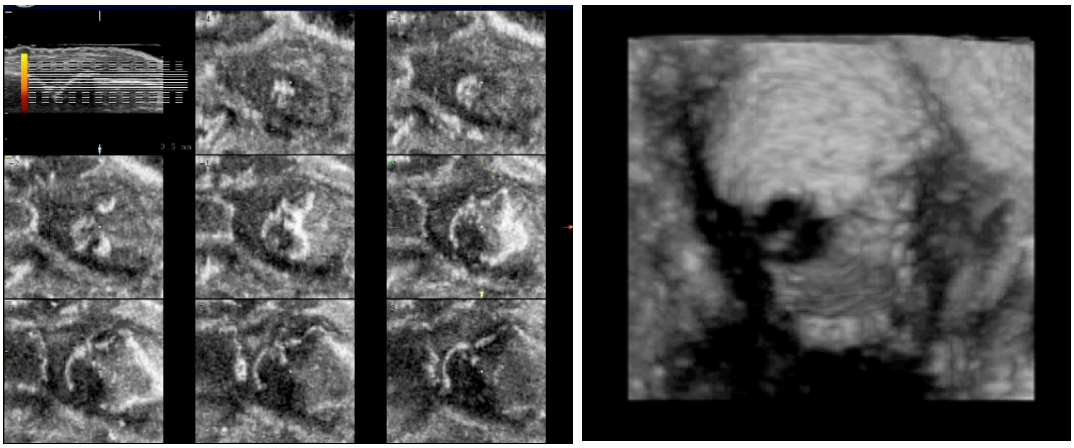

1.5.4 Ultrasound as an aid to diagnosis and prognostic biomarker

The predictive value of US in RA is a critical aspect of its validation if it is ever to be formally incorporation into routine clinical care. Classically, outcome measures in RA refer to functional ability and structural joint damage over time. Whilst these endpoints are of importance, a challenge for the Rheumatologist is often teasing out patients with true inflammatory arthritis versus non-inflammatory disease. In a seminal paper by Freeston et. al. they examined the use of US as an additional tool in predicting patients with inflammatory vs non-inflammatory arthritis[188]. In a relatively

small cohort of patients (50), the addition of ultrasound data to clinical, serology and plain radiographs increased the probability of an inflammatory arthritis being diagnosed in a seronegative patient from 30% to 94%. Similarly, van de Stadt LA, showed an predictive value for US, and in particular power Doppler, at a single joint level in predicting the development of clinically apparent synovitis. Unfortunately th study did not reach significance at the patient level[189]. In a cohort with definitive clinical evidence of synovitis, Filer et. al. showed that in patients with very early arthritis (less or equal to 3 months duration), the addition of US parameters, specifically power Doppler and grey scale synovial thickening of the MCPs, MTPs and wrists predicted the fulfilment of the 1987 American College of Rheumatology (ACR) if used in conjunction with the Leiden algorithm[39]. The studies above collectively show the utility of US data in the diagnosis and classification of patients presenting with either arthralgia or frank arthritis at an early stage.

Whilst the diagnosis and classification of a patients symptoms are important, this inherently should prompt a consideration of the long term outcome. A number of factors are classically used to help the clinician to formulate a predictive view such as erosions on radiographs, seropositive (RF / CCP), insidious onset of symptoms and high DAS score[21 190-192]. However, US seems to have a role to play in this context. In 2007, Naredo et. al. evaluated the predictive value of PDUS parameters in disease activity and radiologic outcome in patients with early RA[114]. The time-integrated values of PDUS parameters demonstrated a significant correlation with DAS28 and radiographic progression after 1 year. This would suggest a role for US assessment at an early stage which may influence therapeutic intervention. Whether US based decisions in an early arthritis cohort benefit outcome is still under investigation. It is likely that using US in addition to clinical predictors of outcome a more tailored approach to early arthritis patients can be implemented.

In established RA patients, the response to therapy and progressions of erosive disease is pertinent question. Taylor et. al. showed in a randomised controlled study with Infliximab, that baseline US synovial thickening and power Doppler predicted

erosive changes using the van der Heijde modified Sharp score for the placebo group. This relationship was abolished in the active treatment arm[131]. Also in a prospective study, Ellegaard has also shown that the baseline US characteristics of patients treated with anti-TNF therapy predict response and on going treatment at 1 year[193]. These findings would argue that US assessment of patients prior to anti-TNF therapy may provide clinicians with the ability to stratify patients and tailor therapy to those where the likelihood of success is greater. This may be a welcome tool in this current climate of economic strain.

The predictive value of US imaging therefore would argue for its incorporation by Rheumatologists to decision making processes both in terms of diagnosis, classification and therapeutic response.

1.5.4.1 Reliability of ultrasound imaging

Multiple reports indicate that ultrasound grading can be reliably conducted[117 194 195]. Reliability is an integral aspect of an assessment tools validity. While an assessment tool may fulfil a number of aspects of validity, it may not be reliable. However, a reliable and reproducible assessment tool does not signify that it is a valid test. The reliability of any assessment tool is inextricably linked to the scoring method used to assess it. In the case if US a number of scoring methods have been employed and reported in the literature. The simplest assessment is a binary outcome of absence or presence of detectable pathology with the resultant score represented as a joint count similar to the ender or swollen joint count seen in the DAS28 assessment[111 114 152]. Others have sought to categorise synovial thickening and doppler in a 4-point ordinal score while a few groups have suggested a 5-point score[118 196 197]. In addition, quantitative methods for assessment can also be used with dedicated imaging processing software[198-200]. Power Doppler however is most often reported using a Likert scale of 0-3, where 0 indicates no synovial blood flow, 1 mild synovial blood flow, 2 moderate synovial blood flow, and 3 extensive synovial blood flow[115]. Naredo reported the results of a training session of ultrasound where the agreement for

shoulder, wrist, ankle, foot and knee assessments were evaluated by 'experts'. The agreement varied somewhat between the anatomical region being scanned and the lesion being assessed. The Kappa however scores were comparable between region (hand and wrist - Kappa 0.61)[201]. Others have also reported similar robust levels of agreement[202-207]. Naredo again demonstrating not only high levels of agreement for US assessment but also that this was superior to clinical assessment[112]. The interobserver reliability for MCP joint US scoring had a reported kappa of 0.88, whereas the reliability of the individual clinical examination of MCP swelling had a reported kappa of only 0.36.

Table 1-5: Agreement between ultrasonographers for various pathologies at different joints.

Overall agreements by ultrasonographic diagnosis in each region and in all regions. NE, diagnosis not evaluated. Reproduced from Naredo et. al. Ann Rheum Dis 2006;65:14-9 [201].

Diagnosis	Shoulder	Wrist/ hand	Ankle/foot	Knee	All regions
Joint effusion/synovitis	88.5%	95%	89%	91.5%	91%
Bony cortex abnormalities	84.5%	88.5%	92%	84.5%	87%
Tenosynovitis/ paratenonitis	76%	88.5%	88.5%	NE	84%
Tendon lesions	88%	NE	92%	94%	91%
Bursitis/cyst	85.5%	NE	73.5%	92%	83.5%
Power Doppler signal	NE	92.5%	73.5%	NE	83%

The majority of the studies examining the reliability of US have been performed using a binary outcome or qualitative assessment of synovitis. However, others have shown that both qualitative, quantitative scoring techniques and resistance index calculations can also be shown to be reproducible[128 200 208-210].

The normal approach to acquiring US images involves a number of steps which may contribute to the overall agreement in scores. A list of 5 variables is given below:

1. Machine / probe - different machines have differing doppler sensitivities and contrast resolution.
2. Image optimisation and probe settings for depth, pulse frequency and gain.
3. Positioning of patient and joint.
4. Timing of scan (morning / afternoon).
5. Position of probe for image recording.

Many reported reliability data combines a number of aspects of US image acquisition and scoring. This combinatorial approach is likely to weaken the agreement between individual as the dedicated image acquired is not standardised. This 'free hand' scanning may increase sensitivity of the imaging technique to detect pathology but will have an impact on agreement. In this thesis I present data from a randomised controlled, multi-centered study examining both the issue of imaging acquisition and scoring from different ultrasonographers / readers and repetitive scanning and scoring from the same ultrasonographer.

1.5.5 Limited ultrasound data sets

Having shown over the past 15 years that US imaging has a valid part to play in the assessment and diagnosis of patients with inflammatory arthritis, a significant question still remains unanswered. In many of the studies described above various joints were imaged and scored but no systematic approach has dominated the literature. The number of joints imaged varies considerably, with a one author demonstrating a relationship between clinical parameters of disease activity and a single wrist joint while others have examined up to 78 joints. A list of publications and joints counts can be seen in the table below.

Table 1-6: List of published US data sets and joints counted

Authors of publications along with the joints data set imaged are shown below. The patient cohort (early RA vs Established RA) is noted and whether there is evidence of the data set being responsive to therapeutic intervention.

Author	Number of joints scanned	Early / Established RA	Response to Therapy
Naredo et al. 2008[396]	12 joints (Elbow, Wrist, 2 + 3 MCP, Ankle, knee)	Established RA	Anti-TNFa
Backhaus et al. 2009[405]	7 joints (2 + 3 MCP, 2+3 PIP, wrist, 2+5 MTP - dominant side)	Established RA	DMARD / Anti-TNFa
Filer et al. 2011[39]	38 joints (MCP, PIP, wrists, elbow, shoulder, 2-5 MTP)	Early RA	DMARD
Scire et al. 2009[124]	44 joints (MCP, PIP, wrist, elbow, shoulder, knee, ankle, MTP, sternoclavicular, acromioclavicular)	Established RA	DMARD
Hammer et. al. 2011[404]	78 joints (PIP, MCP, CMC, wrist, elbow, shoulder, hip, knee, ankle, Mid-foot x 4, TMT, MTP, PIP)	Established RA	none
Naredo et al. 2005[112]	28 joints (MCP, PIP, Wrist, elbow, shoulder, knee)	Established RA	none
Seymour et. al. 2011[128]	10 joints (MCP)	Established RA	Biologic NO inducible agent
Ellegaard et al. 2011[193]	1 joint (wrist)	Established RA	Anti-TNFa

The wrist and MCP joints have been incorporated most often in scoring systems and this reflects the typical joint involvement detected clinically. Unlike the DAS28, a number of US data sets have included the ankles and feet (including MTP joints). There does appear to be value in extending the examination to the lower limb however this does require more time. Using a distal upper limb data set has its attractions as it requires no undressing of patients and as such should be easily incorporated into routine clinical practise. Therefore, more work is required to clarify the optimal joint data set to be imaged. However, it is likely that the optimal US data

set may change depending upon the clinical scenario and purpose of the assessment. For example, the assessment of a patient with new onset of inflammatory symptoms is likely to merit a more comprehensive data set than a patient with established RA commencing anti-TNF therapy. A more focused data set may be used following the initial assessment to include a core joint count + a sentile joint. Conversely, If the data set is designed to detect change following therapy in a clinical trial setting, a smaller data set may be sufficient. In this scenario a baseline of US defined disease activity may be required to facilitate a sufficient change and avoid a flooring effect. This is already done in clinical studies with a pre-specified number of swollen and tender joints along with adequate levels of CRP / ESR required before patients can be enrolled. Currently this is designed to provide a minimum DAS28 score ensuring a controlled population of patients entering the study. A similar criteria may need to be applied to an US driven therapeutic study.

1.6 Synovial biopsy

Synovial biopsy is a safe and generally well-tolerated procedure. Synovial tissue is most often acquired from knee joints in affected patients but with the development of minimally invasive procedures, a greater number of joints may be exploited for the harvesting of synovial tissue. Synovial tissue examination is not considered a routine investigation for most patients attending the Rheumatology clinic. Occasionally this investigation is required when a joint infection is considered and synovial fluid and blood cultures have been unable to identify an infectious organism. In a study in patients with suspected infected knee replacement synovial fluid analysis had a sensitivity of sensitivity of 72.5%, a positive predictive value of 85.3% and a negative predictive value of 90.1%. Synovial tissue analysis showed a sensitivity of 100%, a positive predictive value of 95.2% and a negative predictive value of 100%[211].

Examination of synovial biopsies may also help to make a diagnosis in some relatively rare infiltrative and deposition diseases afflicting the joints such as

amyloidosis[212], ochronosis[213], haemochromatosis[214], and proliferative disorders such as pigmented villonodular synovitis (PVNS)[215].

1.6.1 Blind needle biopsy

This procedure can be performed under local anaesthetic and essentially involves the insertion of a trochar into the joint cavity through a small incision in the skin. The usual apparatus used is the Parker-Pearson needle[216] although other modified needles have been used and reported to achieve reasonable synovial samples. The procedure appears to be relatively safe and tolerable however, the lack of visualisation of the tissue being sampled may be a problem. It may be less favourable in the setting of a clinical trial setting given a failure rate of 15% in terms of suitable harvested synovial tissue[217].

If the supra-patella approach is to be used, it is usual for the pouch to be expanded with 30-50 mils of normal saline before passage of the trochar. Once in place, the biopsy forceps are then introduced through the trochar and the biopsies are performed with multiple samples being taken by changing the angulation of the apparatus. Other joints can be biopsied using this technique but small joint of the hand are exceedingly difficult due to the blinded nature of such a procedure.

1.6.2 Arthroscopic biopsy

Synovial tissue obtained by an arthroscopic procedure has been used extensively in the context of synovial tissue harvesting within clinical trials on new therapeutic agents. A survey by Kane et. al. showed that this technique was being performed by a significant number of Rheumatologists within Europe[218]. Both large and small joints are accessible to this technique which may be performed under local anesthetic. Typically, the biopsy forceps require to be inserted via a second portal; however some equipment allows this through the same introducer as the small bore camera. An infra-patellar portal for the camera insertion is usual with a second supra-patellar portal for the biopsy procedure. This makes it possible to obtain synovial biopsy samples under direct visualisation. This has the advantage of being able to guide the

biopsy forceps to a number of anatomical sites with great accuracy e.g. the cartilage–pannus junction or patellar gutters. Arthroscopy would appear to be reasonably well tolerated with the commonest complain being of mild post procedural pain in the joint in approximately 35% of patients[219]. More serious complications such as haemarthrosis, deep vein thrombosis and joint infection have been quoted as 0.9%, 0.2% and 0.1% respectively[218]. In a study examining diagnostic arthroscopies of the knee alone, an overall complication rate of 1.2% was quoted[220]. Whilst this procedure returns good quality synovial tissue and has been validated as useful tool in harvesting synovial tissue[221], it required a moderate financial outlay for equipment and the need for dedicated surgical suites.

1.6.3 Ultrasound guided synovial biopsy

Once again this procedure can be performed under local anesthetic. A similar approach is taken to that of a blind needle biopsy but with the added advantage of being able to view both the needle insertion into the joint and the biopsy forceps when introduced. Koski et. al. described an ultrasound technique in 2005 using a portal and forceps approach to performing synovial biopsies[222]. This technique was used to biopsy 37 patients with mono- or polyarthritis, with suffcient amounts of synovial tissue harvested in 33/37 cases. One case of skin infection was reported in this small cohort. Van Vugt also demonstrated that, using a Tru-Core needle, an ultrasound guided approach to wrist synvoial biopsies could be achieved with suitable tissue being sampled in 7 patients. However only 2 passes were made with this particular needle technique during the procedure and no specific histological validation was performed on the biopsied tissue[223].

An ultrasound guided technique still requires an aseptic approach and to be performed with the appropriate clothing (sterile gown, mask, gloves and head cover). The ability to guide needles and biopsy forceps improves the safety of this procedure as does the use of a single portal of entry. The added benefit of this procedure is that not only can the biopsy samples be harvested from different compartments of the

joint but using PDS, biopsies can be taken from areas of high vascular signal. The single portal of entry and ability to monitor all aspects of the procedure under US guidance makes this technique particularly suited to sampling tissue from small joints. A recent publication by Scirè et al. showed that US-guided synovial biopsy in small joints represents a reliable approach for good quality tissue collection and that the tissue harvested was representative of the joint cellular infiltration in these joints[224].

1.6.4 Are synovial biopsy samples representative of the whole joint?

The definition of a 'Representative Sample' is: a subset of a statistical population that accurately reflects the members of the entire population. A representative sample should be an unbiased indication of what the population is like. There are a number of different ways of sampling, however the most common is a simple random sampling method. Sampling ‘without replacement’ is common within biological systems as opposed to sampling ‘with replacement’. The theoretical disadvantage of sampling without replacement is that the probability of sampling an individual or object on each subsequent pick becomes reduced. In large populations this change in the population number is relatively small, and as such can be ignored. This is a reasonable approach when researchers know very little about the characteristics of the population being sampled. An alternative sampling method can be used where specific subgroups within the population are well established with random sampling taking place within each group or strata.

Taking this into consideration, an important question to be addressed is the number of samples required at biopsy to be representative of the synovium as a whole. This is a particular important question in the context of clinical trials in early stage drug development where changes in the sub-lining CD68+ macrophage number are thought to be a good indicator of therapeutic response. With respect to synovium sampling within a diarthrial joint, the knee joint has been most extensively investigated. Pannus formation can be detected at the cartilage pannus junction (CP-J), commonly the site of erosions, and as such may represent a discrete population of inflammatory cells with its own characteristic synovial pathobiology. A number of studies have examined tissue from the

CP-J and the rest of the synovium. Whilst an exhaustive comparison of cellular infiltrates has not been made, there is some suggestion that subtle differences may exist. Yousef et. al. examined the distribution of CD3+ and CD68+ mononuclear cells within the suprapatelar pouch (SPP) and at the CP-J[225]. While there was no significant difference detected in CD3+ and lining CD68+ cells a difference was seen between the SPP and CP-J with CD68+ sub-lining cells. However, only 5 out of the 14 patients recruited to this study had tissue harvested form the CP-J providing a relatively small sample size for comparison. Contradictory findings were reported by Smeets also compared the SPP and CP-J in 17 patients[226]. Using a more comprehensive immunohistochemistry staining panel, including T cells, B cells and macrophages along with metalloproteinases, no significant difference was detected between these two sites. In support of this Kane et. al., showed that in addition to there being little difference in MMP and TIMP synovial expression between PsA and RA patients, no significant difference was found within patients at the SPP and CP-J[227]. In line with this, Rooney et. al. recruited 29 clinically active RA patients to a study examining the variability of a number of synovial parameters (synoviocyte hyperplasia, fibrosis, vessel proliferation, perivascular infiltrates, focal aggregates, and diffuse infiltrates of lymphocytes) between biopsy samples. All parameters, scored on a 1-10 semi-quantitative scale, performed well with similar overall involvement. A good level of agreement was also seen within synovial tissue samples suggesting that there is a degree of homogeneity within and between synovial biopsy samples form the knee joint. Work by Dolhain has suggested that minimum of 6 samples of synovial tissue are required to be a representative sample size. Dolhain used synovial tissue form 3 patients undergoing knee joint replacement surgery and sampled 4 sties in 1 patient with 6 samples in two others. An important observation in this report is that the variance between immunohistochemistry markers reducing significantly when slides from different samples were used for scoring rather than samples form the same tissue specimen. They suggest 6 tissue samples as a minimum number required to reduce the variance between markers within the synovium. However the sampling procedure here is was not arthroscopic and may not be whole applicable to the *in vivo* scenario of arthroscopic or ultrasound guided procedures. An attempt to address this issue and validate ultrasound guided synovial biopsies in small joints was undertaken by Scire et.

al. following a US guided biopsy, patients received a arthroplastic procedure on the same joint with the total sample being processed for a number of cellular infiltrates including CD68, CD3 and CD20 by immunohistochemistry. A comparison was made between the US guided synovial tissue samples and with the total tissue analysed from the arthroplastic procedure. The number of high powered fields required to reduce the US guided tissue sample mean to within 10% of the overall arthroplastic sample mean was set as the efficiency threshold for the analysis. This analysis would suggest an area of 1.2mm^2 for CD68 macrophages and 2.5mm^2 for CD3 lymphocytes and CD20 B cells is required to provide a representative assessment of the overall synovial lining[224]. This equated to a minimum of 7 samples being retrieved at a single sitting. These findings however are relevant to the sampling procedure employed and not necessarily relevant to alternative techniques as tissue sampled may vary considerably depending upon the gauge of instrument and sampling method used.

1.7 The Rheumatoid joint

1.7.1 Normal synovium

Synovium can be found lining diarthrodial joints and tendons. It also seen within bursae at various locations at points of bone and ligament or tendon interaction. The normal synovium has a lining (intima) and sub-lining (subintima) layer. The lining layer consists of CD68+ macrophages (type A synoviocytes) and CD55+ fibroblasts (type B synoviocytes)[228 229]. In the non-inflamed joint there is normally a predominance of Type B fibroblast-like synoviocytes in the intima with this ratio changing dramatically during inflammation to favor a predominance of Type A synoviocytes[230 231].

Figure 1-10: Microscopic view of normal and RA synovium

Normal and RA synovium. **A:** Normal synovium stained for CD55+ fibroblasts (red). Synovial fibroblasts make up most of the cells in the lining layer in the normal synovium intimal layer **B:** RA synovial tissue stained for CD55+ fibroblasts (red). *RA synovial tissue* contains fewer fibroblast than macrophage lineage cells. **C:** Normal synovium stained for CD68+ macrophages **D:** *RA synovial tissue* stained for CD68+ macrophages (red). The majority of the lining layer cells in RA synovial tissue are of macrophage origin. Reproduced from Smith et. al. The normal synovium Open Rheumatol J 2011;5:100-6.

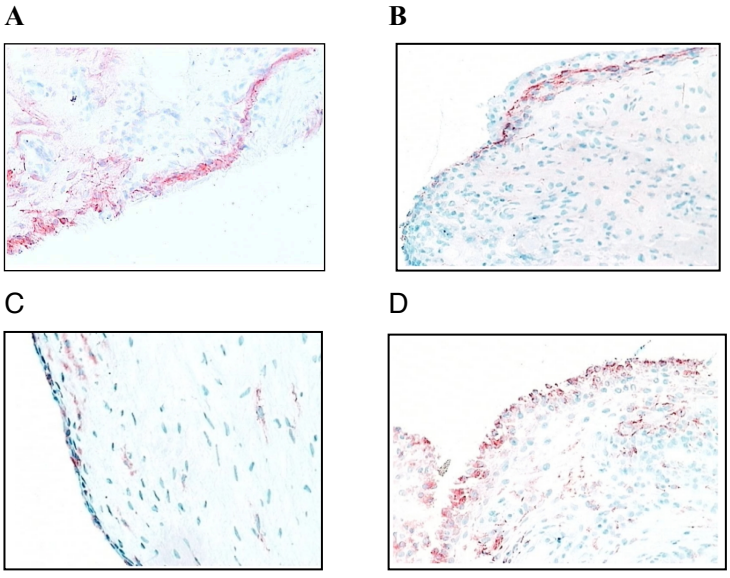

The intimal matrix contains a number of types of collagen (I, III - VI) but importantly no basement membrane. The lack of entactin, essential for binding basement membrane components, would appear to be missing in the intima explaining to some extent this aberration. This presumably facilitates the movement of cells through the intimal layer, although the up regulation of VCAM-1 on intimal type B synoviocytes may inhibit mononuclear cell transit such as macrophage and lymphocytes expressing the complementary ligand (α4 β1 integrin)[232]. Hyaluronan is also found in the matrix but the concentration drops of as deeper layers of the subintima are reached[233]. The non-αdherent intima surface certainly owes its this mechanical property, in part, to the production of hyaluronan by fibroblast-like synoviocytes. Singh et. al. demonstrated by immunohistochemistry that CD4+ and CD8+ lymphocytes can also be seen in normal synovial tissue[234]. However in 9 normal controls, no B cells were identified in the lining or sublining. Another report by Smith et. al. However demonstrated similar findings but also showed a small number of B cells (CD22+) to occasionally to be present within the synovium but no plasma cells (CD38)[235]. The patients identified in this study were form sports clinics with unexplained knee pain undergoing a subsequent arthroscopic investigation and therefore not arguably 'normal' knee joints. Smith also confirmed high levels of IL-1 receptor antagonist in addition to low levels of RANK ligand and OPG expression important in promoting osteoclastic activity.

Normal synovium is vascular and has a rudimentary lymphatic drainage system located in the deeper sub-lining layer. Cell trafficking and the provision of oxygen and nutrients is certainly provided by this network of capillaries. Deeper in the sub-lining these vessels begin to form arterioles and venules in a plexus before ultimately merging with local joint feeding vessels[233 236]. IL-1, TNF-α and IL-6 can all be detected in normal synovial tissue albeit in vastly reduced concentrations as that seen in the actively inflamed joint[234]. There is a significant elevation in levels of IL-1 receptor antagonist levels seen in the normal joint which may mediate an anti-inflammatory cytokine profile inhibiting up regulation of adhesion molecules, cellular activation and recruitment of leukocytes into the joint[237].

Figure 1-11: Microscopic appearances of synovial vascular and lymphatic vessels. Vascular and lymphatic network in normal synoviumA: Normal synovium stained with factor VIII (red) to demonstrate the vascular network. B: Normal synovium stained with LYV-1 antibody (red) to demonstrate the lymphatic network.

A B

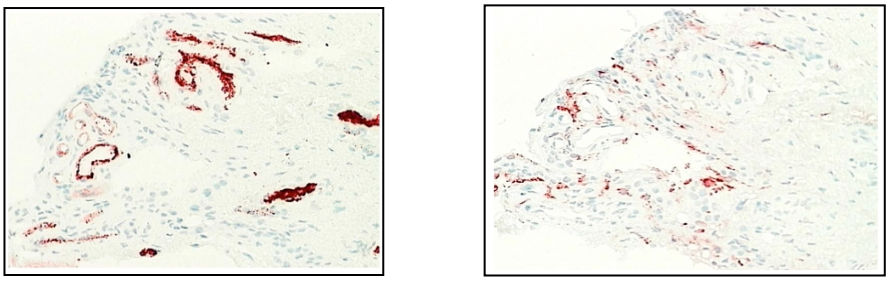

1.7.2 RA synovium

Within RA patients, synovial tissue analysis confirms the hypertrophy of the synovial lining layer with a reverse in the ratio of type A and type B synoviocytes. In addition there is significant influx of many other mediators of inflammation such as T cells, B cells, plasma cells and macrophages. Neutrophils and mast cells are also found in the sub-lining layer. The archetypical synovial pannus consists of synovial lining, synovial stroma with inflammatory cells and fibroblasts and is directly responsible for the erosions seen in the rheumatoid joint. The organization of these cells into lymphoid aggregates in some patients has been well described and will be discussed later. A number of authors have compared histological changes in both early and late RA. The number of cellular types seen within the synovium are broadly similar and independent of the disease duration although few studies have suggested at a tendency for chronic synovial changes to be represented by a greater macrophage number and more synovial organisation of T / B cells into lymphoid like structures. In addition, little difference is seen in cytokine and adhesion molecule expression depending upon disease duration. In a cross-sectional study Kraan et. al. demonstrated in 95 patients with inflammatory arthritis and OA, CD68 macrophages in the sub-lining and CD22+ B cells were helpful in differentiation of RA and non-RA samples although these findings were not exclusive of PsA and OA synovium. A high number of B cells and plasma cells have also reportedly been seen in early RA compared to other non-RA inflammatory arthropathies.

Increased vascularity is also a feature of the RA synovium although this is also seen in other arthropathies. A few studies have suggested that the development of new vessels in the RA synovium tends to result in relatively straight vessel formation rather than a more tortuous morphology seen in PsA and other SpA's. In addition others have reported higher levels of VEGF expression in non-RA synovium than in RA. The up regulation of adhesion molecules are also seen in ealry and late disease with ICAM-1 and VCAM-1 expression being of particular importance. VCAM-1 is up regulated on both endothelial cells and lining layer cells with ICAM -1 expressed through out the synovium. αvβ3 and αvβ5 integrins are also up regulated in both early and late disease with similar distribution and profile suggesting any differences form early to late disease cannot be fully explained on differential integrin expression alone.

Histological evidence of synovitis can be see in asymptomatic joints in patients with RA with samples showing macrophage infiltration and synovial lining layer hypertrophy. Similarly, imaging studies in patients with oligoarticular showed approximately 13 percent of joints could be reclassified as having ultrasound determined synovitis re-enforcing the concept of subclinical synovitis. However in the synovial histology studies no long term data is available to confirm the development of clinical synovitis in biopsied, asymptomatic joints and whether this consequently leads to joint damage.

1.7.3 Synovial ectopic lymphoneogenesis and lymphoid structures (ELS)

As previously described, there is a large influx of immune cells into the rheumatoid synovium during the acute inflammatory process. These immune-cells can be found either randomly distributed within the synovial sublining or spatially grouped into follicular structures[238]. These structures may acquired features of secondary-lymphoid-organs-(SLO) to include high-endothelial venules (HEV), T/B-cell segregation, follicular-dendritic-cells networks and are defined as ectopic/tertiary lymphoid-like structures (ELS/TLS)[239-242]. Notably, these structures are also seen in other autoimmune diseases besides RA such as Sjogren's syndrome (SS) and Hashimoto"s thyroiditis. The true distinction and functional consequences of the presence or absence of ELS/TLS within the synovium is still debated[240-244]. Here we

would like to emphasize that these two patterns, defined as “follicular” and “diffuse”, are not necessarily mutually exclusive and individual tissues may feature variable levels of diversity or overlap[243]. Nevertheless, while in some tissues large, densely distributed ELS predominate, in others ELS are undetectable despite a prominent diffuse tissue inflammation. Studies in large cohorts of RA patients, demonstrate a variable incidence of ectopic/tertiary lymphoid-like structures within the synovium in approximately 30% - 73% of the specimens after arthroscopic biopsy from knee joints deemed clinically inflamed[245-249]. Some difference is seen depending upon the sampling method although e.g. arthroscopic vs arthroplastic samples (36%, n = 29, 68%, n = 22 respectively) although given that arthroplastic sampling tends to occur in patients with long standing disease with concomitant OA and may be a confounder for these findings[249]. Treatment with anti-TNF therapy has also been shown to disrupt such aggregations and this change to be associated with good clinical response[250].

CXCL13 and CCL21 appear to be important chemokines in regulating the inter-cellular interaction within these structures[251 252]. Examination of their mRNA and protein expression demonstrates a clear relationship between CXCL13 and CCL21 expression and the development of ELS with T-β compartmentalisation, CD21(+) follicular dendritic cell differentiation and germinal center formation[239]. A mouse model of SS (C57BL/6 mice) development of ELS was shown to be preceded by expression of lymphoid chemokines CXCL13 and lymphotoxin-β[253]. Similar findings were demonstrated in the NOD mouse model with up-regulation of lymphotoxins β and CXCL13 and CCL19 chemokines with subsequent infiltration of follicular B cells expressing CXCR5[254]. In addition to chemokine expression, our group have demonstrated that these ectopic lymphoid structures do have the ability to function independently as true ectopic lymphoid structures[255]. Activation-induced cytidine deaminase (AID), the enzyme required for class switch recombination and somatic hypermutation, expressed within follicular dendritic cell (FDC) networks, was shown to be present in salivary tissue with ELS but not expressed in its absence.

Figure 1-12: Examples of follicular, diffuse and pauci-immune synovitis

Image of ectopic/tertiary lymphoid-like structures within the Rheumatoid synovium. Microphotographs of prototypical examples of Follicular, Diffuse and Pauci-immune synovitis. Three µm sections of paraffin embedded RA synovial tissues were stained with Haematoxylin and Eosin (H&E) and by Immunohistochemisty (IHC) for B cells (CD20), T cells (CD3), Macrophages (CD68) and Plasma cells (CD138). IHC performed by Dr. B. Hands (Experimental Medicine and Rheumatology, William Harvery Research Institute).

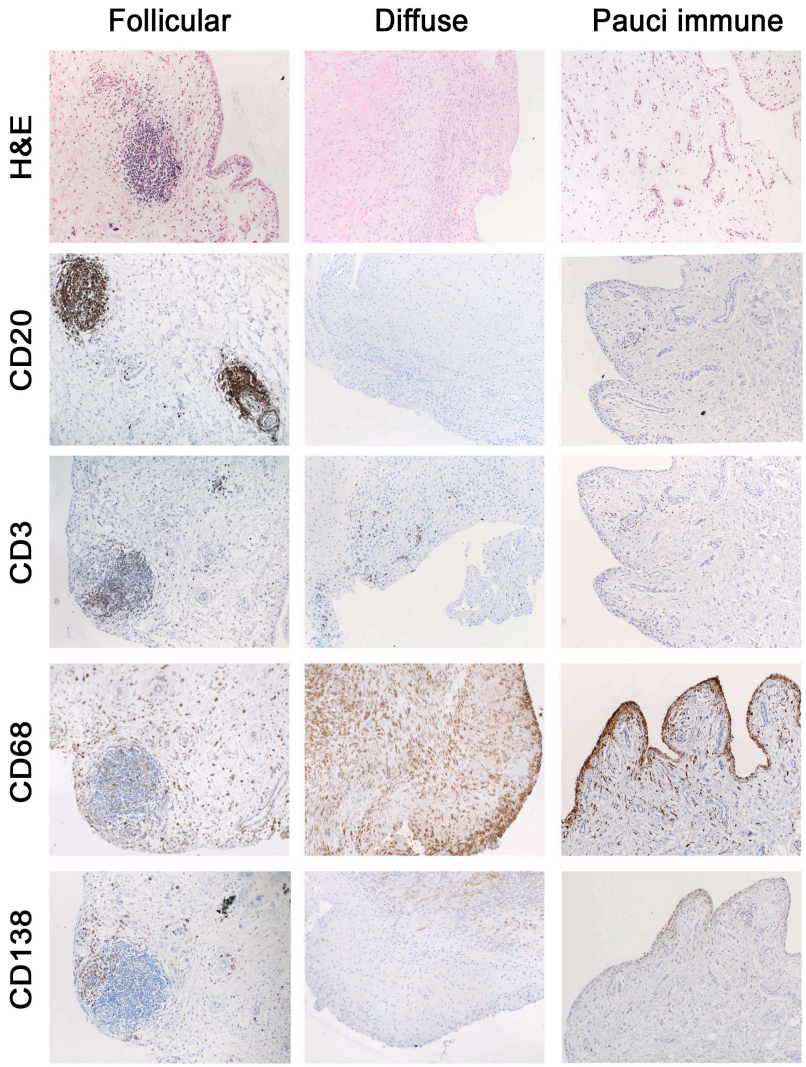

Furthermore, in synovial tissue from 55 patients with RA, we demonstrated that FDC + GC like structures invariably expressed AID with a distribution resembling secondary lymphoid organs[255]. Specifically, AID+/CD21+ follicular structures were

surrounded by ACPA+/CD138+ plasma cell. Transplanted SCID mice with RA synovium demonstrated persistent expression of AID with synovial mRNA levels of AID within the mouse closely associated with circulating human IgG ACPA in sera. This would suggest that these structures are functional and have the molecular machinery to support local autoantibody production and B cell expansion.

Additionally, Prof. Pitzalis group has described a third pattern other than aggregational / diffuse, termed “pauci-immune” synovitis that shows hardly any infiltrating immune-cells (Figure 1-12) and is also found in active disease and early-untreated arthritis therefore not simply the result of “burned out” synovitis[256].

Immunophenotypic characterization of these three histomorphological patterns demonstrates B-cells principally in “follicular” synovitis (30-40% of patients) but absent/low in the “pauci-immune” and “diffuse” pathotypes (60-70% combined), the latter predominated by CD68+ve monocytes[256].

Importantly these histomorphological patterns appear to segregate with specific transcriptomic signatures. In a cross-sectional cohort of arthroplasty samples from 49 RA patients, Genentech scientists observed transcriptomic clustering into: Lymphoid-(L), Myeloid-(M) and two Fibroblast-(F,F/A) prevalent patterns together with a mixed-(X) pattern containing biological aspects of the other 4 as defined using gene set modules (Fig.1-12). The F,F/A patterns are consistent with previous publications reporting diverse transcriptomic profiles associated with specific fibroblast-like synoviocytes (FLS) subsets[257]. Notably, FLS isolated from highly inflamed synovium displayed a transforming-growth-factor-β/activin-α inducible signature characteristic of myofibroblasts, whilst FLS from tissues with low inflammation displayed principally an insulin-like-growth-factor regulated genes signature[257]. The transition from healthy FLS to smooth-muscle actin-positive myofibroblasts is associated with the expression of matrix degrading proteases[258] that might explain the diverse FLS invasive/destructive phenotype described among RA patients [258-260].

Figure 1-13: Transcriptomic clustering of RA synovial subtypes

Transcriptomic clustering of RA synovial subtypes Cross-sectional cohort of arthroplasty samples from 49 RA patients observed transcriptomic clustering into several subtypes: Lymphoid (L), Myeloid (M) and two Fibroblast (F, F/A) prevalent patterns together with a mixed (X) pattern containing biological aspects of the other 4 as defined using gene set module (Michael Townsend, Sarah Kummerfeld, David Fox & Flavius Martin)

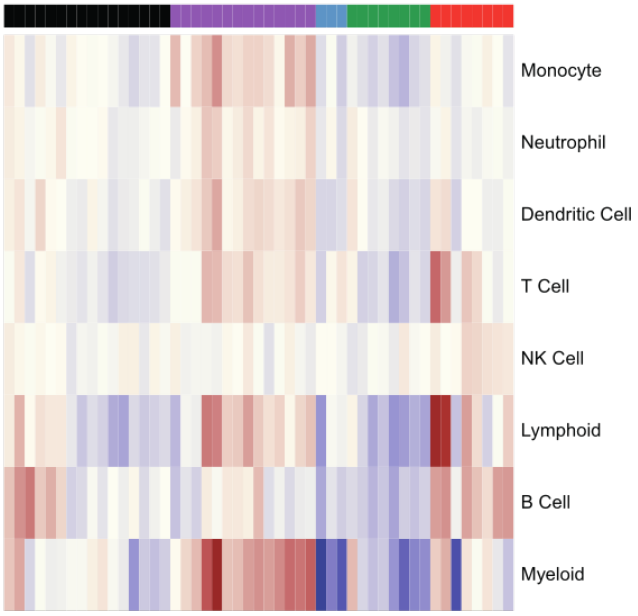

1.7.4 Scoring synovial cellular infiltration

The cellular infiltration with in the synovium can be scored both quantitatively and semi-quantitatively. A number of semi-quantitative inflammatory scores exist. The Rooney and the Tak scoring system have been most widely studied[261] [262]. Using a semi-quantitative score it has been possible to show a correlation between the presence of synovitis and degree of histological inflammation in both early and established RA whilst other cross-sectional studies have also shown a correlation with erosive damage[263]. Krenn has also described a synovitis score based on a 9 point synovitis score for lining layer hypertrophy, synovial stroma cell density and the degree of organisation of the infiltrate[145]. These scoring systems will be discussed further in the next section.

Quantitative analysis can be performed using Digital Image Analysis (DIA) and Prof. Pitzalis group have developed a novel quantitative aggregational scoring system (QAS) that quantifies both the degree of aggregation within the SM and degree of diffuse infiltrate in the remainder of the tissue100. The aggregational score (AS) relates to the area fraction of ST occupied by mononuclear cells in aggregate form and the diffuse score (DS) relates to the area fraction occupied by mononuclear cells in the remaining tissue.

Table 1-7: Krenn histological synovitis score

Krenn scoring system adapted from Krenn et al. Synovitis score: discrimination between chronic low-grade and high-grade synovitis. Histopathology 2006;49(4): 358-64.

Enlargement of the synovial lining cell layer	
0 points	The lining cells form one layer
1 point	The lining cells form 2–3 layers
2 points	The lining cells form 4–5 layers, few multinucleated cells might occur
3 points	The lining cells form more than 5 layers, the lining might be ulcerated and multinucleated cells might occur
Density of the resident cells	
0 points	The synovial stroma shows normal cellularity
1 point	The cellularity is slightly increased
2 points	The cellularity is moderately increased, multinucleated cells might occur
3 points	The cellularity is greatly increased, multinucleated giant cells, pannus formation and rheumatoid granulomas might occur
Inflammatory infiltrate	
0 points	No inflammatory infiltrate
1 point	Few mostly perivascular situated lymphocytes or plasma cells
2 point	Numerous lymphocytes or plasma cells, sometimes forming follicle-like aggregates
3 points	Dense band-like inflammatory infiltrate or numerous large follicle-like aggregates
Sum 0 or 1	**No synovitis**
Sum 2–4	**Low-grade synovitis**
Sum 5–9	**High-grade synovitis**

1.7.5 Prognostic potential of the synovial membrane

Cross-sectional data from histomorphology studies have suggested an association of histomorphology with particular disease phenotypes. Klimiuk et al. have reported that, in established disease, the more organized forms of synovitis with T-β cell aggregates and/or germinal centres (GC) are associated with a more severe disease

phenotype clinically and radiologically77. The authors have suggested that all joints in an individual patient share the same pattern and these remain stable during the course of the disease. However there is little prospective data to confirm this. In fact using the Rooney score to prospectively evaluate histomorphology as a potential prognostic marker, no statistical correlation with erosive disease over a 2 year period was found. It remains to be seen if the QAS performs better in a prospective study in early or established Rheumatoid arthritis.

As already described macrophages have been more widely studied with studies indicating that the intensity of CD68+ macrophage synovial infiltration at baseline is associated with progressive joint damage. Recently a study of patients with early arthritis demonstrated a good correlation between the proportion of macrophages at baseline and the appearance of new joint erosions101. In early arthritis matrix metalloproteinase-1 gene expression was correlated with the development of erosions in a study involving patients with RA. The macrophage number also correlated with MMP-1 expression and erosive damage after 1 year of follow up. However, despite this promising observation a larger study has failed to confirm the usefulness of these findings in a cohort of early arthritis.

1.7.6 Synovial biomarkers response to therapy

A number of candidate biomarkers exist within the synovium which may be responsive to therapeutic intervention. Some authors have attempted to produce a collective score for a number of histological variables such as Krenn[145 146] and Pettit[264]. Pettit produced a 1 - 10 score for a number of histomorphological features of the synovium and examined the ACR response in 18 patients undergoing knee arthroscopic procedures following treatment with DMARDS. He did not demonstrate a signifiant correlation with the change in any synovial biomarkers e.g. CD68SL or lymphocytic infiltrate and change in ACR score, however, there was a significant correlation with clinical response and his synovitis score. Despite this, over the past decade work by a number of authors have settled on CD68 sub-lining macrophages

as the most responsive and reproducible biomarker in RA patients undergoing treatment.

Tak et. al. demonstrated in two distinct cohorts of RA patients (early < 1 year vs late >5 years disease duration) that there was little difference in the immunohistochemical analysis of the synovium but they did show a correlation betweeen synovial macrophage number and IL-6 with knee pain[262]. Subsequently, the same group examined the peformance of this biomarker against DAS28 in the context of a randomized controlled clinical trial using Prednisolone therapy over a 2 week period. 21 patients with active RA were randomised to either oral prednisolone (n = 10) or placebo (n = 11) for 2 weeks[265]. The effect of prednisolone was large in comparison to DAS28 response suggesting that synovial macrophage numbers could be used as a biomarker for clinical efficacy. Bresnihan et. al. also demonstrated that this biomarker and histological processing across a number of centers was reliable[221]. This is an important step forward in facilitating its use as potential outcome measure in clinical trials. Further work by Tak, in a pooled cohort of 88 patients undergoing a number of therapeutic interventions showed a good correlation with the change in CD68SL macrophages and the patients EULAR clinical response (Pearson correlation 0.874, $p<0.01$) [266] (fig 1-14). There were no correlations between the change in intimal macrophages and the change in DAS28. Linear regression analysis, showed that the mean change in sublining macrophages could significantly explain 76% of the variance in the mean change in the pooled DAS28 scores ($p<0.02$)[266] (figure 1n).

Figure 1-14: Relationship of sublining CD68+ macrophages and mean change in DAS

A: Mean change in CD68+ macrophages within the lining layer of synovial tissue following therapeutic intervention with various medication including biological agents and DMARDS. **B:** A: Mean change in CD68+ macrophages within the sublining layer of synovial tissue following therapeutic intervention with various medication including biological agents and DMARDS. There is a significant difference in patients with good, moderate and no response to therapy. **C:** Plot of regressional analysis of mean change in DAS28 and mean change in sublining CD68+ macrophages. Note: legend should read T1 CCR1 antagonist

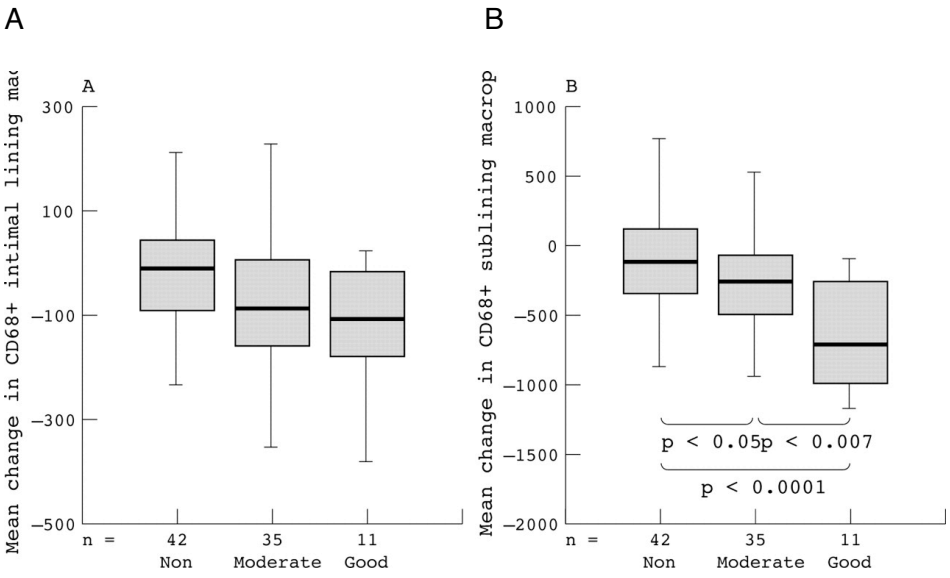

C

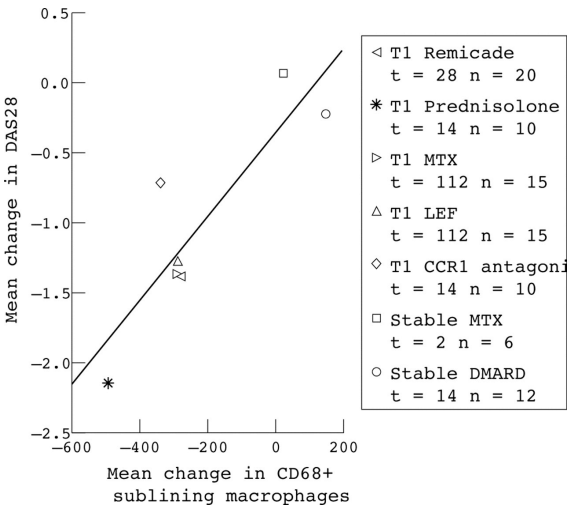

In addition, Baeten et. al. showed in twelve patients with active RA receiving placebo, as part of a placebo controlled trial, over a 14 week duration showed no change in synovial T cell , B cell, plasma cell, dendritic cell or sub-lining macrophages[248]. There was however a trend of decrease in the components of the DAS28 score including ESR suggesting that histological assessment of the synovium may provide greater clarity of response in such placebo controlled studies with the impact of fewer patient recruited with an early read out of response.

Klaasen et. al. examined the presence of synovial germinal centers as baseline predictors to infliximab therapy and showed only a modest relationship using linear regression analysis in a model containing clinical, histological and biochemical parameters ($r2 = 0.1$)[267]. In a similar cohort the same group used large-scale gene expression profiling on synovial tissue samples and identified high levels of synovial inflammation and associated gene up regulation and a significant associated factor in Infliximab response[268]. Although, in a study by Buch et. al. no correlation was seen between baseline synovial tissue TNFα levels and anti-TNFa reposne[269]. The synovial response to anti-TNFa therapy has also been investigated in a cohort of 10 patients undergoing treatment with Adalimumab + MTX vs MTX alone. MMP-3 and CD68 macrophage numbers showed a significant decrease in those treated with the Adalimumab[270].

In patients treated with Rituximab, peripheral blood B cells are shown to be depleted rapidly and almost undetectable at 4 weeks post infusion[271-273]. Within the synovium, Thurlings et. al. demonstrated a significant decrease in CD68L and SL macrophages numbers, CD3+ lymphocytes, B cells (CD20) and plasma cells (CD138). Whilst none of the baseline histological features predicted clinical response there was a trend to B cell numbers being significant[274]. The change in CD68SL macrophages and plasma cells at 4 weeks post treatment predicted clinical response at 24 weeks. A disruption of lymphoid aggregates was also seen at 16 weeks post Rituximab treatment. It is interesting to note that in a study investigating the synovial and MRI response in 16 patients treated with Abatacept, while there was a reduction in pro-

inflammatory gene expression (particularly IFNγ), no change was seen in the synovial cellular infiltrate at 4 months following treatment[275].

The lack of a unifying biomarker of synovial histological response to therapy is clearly demonstrated by the number of studies showing the utility of various cellular and biochemical markers depending upon the drug in use. Further prospective studies are required in larger cohorts to better understand the kinetics of synovial response to differing biological therapies and provide the optimal marker ofresponse. Depending upon the mode of action, particularly in the era of targeted biologic therapy, different biomarkers may be required at varying stages of treatment and disease evolution.

1.8 Angiogenesis

Angiogenesis is a fundamental process, critical for the sustained development of foetal life but also contributing to wound healing and granulation tissue in the adult. Strictly speaking, angiogenesis is the formation of new blood vessels from a pre-existing vascular network. Vasculogenesis, however refers to the *de novo* formation of endothelial cells form mesodermal cell precursors[276].

1.8.1 Vasculogenesis

Within the foetus, the development of a vascular plexus requires the differentiation of mesodermal angioblasts to form primitive blood vessels. Angioblasts are thought to develop under the influence of VEGFR-2 from a bi-potential stem cell (Haemangioblast). The role of VEGFR-2 is suggested by the consequent lack of vasculogenesis and haematopoiesis seen in both mice and humans with a defect in this receptor[277]. The angioblast cell line facilitates the development of a vascular capillary plexus under the influence of a number of angiogenic factors and receptor including VEGF, TGF-β, VEGFR-1, Tie-1, Tie-2, TGF-β receptor[278].

VEGF-R1 absence does not inhibit angioblast formation but the mature arrangement and development of a capillary plexus is disrupted[279]. In addition, a threshold of VEGF expression appears to be of equal importance with mice with only 1 gene copy do not survive gestation with resultant aberrant vessel formation[280]. It would seem that the interplay of VEGF expression and VEGF - R1 and R2 is a critical part of normal vascular development *de novo*.

Once the primary capillary plexus has formed further differentiation and modification is required to facilitate a mature vascular network. This can be achieved in 2 distinct processes:

1. Sprouting angiogenesis: this process occurs most commonly in organogenesis with degradation of the local extracellular matrix, proliferation of endothelial cells along a chemotaxtic induced path, lumen formation and subsequent maturation.[281]

2. Intussusception (non-sprouting angiogenesis): this process involves the splitting of a pre-existing vascular bed by transcapillary pillars of the extracellular matrix[281].

The process of angiogenesis differs form organ to organ, with the lung predominantly developing a vascular network by non-sprouting angiogenesis and the brain using sprouting angiogenesis due to the lack of angioblasts within its substance[282 283]. Both processes may occur together during organogenesis. Tie-2 (endothelial receptor tyrosine kinase) is necessary for sprouting. Tie-2 knockout mice do not sprout vessels within the brain leading to embryological death at day 10[284]. Angiopoeitins act as Tie-1 and 2 receptor agonists and this interaction may underpin the effects of VEGF in determining sprouting or non-sprouting angiogenesis[285].

Figure 1-15: Scanning electron micrographs of sprouting and transcapillary pillars

Scanning electron micrographs of methyl methacrylate corrosion casts of the vasculature in mammary gland tumors of c-neuT transgenic mice. (a, b) The sprouting phenotype, capillary sprouts are indicated by arrows. (c, d) The intussusceptive phenotype, transcapillary pillars are indicated by arrowheads. Scale bars: a=150 μm, b=100 μm; c, d=25 μm. Reproduced from Burri PH, I Molecular aspects of medicine 2002;23(6S):S1-27[281].

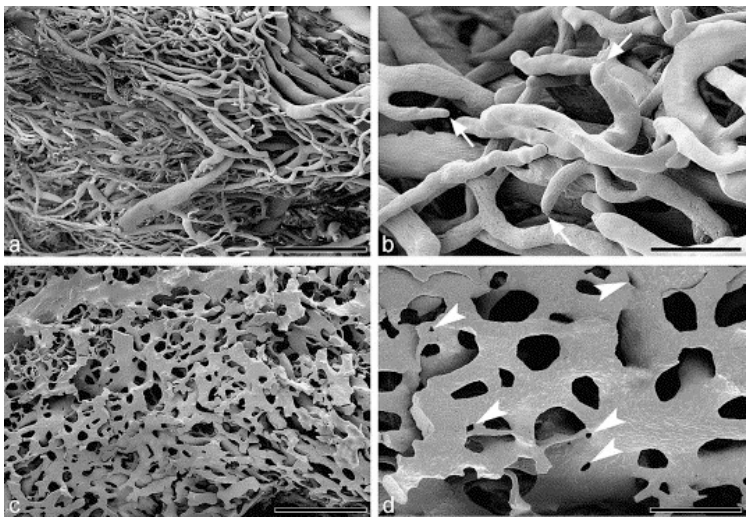

As the vascular plexus matures it undergoes pruning and remodeling. This was first described in the embryonic retina with the process being encouraged with hyperoxia states. Hyperoxia can reduces the expression of VEGF. The withdrawal of this important survival factor results in vessel regression however injection of VEGF inhibits this process[286]. Following the formation of a suitable vascular supply, vessel integrity and stability becomes less dependent upon VEGF[287]. It appears that cell adhesion molecules play an important role in vessel stabalisation and continuing maturation.

1.8.2 Neoangiogenesis

The formation of new vessels form pre-existing vascular network is an integral part of many pathological states including inflammatory arthritis, tumor development and angiogenic ocular disease. It is also seen in the context of response to injury and wound healing[288].

The formation of new vasculature in the Rheumatoid joint occurs by sprouting of new vessels (neovascularisation) in response to angiogenic mediators[289]. Endothelial cell activation results in the release of proteolytic enzymes which degrade the surrounding extracellular matrix and basement membrane[290]. Endothelial cells reproduce and migrate into the extracellular matrix forming a sprout. These primary sprouts form a capillary loop and, following the production of a basement membrane by endothelial cells, form a mature vascular capillary. These early features of angiogenesis are heavily VEGF dependent[291 292]. New vessel sprouting is along a VEGF A concentration gradient with tip and stalk endothelial cells showing differential expression of delta-like 4 (DLL4) - expressing tip endothelial cells and NOTCH1 - expressing sprout stalk endothelial cells[293 294]. Within tumors there is a clear relationship with the stability of immature, developing vasculature and VEGF but this dependency is lost with a more mature vascular network[295-298].

1.8.3 Angiogenic factors

VEGF

VEGF has a central role in the mediation of angiogenesis. The loss of a single VEGF allele in mice results in malformation of the primitive vascular system in utero with a subsequent non-viable phenotype[299]. The early phases of angiogenic sprouting and vascular destabilization show a similar VEGF dependency[300]. Later, following maturation of the newly formed vessels, the expression of VEGF is less important for normal vascular stability. Senger et al. were the first to describe a protein able to induce vascular leakage. This protein was termed 'tumor vascular permeability factor' (VPF) as it was isolated from a tumor cell line[301]. The term 'vascular endothelial growth factor' was first coined by Ferrara and Henzel in 1989 when they reported an endothelial cell-specific mitogen from bovine pituitary follicular cells[302].

VEGF Ligands

VEGF A

The human VEGF-α gene is localized in chromosome 6p21.3. Alternative splicing may result in the generation of four different isoforms which are charachterised by the number of amino acids in their sequence (121, 165, 189 and 206 amino acids)[303]. VEGF165 is the most predominant isoform. VEGF165 is secreted by endothelial cells, however it may remain bound to the cell surface and extracellular matrix (ECM)[304]. The ECM-βound isoforms may be released in a diffusible form by heparin or heparinase with the loss of the heparin binding domain in VEGF has been shown to be critical in maintaining its affect as a survival factor for EC[305 306]. In pathological states, VEGF A has been demonstarted to acts on tumour endothelial cells causing proliferation, inhibiting vessel maturation and providing a positive mitogenic stimulus in hypoxic tissues[307-311].

VEGF B

VEGF-β is expressed early during fetal development and is widely distributed, being prominently expressed in the cardiac myocytes, in skeletal muscle and smooth muscle cells of large vessels[312]. VEGF-β is also expressed in the perichondrium of developing bone and in the nervous system[312-314]. VEGF-β is a selective ligand for VEGFR-1. VEGF-β and VEGF-α have only partially overlapping receptor specificities and as indicated by the lethality of VEGF knockout in embryos, no other growth factor could compensate for the loss of even a single VEGF allele[299].

VEGF C

As well as signaling through VEGF-R2, VEGF-C is a potent inducer of lymphangiogenesis when bound to its principal target - VEGF-R3[315]. Transgenic mice over expressing VEGF-C have a selective hyperplasia of the superficial lymphatic vasculature, however, VEGF164 from the same promoter generates a pure angiogenic anomaly[316]. VEGF-C is also a potent chemotactic for macrophages expressing VEGF-R3, at the sites of inflammation[317]. It has been suggested that pro-inflammatory cytokines, TNF-α or IL-1, stimulate these myeloid cells to produce VEGF-C thus encouraging synovial lymphangiogenesis although these pro-inflammatory cytokines have also been shown to up regulate VEGF-C expression in vascular endothelial cells and fibroblast like synoviocytes[318]. However, a report from Polzer et. al. suggested that lymphangiogenesis was encouraged following treatment of humans with anti-TNF α with a greater expression of lymphatic vessels in synovial tissue when examining pre and post treatment synovial tissue[319].

VEGF D

VEGF-D is a ligand for both VEGF receptors (VEGFRs) VEGFR-2 (Flk1) and VEGFR-3 (Flt4) and can activate these receptors. However, VEGF-D does not bind to VEGFR-1. Expression of a truncated derivative of VEGF-D demonstrated that the receptor-βinding capacities reside in the portion of the molecule that is most closely

related in primary structure to other VEGF family members and that corresponds to the mature form of VEGF-C. In addition, VEGF-D is a mitogen for endothelial cells. The structural and functional similarities between VEGF-D and VEGF-C define a subfamily of the VEGFs. VEGF-D appears to have a negligible role in development in mice. Recent experimental evidence strongly suggests that tumors can actively induce lymphangiogenesis via production of lymphangiogenic factors such as vascular endothelial growth factor (VEGF)-C and VEGF-D, and that the extent of tumor lymphangiogenesis is directly correlated with the extent of experimental metastatic tumor spread to regional lymph nodes. Homozygous deletion of Vegfc leads to the complete absence of the lymphatic vasculature in mouse embryos, whereas Vegfc+/- mice display severe lymphatic hypoplasia16. In Vegfc-null mice, lymphatic endothelial cells initially differentiate in the cardinal veins but fail to migrate and to form primary lymph sacs. This demonstrates that VEGF-C is an essential chemotactic and survival factor during embryonic lymphangiogenesis16. By contrast, deletion of Vegfd does not affect development of the lymphatic vasculature, although exogenous VEGF-D protein rescues the impaired vessel sprouting in Vegfc-/- embryos16, 34. Vegfr3 deletion leads to defects in blood-vessel remodelling and embryonic death at mid-gestation, indicating an early blood vascular function

Placenta Growth Factor (PLGF)

PLGF binds only VEGF-R1. PLGF enhances the recycling of VEGF-R21 and αvβ3 by endothelial cells by phosphorylation of GSK-3β[320]. This may indicate that endothelial cell adhesion and migration during angiogenesis is influenced by integrin expression and activation along side VEGF receptors.

VEGF mediates endothelial cell survival and can be demonstrated both *in vitro* and *in vivo*. *In vitro*, endothelial cell apoptosis induced by serum starvation is inhibited by VEGF and has been shown to up regulate a number of anti-αpoptotoic proteins such as Bcl-2, A1 and survivin[321 322]. *In vivo*, as already described the lack of VEGF results

in a lethal phenotype. Other, non-eptithelail cell types also respond to VEGF as a positive mitogen such as Schwann cells and pancreatic duct cells[323]. Recently, it has been suggested that VEGF A may act as a neuronal survival factor based on the observation that reduced VEGF expression is an associated risk for amyotrophic lateral sclerosis[324].

VEGF has a number of physiological roles in the normal vascular system over and above endothelial cell stabalisation and triggering angiogenesis. VEGF produces vasodilatation, tachycardia and hypotension if infused into monitored rats. A role for endothelial derived Nitous Oxide (NO) in the mediation of these effects has been suggested[325]. A supportive observation in patients undergoing therapy with anti-VEGF antibodies often have a modest elevation of blood pressure. Vascular permeability is also thought to be mediated by NO. Fukumura et. al. demonstrated that endothelial derived Nitrous oxide synthetase knockout (eNOS - / -) mice do not show a significant response to VEGF but inducible NOS (iNOS) and wild type animals do when measuring angiogenesis, blood flow rate, and vascular permeability[326]. Both the eNOS-/- and iNOS-/- mice show normal development suggesting that while NO is an important mediator of VEGF function in the normal physiological processes, it is not necessary for vasculogenesis and development of a competent vascular system.

Regulation of VEGF Expression

Oxygen tension

Tissue hypoxia plays an important role in mediating the expression of VEGF and some similarities with the regulation of erythropoietin (Epo) production. A similar binding site is seen on the VEGF and Epo promoter. In response to hypoxia, HIF-1 binds to DNA binding sites within regulatory sequences of hypoxia-inducible genes such as VEGF[327]. HIF-1 is a heterodimeric protein consisting of two subunits, HIF-1α and HIF-1β. HIF-1α is continually produced but just as quickly degraded. This process is mediated by von Hippel–Lindau tumor suppressor factor[328]. The effect of

hypoxia is to inhibit the function of this factor, allowing the survival and stabalisation of HIF1- α followed by it's binding to the appropriate DNA site in conjunction with HIF 1- β. Loss of the expression of VHL tumor suppressor factor, as seen in von Hippel–Lindau disease, results in continued availability of HIF-1α, over expression of angiogenic factors and disorganized vascular growth manifest clinically as multiple capillary haemagiomas. Whilst HIF-1 up regulates VEGF and other related peptides, it also functions to prepare cells for anaerobic conditions. This is achieved by by inducing glycolytic enzymes and glucose transporters which improves cells energy production in such hypoxic states[329]. HIF-1 also decreases mitochondrial oxygen consumption and halts the citric acid cycle.

Hypoxia-independent regulation

A number of growth factors are known to up regulate the expression of VEGF such as TGF-α, TGF-β, FGF, and PDGF[330]. A number of authors have also reported the ability of inflammatory cytokines such as IL-1-α and IL-6 and TNF-α to induce expression of VEGF in a number of cell linages including synovial fibroblasts in a HIF-1 dependent fashion. Interleukin-1 (IL-1) and tumor necrosis factor-α (TNF-α), stimulate HIF-1 dependent gene expression even in normoxic cells[331] [332]. It would appear that, although HIF-1a degradation is not inhibited in the normoxic scenario, the increased transcription of the gene is sufficient to alter the balance with the cell to favour dimerization with HIF-1β and fulfill its combined function. In addition, TNF-α may activate HIF-1 by radical oxygen species and NO production and/or NF-κB activation[332].

VEGF receptors

All VEGF splice variants bind in an overlapping pattern to three receptors (VEGF-R1,2,3). All three VEGF receptors are expressed on vascular endothelial cells to differing degrees.

VEGFR1

Also known as Flt-1.

In addition to endothelial cells, VEGFR1 expression can also be found on dendritic cells, osteoclasts, monocytes and macrophages. VEGFR1 null mutant mice die at the embryonic stage as a result of endothelial cell proliferation and disorganized vascular overgrowth[280]. This would suggest that VEGF-R1 may have a regulatory effect (negative) on vasculogenesis. However, mice expressing the transmembrane and extracellular component of VEGF-R1 but not the intracellular signaling domain develop normally suggesting that VEGF-R1 tyrosine kinase has redundancy. It has been postulated that the mopping up of VEGF is the critical aspect of the receptor during embryogenesis thus preventing VEGF signaling through VEGF-R2[333]. VEGFR1 transduces weak signals for endothelial cell and pericyte growth and survival as well as for cell migration of macrophages[334 335]. This may have a role to play in the on set and sustained inflammatory component seen in Rheumatoid Arthritis.

VEGF-R2

Up regulation of VEGF-R2 expression can be seen on vascular endothelial progenitors in early embryogenesis. During later stages of vascular development, VEGFR2 expression declines but can be up regulated in pathological angiogenesis such as in malignancy[336]. Up regulation of VEGF-R2 expression is seen principally on tip endothelial cells in keeping with vascular VEGF A mediated response[337]. The subsequent release of Ang 2 from activated endothelial cells further destabalises the local vascular network facilitating loss of the local basement membrane, cell

migration and sprouting. If the VEGF-R2 gene is inactivated in mice, embryonic death occurs due to a lack vascular development especially within the yoke sac[338]. Comparing this to the VEGF-R1 knock out mice who die of a over growth of poorly organized vessels, it would appear that a balance is maintained between the binding and signaling of VEGF- R1 and R2. Once again VEGF-R2 has been identified on other cell lines including osteoblasts, megakaryocytes and neuronal cells. Their role on these cells remains unclear however on vascular endothelium, VEGF A binding to VEGF-R2, promotes endothelial cell differentiation[339].

VEGF-R3

VEGF-R3 has a more limited pattern of expression, being principally found on lymphatic endothelial cells and fenestrated capillaries. Although the initial stages of lymphatic development form the cardinal vein in the embryo appears not to be significantly influenced from VEGF-R3 signaling, sprouting of lymphatics at a later stage does requires the interaction of VEGF C and R3[340 341]. Dysfunction of VEGF-R3 can be seen in congenital lymphedema due to mutations in the gene resulting in defective signal transduction[342]. This condition, characterised by a decrease in the lymphatic systems ability to collect and transport lymph form the extracellular matrix back into the circulation. Within tumours, VEGF-C expression, binding to VEGF-R3 may increase lymphatic vessel development within the tumour microenvironment. Certainly in orthotopic mice models, over expression of VEGF-C and D results in peritumoral lymphatic vessels formation and increases metastasis to regional lymph nodes[343 344].

VEGF co-receptors

Neuropilins (NRPs)

There are two NRP homologues, NRP1 and NRP2. The NRPs are a family of soluble molecules with neuronal guidance functions, and subsequently have been suggested

to be important receptors for normal vascular systems. NRPs are VEGF receptors and in help mediate the pro-αngiogenic and lymphangiogenic effects of VEGF.

NRP1 is a co-receptor for VEGFR1/2 and NRP2 is a co-receptor for VEGFR3. NRP1 contributes to VEGFR2 signaling with the subsequent effects of increased endothelial cell survival, vascular permeability and promotes cell migration[345] [346]

1.8.4 Angiopoietins - TIE signalling system

The Angiopoietin (Ang) - Tie signaling system consists of two tyrosine kinase receptors and 2 principal ligands (Ang 1 and 2). Ang 3 is the mouse orthologue of human Ang 4. Ang 4 is thought to influence vascular remodeling and maturation as an angiogenic inhibitor. Ang 3 and 4 will not be discussed further in this section.

Ang 1 would appear to have a stabalising effect on vascular endothelium. Ang 1 binding to Tie 2 tyrosine kinase, resulting in dimerisaton of the receptor and is autophosphorylated[347]. Activated Tie 2 on endothelial cells activates a number of downstream effectors important in maintaining endothelial cell stability and equilibrium. Ang 1 interaction with Tie-2 appears to act as a survival signal in endothelial cells in mature vascular networks[348] [349]. Under physiological it has a role in the integrity of existing vessels through maintenance of the contacts between endothelial cells and mural cells. If there is a lack of Ang 1 signaling there is loosening of tight junctions permitting greater vascular permeability in the presence of on going VEGF expression[349]. This is obviously a favorable situation with leukocyte migration in infection but not ideal in the context of a persistent inflammatory condition such as RA.

Ang 2 has an antagonistic effect, compared to Ang 1, on endothelial cell function despite studies confirming that it binds to Tie 2[350] [351]. It would seem that the competitive binding of Ang 2 is a negative regulator of Tie 2 signaling resulting in degradation of the endothelial basement membrane. However this relationship cannot be viewed in isolation with the presence of VEGF significantly modifying the

endothelial response to the Angiopoietin. VEGF stimulates the release of Ang 2 from Weibel-Palade bodies[352]. These are storage granule of endothelial cells which contain Ang 2, von Willebrand factors, P-selectin and several other chemokines. This facilitates the disrupted intercellular endothelial junctions, sprouting of endothelial cells and degradation of the basement membrane[353 354]. The formation of vessel lumen are also vital for the maturation of new vessels and seem to be under the influence of epidermal growth factor-like domain multiple 7 (EGLF 7). EGLF 7 promotes the movement of angioblasts and the formation of EC tube lumens. In its absence vessels continue to appear but lack a functional lumen.

1.8.5 Lymphangiogenesis

The lymphatic system is an essential component of our normal vascular system acting as a collection and return system for excess extracellular fluid and cells to the circulatory system via the thoracic duct. Inhibition of this process quickly result in extracellular fluid accumulation and the clinical picture of lymphodema. The lymphatic system also acts as a conduit for the movement of immune cells and antigens through out the body[355]. Although there are some similarities between the endothelial cells of he lymphatic and vascular system, many difference have been elicited. Endothelial cells lining lymphatic vessels have less tight intercellular junctions and fragments of broken basement membrane intergity[355]. VEGEF-R3 seems to play an important role in lymphangiogenesis although its expression is seen in the early stages of angiogenesis its role becomes more restricted to lymphatic endothelial cells[356]. VEGF C and binding with VEGF-R3 also play an important role in encouraging lymphatic sprouting from the embyologic venous system with VEGF C knockout mice failing to form any lymphatic vessels, developing severe oedema[341 356 357].

The lymphatic vessels also have smooth muscle cells located around the vessels although less concentrated than in normal vessels. Smooth muscle cell recruitment to the lymphatic vessels is inhibited in the absence of Ang 2 as seen in the knockout

mouse[358 359]. Ang 1 can also promote lymphangiogenesis, and the abnormalities of Ang 2 deficiency can be completely reversed by the administration of Ang 1. Interestingly, this may suggest that both angiopoeitins, acting via Tie 2 within the lymphatic system, have agonistic effects rather than the previously described the agonist / antagonist roles seen on the normal vascular system[358].

1.8.6 Angiogenesis and lymphangiogenesis in Rheumatoid Arthritis

There are many mediators of angiogenesis within the inflamed RA synovium. Normal synovium has a small number of vessels which supply sufficient nutrients and oxygen for its optimal function. In the pathological state, there is a significant increase in the vascular density which facilitates the continued synovial proliferation and on going inflammatory response[360]. A common analogy is drawn with tumour growth and development although the vascular supply here develops *de novo* (combination of both angio- and vasculogenesis) rather than a pre-existing vascular network[361 362].

Within the inflamed synovial joint there are many mediators of angiogenesis. Table 1-8, outlines the plethora of mediators and some inhibitors of angiogenesis within the RA joint.

Table 1-8: List of mediators and inhibitors of angiogenesis within the Rheumatoid synovium

Modified from: Szekanecz Z, et. al. New insights in synovial angiogenesis. Joint Bone Spine 2010;77:13-9.[360]

	Mediators	Inhibitors
Growth factors	VEGF, aFGF, bFGF, HGF, HIF-1, HIF-2, PDGF, EGF, KGF, IGF-I, TGF-β	-
Cytokines	TNF-α, IL-1, IL-6[a], IL-8, IL-15, IL-17, IL-18, G-CSF, GM-CSF, oncostatin M, MIF	IFN-α, IFN-γ,IL-4, IL-12, LIF
Chemokines/receptors	IL-8/CXCL8, ENA-78/CXCL5, groα/CXCL1, CTAP-III/ CXCL6, SDF-1/CXCL12[a], MCP-1/CCL2, fractalkine/ CX3CL1 CXCR2, CXCR4[a], CCR2	PF4/CXCL4, Míg/CXCL9, IP-10/CXCL10, SLC/ CCL21, CXCR3
Matrix molecules	Type I collagen, fibronectin, laminin, vitronectin, tenascin, proteoglycan	Thrombospondin-1
Cell adhesion molecules	β1 and β3 integrins[a], E-selectin[a] VCAM-1, ICAM-2, CD34, Lewis^{y}/H, MUC18, PECAM-1, endoglin, JAM-α, JAM-C	-
Proteolytic enzymes	MMPs, plasminogen activators	TIMPs, PAIs
Environmental factors	Hypoxia	-
Others	Angiopoietin 1 /Tie-2, angiotropin, pleiotrophin, angiogenin, survivin, COX/prostaglandin E2, PAF, Nitric oxide (NO), endothelin-1,	Angiopoietin 2, angiostatin, endostatin, taxol, osteonectin, opioids, troponin I, chondromodulin, etc.

VEGF: vascular endothelial growth factor; FGF: fibroblast growth factor; HGF: hepatocyte growth factor; HIF: hypoxia-inducible factors; PDGF: platelet-derived growth factor; EGF: epidermal growth factor; KGF: keratinocyte growth factor; IGF: insulin-like growth factor; TGF-β: transforming growth factor-β; TNF: tumor necrosis factor; G-CSF: granulocyte colony-stimulating factors; GM-CSF: granulocyte-macrophage colony-stimulating factors; MIF: migration inhibitory factor; JAM: junctional cell adhesion molecules; PECAM-1: platelet-endothelial cell adhesion molecule-1; MMP: matrix metalloproteinases; TIMP: tissue inhibitors of metalloproteinases; PAI: plasminogen activator inhibitors.

Numerous growth factors are found within the RA synovium with VEGF playing a central role in the development of new vessels in response to inflammation. The release of TNF-α by synovial macrophages and fibroblasts has been shown to increase VEGF levels with the result of endothelial cell proliferation and subsequent

degradation of the basement membrane with a rudimentary sprout formation[363 364]. Taylor et. al. has also reported a significant correlation with serum VEGF levels and radiographic damage, as measured by a modified Sharp's score, over the course of one year[365]. Furthermore, this group have also described elevated serum VEGF levels at presentation, in a cohort of RA patients with persistent disease activity despite conventional therapy. In addition, Klimiuk et al. have shown correlation between soluble adhesion molecules and VEGF[366]. Soluble adhesion molecules such as intercellular adhesion molecule-1(ICAM-1), vascular cell adhesion molecule-1 (VCAM-1) and E-selectin play a key role in activation, circulation, and migration of mononuclear cells to inflammatory sites perpetuating the immune response.

VEGF would appear to have 3 main receptors within the RA synovium including VEGF-R1, VEGF-R2 and neuropilin-1 (NP-1). VEGF-R1 and R2 are both expressed on the majority of endothelial cells. VEGF-R2 would seem to be a driver of endothelial cell proliferation and activation. This enhances cell surface expression molecules increasing peripheral leukocyte adhesion and migration into the inflamed joint[367 368]. VEGF-R2 promotes endothelial cell release of chemokines, such as TNF-a, IL-6, and MCP-1, critical for the on going inflammatory response[369]. NP-1 is also a co-receptor of VEGF, and has been shown to regulate VEGF-R2[370]. NP-1 has anti-αpoptotic functions in breast carcinoma suggesting that ligation of this particular receptor may act as a survival signal for endothelial within the joint.

Hypoxia plays a key role in neoangiogenesis that is typically seen in the rheumatoid synovium and contributes to the tissue hypertrophy by supplying oxygen and nutrients to the proliferating synovial cells. Etherington et al. demonstrated exceptionally low levels of pO2, using silver micro-electrodes, in the synovium of mice with established collagen-induced arthritis and similar levels in patients with inflammatory arthritis[371]. Lund-Olesen et al. reported the mean synovial fluid pO2 in RA knee joints to be as low as 27 mm Hg compared with 43 mm Hg in osteoarthritis patients[372]. Other authors support these findings and have recorded pO2 values

below 15 mm Hg[373]. VEGF, under the control of hypoxia-inducible factor (HIF), appears to mediate the hypoxic effects found within the RA joint. Cultured synovial cells are able to secrete VEGF under hypoxic conditions or when stimulated with IL-1, IL-6[374]. The induction of HIF-1 is highly specific and sensitive to tissue hypoxia. HIF-1 is a heterodimer consisting of HIF-1α and HIF-1β subunits. HIF-1α, in the normoxic state, is undetectable because of rapid ubiquitination followed by proteosomal degradation mediated by von Hippel–Lindau tumor suppressor factor (VHL)[373]. This is inhibited in hypoxic conditions allowing the dimerisation with the constitutively expressed β subunit. The resulting HIF-1 dimer up-regulates several genes including VEGF promoting angiogenesis[332]. The up-regulation of HIF through NF-κB also occurs in the response to pro-inflammatory cytokines such as TNF-α, IL-1 and IL-6 which may occur in a relative normoxic conditions.

Chemokine-driven recruitment of inflammatory cells is seen in the Rheumatoid synovium. Chemokines containing glutamyl-leucyl-αrginyl (ELR) amino acid sequences (CXC) have been shown to stimulate angiogenesis as well as lymphangiogenesis. These include, but not limited to, IL-8/CXCL8 and epithelial neutrophil activating protein-78 (ENA-78)/CXCL5, while Stromal cell-derived factor-1 (SDF-1)/CXCL12 seems to be important in promoting lymphangiogenesis[375-377].

1.9 Vascular vasodilatation and constriction

The control of peripheral vascular tone is an important homeostatic process which facilitates appropriate tissue perfusion and maintenance of systemic blood pressure. This control is exerted at a number of levels and includes neuronal, hormonal and local mediators of vascular constriction and vasodilatation. Excessive peripheral vasoconstriction certainly contributes to systemic hypertension and is considered a pathological extension of the normal appropriate, physiological response encountered in low cardiac output states such as hemorrhage or cardiogenic shock. In Raynaud's phenomenon a more subtle aberration exists with profound vasoconstriction with eventual correction of the digital vessel excessive tone. A

neuronal mediated response is the principal driver of vasoconstriction in Raynaud's phenomenon.

Vasodilatation is seen in the setting of acute inflammation. While neovascularisation is seen in chronic synovial inflammation, this may only partly explain the rapid alteration in vascular signal seen in patients with a 'flare' of their rheumatic disease. Patients can rapidly oscillate between low, stable disease and significant joint inflammation characterised by the classic calor, dolor, rubor and tumor (heat, pain, redness and swelling). The infrastructural changes in tissue vasculature take significant time to develop as a chronic inflammatory response takes hold. It is likely that subclinical disease facilitates this significant vascular ingress however the dramatic and sudden change in vascular flow, which can occur with a disease flare, is likely to be mediated by local pro-inflammatory mediators and local vasodilatation. The opposite observation is seen in with the administration of steroid therapy during disease flares with rapid resolution of swelling and redness within 24-48hrs. This once again this suggests a down regulation of local inflammatory mediators and improved tonal control of afferent vessels.

Vasodilatation may not be sufficient to explain all aspects of clinically observed joint inflammation. Acute swelling of joints during a flare or reduction in size following therapy is not likely to be purely related to vasodilatation but include a reduction / increase in vascular permeability with a resultant fluid shift. Synovial lymphatics have been demonstrated in synovial samples of both normal joints and in Rheumatoid Arthritis. It is likely that these vessels would promote the rapid redistribution of excessive intercellular fluid generated by both increased vascular permeability and increase hydrostatic pressure from greater blood flow during periods of inflammation and subsequent low disease activity. Polzer et. al. demonstrated that in both animal and human studies that lymphatic tissue expansion occurs on successful suppression of the joint inflammatory response[319]. This would indicate a role for this network in promoting the efflux of fluid and cells from the synovium.

Neuronal control of vascular tone

Dual vasoconstrictor nerves and vasodilator nerves in skin were first suggested in 1931 by Lewis and Pickering. To date cutaneous vascular control being the most extensively investigated. This is in part due to easy access of the organ involved and simple thermoregulation techniques which can be employed to manipulate the underlying vasculature. Neuronal vascular control of cutaneous vessels is mediated by a nor-αdrenergic sympathetic vasoconstrictor system, and a non-noradrenergic vasodilator system. In the normothermic state the nor adrenergic system is active to maintain vascular tone although this often is dependent upon the ambient environment temperature. Stephens et al. showed that complete postsynaptic blockade of adrenergic receptor mediated vasoconstriction did not completely inhibit the vasoconstrictor response to cold but required the additional use of a pre-synaptic blockade suggesting that nor-αdrenergic mediated vasoconstriction is dependent not only upon nor-αdrenaline but also co-transmitters. Neuropeptide Y, was identified as the likely co-transmitter since antagonism of this molecule with BIBP-3226, in addition to α 1 and α 2 blockade of adrenergic receptors, completely abolished the vasoconstrictor response.

The control of vasodilatation is less well understood but once again co-transmitters have been implicated along side acetyl-choline as important mediators of neuronal mediated affects. It is interesting to note that post-synaptic blockade of muscarinic receptors completely abrogates sweating but has almost no effect on cutaneous reflex vasodilatation suggesting additional mediators of this phenomenon. Vasoactive intestinal peptide (VIP), Nitrous oxide (NO) and substance P have all been shown to act as co-transmitters. McCord et al. (58) used intradermal ketorolac (a nonselective cyclooxygenase inhibitor) and l-NAME (NOS inhibitor) in a model of vasodilatation and found that both treatments significantly reduced the vasodilatory response in their model with some additional synergistic effects demonstrated by combination therapy.

A number of disease processes have a modifying effect on both vasodilatation and constriction. Patients with systemic hypertension and diabetes tend to have a diminished response to reflex vasodilatation. Holowatz et. al. showed that in hypertensive patients the administration of arginase (which may compete with NOS) improves reflex vasodilation thermoregulation but not in a normotensive cohort. In addition the same group showed that older individuals have both an inhibited vasodilation and vasoconstriction to warming and cooling respectfully.

Local mediators of vascular tone

The release of endothelium-derived contractile mediators is governed by a number of steps including an increase in intracellular calcium concentration and activation of cyclo-oxygenase-1 (COX-1). One of the first identified endothelial derived vasoactive mediators was prostaglandins and Thromboxane A2. Increased intra-luminal pressure or mechanical shear force can cause hyperactivation of COX-1 with the subsequent effect of prostaglandin synthesis and increase in smooth muscle activation and vascular tone. A counter balance exist with NO being at the centre of endothelial derived vasodilatation. However in the pathological state, such as systemic hypertension, there seems to be an imbalance between these two control mechanisms. COX-1 is constitutively expressed in cells although following shear stresses hyper-expresion may occur. COX-2 in normally inducible but in vascular endothelial cells it appears to be constitutively expressed also.

Thromboxane A2 is the most potent inducer of smooth muscle contraction and increase in vascular tone through activation of smooth muscle TP receptors. This tends to be derived form platelet COX-1 but can be produced form endothelial cells. Conversely, Prostacyclin is a potent vasodilator and over expression of prostacyclin synthase in mice prevents injury-induced intimal hyperplasia, pulmonary hypertension and vascular remodeling.

1.9.1 Endothelial permeability

Vascular smooth muscle is the muscular component of blood vessels but no smooth muscle cells are found in capillaries. Instead, arterioles and to a lesser extent venules control the pressure differential across capillary networks directly influencing the hydrostatic pressure within them. In the setting of acute inflammation, arteriolar dilation causes an increase in hydrostatic pressure in combination with endothelial cell up-regulation of adhesion molecules and reduction in cell-cell junctions. Changes to the cytoskeleton and alterations in the plasma membrane of endothelial cells are responsible for the changes in vascular permeability. These changes are thought to be mediated by protein kinase C (PKC) activation and tyrosine-kinase-regulated pathways. Pro-inflammatory cytokines, such as IL-1β, IL-6 and TNF-α, mediate NF-κB up-regulation and subsequent expression of both VCAM-1 and ICAM-1 on the endothelium during inflammation. This facilitates both an exudative fluid shift into the extracellular space and cellular trafficking. Up regulation of endothelial adhesion molecules (ICAM-1, allow circulating neutrophils to initially roll along the endothelial surface, become apposed to endothelial cells (pavementing), followed by migration through the vessel basement membrane to access the intercellular space. These changes can occur within 6 hours on the initial stimuli. Vascular permeability can be though of in three separate scenarios, although there will be significant overlap in these constructs at various times.

BVP - Basal Vascular Permeability

In the normal setting vascular movement of small molecules takes place at the level of the capillary bed. Small molecules, such as gases, salts and sugars, pass through the endothelial barrier relatively easily. Capillary endothelial cells contained small vesicles referred to as caveolae (Fig. 2a, b) which appear to transport molecules across the endothelial cells. The normal hydrostatic pressure permits movement of fluid in the inter-cellular spaces but with a continuous basement membrane and

relatively firm adherent junctions cellular trafficking or the movement of large molecules are not typical features in this setting.

AVH - Acute Vascular Hyperpermeability

The local production and release of vasoactive molecules such as TNF-α, bradykinin, VEGF-α or histamine has a dramatic effect on the local vascular network and its permeability to large molecules and cellular trafficking. These changes can be rapid (within 30mins) and produces an exudative fluid leak. The importance of eNOS in the signaling pathway for PAF and VEGF mediated vessel permeability has been clearly demonstrated in eNOS knockout mice and may be an attractive target in chronic inflammatory conditions with persistent elevated VEGF expression. Paradoxically eNOS and NO appear to have a stabilizing effect on intercellular junction in the normal basal vascular permeability state as shown by Predescu et. al. while others have shown that increased NO synthesis in the acute inflammatory state results in vasodilatation, changes in the cytoskeleton and effective loosening of the same intercellular junctions. An important finding by Majno et. al. was that maximum vascular permeability occurs at post-capillary venules rather than at the capillary level. This region is highly specialized with cuboidal endothelial cells, which readily undergo cytoskeleton changes to disengage producing inter-cellular spaces. In addition, dedicated organelles have been described as alternative routes for larger molecules to pass through the cell itself into the extracellular space. In the acute setting however there is persistence of the basement lamina and pericyte adhesion further limiting movements of cells and large proteins.

CVH - Chronic Vascular Hyperpermeability

Chronic inflammation brings about further changes to the post-capillary venules which are important adaptations. These are often seen in neoangiogenesis in the context of tumors and inflammatory arthritis. New vessels form so called mother vessels (MV). These vessels form by a process of pericyte detachment and

degredation of the basla lamina, likely to be in part encouraged by the release of MMPs from inflammatory cells and fibroblasts. These greatly enlarged sinusoids arise from preexisting normal venules by a process that involves pericyte detachment, vascular basal lamina degradation, and a 4–5-fold increase in lumen size that is accompanied by extensive endothelial cell thinning. Large molecules still pass through the endothelial barrier by the trans-cellular route already described with pores developing as cellular reorganization of the cytoskeleton infrastructure disengages cells form one another and more readily facilitates cellular trafficking.

Figure 1- 16: Diagram of a normal venule architecture and following acute and chronic inflammatory changes.

(a) Schematic diagram of a normal venule comprised of cuboidal endothelium with prominent VVOs and closed inter-endothelial cell junctions. Basal lamina (BL) is intact and the endothelium is completely covered by pericytes. (b) AVH. Acute exposure to VEGF-α causes VVO to open, allowing transcellular passage of plasma contents, possibly by mechanical pulling apart of stomatal diaphragms (3). Others have suggested that fluid extravasation takes place through an opening of intercellular junctions (4, here shown closed). BL and pericyte coverage are as in (a). (c) CVH. Prolonged VEGF-α stimulation causes endothelium to transform into mther venules, greatly thinned, hyperpermeable cells with fewer VVOs and VVO vesicles/ vacuoles, degraded BL, and extensive loss of pericyte coverage. Plasma may extravasate either through residual VVO vesicles (5) or through fenestrations (6). Reproduced from Nagy JA, et al. Vascular permeability, vascular hyperpermeability and angiogenesis. Angiogenesis. 2008;11:109-119.

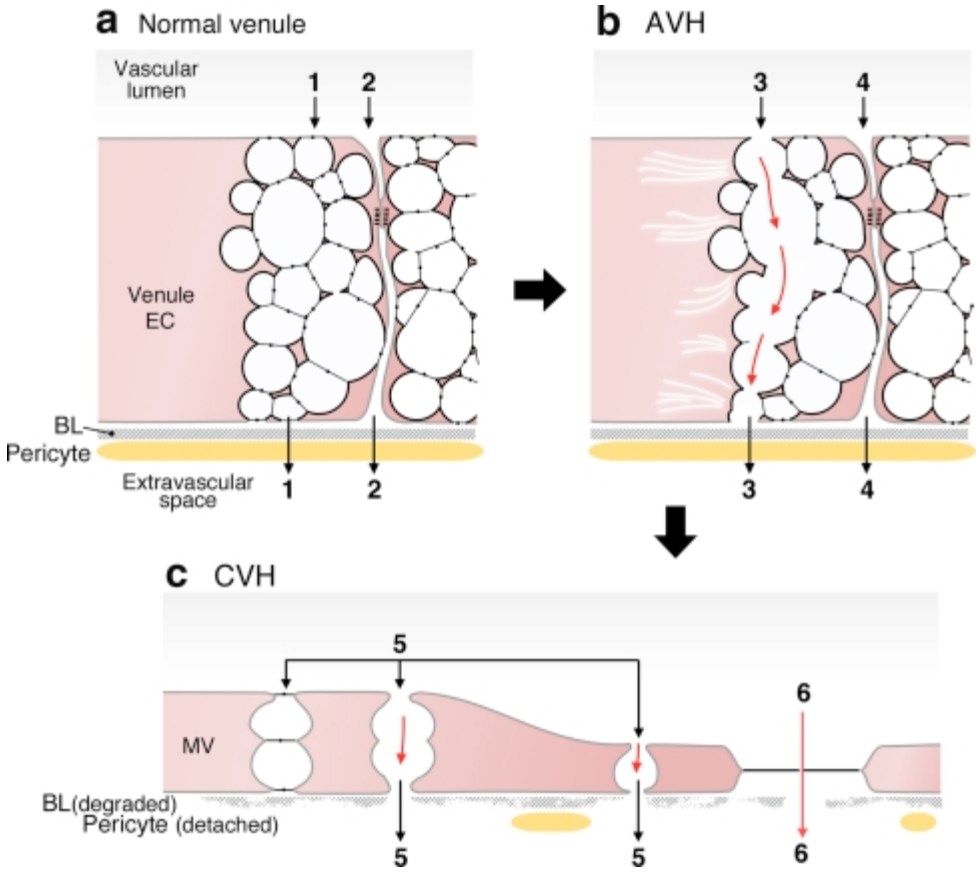

2. General methods

2.1 Ultrasound Guided Synovial biopsy

2.1.1 Equipment

- Quick-Core biopsy needles (16G)
- 21G / 19G needles
- Sterile drapes
- Sterile Ultrasound sheath
- Sterile gown and gloves
- Procedure pack
- Face mask / hair cover
- Sterile swabs
- Antiseptic solution (Chlorhexidine 2%)
- 10mls / 20mls syringes
- 1 % Lignocaine (20-30mls)
- Non-adhesive dressing
- Sample container for processing

2.1.2 Personnel

Ultrasonographer performing the biopsy

Technician / nurse / clinical fellow for tissue processing and assisting

2.1.3 Consent and adverse events

Consent should be gained prior to the patient attending for the synovial biopsy. This can ideally be done during clinic with the patient's permission to perform he biopsy is initially sought.

There are no large prospective studies of complication rates for Ultrasound (US) guided synovial biopsies using this particular technique. Our own experience would suggest that this procedure is well tolerated and safe. We have listed the quoted complications for diagnostic arthroscopy, however we expect the complication rate for this procedure to be significantly better. An audit of our practice in 400 patients revealed only 1 wound infection with no other serious complications

Approximately 25% of patients will have minor discomfort after the procedure. This is effectively managed with simple analgesia (non-steroidal anti-inflammatory drugs /

Paracetamol) and should dissipate after 24hrs. Patients are able to walk after the procedure and can go home on the same day. Patients are asked to refrain from overuse of the biopsied joint and should ideally be accompanied home by a friend / relative.

Below is a list of most commonly experienced complications with arthroscopic procedures (approximate frequency in brackets) and should be discussed with the patient as potential complications.

i) Joint infection (0.2%)

ii) Deep venous thrombosis (0.2%)

iii) Haemarthrosis (1%)

iv) Neurological damage (0.02%)

v) Wound infection (0.5%)

vi) Thrombophlebitis (0.08%)

Patients be given a contact telephone number if they have any concerns following the synovial biopsy, specifically if there is pain, swelling, warmth or redness from the joint which may indicate infection.

2.1.4 Biopsy procedure

Orientation of patient

Wrist

The patient should be placed supine on a bed. The patient may remain recumbent at 45 degrees, with the hand placed on a table next to the bed. Care should be taken not to elevate the hand or abduct the shoulder significantly as this will cause patient discomfort during the procedure. The hand should be place with the palm downwards.

Knee

The patient should be placed supine on a bed. The patient may remain recumbent at 45 degrees or preferably lie completely flat during the procedure. With the knee

slightly flexed (25-30 degrees) to improve imaging of the supra-patella pouch and a suitable point marked on the patient for introduction of the biopsy needle.

Preparation

Wrist

With the patient suitably placed on the bed, suitable absorbent pads should be placed under the wrist. The skin should be prepped with appropriate sterilization fluid. A wide field should be sterilized in excess of the immediate area of interest, approx. Hand to mid-forearm (dorsal and ventral aspects).

Sterile drapes should be positioned below the wrist on the table and a sterile drape used as a cuff at the mid forearm.

The wrist should be placed in slight palmar flexion to improve access and identification of the synovial recesses. This can be facilitated by placing a few sterile sections of gauze under the wrist

The operator should now evaluate his equipment tray including biopsy needle and commence personal preparations for the procedure (hand washing, gloves, face mask, hair net, sterile gown).

The US probe should be placed within the sterile sheath. US gel should be placed first upon the probes foot-print and slowly lowered into the sheath. The upper end of the sheath should be secured with a sterile tie or elastic band usually provided with the sheath.

10mls of 1% lignocaine should be aspirated into a syringe.

US examination of the wrist should be performed prior to the biopsy to identify the extensor tendons of the 4th, 5th and 6th compartments, the scaphoid lunate junction and suitable synovial tissue. A suitable path should be planned as the normal anatomical relations may be disturbed in chronic Rheumatoid Arthritis. A suitable path can usually be identified inserting the needle superior to the Extensor Carpi Ulnaris (ECU) tendon and passing inferior to the Extensor Digiti Quinti Proprius (EDQ) and Long flexors (Extensor Digitum longus). The typical region for biopsy lies just superior to the scaphoid lunate ligament (Figure 1).

Knee

With the patient suitably placed on the bed, suitable absorbent pads should be placed under the knee. The skin should be prepped with appropriate sterilization fluid. A wide field should be sterilized in excess of the immediate area of interest, approx mid-thigh to mid calf both anteriorly and posteriorly.

Sterile drapes should be positioned above, below, medial and lateral to the knee leaving sufficient space for access to the supra-patella pouch and placement of the U.S. probe for the purposes of imaging.

The operator should now evaluate his equipment tray and commence personal preparations for the procedure (hand washing, gloves, face mask, hair net, sterile gown).

The US probe should be placed within the sterile sheath. US gel should be placed first upon the probes foot-print and slowly lowered into the sheath. The upper end of the sheath should be secured with a sterile tie or elastic band usually provided with the sheath.

10mls of 1% lignocaine should be aspirated into a syringe and a second syringe of 40mls of normal saline mixed with 10mls 1% lignocaine prepared which will be introduced into the synovial space later.

Procedure

Wrist

Inject the 2-5mls of 1% lignocaine into the subcutaneous tissue up to the extensor retinaculum. Leave a minimum of 3-5 mins for effect.

Using a 19G needle and under US guidance, aspirate any fluid. This should be stored for analysis. This is an opportunity to plan for the biopsy needle insertion. Now introduce 2-5 mls of 1% lignocaine. This will enable a better image to be acquired during the procedure and facilitate clear identification of synovial tissue.

The quick core biopsy needle should be primed before its introduction to the synovial space.

Introduction of the biopsy needle into the wrist can now be performed under ultrasound guidance. This is best achieved by imaging the needle in a longitudinal plane as seen in figure 1.

The needle should be extended and the throw identified on the US images (Figure 2). The throw of the needle should be placed against the surface of the synovium to maximize the opportunity for capturing the lining layer. Gentle pressure should be placed on the needle to oppose the throw and synovium. Triggering of the needle mechanism should be performed with a small forward movement of the whole needle. NOTE: if the tip of the extended needle is abutting a boney surface, backwards movement of the needle will occur at this stage with poor retrieval of tissue.

After sufficient numbers of specimens have been harvested, any remaining fluid should be aspirated.

Figure 2-1: US guided synovial biopsy of the right wrist

Figure 2-2: US image of wrist joint with Quick Core™ biopsy needle in situ.

EDL - extensor digitorum longus, EDQ - extensor digiti quinti

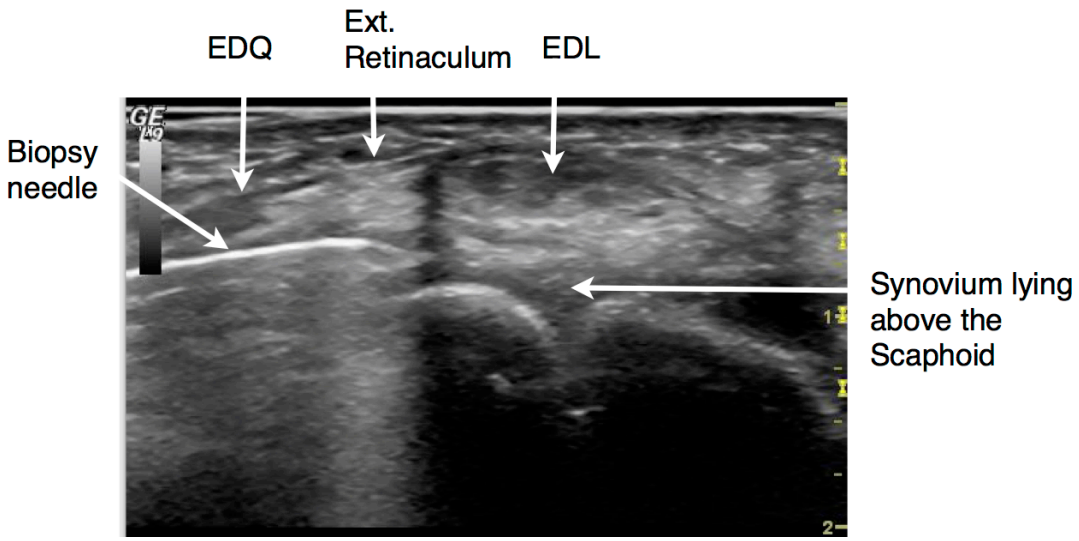

Figure 2-3: US image of wrist joint with Quick Core™ biopsy needle open with throw lying within the synovium.

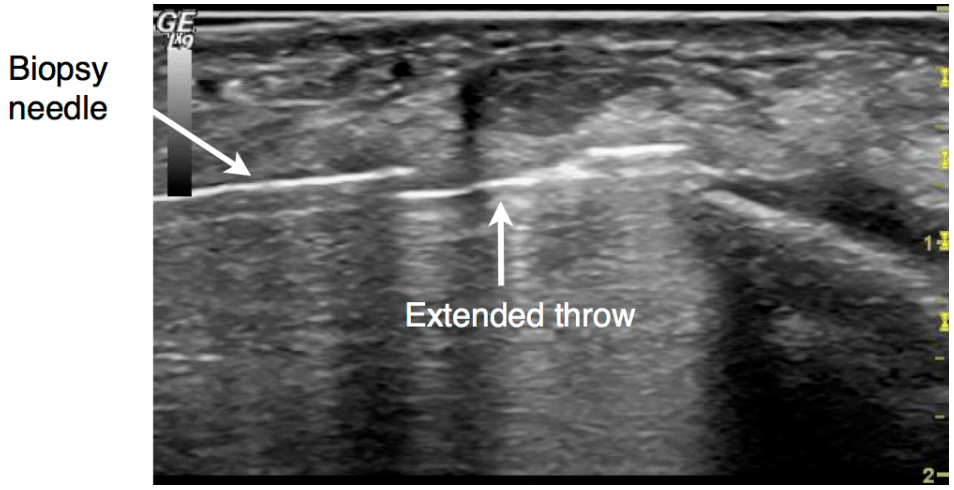

Knee

Inject the 10mls of 1% lignocaine into the subcutaneous and deep tissue at the predetermined point of incision as previously identified by the initial US scan. Leave for 3-5 mins for the effect to take hold.

Using a 19G needle and under US guidance, aspirate as much fluid as possible from the supra-patella pouch. This should be stored for analysis if required. Disconnect the syringe leaving the needle in situ. Now introduce the 30-50ml mix of normal saline and lignocaine. A total of 10mls of 1% lignocaine can be introduced mixed with normal saline into the suprapatella pouch. This will enable a better image to be acquired during the procedure.

Introduction of the biopsy needle can be performed through the anesthetized skin on the lateral aspect of the suprapatella pouch. The needled should be identified by the ultrasound probe in the longitudinal position as soon as it enters the subcutaneous tissue. The needle should then be advanced into the supra patella pouch. Repeated biopsies can be taken using the same tract.

Chlorhexidine can be used as a suitable contact medium for the ultrasound probe . A syringe (20mls) containing Chlorhexidine can be used to cover the skin during the procedure acting as a contact medium and maintaining sterility.

2.1.1 Post procedure care

1. A small dressing can be used to cover the wound.
2. A Neurovascular assessment should be made of the hand following the procedure and documented on the patients notes
3. The patient should remain in the department for a minimum of 30 mins post procedure. No specific monitoring is required.
4. Contact details in case of complications should be provided to the patient. Specifically, patients should be asked to contact the team if there is significant pain, swelling or redness of the biopsied joint within the next 5-7 days.

It is recommended that patients are followed up 3-5 days following the procedure either in person or by telephone.

2.1.2 Tissue processing

Tissue should be collected in the appropriate method for processing as described below depending upon local study protocols. Typically for studies described in this thesis I have harvested approximately 20-30 samples per joint biopsy. The tissue was processes for both histological evaluation and gene microarray analysis.

2.2 Ultrasound image scoring

2.2.1 2D Qualitative score MCP / Wrist / knee joints

Synovial thickness measurement

2D images were stored and analyzed according to a standardized image set on an ordinal scale ranging from 0 to 4: 0, no synovial thickening; 1, minimal; 2; mild; 3, moderate; 4, severe. (appendix 1) which represented the spectrum of synovial thickening for both longitudinal and transverse images at MCP, wrist and knee joints. Synovial fluid was not considered in the scoring of these still images. Images were displayed using Image J viewing platform (NIH, http://rsb.info.nih.gov/ij/. 1997-2008). The images were reviewed in a standard format with pixel area of 1024 x 768. Synovium was defined as hypoechoic structure lying between the bone and tendons.

This measurement is referred to in thesis thesis as the STi (synovial thickness index). The scores from each of the 10 MCPJs were summated to create a Synovial Thickness Index (minimum score of 0 and a maximum of 40) for each plane; the 10MCP Trans STi and 10MCP Long STi.

Power Doppler Signal

2D power doppler images were acquired using a 2D M12L (2D settings). A 3 second cine loop was acquired after resting the probe on the joint. The cine loop represented the previous 3 seconds of data capture. This loop was stored and analysed using Image J viewing platform. This platformed displayed the cine loops in a constant 532 x 434 pixel constraint allowing for consistent interpretation of the images. The cine loop was played and the frame with the greatest doppler area chosen and scored using a semi-quantitative 0-to-4 vascularity scale: 0, no PD signal; 1, minimal; 2; mild; 3, moderate; 4, severe. As for the PDA the longitudinal and the transverse region of interest at the MCPJs were the same as the respective STA region of interest. Images were graded against a library of representative images i.e. for each selected image I visually estimated the amount of coloured pixels within the joint capsule, compared this with the library, decided which representative image was the closest fit and allocated a score. The scores from each of the 10 MCPJs were summated to create a Vascularity Index (minimum score of 0 and a maximum of 40) for each plane; the 10MCP Trans VASCi and 10MCP Long VASCi.

2.2.2 2D Quantitative score (MCP / Wrist / Knee)

Synovial thickness measurement

Still images were recorded and Images were displayed using Image J viewing platform (NIH, http://rsb.info.nih.gov/ij/. 1997-2008). The images were reviewed in a standard format with pixel area of 1024 x 768. The synovial area was outlined as described above using a free hand drawing tool and the total pixel area recorded.

The Synovial Thickness Area (STA), is a count of the number of pixels within a defined region of interest in a standardized 2-dimensional image of the joint. For the Longitudinal STA the region of interest should envelop the synovium over the phalangeal base, triangular structure, metacarpal head and metacarpal notch. For the transverse STA the region of interest should envelop the MCP joint synovium from the lower border of the triangular structure (if bone this is indicated by a continuous hyperechoic line or if cartilage by a homogenous anechoic line above bone) to the joint capsule superiorly.

Power Doppler Signal

Recorded ultrasound cine clips were recorded and quantitate analysis performed using Image J (NIH, http://rsb.info.nih.gov/ij/. 1997-2008) with a customised macro application for pixel area measurement. The macro enabled sequential measurements of all cine loops within each file and the output file saved as an excel spreadsheet. For each recording the cine loop was played and the frame representing the maximum doppler signal selected by the reader. The Power Doppler Area (PDA) is a count of the number of pixels with PDUS signal, uncorrected for pixel intensity, within a defined region of interest in a standardized 2-dimensional image of the joint (figure 2-4). Separate Quantitative measurements provided included power doppler pixel area (PDA), doppler pixel area over a predetermined colour threshold (PDThA) and a ratio of synovial to doppler area (PDA/STA).

2.2.3 Power doppler Pixel intensity calculation

This is a measure of the luminance of the color scale seen in the left hand side of the still image in figure: 2-4. This reflects the intensity of the PD signal. Yellow indicates a higher flow (and therefore intensity) than red according to the colour scale used. In order to extract the luminescence of the PD pixels the RGB (Red,

Green, Blue) image was split into their individual components. The Red and Green channels were subsequently combined (minus Blue) according to the formula below:

Image Intensity: $Y = 0.35*(R-\beta) + 0.65*(G-\beta)$

This provided a luminescence score for each pixel. This calculation was performed of a spectrum of cine loops with varying PD signal and intensity. Using a step wise approach, a threshold of 100 was deemed to identify > 98% of high intensity pixels. The resultant number is recorded as the PD pixel intensity (PDThA).

Figure 2-4: Quantitative assessment of MCP Power Doppler signal using Image J.

A: Frame 9 / 27, selected still image of MCP with maximum PD signal. A yellow free hand drawn line depicts the region of interest equivalent to the synovial area. **B:** A graphic representation of the analysis indicating the maximum PD pixels analysed for each frame of the cine loop. **C:** Spreadsheet output from the Image J macro indicating the frame analysed, the pixel area drawn as the region of interest, the PD pixels within this region of interest, the number of PD pixels over a designated threshold and the frame chosen as the maximum representative PD signal (in this case frame 9).

A

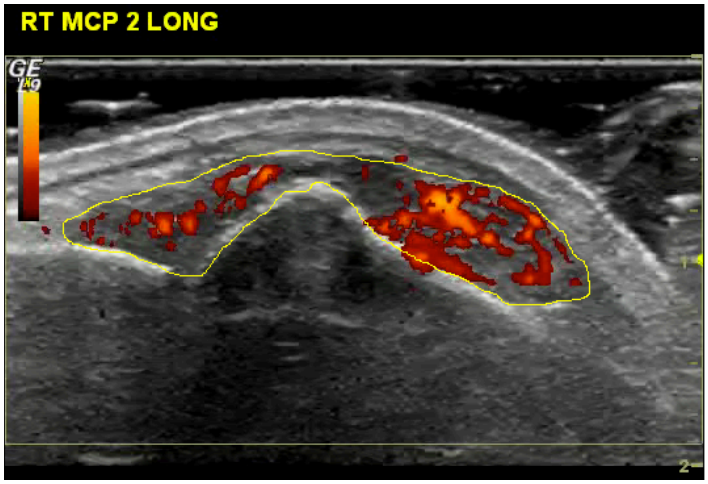

B

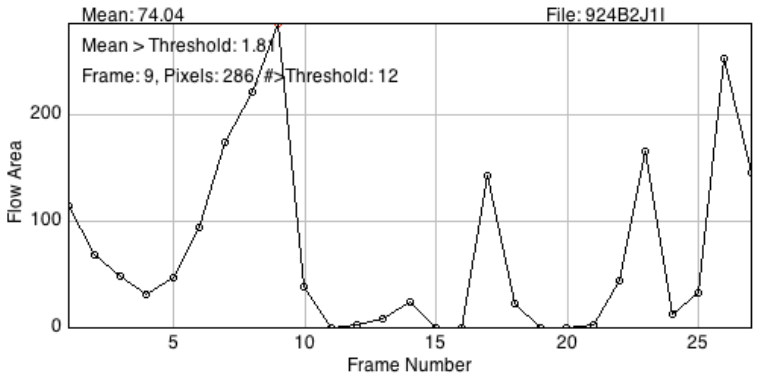

C

Frame	Area_Pixels	PD_Pixels	PDTh_Pixels	Chosen Frame
1	19483	115	0	0
2	19483	70	0	0
3	19483	49	0	0
4	19483	32	0	0
5	19483	48	0	0
6	19483	95	0	0
7	19483	175	0	0
8	19483	223	0	0
9	19483	286	12	1
10	19483	39	0	0
11	19483	0	0	0
12	19483	4	0	0
13	19483	9	0	0
14	19483	25	6	0
15	19483	0	0	0
16	19483	0	0	0
17	19483	144	2	0
18	19483	24	0	0
19	19483	0	0	0
20	19483	0	0	0
21	19483	3	0	0
22	19483	45	0	0
23	19483	166	0	0
24	19483	14	0	0
25	19483	33	0	0
26	19483	254	15	0
27	19483	146	14	0

2.2.4 3D Qualitative score MCP / Wrists

3D images were acquired from MCP an wrist joints. Only the vascular score was examined in this thesis. The acquired 3D volumetric DICOM image was processed in a DICOM viewing platform (4D View® GE Healthcare). The resultant DICOM image was displayed as three 2D images (longitudinal x axis, transverse z axis and coronal y axis) and as a 3D composite image. The reconstructed image was set to ‘3D angio’ which removed all grey scale voxels leaving only Power Doppler Voxels and producing a ‘3D angiogram’. The resultant image was analyzed according to a standardized image set on an ordinal scale ranging from 0 to 4: 0, no synovial thickening; 1, minimal; 2; mild; 3, moderate; 4, severe. (appendix 1) which represented the spectrum of 3D vascularity.

2.2.5 3D Quantitative score MCP / Wrists

The 3D volume data was acquired using the dedicated 4D16L Probe (3D Settings). This provided a standard 19 degrees mechanical sweep from the baseline (38 degrees from start to finish of volume data acquisition). This took approximately 5 seconds whilst the probe was lightly held over the joint being imaged. For MCP joints a transverse 2D image through the centre of the joint was used as the mid reference point of the 3D probe. Once this image was acquired, the 3D settings were activated. The linear array within the probe swings to the edge of the probes foot print to being the mechanical generated sweep. Provided there is no movement of the probe the mid point should correspond to the centre of the joint as identified on with the 2D settings.

The acquired 3D volumetric DICOM image was processed in a DICOM viewing platform (4D View® GE Healthcare). The resultant DICOM image was displayed as three 2D images (longitudinal x axis, transverse z axis and coronal y axis) and as a 3D composite image.

The 3D image was selected and the VOCAL^{TM} function on the software enabled to provide volumetric measurements. The grey scale component to the 3D image was removed leaving only the PD signal (3D angiogram). Using the scalpel mode the digital vessels were removed leaving only the synovial 3D vascular signal.

The remaining volume was calculated in cm^3. The PD volume calculation was made by using the vascular index (VI). This is the percentage of voxels within the defined region of interest. Therefore the PD volume (cm^3) was measured by:

PD volume = (Histogram Volume x VI) / 100

Flow Index (FI) was also recorded and is a measure of the intensity of the doppler signal and an attempt to quantify the velocity of blood flow.

Vascularization flow index (VFI) is a related calculation which attempts to quantify the number of high intensity (fast moving) voxels in the Histogram Volume.

Figure 2-5: Quantification of 3D Power Doppler volume data set

A: 3D reconstruction of volumetric data to provide longitudinal, coronal and transverse images. There is a 3D reconstruction of the Power Doppler image which can be manipulated and rotated about each axis. **B:** identification and outline of the right digital vessel using the scalpel function. This allows the region encircled to be eliminated from the 3D reconstruction. **C:** Further use of the scalpel function to remove other vessels. **D:** Remaining synovial Power Doppler voxel signal for analysis.

A

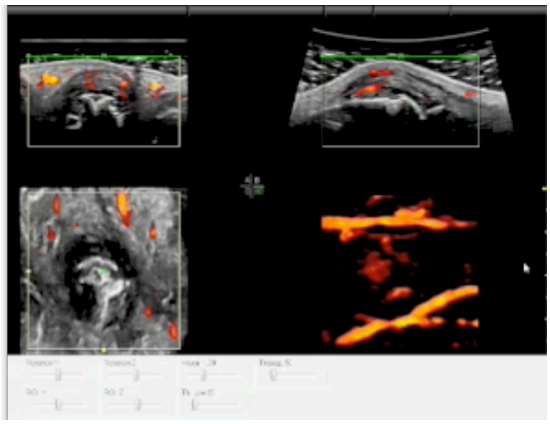

B

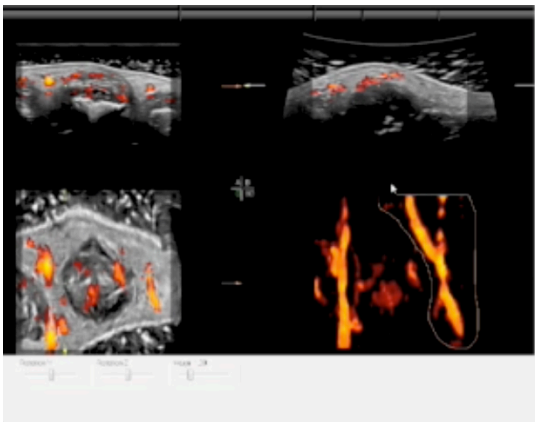

C

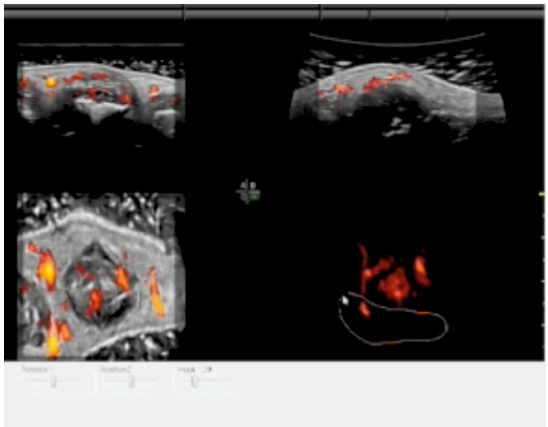

D

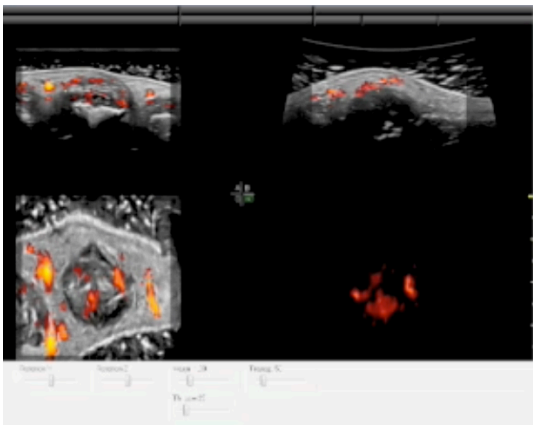

2.2.6 Topographical Image Scoring (TUI)

The 3D volume data may be analysed by topographical sections as well as the reconstructed global image described in the sections above. To facilitate the topographical scoring of the volumetric data set the 3D DICOM viewing platform (4D View® GE Healthcare) can be selected to display the topographical image by selecting TUI on the viewing menu. This produces a topographical display of longitudinal images through the acquired volume data. Further manipulation can be performed by modification of the central reference slice, the number of slices and distance between slices. The display shows 9 images at any given moment but sections can be scrolled through to gain an overall view of the data set. Care was taken on acquiring the data set that the mid point of the 3D probe was placed in the transverse position within the centre of the joint in a similar fashion as the 2D transverse probe position. This allows the 19 degrees sweep to cover the extent of the dorsal surface of the joint and the subsequent topographical longitudinal images to extend form the head of the proximal phalange to the synovial recess behind the neck of the metacarpal bone.

For standardisation the topographical settings used were:

No. Slices - 15

Distance between slices - 0.5mm

Central slice - positioned on the mid point of the metacarpal head

Topographical scores recorded were based on the TUI slice deemed to show maximal PDS. include:

TUI - PDS score - 0-4

TUI - ST score - 0-4

Figure 2-6: Topographical imaging of the 2nd MCP joint showing PDS.

Topographical display of the an MCP joint form a 3D volumetric data set. A reference image is positioned in the top left hand corner in a transverse view with longitudinal sections displayed in the remaining 8 spaces. The reference image can be used to orientate and aline the central slice as the number and distance between each slice can be adjusted.

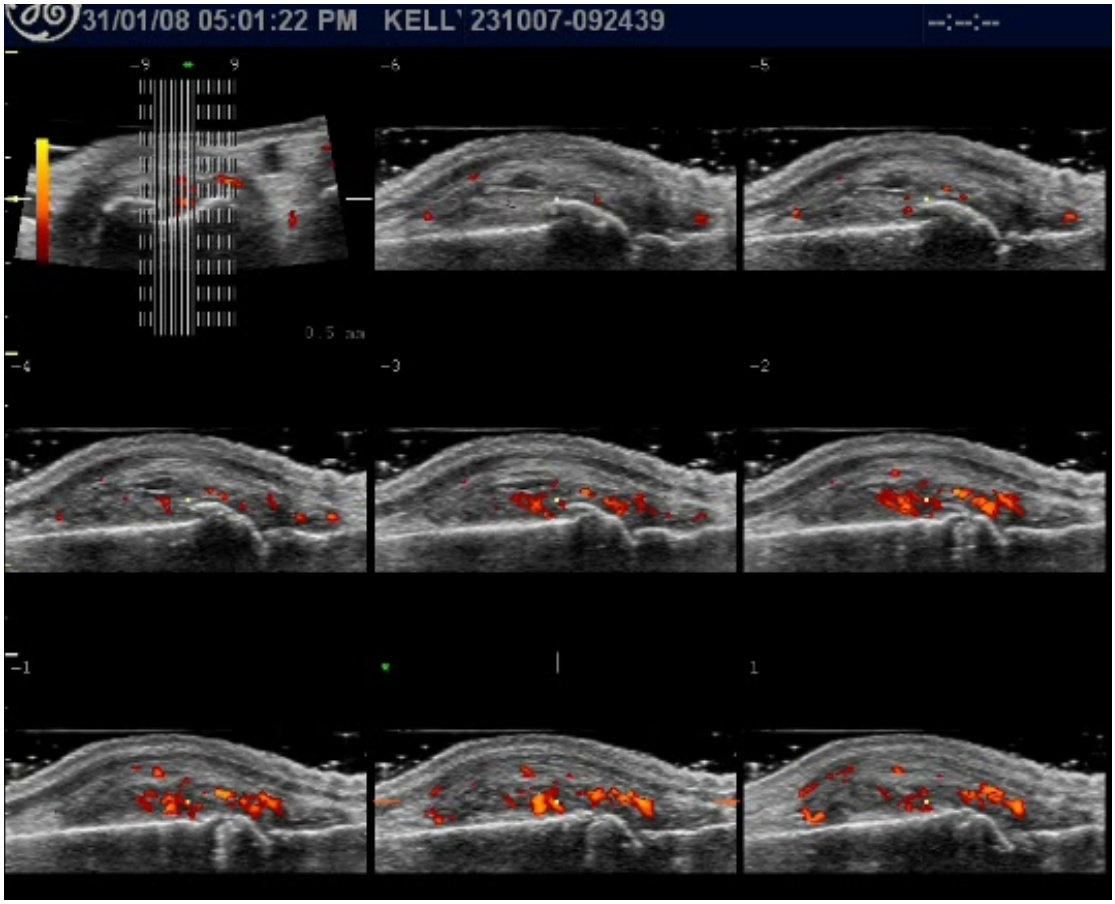

2.3 Clinical Efficacy Assessments

2.3.1 Disease Activity

The primary measure of disease activity in this study is the DAS28(CRP). The components of the DAS28(CRP) are the number of tender joints (28 joint count), the number of swollen joints (28 joint count), a Global Health index (100 mm VAS), and the CRP (in mg/L). An example of the form that can be used for the DAS28(CRP) calculation is found in Appendix 6.8. The formula for determining the DAS28(CRP) is as follows:

$$DAS28(CRP) = 0.56*\sqrt{(TJC28)} + 0.28*\sqrt{(SJC28)} + 0.36*\ln(CRP+1) + 0.014*GH(VAS) + 0.96$$

Assessment of Tenderness – 28 Tender Joint Count (TJC28): The following 28 joints will be assessed for tenderness in response to pressure and/or passive motion.

Finger Proximal Interphalangeal Joints (8), thumb interphalangeal joint (2), metacarpophalangeal (MCP) (10), wrists (2) (includes carpometacarpal, intercarpal, and radiocarpal), elbows (2), shoulders (2), and knees (2).

During the assessment of pain on passive motion, no concurrent pressure will be applied to the joint margin. During pain on passive motion testing, the joint will be moved through the full available range in order to detect any end range pain.

Joint pain with palpation or pain on passive motion (either is sufficient) will be scored according to the following scale:

No pain (0)

Patient states that there is pain (1)

Assessment of Swelling – Swollen Joint Count (SJC): 28 joints will be assessed for the presence of swelling. The joints to be evaluated will be the same as those evaluated for tenderness. Joint swelling on palpation will be scored according to the following scale:

No swelling (0) Swelling (1)

Examination of the upper extremities will be performed with the patient in the sitting position. Any joint that has undergone a replacement arthroplasty, small joint synovectomy, or has had an intraarticular corticosteroid injection within the last 3 months, should not be included in the SJC/TJC or ultrasound measures. NA will be used to grade such joints.

Patient's Global Assessment of Arthritis Condition

The patient will be evaluated for their global status of arthritis condition using the 100 mm ungraded visual analogue scale (VAS).

2.3.2 Health Assessment Questionnaire (HAQ; Disability Scales)

The HAQ is usually self-αdministered, but may also be given face-to-face in these clinical studies. The Disability Index consists of eight categories assessed by the Disability Index are 1) dressing and grooming, 2) arising, 3) eating, 4) walking, 5) hygiene, 6) reach, 7) grip, and 8) common daily activities. For each of these categories, patients report the amount of difficulty they have in performing two or three specific activities. Patients usually find the HAQ Disability Index entirely self-explanatory. The HAQ – Disability Index questionnaire is in Appendix 6.6.

2.4 Ethics

All studies described in this thesis were reviewed and approved by local ethics committees. All study procedures, patient management and data collection was performed according to Good Clinical Practice (GCP).

Relevant ethics approvals are listed below:

1. An exploratory investigation into the molecular mechanisms of Response-Relapse-Resistance to Rituximab therapy in RA patients (R4-RA study) - REC reference number: 10/H1109/23
2. Clinical responsiveness to anti-TNFα therapy and modulation of synovial lymphoid structures and B cell function in RA - REC reference number: 10/H0801/47
3. Lymphoid Neogenesis In Rheumatoid Arthritis: The histomorphological pattern of the synovial membrane (SM) predicts disease outcome - REC reference number: 05/Q0703/92
4. A Randomized, Double-βlind, Parallel Group, Placebo Controlled Study to Assess the Effects of Oral Prednisone on Clinical Efficacy and the Power Doppler Ultrasound Signal of Synovium in Patients with Rheumatoid Arthritis - REC Reference Number: 08/H0718/37
5. Mechanisms of joint inflammation in rheumatic diseases - Guys Hospital REC Reference Number: 01/05/02

3. Reliability of 2D and 3D ultrasound imaging endpoints

3.1 Introduction

The acquisition and scoring of ultrasound images is an important aspect of its validity and utilization in both clinical and research settings. Previous authors have examined the variability of reading images but few have attempted to address the issue of variability in respects to image acquisition and the consistency of agreement between readers at different points in the study timeline.

In collaboration with a colleague, Matt Seymour - based at the Kennedy Institute of Rheumatology, we incorporated in to the design of a randomized controlled study serial ultrasound assessments at baseline and the end of study assessment (Day 15) to address these questions.

3.2 Aims

This component of the study evaluated a number of the systematic processes involved in image acquisition and interpretation. Specifically, we investigated the reliability of 2D and 3D ultrasonographic endpoints (quantitative and qualitative measures of synovial thickness and vascularity) in MCPJs and wrists.

3.3 Reader Definitions

Assessment of reliability has been complicated by a diversity of nomenclature employed by different investigators. Terms for assessment of reliability are redefined below to avoid confusion. The ultrasonographer also a reader of the anonymised images. Imaging was performed at two centers (Barts Health NHS Trust - BH and Kennedy Institute of Rheumatology - KIR) by two ultrasonographers Stephen Kelly (SK) and Matt Seymore (MS). Both myself and Matt have over 5 years of US experience as ultrasonographers. We were both blinded to the subjects' group allocation (i.e. Placebo or treatment group). We spent approximately five, three hour sessions before the study to gain consensus on image acquisition and analysis. A data set denotes 2D (longitudinal and transverse) and 3D images of the MCP and wrists.

Within scan intra-reader

1 patient, 1 ultrasonographer acquires one data set, 1 reader reads the scan set twice; each reading is separated by a fixed time period (previously called intra-reader and intraobserver).

Within scan inter-reader

1 patient, 1 ultrasonographer acquires one scan set, 2 independent readers (previously called inter-reader, interobserver and inter-investigator).

Parallel scan intra-reader

1 patient, 1 ultrasonographer acquires two scan sets sequentially, 1 reader independently reads both scan sets (previously called intraobserver).

Parallel scan inter-reader

1 patient, 2 ultrasonographers each acquire a scan set independently, 2 readers each read their own acquired scan set independently (previously called interobserver).

To determine reliability (within scan inter-reader, parallel scan intra-reader and parallel scan inter-reader) three scans were sequentially acquired at Day 1 (baseline) and on Day 15 according to table 1.

3.4 US endpoint definitions

2D US endpoint definitions

A detailed description of these measurements can be found in chapter 2 .

2D Trans PDA - Sum of 10MCP Joints Quantitative Transverse Power Doppler Area

2D Long PDA - Sum of 10MCP Joints Quantitative Longitudinal Power Doppler Area

2D Long VASCi - Sum of 10MCP Joints Qualitative Longitudinal Synovial Vascularity

2D Trans VASCi - Sum of 10MCP Joints Qualitative Transverse Synovial Vascularity

2D Long STi - Sum of 10MCP Joints 2D Qualitative Longitudinal Synovial Thickness

2D Trans STi - Sum of 10MCP Joints 2D Qualitative Transverse Synovial Thickness

2D Long STA - Sum of 10MCP Joints Quantitative Longitudinal Synovial Thickness Area.

2D Trans STA - Sum of 10MCP Joints Quantitative Transverse Synovial Thickness Area.

3D US measures definitions

3D VASCi - Sum of 10MCP Joints 3D Qualitative Synovial Vascularity Score

3D PD Vol - Sum of 10MCP Joints 3D Quantitative Power Doppler Volume

3D VFI - Sum of 10MCP Joints 3D Quantitative Power Doppler Volume qualified for a predetermined thresholded of signal intensity.

3.5 Method

The study design is shown in figure 3-1. This was a randomized, double-βlind, parallel group, placebo controlled study to assess the effects of oral prednisone on clinical efficacy and power Doppler ultrasound signal of synovium in patients with Rheumatoid Arthritis. The study was divided into a Panel A (18 patients receiving 15mg of Prednisone daily or placebo) and Panel B (27 patients receiving 7.5mg Prednisone daily or Placebo). The ICC data was collected form Panel A patients only. This study was conducted over 2 centers both using a GE Logiq9 ultrasound machine. The treatment group received 15mg of Prednisone daily for the duration of the study. 2D images were acquired with a 2-dimensional M12L transducer and 3D images with a 4D16L Probe. Subjects were imaged over the dorsum of all 10 MCPJs and the dorsum of the wrist for 3D scans only.

Serial scanning (3 scans, 2 ultrasonographers) occurred at Days 1, and 15 in the longitudinal and transverse planes for 2D imaging and for all MCPJs and wrists for 3D imaging. Longitudinal images were recorded in the midline with the hand of the metacarpal bone, proximal phalenge and extensor tendon in view. Transverse images were acquired through the centre of the joint with the image centralised to show both the medial and lateral aspects of the joint. Settings were identical on both GE Logiq9 ultrasound machines (appendix 1). To standardise data acquisition, the hands were maintained in a position of rest by a splint (identical at both sites). The time of day of scanning at each visit was within 1 hour of the time of the baseline visit. Care was taken when scanning to avoid undue pressure with the probe in case this altered blood flow in the joint. This was achieved by maintaining a distance of at least 1 mm of gel between the probe and the subject as visualised on the US monitor. Three scans were sequentially acquired at baseline and on Day 14

according to the scheme described in table 3-1. Each 2D scan data set consists of a grey scale still images and power doppler movie clip that covers 3 or 4 cardiac cycles of all 10 MCPjs. The 3D scan data set involved all 10 MCPJs and both wrists. Each data set was identified with a unique ID number for blinding purposes.

Figure 3-1: Overview view of randomised controlled study design showing ultrasound and clinical assessments.

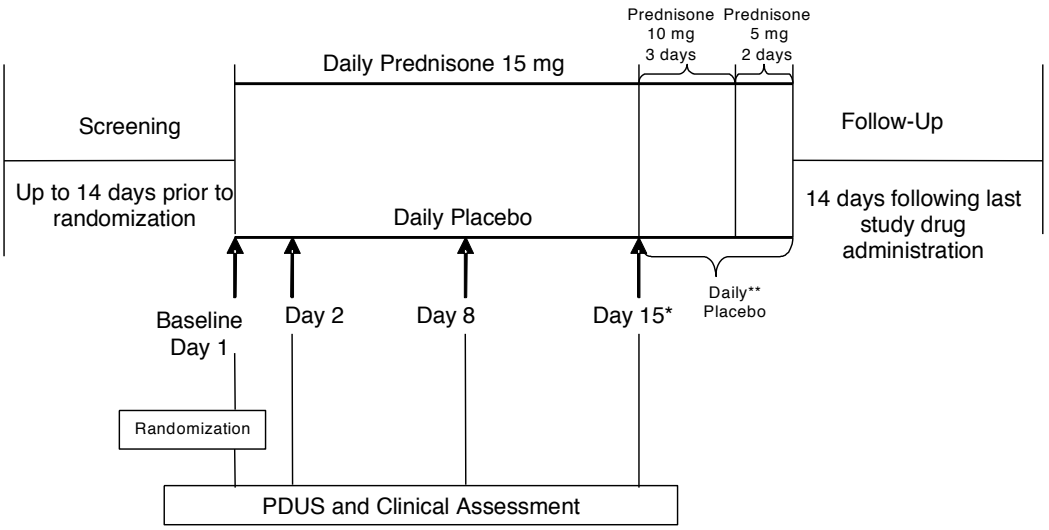

Table 3-1: Table describing the scan order at each site and from each ultrasonographer during the coarse of the study for panel A only.

Site	Scan	Ultrasonographer	Reader
BH	1	SK	SK
			MS
	2	MS	MS
	3	SK	SK
KIR	1	MS	SK
			MS
	2	SK	SK
	3	MS	MS

Patients suitable for this study all met the 1987 ACR criteria for diagnosis of Rheumatoid Arthritis and will had at least moderate disease activity, measured by a DAS28(CRP) score of at least 3.2 at screening. In addition, patients had evidence of

moderately active synovitis in at least 2 MCP joint characterized by a score of ≥2 or high synovial activity in at least 1 MCP joint characterized by a score = 4. The synovial activity was assessed by a 2-dimensional Transverse Synovial Vascularity Score (2D Trans VASCi) of synovial blood flow on PDUS of the MCP joint, using a 0 to 4 scale, with 4 being severe PDUS signal (Appendix 1 for US atlas). Rather than investigating the reliability on an individual joint basis, the of a summation of 10 MCPJs was used as this represented the primary outcome measure. 3D MCP joints scans were also treated similarly with a summation of the scores over 10 MCPJs whilst the wrists were treated as a sum of 2 scans.

Both myself and MS were blinded in the reading of the scan data set to both the patient and the timing of the scan (e.g. Day 1 / 2 / 8 / 15). Unblinding took place after all data sets had been scored.

3.6 Results

3.6.1 2D US Endpoints

Within scan intra-reader reliability was not examined in this study i.e. reading of the same scan by the same reader on 2 occasions. The results of all the baseline and Day 15 Interclass Correlation Coefficients (ICC) values and Coefficient of Variation (CV) can be found in table 3-1 and 3-2.

Within scan inter-reader:

For the primary end point of the study the (2D Trans 10MCP PDA) the intraclass correlation coefficient for the readings made in the 2 centers was very high, 0.99 (CI 0.98 - 1.00) (Table 3-1). Visual inspection of Bland-ɑltman plots (scatterplots of the average of the two baseline measurements read by the 2 readers versus the difference of the 2 measurements) didn't provide any evidence that the magnitudes of the differences are not constant throughout the range of baseline measurements. The mean difference (bias) between the readings of the baseline value was 0.54 with a 95% CI equal to (-0.01, 1.1); the 95% limits of agreement were equal to (-1.7, 2.8)

i.e. approximately 10% of the measurement scale. At Day 15, the ICC remained high 1.00 with a lower bound for the 95% CI greater than 0.99 (table 3-1). Generally, the synovial greyscale, qualitative and quantitative, measurements for synovial area were less robust than for their corresponding PD measurements. As already described, the primary end point of this study showed near perfect agreement (ICC 0.99) as did the qualitative Trans VASCi score (ICC 0.92, CI 0.84-0.99), however both the Trans synovial thickness measures showed moderate agreement (Trans STA - 0.52, Trans STi - 0.48).

At Day 15, there was similarly good / excellent agreement between all longitudinal endpoints with the best results seen with 2D Trans PDA (ICC 1.00, CI 0.99-1.00) followed by 2D Long VASCi (ICC 0.94, CI 0.88 - 1.00). For the primary endpoint (2D Trans PDA), the Bland-αltman plots didn't provide any evidence that the magnitudes of the differences are not constant throughout the range of measurements; see Figure 3-2. The mean difference (bias) between the readings of the difference value was -0.13 with a 95% CI equal to (-0.6, 0.3) in the placebo group and was 0.08 with a 95% CI equal to (-0.9, 1.1); the 95% limits of agreement were (-1.5, 1.2) and (-2.3, 2.5) in the placebo and prednisone groups respectively; these limits are therefore between 5% and 10 % of the measurement scale.

Figure 3-2: Bland-altman Plot of the primary end point (2D Trans PDA) for two readers evaluation of baseline data set.

The red line represents the difference between the 2 readings (bias) for both groups combined, the green lines are the limits of agreement.

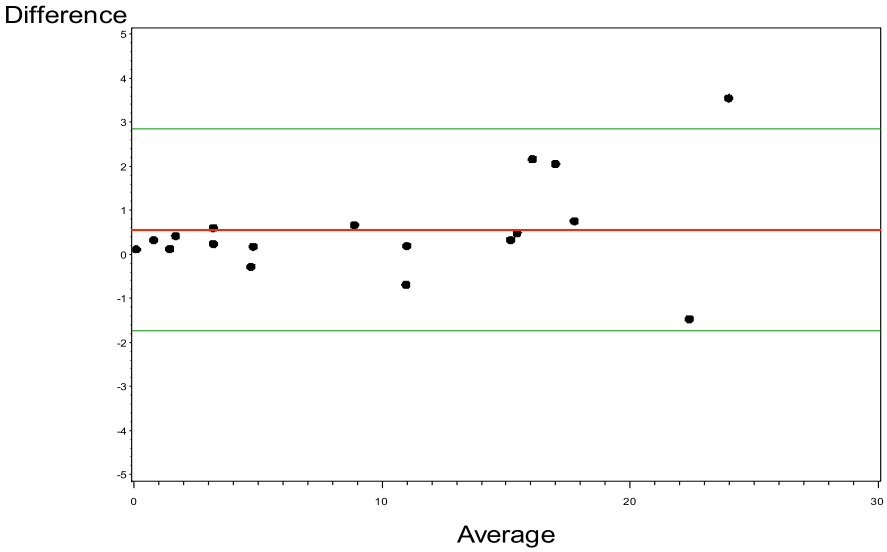

Figure 3-3: Bland-altman Plot of the primary end point (2D Trans PDA) for two readers evaluation of the Day 15 data set for placebo and treatment groups

The red continuous lines present the difference between the 2 readings (bias) and limits of agreement for the placebo group; the green dashed lines present the difference between the 2 readings (bias) and limits of agreement for the prednisone group. (● - Prednisone, * - Placebo).

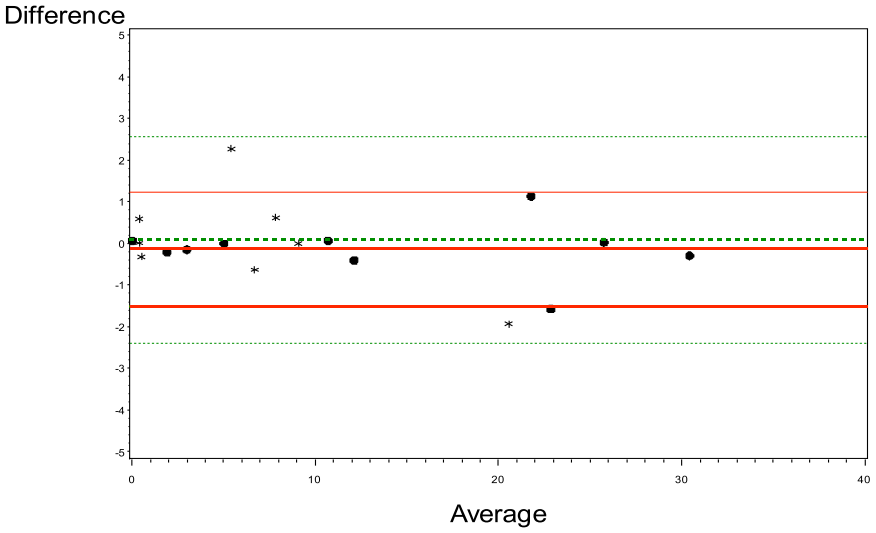

Parallel scan intra-reader:

Agreement between the 2 baseline scans readings by the same reader was good e.g. ultrasonographer SK performs 2 scan data sets on day 1 and SK scores both) The ICC values were > 0.70 for all endpoints; the coefficient of variation was smallest for the 2D Long STA (7%) and largest for the 2D Long PDA (57%).

At Day 15, a good or excellent agreement was seen with all end points, ICC > 0.76, except for 2D Long PDA which showed moderate agreement ICC 0.62 (0.36; 0.88). Visual inspection of the Bland-αltman plots didn't provide any evidence that the magnitudes of the differences are not constant throughout the range of measurements both at baseline and Day 15. The coefficient of variation at baseline for all endpoints was less than 30% but increased significantly to Day 15.

Parallel scan inter-reader:

Agreement between the 2 baseline scans readings by different readers was good with ICC values > 0.68 for all endpoints except for Trans STA and STi. The coefficient of variation was smallest for the 2D Long STA (12%) and largest for the 2D Long PDA (60%). Significant differences between the 2 readings were detected for each of the endpoint.

At Day 15, the endpoints concerning synovial thickness and in particular Trans STi shoed poor agreement. Trans VASCi continues to show excellent agreement between readers, ICC 0.85 (CI 0.72 - 0.99) with a coefficient of variation of 40%.

Table 3-1: Inter class correlation coefficient (ICC) baseline results for all US endpoints

Inter class correlation coefficient (ICC) baseline results for all US endpoints (95% CI) and co-efficient of variation (CV) expressed as a percentage with 95% CI.

End Point	Scan and reader	ICC	95% CI	CV	95% CI
2D Long PDA	Within scan inter-reader	0.89	(0.80; 0.99)	30.8	(23.7; 44.7)
	Parallel scan intra-reader	0.80	(0.64; 0.96)	57.3	(42.5; 90.4)
	Parallel scan inter-reader	0.78	(0.59; 0.97)	60.1	(44.4; 96.0)
2D Long STA	Within scan inter-reader	0.76	(0.56; 0.95)	12.4	(9.7; 17.4)
	Parallel scan intra-reader	0.95	(0.90; 1.00)	7.1	(5.6; 10.0)
	Parallel scan inter-reader	0.85	(0.72; 0.98)	11.6	(9.1; 16.3)
2D Long STi	Within scan inter-reader	0.67	(0.40; 0.93)	14.0	(11.0; 19.8)
	Parallel scan intra-reader	0.87	(0.75; 0.99)	10.9	(8.5; 15.3)
	Parallel scan inter-reader	0.67	(0.42; 0.93)	14.8	(11.6; 20.9)
2D Long VASCi	Within scan inter-reader	0.90	(0.81; 0.99)	18.7	(14.6; 26.6)
	Parallel scan intra-reader	0.93	(0.87; 0.99)	16.8	(13.1; 23.8)
	Parallel scan inter-reader	0.83	(0.67; 0.98)	27.9	(21.5; 40.2)
2D Trans PDA	Within scan inter-reader	0.99	(0.98; 1.00)	7.7	(6.0; 10.8)
	Parallel scan intra-reader	0.75	(0.57; 0.93)	43.7	(33.1; 65.7)
	Parallel scan inter-reader	0.72	(0.51; 0.93)	51.0	(38.2; 78.7)
2D Trans STA	Within scan inter-reader	0.52	(0.33; 0.72)	6.1	(4.8; 8.6)
	Parallel scan intra-reader	0.83	(0.68; 0.98)	9.7	(7.6; 13.6)
	Parallel scan inter-reader	0.57	(0.24; 0.89)	13.8	(10.8; 19.5)
2D Trans STi	Within scan inter-reader	0.48	(0.19; 0.76)	20.2	(15.7; 28.7)
	Parallel scan intra-reader	0.83	(0.68; 0.98)	15.3	(12.0; 21.7)
	Parallel scan inter-reader	0.00	(-0.46; 0.46)	32.1	(24.7; 46.7)
2D Trans VASCi	Within scan inter-reader	0.92	(0.84; 0.99)	15.7	(12.3; 22.2)
	Parallel scan intra-reader	0.73	(0.52; 0.94)	30.8	(23.8; 44.8)
	Parallel scan inter-reader	0.68	(0.45; 0.92)	32.4	(25.0; 47.3)

Table 3-2: Inter class correlation coefficient (ICC) results for all US endpoints at DAY 15

Inter class correlation coefficient (ICC) results for all US endpoints at DAY 15(95% CI) and co-efficient of variation (CV) expressed as a percentage with 95% CI.

End Point	Scan and reader	ICC	95% CI	CV	95% CI
2D Long PDA	Within scan inter-reader	0.98	(0.95; 1.00)	21.8	(16.9; 31.6)
	Parallel scan intra-reader	0.62	(0.36; 0.88)	259.8	(126.1; 788)
	Parallel scan inter-reader	0.68	(0.45; 0.92)	153.5	(92.3; 496.3)
2D Long STA	Within scan inter-reader	0.81	(0.65; 0.97)	13.0	(10.1; 18.6)
	Parallel scan intra-reader	0.83	(0.68; 0.98)	12.4	(9.6; 17.7)
	Parallel scan inter-reader	0.71	(0.48; 0.95)	17.6	(13.6; 25.2)
2D Long STi	Within scan inter-reader	0.54	(0.20; 0.88)	20.5	(15.9; 29.6)
	Parallel scan intra-reader	0.82	(0.66; 0.98)	12.9	(10.1; 18.5)
	Parallel scan inter-reader	0.46	(0.07; 0.85)	23.9	(18.4; 34.7)
2D Long VASCi	Within scan inter-reader	0.94	(0.88; 1.00)	27.4	(21.1; 40.0)
	Parallel scan intra-reader	0.94	(0.88; 1.00)	31.9	(24.4; 47.1)
	Parallel scan inter-reader	0.85	(0.72; 0.99)	40.5	(30.6; 61.2)
2D Trans PDA	Within scan inter-reader	1.00	(0.99; 1.00)	10.2	(7.9; 14.5)
	Parallel scan intra-reader	0.76	(0.57; 0.94)	83.4	(58.4; 152.1)
	Parallel scan inter-reader	0.75	(0.55; 0.96)	74.3	(53.0; 129.0)
2D Trans STA	Within scan inter-reader	0.57	(0.36; 0.79)	7.9	(6.2; 11.2)
	Parallel scan intra-reader	0.92	(0.85; 0.99)	7.6	(5.9; 10.8)
	Parallel scan inter-reader	0.40	(0.01; 0.80)	18.0	(13.9; 25.9)
2D Trans STi	Within scan inter-reader	0.36	(0.10; 0.62)	21.7	(16.8; 31.4)
	Parallel scan intra-reader	0.77	(0.58; 0.97)	22.9	(17.7; 33.1)
	Parallel scan inter-reader	0.01	(-0.46; 0.48)	35.1	(26.8; 52.3)
2D Trans VASCi	Within scan inter-reader	0.96	(0.92; 1.00)	20.1	(15.6; 29.0)
	Parallel scan intra-reader	0.91	(0.84; 0.99)	23.4	(21.4; 61.3)
	Parallel scan inter-reader	0.78	(0.60; 0.96)	37.1	(12.6; 84.9)

3.6.2 3D US Endpoints

For the selected 3D vascular endpoints, Within scan intra-reader reliability was also examined. The results of all the baseline and Day 15 Interclass Correlation Coefficients (ICC) values and Coefficient of Variation (CV) can be found in table 3-3 and 3-4.

Within scan intra-reader

The baseline and Day 15, 3D US endpoint data set was read and re-read after a 2 month delay. The agreement between these two readings at baseline were excellent with a 3D PD Vol ICC of 0.98 (CI 0.97 - 1.00) and 3D VASCi, qualitative measure, of 0.95 (CI 0.91 - 0.99). The agreement continued to be excellent following treatment at Day 15. The Bland-αltman plots didn't provide any evidence that the magnitudes of the differences are not constant throughout the range of measurements Figure 3-4 and 3-5

Within scan inter-reader

Excellent ICC results were obtained with all 3D endpoints ICC > 0.89. This was observed at baseline and at Day 15.

Parallel scan intra-reader

This reading provided the poorest agreement with all endpoints giving only moderate agreement with 3D VASCi having an ICC of 0.53 (CI 0.22- 0.84) and a coefficient of variation 59% (CI 43.8-94.4).

Parallel scan inter-reader

Excellent ICC results were obtained with all 3D endpoints and this was observed at baseline and at Day 15.

Figure 3-4: Bland-altman Plot of the 3D VASCi endpoint for two readers evaluation of a baseline data set.

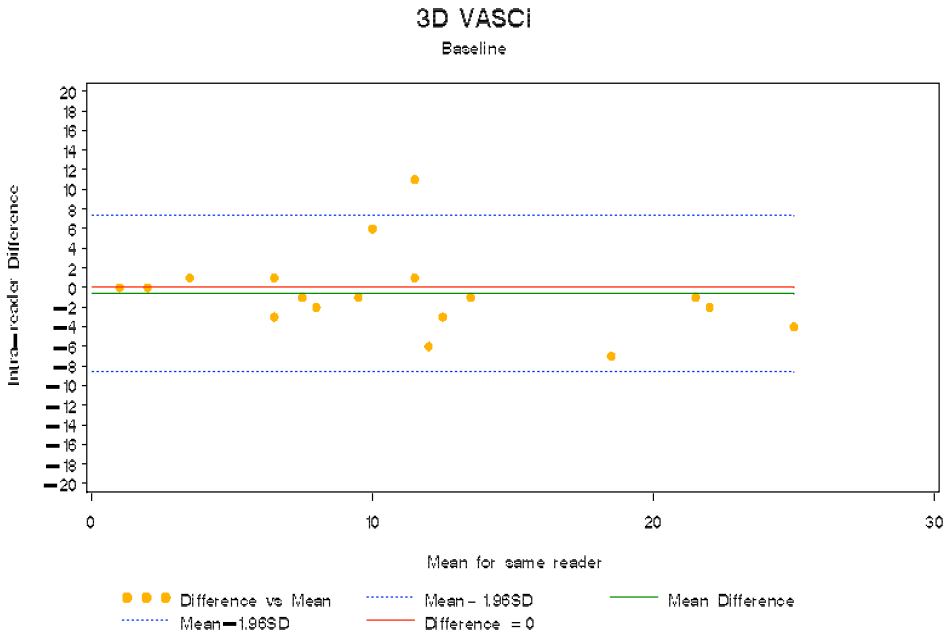

Figure 3-5: Bland-altman Plot of the 3D Power Doppler volume (3D PD Vol) endpoint for two readers evaluation of a baseline data set.

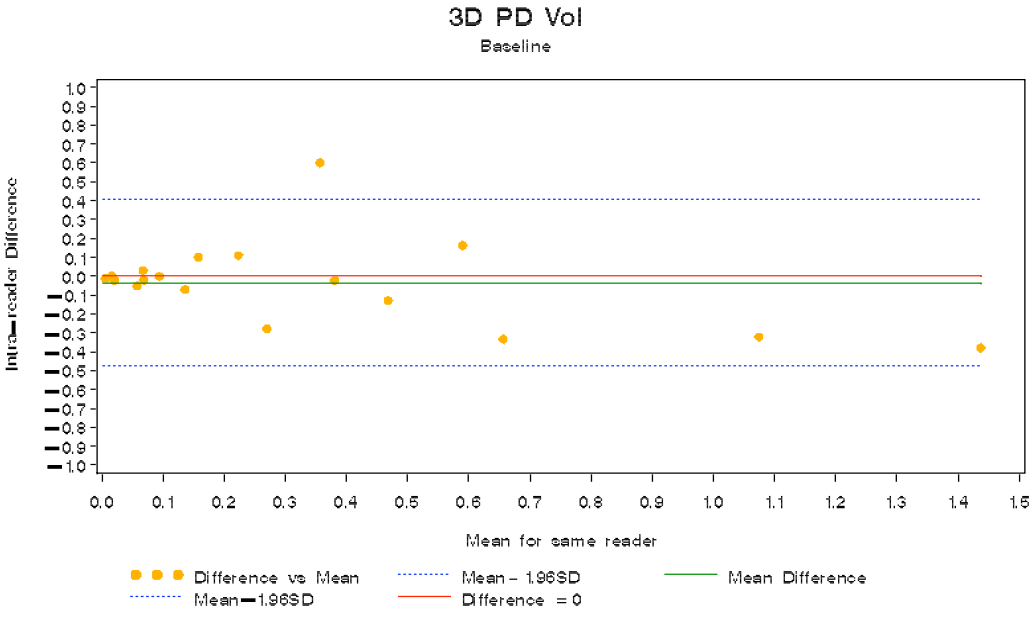

Table 3-3: Inter class correlation coefficient (ICC) baseline results for all 3D US endpoints

Inter class correlation coefficient (ICC) baseline results for all 3D US endpoints (95% CI) and co-efficient of variation (CV) expressed as a percentage with 95% CI.

Endpoint	Comparison	ICC	95% CI	CV	95% CI
3D PD Vol	Within scan intra-reader	0.98	(0.97; 1.00)	9.3	(4.2; 17.9)
	Within scan inter-reader	0.97	(0.95; 1.00)	18.9	(14.7; 26.8)
	Parallel scan intra-reader	0.69	(0.44; 0.94)	121.7	(79.2; 277.2)
	Parallel scan inter-reader	0.85	(0.73; 0.98)	49.2	(37.0; 75.4)
3D VASCi	Within scan intra-reader	0.95	(0.91; 0.99)	12.1	(6.8; 22.6)
	Within scan inter-reader	0.89	(0.79; 0.99)	22.4	(17.4; 32.0)
	Parallel scan intra-reader	0.53	(0.22; 0.84)	59.3	(43.8; 94.4)
	Parallel scan inter-reader	0.84	(0.70; 0.98)	26.4	(20.5; 38.0)
3D VFI	Within scan intra-reader	0.99	(0.98;1.00)	9.8	(3.2; 15.7)
	Within scan inter-reader	0.97	(0.93; 1.00)	22.8	(17.7; 32.5)
	Parallel scan intra-reader	0.70	(0.45; 0.94)	124.8	(80.7; 291.4)
	Parallel scan inter-reader	0.83	(0.69; 0.98)	54.5	(40.6; 85.2)

Table 3-4: Interclass correlation coefficient (ICC) Day 15 results for all 3D US endpoints

Interclass correlation coefficient (ICC) Day 15 results for all 3D US endpoints (95% CI) and co-efficient of variation (CV) expressed as a percentage with 95% CI.

Endpoint	Comparison	ICC	95% CI	CV	95% CI
3D PD Vol	Within scan intra-reader	0.98	(0.94; 1.00)	10.4	(7.8; 19.3)
	Within scan inter-reader	0.96	(0.92; 1.00)	42.5	(32.1; 64.8)
	Parallel scan intra-reader	0.72	(0.51; 0.93)	468.9	(163.0; .)
	Parallel scan inter-reader	0.91	(0.83; 0.99)	79.0	(55.8; 140.8)
3D VASCi	Within scan intra-reader	0.94	(0.88; 0.97)	10.5	(6.2; 15.3)
	Within scan inter-reader	0.91	(0.82; 0.99)	29.8	(22.8; 43.7)
	Parallel scan intra-reader	0.39	(0.03; 0.76)	97.9	(66.4; 194.8)
	Parallel scan inter-reader	0.94	(0.89; 1.00)	22.3	(17.2; 32.2)
3D VFI	Within scan intra-reader	0.96	(0.92; 0.99)	14.2	(4.7; 23.4)
	Within scan inter-reader	0.93	(0.87; 0.99)	42.2	(31.8; 64.1)
	Parallel scan intra-reader	0.63	(0.37; 0.89)	743.0	(187.5; -)
	Parallel scan inter-reader	0.86	(0.74; 0.98)	99.4	(67.2; 199.8)

3.7 Discussion

Interclass correlation coefficient (ICC) was calculated for a number of measurements outlined above at baseline and at Day 15 of this placebo controlled, randomised study (Panel A). As a ultrasound measurement of disease activity was chosen as the primary end point it was important to identify if the ICC remained constant over the course of the study and specifically if a significant change to the US scores following treatment resulted in a deterioration in the reliability of the endpoint. Therefore all US endpoints were calculated at baseline and day 15.

2D US endpoints

The ICC results for the 2D data set used in this clinical study showed good to excellent agreement in many of the US endpoints examined. Generally, the synovial thickness measurements performed less well than the power Doppler counterparts at both baseline and Day 15. In particular the 2D Trans STi showed no agreement for 'Parallel scan inter-reader' measurements and only poor to moderate agreement for 'Within scan inter-reader' measurements. There was a high degree of consistency for all endpoints, including Trans STi ,for 'Parallel scan intra-reader' measurements. The dimensions of the transducers available for use in this study may have been a limitation resulting in weak inter-reader reliability (within-scan or parallel scan) for the Trans STi and Trans STA endpoints. The transducer used in this study had a large foot print relative to the deepest point of the triangular structure (which is a narrow precise location), more than one hyperechoic line, representing bone, is often observed on the saved gray-scale image. This is often the co-localisation of the head of the MCP and PIP joint coming into view. Therefore, myself and MS may have chosen different region of interests depending on which line was selected to represent the lower border of the triangular structure, even though a consensus to use the lowest hyperechoic line was instigated at the beginning of the study.

Most US studies have investigated reliability on a joint by joint basis. Few have assessed reliability of a summation of scores for a selected group of joints. Naredo et

al assessed within scan intra-reader reliability with a resultant excellent ICC value of 0.99 [10] for summated 4-point semi-quantitative PDUS imaging of 28 joints, called the “overall US joint index for power Doppler signal”. Backhaus et al (2009) [31] developed a composite US score called the “German US7 score”. They measured US grey scale synovitis and PD synovitis using 4-point semi-quantitative scales in 7 joints and the within scan inter-reader reliability kappa value was 0.6. The most clinically relevant measure of reliability is the “parallel scan inter-reader” because it is a comparison between two ultrasonographers acquiring and reading their own scans. The images are read independently, as might be the case in multi-site clinical trial or routine clinical practice. As expected the overall reproducibility for ‘parallel scan inter-reader’ reliability was lower than ‘within scan inter-reader’ reliability; the difference between these two methods most likely representing the loss of concordance due to image acquisition. A similar observation was reported by Kamishima et al [32]. Despite this shortfall, in the current study good agreement was observed for the overall ‘parallel scan inter-reader’ reliability. This would suggest that the greatest variable is the source of the US examination i.e. a second ultrasonographer acquiring the data set. This has implications for multi-centered studies using US imaging a dedicated endpoint however the excellent ‘Within scan inter-reader’ agreement would suggest that this effect can be minimized by central analysis of acquired images.

Visual inspection of the The Bland - Altman plots may provide evidence that the magnitudes of the differences in scores are not constant throughout the range of measurements. This was performed at baseline and at the end of the study on Day 15 for all US endpoints . As describe above, 4-point score has been widely used in published US studies. This 5-point score, based upon a standard atlas of images, was used with the hope that it may be more sensitive to change than a 4-point scale. However, with a larger scale there is an inherent risk of reducing the level of agreement between readers. Whilst generally this was not seen, agreement between readers can vary at different points along the scale. The Bland - Altman plots provide

a visual interpretation of agreement by plotting the average of the two baseline measurements read by the 2 readers versus the difference of the 2 measurements. This may also give an indication of bias between the 2 readers. Within this study, there was no indication of significant bias although with 2D Trans STi and Long STi baseline endpoints, some diversion was seen at the high end of the scale.

Quantitative ultrasonographic measures of synovitis demonstrated better overall reliability than semi-quantitative measures although the difference was not statistically significant. Therefore, within future studies there may still be a place for more time-consuming measures of synovitis, by computationally quantifying pixel counts, but quicker semi-quantitative scales may be an acceptable substitute. Power Doppler measures of synovitis were significantly more reproducible than gray-scale measures of synovitis in this study and thus I would advocate that future ultrasound studies include power Doppler vascularity endpoints to deliver optimum reliability.

3D US endpoints

All 3D endpoints showed good to excellent agreement for both baseline. At Day 15 the 3D VASCi 'Parallel scan intra-reader' endpoint had reduced from 0.53 to 0.39 from baseline. All of the other 3D endpoints performed well at both time points. No synovial grey scale 3D images were scored as this was felt that the virtual reconstruction of the image showed insufficient grey scale definition to appreciate synovial and extra-synovial tissue.

The vascular power doppler endpoints were easily identified by the subtraction of all grey scale information on the image leaving only the power doppler voxels, so called '3D angio'. There was excellent agreement in all endpoints for 'within scan intra-reader', 'Within scan inter-reader' and 'Parallel scan inter-reader'. Surprisingly the 'Parallel scan inter-reader' ICC values were consistently less both at baseline and Day 15. Given the excellent 'Within scan intra-reader' results for all the endpoints the lack of agreement in the 'Parallel scan inter-reader' would suggest a that the lack of correlation was due to the image acquisition rather than the reading of the scan data

set. There are two possible explanations for this observation. Firstly, the 3D probe is a single linear array which sweeps through the chosen region of interest at a constant speed recording still images at every 1 degree step. The reconstruction of these still images provides the '3D angio' which is then scored and manipulated. Synovial blood blow varies according to heart rate (figure 3-6). Given that only a single still image is recorded during each increment of the swing of the linear array, it is conceivable that at a number of points along its path a diastolic image is acquired. Should this occur at a site of significant vascular PD signal there may be up to a 50% reduction in signal recorded. As the PD within the synovium is often localised rather than confluent, especially at low grades of signal, there is a significant possibility of signal being completely missed during the 3D sweep of the probe. One possible improvement on current technology is Spatio-temporal image correlation (STIC). This is an automated volume acquisition similar to the 3D technology used in this study however there is a significantly high number of 2D frames recorded (approximately 150 / second). This technology is currently used in foetal heart imaging due to the small region of interest required. This essentially facilitates the alignment of images according to time and space, providing a 4D 'real - time' image. The region of interest is necessarily small and for doppler signal registration, high rates of flow are required which are not seen in the synovium. However, with regards to the reduced ICC seen in the 'Parallel scan intra-reader' 3D endpoints, if a systematic error occurred one might expect that the 'Parallel scan inter-reader' endpoints would have been similarly affected and this was not the case. The large foot print of the 3D probe covers all the MCP dorsal surface and it was not likely that positioning of the probe has a contribution to the variability of image acquisition.

A second possibility, and perhaps more likely, was that there was a thermo-regulatory influence. Each data set required approximately 30mins of scanning. This included 2D images and 3D imaged of MCPJs and Wrists. Warm gel was used at the beginning of the scan data set acquisition, after 90 mins of imaging patients often remarked that their hands felt cold suggesting a degree of cooling may have

occurred reducing the vascular signal seen. The 'Parallel scan intra-reader' ICC results were marginally less than the 'Within scan inter-reader' results for the 2D data set suggesting that this may have an effect here as well.

Figure 3-6: Graphical representation of the change in power doppler pixel count over a 27 frame cine loop

A graph showing the variation of PD pixels over a 3 second cine loop from a longitudinal 2D PD scan within the synovium. 27 frames are recorded in the cine loop (9 frames per second). Patient's heart rate was 62 bpm at the time of the scan.

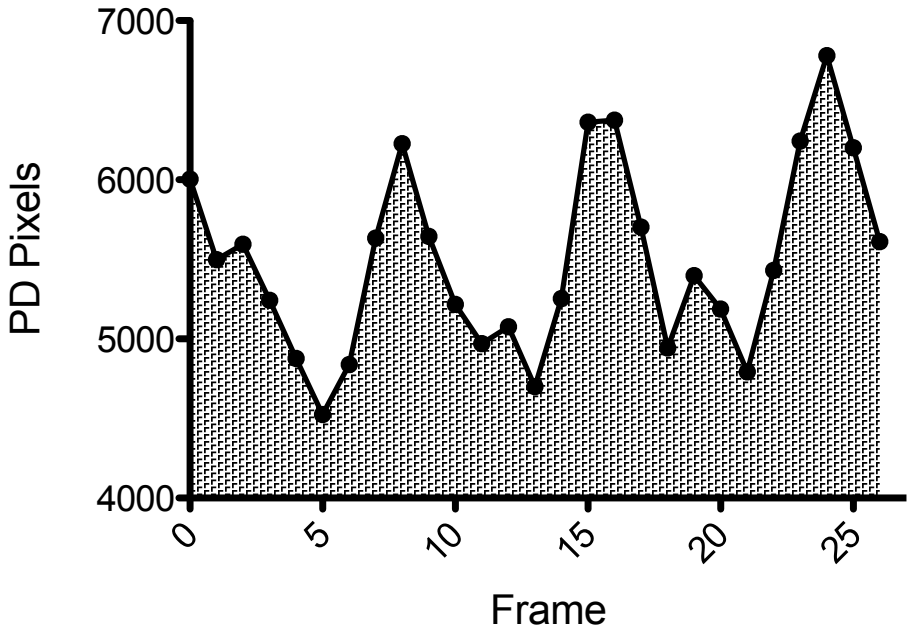

The reproducibility of the clinical examinations was not collected or tested in this study, and so a formal comparison of the precision of synovial US with clinical examination is not possible. Literature references demonstrate that the reproducibility of joint examination is poor. The reliability of the individual clinical examination of MCP swelling had a reported kappa of only 0.36 (Naredo, 2005). A published study examining the ICC for a number of clinical and US measures of disease activity came to the similar conclusions that ultrasound was at least as relevant as clinical examination in the assessment of disease status of patients in an open-label longitudinal treatment study of Humira in rheumatoid arthritis (Dougados, 2009).

Reproducibility was determined for physical examination and ultrasound. The reproducibility of physical examination of MCP and metatarso-phalangeal joint swelling (0-2 score) had a weighted kappa of 0.48 (-0.11 to 1.00) and the reproducibility of Power Doppler ultrasound score (0-3 score) had a weighted kappa of 0.90 (0.78-1.00).

The Ultrasound measures of synovitis used in this clinical study are reliable and perform well in a multi-centered clinical trial. The objective assessment of synovitis in patients with inflammatory arthritis underpins the development of new therapies for Rheumatoid Arthritis and as such ultrasound imaging in this study has shown to be a reproducible imaging modality.

4. Thermoregulation attenuates 2D and 3D power Doppler signal in inflamed Rheumatoid joints.

4.1 Introduction

Joint inflammation is a focal point of the systemic inflammatory disease process known as Rheumatoid Arthritis. In addition to cellular infiltration, one of the first pathological adaptations to take place is the development of new vessels supplying the synovium. This in parts facilitates the influx of cellular mediators of inflammation whilst sustaining the process by delivering essential nutrients and oxygen. Synovial inflammation can be seen clinically as swollen, red warm joints. On ultrasound examination synovial thickening is often marked with evidence of vascular signal within the synovium on power Doppler examination. Histological examination of joint synovium demonstrated a small number of blood vessels in the normal, un-inflamed state but these become greatly expanded in the inflamed joint. Histologically these capillaries are often poorly formed, leaky and lack the mature infrastructure seen elsewhere.

Changes in vascular density may contribute to changes in doppler signal in patients receiving treatment, however dismantling of this network is not immediate following therapy. Reduction in local inflammatory mediators will affect afferent vasculature reducing blood flow however changes in synovial blood flow are often seen immediately in response to cold stimuli suggesting a neuronal mediated afferent control in vascular flow. Thermoregulation of vascular has been most extensively explored in the setting of cutaneous vascular changes with evidence that underlying systemic disorders such as hypertension and Diabetes may inhibit normal vascular reflexes. Little information exists regarding the control of vascular tone in patients with RA although resistance indices within larger vessels in patients with RA have been shown to be consistently higher.

Prior to the advent of effective pharmacotherapy, thermoregulation was used for symptomatic relief of both pain and swelling. The application of an ice pack on an

inflamed joint relieves discomfort within a few minutes with gradual reduction in swelling after sustained application. Thermoregulation is employed less often today in the setting of acute inflammatory arthritis. However manipulation of temperature may provide a reasonable platform on which to test, *in vivo,* the utility of various US parameters such as 2D and 3D Doppler signal. The assessment of responsiveness for most clinically relevant parameters in patients with RA require the administration of a pharmacological therapy to provide sufficient biological change. In this study I will investigate the sensitivity to change of both three dimensional (3D) and two dimensional (2D) ultrasound imaging of power Doppler signal (PDS). The use of thermoregulation, as a broadly physiological stressor, provides an inexpensive, safe and consistent stimulus for a preliminary exercise in examining these vascular assessment imaging tools.

4.2 Aims

The aims of this study were:

1. Correlate 2D longitudinal and transverse power doppler scores with 3D volumetric and topographical scores in a limited US data set (10 MCP joints).
2. To demonstrate the effects of cooling on Power doppler signal (2D & 3D) and synovial thickness (2D) within a limited US data set (10 MCP joints).
3. To determine the responsiveness of 2D (longitudinal and Transverse) and 3D Doppler signal (3D volume rendering and TUI) following cooling.

4.3 Definitions

i) Long STi - Synovial thickness index scored from longitudinal orientated images summed over 10 MCP joints

ii) Trans STi - Synovial thickness index scored from transverse orientated images summed over 10 MCP joints

iii) Long VASCi - Vascular index score from longitudinal orientated images summed over 10 MCP joints

iv) Trans VASCi - Vascular index score from transverse orientated images summed over 10 MCP joints

v) 3D VASCi - Vascular index score from 3D rendered images summed over 10 MCP joints

vi) TUI (max) VASCi - Maximum vascular index slice determined by topographical ultrasound imaging vascular index summed over 10 MCP joints.

vii) TUI (mid) VASCi - Vascular index score from the midline image determined by a topographical ultrasound imaging midline slice summed over 10 MCP joints.

4.4 Methods

Patients

13 patients fulfilling the ACR diagnostic criteria (1987) for Rheumatoid Arthritis with a DAS 28 > 3.2 were recruited from the weekly US clinic based at the Rheumatology Department, Barts Health NHS trust, Mile End Hospital. All patients had grade 2/4 PDS in a least 2 MCP joints at enrollment. Patients were excluded if they had a prior diagnosis of, or symptoms suggestive of, Raynauds phenomenon, peripheral vascular disease, diabetes mellitus or systemic hypertension. Patients were also excluded if they were receiving therapy which potentially may have a peripheral vasodilatory effect e.g. Calcium channel antagonist or received recent escalation in their current corticosteroid therapy within the last 2 weeks (including intra-muscular depomedrone).

US assessment and scoring

All US images were acquired using a Logiq 9 (GE Healthcare) machine with a 4D16L transducer (3D data) and a M12L transducer (2D) probes. At each time point all 10 MCP joints were imaged by 2D (longitudinal and transverse views) and 3D volumetric scans. 2D US images were scored qualitatively as described in Section 2.2.1. 3D rendered volumetric imagines were analysed qualitatively and as described in section 2.2.4. Topographical scores were performed using the maximal PDS signal slice and the midline reference image as described in section 2.2.6.

Each data set was analysed by 2 readers (SK and MW) both with more than 3 years of US experience. 2D and 3D data was read in a paired fashion (non-chronological). ICCs were calculated for each data set before and after cooling. For statistical analysis the scores of SK we used for the outcome measures of response.

Time schedule

Prior to assessment patients were resting at an ambient room temperature (18^0C) for at least fifteen minutes. The temperature of the room was measured using a standard room thermometer.

A baseline data set was acquired prior to cooling. The patients hands were immersed in a water bath at 5^0C for 5 minutes and an US data set acquired immediately. Following this, after 5 mins and again after 15 mins another US data set was acquired. A 4 litre water bath was used with constant temperature monitoring providing a sufficiently large volume to minimise temperature rises during the 5 mins of hand submersion.

4.5 Statistical analysis

Multiple comparisons procedures are used to control for the familywise error rate. For example, suppose that we have four groups and we want to carry out all pairwise comparisons of the group means. There are six such comparisons: 1 with 2, 1 with 3, 1 with 4, 2 with 3, 2 with 4 and 3 with 4. Such set of comparisons is called a family. If we use, for example, a t-test to compare each pair at a certain significance level

4.6 Results

4.6.1 Patient demographics

61.5% of patients recruited were female with an overall average age of 48 (73 - 29). There was a relatively high mean DAS score (5.01 +/- 0.7) with an average ESR of 36 +/- 13.65). 9/13 patients were receiving Methotrexate either alone or in combination with other DMARDs or biological therapy with 4 pateints currently receiving a biologic (1 Rituximab, 3 anti-TNF therapy). 5 patients were currently receiving Prednisolone therapy with at and average dose of 6.5 mg daily.

Table 4-1: list of patient receiving cryotherapy including demographics

Patient baseline demographics. MTX - Methotrexate, SZP - Sulpahasalzine, HCQ - Hydroxychloroquine, Pred - Prednisolone.

Patient	Age	Gender	DAS28(ESR)	ESR	RF	Erosions	Duration of RA (months)	Current therapy
1	56	M	5.4	49	+	+	96	MTX, HCQ, Pred,
2	65	M	4.5	23	+	+	55	MTX, HCQ, Pred,
3	34	M	5.31	65	-	+	69	SZP, Pred
4	37	F	6.23	51	-	+	23	MTX, HCQ, Pred,
5	29	F	4.75	28	+	+	65	MTX, Adalimumab
6	48	F	3.91	15	+	+	77	HCQ
7	51	F	4.76	29	+	+	113	MTX, Rituximab
8	57	M	5.32	35	+	+	12	MTX, Etanercept
9	62	F	5.68	31	-	+	9	MTX, SZP
10	30	M	3.78	27	-	-	6	MTX, SZP, Pred,
11	53	F	5.73	49	-	+	19	MTX
12	73	F	5.39	38	+	-	38	SZP, HCQ
13	30	F	5.21	35	+	+	29	Adalimumab

4.6.2 Good to moderate reliability of 2D, 3D and topographical VASCi scores

Both readers scored all US images and reliability was calculated using Inter class correlation coefficients (ICC) at baseline and following cooling. Both 2D VASCi scores showed excellent within scan inter-reader reliability (Long VASCi - 0.96, Trans VASCi - 0.92). Similarly good reliability was demonstrated for both the topographical VASCi scores (TUI (max) VASCi - 0.89, TUI (mid) VASCi - 0.95), however the 3D VASCi was least reliable (0.79).

ICC measurements repeated following cooling of the MCP joints showed some improvement in the 2D image ICC readings but a marked improvement in respect to the 3D VASCi (0.79 to 0.85).

Table 4-2: ICC results for Pre and Post cryotherapy VASCi for 10 MCP joint scores

ICC results and 95% confidence intervals for all VASCi US parameters prior to and following cooling of peripheral MCP joints in 5^0C water bath. Pre-Cryo: Prior to application of cryotherapy, Post-Cryo: After application of cryotherapy.

A

Pre-Cryo	ICC	95% CI
Long VASCi	0.96	(0.89; 0.99)
Trans VASCi	0.92	(0.90; 0.95)
3D VASCi	0.79	(0.73; 0.85)
TUI (max) VASCi	0.95	(0.91; 0.99)
TUI (mid) VASCi	0.89	(0.82; 0.92)

B

Post-Cryo	ICC	95% CI
Long VASCi	0.97	(0.95; 1.00)
Trans VASCi	0.98	(0.97; 1.00)
3D VASCi	0.75	(0.73; 0.77)
TUI (max) VASCi	0.95	(0.91; 0.98)
TUI (mid) VASCi	0.97	(0.96; 0.99)

Inspection of the Bland - Altman plot would suggest that there is some deviation at the lower level of 3D VASCi scores which has contributed to the moderate ICC values for 3D VASCi scoring. 4 data points below a mean of 5 demonstrate movement in the same direction.

Figure 4-1: Bland - Altman plot for 3D VASCi scores at baseline prior to cryotherapy.

Bland - Altman plot for 3D VASCi scores at baseline demonstrating some deviation at the lower 3D VASCi scores. This may suggest a systematic error or discrepancy in scoring by one of he readers at low levels of 3D doppler scores.

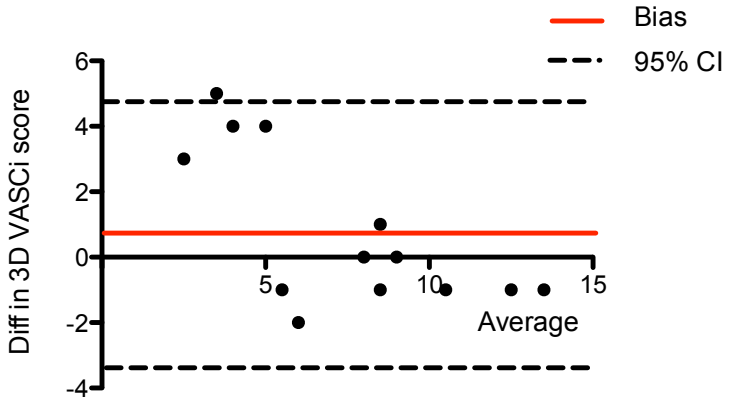

4.6.3 2D VASCi scores correlate with 3D VASCi and TUI(max) VASCi scores

Table 4-3 shows a correlation matrix between the 2D VASCi, 3D VASCi and topographical VASCi scores at baseline prior to cooling. There is a significant correlation between 3D VASCi and both 2D VASCi scores and this greater than for the TUI(max) VASCi score. The TUI (mid) VASCi did not correlate with either of the 2D VASCi scores although a modest relationship was detected between it and the TUI(max) VASCI (Pearson's coefficient - 0.31, $p < 0.045$). The correlations were generally weaker following cooling at time 0 with 3D VASCi scores continuing to be correlated with 2D long and Trans VASCi scores but no significant relationship was detected for any of the TUI VASCi scores.

Table 4-3: correlation matrix for 2D, 3D and TUI VASCi parameters at baseline prior to cryotherapy.

A: Table showing a correlation matrix for 2D, 3D and TUI VASCi parameters at baseline prior to cooling. Significance at $p < 0.05$ **B:** table showing a correlation matrix for 2D, 3D and TUI VASCi parameters following cooling in water bath for 5^{o}C cooling. Significance at $p < 0.05$

* - no significant correlation demonstrated using Pearson's Correlation coefficient

A

2D US images	3D VASCi	TUI (max) VASCi	TUI (mid) VASCi
Long VASCi	0.69	0.64	0.07*
Trans VASCi	0.84	0.50	0.014*

B

2D US images	3D VASCi	TUI (max) VASCi	TUI (mid) VASCi
Long VASCi	0.65	0.40*	-0.23*
Trans VASCi	0.68	0.13*	-0.08*

Figure 4-2: Graphical representation of the correlation of 2D and 3D scores prior to cryotherapy

A: Correlation of 2D VASCi and 3D VASCi (Pearson's Correlation coefficient r=0.84, p<0.001) **B:** Correlation of 2D Long VASCi and TUI(max) VASCi (Pearson's Correlation coefficient r=0.64, p<0.001).

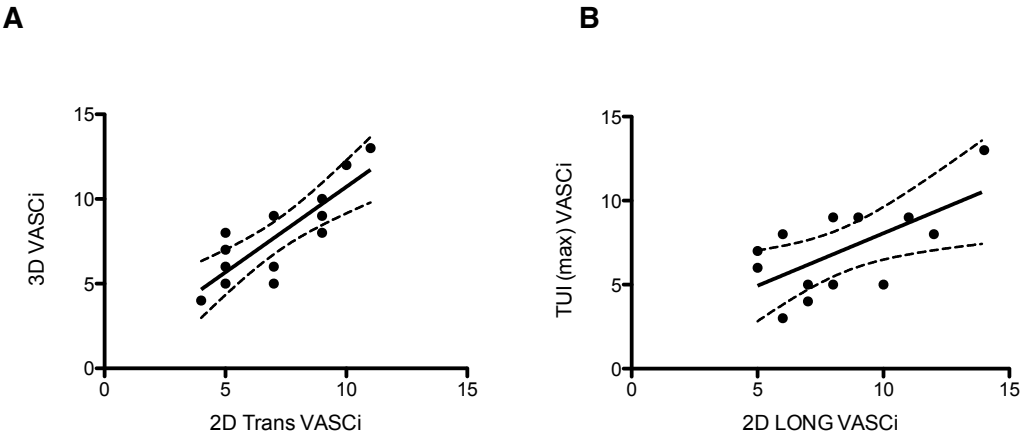

4.6.4 VASCi but not STi scores show a significant change from baseline

All power Doppler indices showed a significant change form baseline with the magnitude of change being greatest for 2D long VASCi (50% change). Synovial thickness scores showed no significant change from baseline (two tailed t-test, Long STi p =0.54, Trans STi p=0.32). The TUI(mid) mean VASCi score was significantly lower at baseline compared to all other baseline VASCi scores (Repeated-measures ANOVA $p < 0.0001$) but still showed a significant change following emersion of the hands in the water bath.

Figure 4-3: change in VASCi parameters pre and post emersion of patients hands in a 5^0C water bath.

A: No change is demonstrated from baseline following water bath emersion for mean STi scores**B**: Longitudinal and and Transverse VASCi change following cryotherapy. **C:** Change in 3D data set including 3D rendered PD volume, TUI (max) and TUI (mid) VASCi. **STi** - synovial thickness index, **VASCi** - Vascular index, **TUI (max)** - topographical ultrasound imaging maximum signal slice vascular index. **TUI (mid)** - topographical ultrasound imaging midline signal slice vascular index

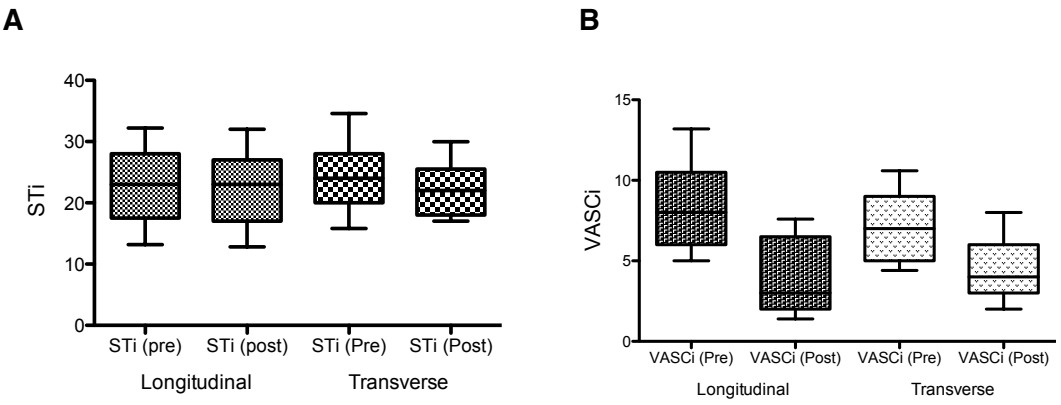

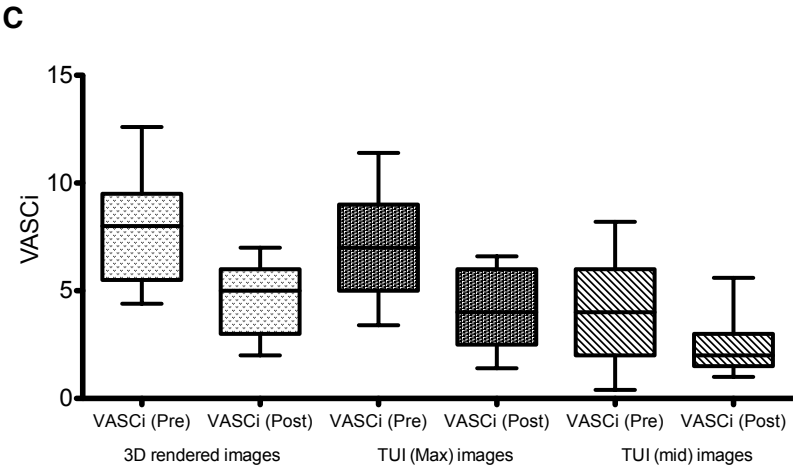

Examining the change in individual scores, it is noticeable that patients number 4 and 12 did not show only a modest reduction in any VASCi following crypotherapy for all of the VASCi parameter scores (figure4-4). Patient 12 showed an increase in VASCi only for longitudinal VASCi scans.

Figure 4-4: Before and after cryotherapy plots of individual patients VASCi scores

A: Individual longitudinal VASCi scores. Patient 4 showed only a small reduction in VASCi while patient 12 shows a small increase in VASCi. **B:** Individual transverse VASCi scores demonstrating a small decrease in both patients VASCi. (Pre) - prior to cryotherapy, (Post) - immediately following cryotherapy.

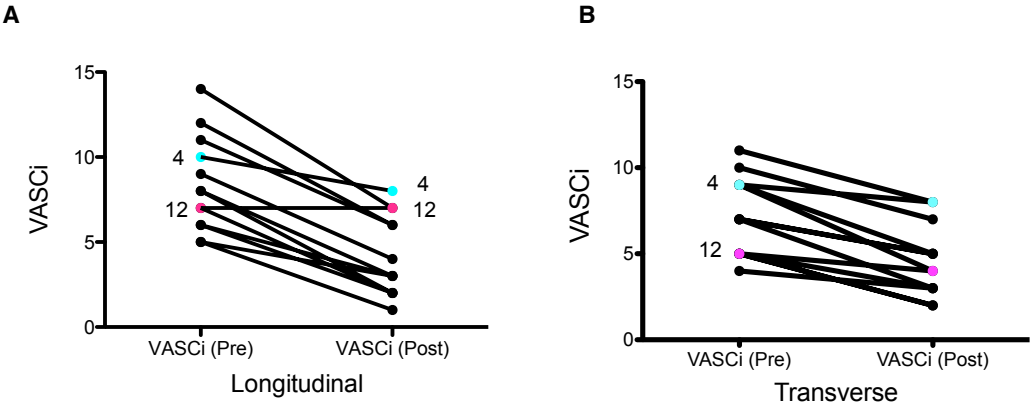

4.6.5 Reduction of mean VASCi score persists following re-warming

A significant reduction was seen with all VASCi scores following cooling. 3D VASCi was the only variable to show a significant increase form time 0 to 5 mins post cooling (Paired T test, $p < 0.001$). However, a significant increase in VASCi score was seen for all parameters from Time 0 to 15mins (Paired T test, $p < 0.003$). Using 2D Long VASCi scores, patient no. 4 achieved only a 20% reduction in signal with patient no. 12 having a 14% increase immediately after cooling at time 0. Similar modest responses were observed with other VASCi scores for both these patients with patient 12 demonstrating a maximum of 13% reduction in 3D VASCi. Overall 4/13 patients achieved an similar of greater VASCi score at 15mins compared to baseline. Patient no. 3 consistently showed a higher VASCi score at 15mins on all parameters compared to baseline with a maximal increase of 40% detected with the 2D Trans VASCi score. Patient no. 7 had a reduction of 65% in Long VASCi following cooling at time 0 with no change at 15mins. This was similarly observed with other VASCi scores with only 2D Trans VASCi showing a small improvement at 15mins.

Figure 4-5: Kinetics of response to cryotherapy and change in VASCi parameters on re-warming

A: Graph of change in mean VASCi over time for 2D Long and Trans VASCi scores. (Mean and 95%CI) **B:** Graph of change in mean VASCi over time for 3D VASCi, TUI (max) and TUI (mid) VASCi scores. (Mean and 95%CI). A clear decrease in all cores can be seen between baseline and time 0. Subsequent warming over a 15 min period causes a return of doppler signal within the synovium demonstrated by the gradual increase in VASCi scores. Day 15 VASCi scores however do not return to pre-cryotherapy levels.

A

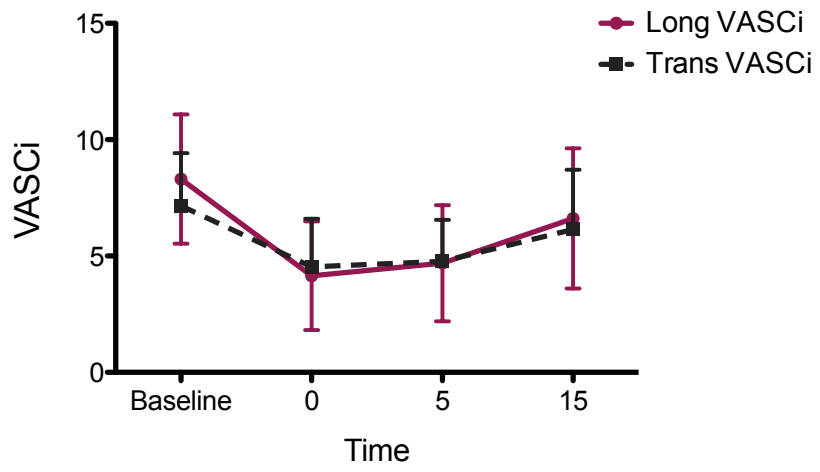

B

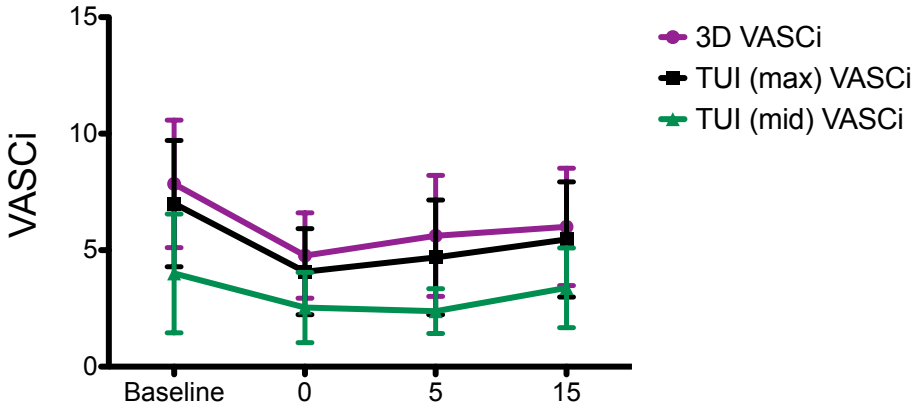

4.6.6 2D VASCi scores are more responsive than 3D scores

The Standardised Response Mean (SRM) was calculated for each Power Doppler score as the mean change in VASCi score form baseline to time 0 divided by the standard deviation of the change in VASCi. As expected the TUI (mid) VASCi performed poorly in comparison with the other VASCi scores with an SRM of 0.72. 2D Longitudinal and transverse VASCI and 3D VASCi performed similarly with a SRM of approximately 2. The TUI(max) VASCi was less responsive but still demonstrated a significant change. Table 4-4 summaries the SRM for each VASCi score.

Table 4-4: Standardised response mean (SRM) for all US parameters following cryotherapy

SRM (standardised response mean) results for VASCi scores. Change from baseline to Time 0 following cooling was used to calculate the mean change in VASCi score and standard deviation.

2D Long VASCi	2D Trans VASCi	3D VASCi	TUI (max) VASCi	TUI (mid) VASCi
2.12	2.07	1.92	1.62	0.72

4.7 Conclusions

Cryotherapy has been used in the setting of arthritis since antiquity and is still a central theme in the management of acute sporting injuries. Application of cyrotherapy can take many forms including, ice and gel packs, inflatable splints as well as complete submersion in ice baths. There is purported benefits to recovery time and improved rehabilitation after injury with cryotherapy although a number of authors have questioned the lack of stringent randomised controlled trials to support some of these claims[378-380].

Cryotherapy is a convenient method for inducing change in vascular perfusion as demonstrated by variation in power Doppler signal[381 382]. This study exploits a physiological response to cryotherapy to induce change in a limited ultrasound joint set of 10 MCP joints. This platform was used to examine the relationship of 2D and 3D vascular index scores and their response following application of cryotherapy. Patients with potentially confounding factors, such as anti-hypertensive agents or systemic disease processes, known to effect vascular response were excluded. Patients recruited had a minimal PDS score of 2/4 in at least 2 joints. Given the potentially dramatic reduction in vascular flow anticipated, only 1 patient completely abated all doppler signal from the 10 MCP joints on 2D imaging following immersion in the 5oC water bath. This would suggesting the selected benchmark of baseline PD signal provides some protection against a flooring effect in this model. A significant reduction in vascular flow was noted with all VASCi scores which allows the responsiveness of each modality to be compared. Both 2D Long and Trans VASCi scores performed well, with a SRM of 2.12 and 2.07 respectfully. The 3D VASCi and TUI (max) VASCi were also demonstrated to be responsive, however the utility of TUI (mid) VASCi was limited in this model. The incorporation of the TUI (mid) VASCi score was planned in an attempted to identify a similar region interest as would normally be assessed by the 2D Long VASCi score. This would provide a comparison between the PDS generated by 2D US, and that captured with 3D volumetric imaging within a strict region of interest. A 50.6% difference in mean

VASCi score can be seen between the baseline Long VASCi and TUI (mid) VASCi which reduces to 34.8% following cryotherapy. This would suggest a significant loss in Doppler signal detection with 3D PD imaging. The fact that 3D VASCi is still responsive, is likely to relate to the volume of tissue being imaged rather than the sensitivity of the technique in detecting PDS. Despite its shortcomings, the TUI VASCi endpoints appear to be reliable with excellent ICC values generated for both TUI (mid) and TUI (max). The poor 3D VASCi ICC value may reflect the lack of experience of MW with 3D imaging. Both myself and MW spent time prior to scoring discussing a number of standard images however the variability on 3D signal is much more difficult to capture on 2D images which may have lead to discrepancies when scoring. The Bland-αltman graph does suggest that scoring for lower 3D VASCi scores may be less reliable between myself and MW. The clustering of 4 data points in the same direction may represent a systemic scoring tendency for one of the readers.

2 patients failed to demonstrate a significant fall in vascular signal following cryotherapy. The aberration of normal control of vascular tone may explain these finding although I cannot exclude the possibility that an initial reduction in vascular flow did occur with subsequent loss of the neuronal mediated vasoconstriction. This has been previously observed in 2 scenarios. Beste et.al. showed that initial reduction of the US pulsitile index of the doralis pedis artery could be mediated through application of cryotherapy to the knee and lower leg[383]. After 5 mins of therapy a slow improvement in pulsitile index was noted despite continued application of the cyro-pack. Similarly, Albrecht et.al. demonstrated that cooling of the skin over an inflamed wrist joint resulted in minimal vasodilatation and reduction in PDS on US examination but curiously a marked increase in PDS was seen after 10 mins of withdrawing the cooling agent[381]. However, in this study a clear reduction in the PDS was demonstrated in the wrist if a more potent cooling method was used such as an ice pack presumably allowing greater penetration rather than only superficial dermal cooling.

A number of limitations exist within this model. Following cooling of the hands in a water bath, the patients hands were place on the bench to facilitate the US examination. This examination required approximately 2 mins to complete. 2D images were acquired first followed by 3D images. The subsequent warming over this period may have been responsible for artificially reducing the SRM given an increase in PDS at time 0 with the 3D VASCi score. Two containers of US gel were used for each patient - one maintained at 50C and the other at room temperature. The initial assessment at time 0 was preformed using the cooled US gel with all subsequent assessments using gel at room temperature. In addition, the on going depletion of doppler signal seen after 15 mins would argue for a longer time frame of assessment. An important question to address is the time that is required for patients to return to their pre-cooling state. This has significant implications for clinical trial assessments using US as well as the sensitivity of US to detect Doppler signal in clinical practice. Presently, from this data set a recommendation can only be given that patients should wait more than 15 mins in at ambient room temperature prior to US examination. Our current practice is for patients to wait a minimum of 30 mins prior to US assessment in the setting of a clinical trial. To standardise imaging acquisition the response of synovial vasculature to temperature changes should be bourn in mind when integrating US imaging into therapeutic study design.

Cryotherapy is not the only potential physiological variable which may alter patients vascular flow on PD examination. Diurnal variation has been shown to have an impact on synovial flow and doppler detection with in the MCP joints of the hands[384]. In addition, many of our patients receive daily therapy which is often administered first thing in the morning and may have an impact on vascular tone such as anti-hypertensive agents. Diurnal variation of endogenous cortisol and bioavailability of anti-inflammatory medication such as Prednisolone or NSAIDS may significantly alter the baseline characteristic of patients synovial vascularity. More work is needed to document the influences of these parameters of synovial vascular flow.

This model is a safe and convenient method of applying a physiological stressor to synovial blood flow. Within this model, the ability of 2D and 3D US parameters to detect change in synovial vascular flow over a relatively short period of time can be demonstrated. The vascular index scores used over 10 MCP joints would seem to be both responsive and reliable.

5. Ultrasound assessment of Rheumatoid synovitis is more responsive than clinical assessment to Prednisolone therapy. A randomised, placebo controlled study

5.1 Introduction

The development of new therapeutics for RA involves clinical assessment of response by endpoints that include composite measures of disease activity, such as the Disease Activity Score (DAS28)[46], a continuous measure, and American College of Rheumatology (ACR) categorical responses[148 385].

For early testing of novel therapeutics, we require a sensitive method to distinguish between treatment groups in cohort studies that permit small patient numbers and provide a reliable, early indicator of efficacy. Ideally, such measures would be quick, non-invasive, objective, predict longer-term response to repeated medication and give an early indication of disease modification. Due to ethical constraints of performing placebo controlled trials and the resultant trend towards comparator controlled trials, the requirement for sensitive endpoints is greater than ever.

Synovial inflammation in Rheumatoid Arthritis, has as a hallmark, a number of pathological features including inflammation, angiogenesis, synovial proliferation and tissue destruction[386 387]. The detection of synovitis is of great importance to optimize patient therapy with the purpose of suppressing this process completely to help prevent joint damage[388]. Techniques that quantify synovial inflammation and are sensitive to treatment effects may allow faster decision-making and more efficient clinical trials.

Swollen joints are a characteristic feature of RA but they are not well-correlated with longitudinal outcome or disability or radiographic erosions. In part, this is probably because clinical examination is not very sensitive for synovial inflammation (Hansen 1979). Current composite indices of disease activity, such as Disease Activity Score (DAS) or the American College of Rheumatology (ACR) responder criteria, themselves based on aggregating individual clinical findings such as swollen joint counts to derive a more responsive and valid outcome measure[46 389]. As a

consequence, using such a dichotomous outcome measure, the sample sizes to detect moderate drug effects using the ACR20 responder endpoint are approximately 100 patients per treatment group, representing a substantial challenge when prolonged dosing regimens and placebo controls are required[390].

Power Doppler Ultrasound (PDUS) is proposed as a valid, reliable method for quantifying synovial blood flow. As such, it has the potential to serve as a broadly applicable pharmacodynamic marker of synovial inflammation. In Chapter 3, I have already discussed the reliability of a number of ultrasonographic endpoints used in this study for both 2D and 3D imaging modalities. For early testing of novel therapeutics, we require a sensitive method to distinguish between treatment groups in cohort studies that permit small patient numbers and provide a reliable, early indicator of efficacy. Ideally, such measures would be quick, non-invasive, objective, predict longer-term response to repeated medication and give an early indication of disease modification. Due to ethical constraints of performing placebo controlled trials and the resultant trend towards comparator controlled trials, the requirement for sensitive endpoints is greater than ever.

There is only one single-center, double-blind, placebo controlled clinical trial that included both PDUS and conventional clinical endpoints in RA (Taylor, 2004). There are numerous open-label treatment studies, but none that have explored the ability of PDUS to identify a dose-response for an efficacious therapeutic agent (Newman 1996, Fiocco 2005, Stone 2001, Filippucci 2004, 2006, Salaffi 2004).

This study compared the responsiveness of PDUS and the traditional composite endpoint of disease activity, the DAS, in a randomized, parallel group, double blind trial of prednisone in patients with rheumatoid arthritis. This study involved two clinical centers to assess the feasibility of conducting a multi-center study using PDUS with centralized grading.

Metacarpophalangeal joints (MCPJs) are invariably involved in RA and so their evaluation is important. These superficial joints are amenable to assessment with ultrasound utilizing frequencies that produce high resolution images. High-frequency ultrasonography (HFUS) and power Doppler ultrasonography (PDUS) are

reproducible tools for determining synovitis and more sensitive than clinical scoring in determining disease activity. The synovial vascular signal on PDUS closely correlates with the dynamic contrast enhanced MRI in RA MCPJs and synovitis detected by ultrasound (US) predicts erosive disease.

5.2 Aims

By using a known efficacious treatment for RA, our objectives were:

i) To determine the potential of 2D ultrasonographic endpoints to provide an early and objective indication of a therapeutic response to treatment intervention in rheumatoid arthritis (RA).

ii) Using two different doses of Prednisone (15 mg and 7.5 mg) to investigate whether ultrasonographic endpoints are able to demonstrate a dose-response relationship of two relatively low doses of corticosteroid.

iii) To compare the ultrasound endpoints with DAS28(CRP) and to explore the potential of composite endpoints (DAS28 combined with US endpoints) to improve the registration of a significant treatment effect.

iv) To explore the responsiveness of 3D ultrasound imaging in response to therapeutic intervention.

5.3 Methods

5.3.1 Patients

This was a randomized, double-βlind, parallel-group, placebo-controlled trial conducted at 2 academic research centres in UK (clinicaltrials.gov identifier: NCT00746512).

Two panels were planned for the study:

1. **Panel A:** Subjects were randomized in a 1:1 ratio to oral prednisone 15 mg daily or matching placebo for 15 days. After a total of 18 subjects completed the study, an interim analysis was planned to determine if this smaller sample size could significantly ($\alpha = 0.03$, 1-sided) discriminate prednisone 15 mg from placebo based on the primary endpoint.

Figure 5-1: Diagrammatic representation of the study schedule for Panel A patients

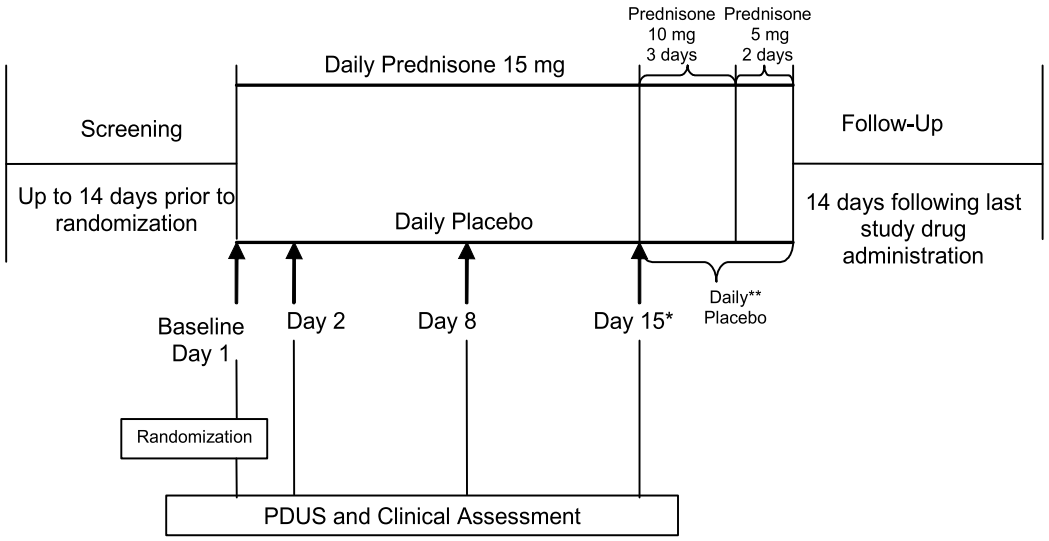

2. **Panel B:** If Panel A was able to discriminate treatment form Placebo, then enrollment in the prednisone 15 mg group would cease. Panel B would recruit 27 additional subjects and be randomized (2:1 ratio) to prednisone 7.5 mg or matching placebo for 15 days.

Figure 5-2: Diagrammatic representation of the study schedule for Panel B patients

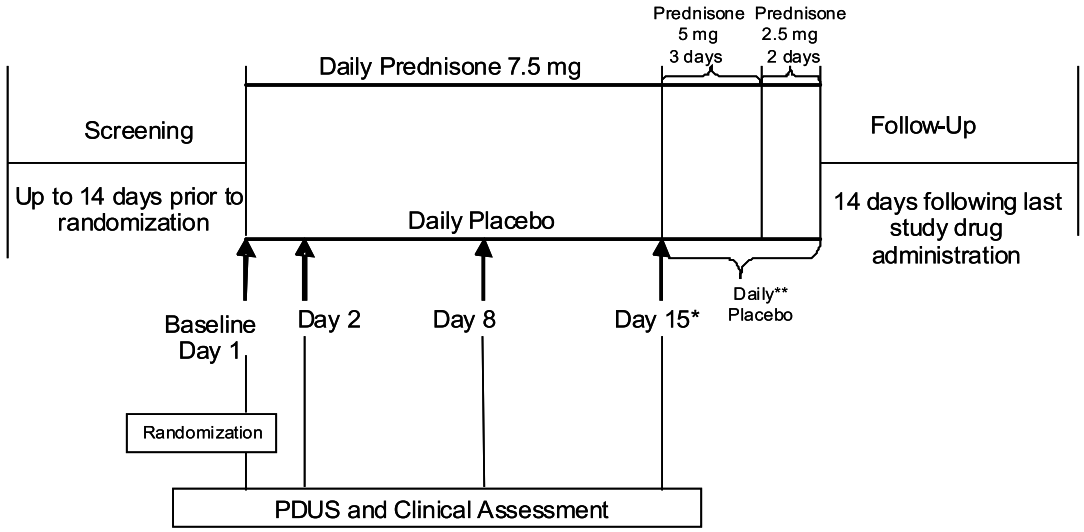

Men and non-pregnant women ≥18 years with RA ≥6 months duration meeting the 1987 American College of Rheumatology criteria for the diagnosis of RA were eligible. Subjects were required to have at least moderate disease activity [DAS28(CRP≥3.2] and moderate dorsal transverse synovial vascularity in 2 MCPJs (score≥2) or severe in 1 MCPJ (score=4) as measured on a semi-quantitative 0-to-4 scale.

Non-steroidal anti-inflammatory drugs (NSAIDs) at stable doses ≥4 weeks were permitted, as were disease modifying anti-rheumatic drugs (DMARDs) at stable doses for ≥6 weeks, topical or inhaled glucocorticoids at stable doses for ≥2 weeks, and opiates at stable doses ≥2 weeks. Acetaminophen (paracetamol) was allowed for breakthrough pain, but NSAIDs were not to be taken on an as-needed basis.

Pertinent exclusion criteria included intra-αrticular glucocorticoid injections to MCPJs within 3 months or to non-MCP Js within 6 weeks of baseline; oral glucocorticoid use within 4 weeks; and current biological therapies.

Tolerability was assessed by clinical and laboratory examination and adverse event (AE) reporting during the study. After baseline measures subjects were randomized (by a sponsor statistician using a computerised Clinical Allocation Schedule System [CASS] with blocking factors to ensure blinding based on a multiple of the number of treatment groups and subjects) and then received their first dose of study medication.

All subjects gave informed written consent to participate. The study was conducted in accordance with principles of Good Clinical Practice and approved by the institutional review board for human research.

5.4 Ultrasonography

2D ultrasound images were obtained as described in chapter 2.

Synovial thickness and Power doppler quantitative and qualitative scores are described in chapter 2.

Quantitative vascularity and synovial thickness measurements were described in chapter 2.

3D US assessment of patients is described in chapter 2. All patients were scanned in the same order depending upon the location of the ultrasound examination. The primary US assessment used for analysis of the primary endpoint in the study was the 1st scan at each site, read by SK.

Table 5.1: Table describing the scan order at each site and from each ultrasonographer.

This table represents the scanning order of patient assessments for Panel A at each intitution. Also descibed is the reading of scans for ICC results. BH - Barts Health NHS Trust, KIR - Kennedy Institute of Rheumatology, SK- Stephen Kelly, MS - Matt Seymour

Site	Scan	Ultrasonographer	Reader
BH	1	SK	SK
			MS
	2	MS	MS
	3	SK	SK
KIR	1	MS	SK
			MS
	2	SK	SK
	3	MS	MS

5.4.1 Clinical Efficacy Assessments

Clinical efficacy was assessed by the DAS28(CRP), which includes the number of swollen and tender joints (28-joint count), a patient's global assessment of arthritis index (visual analogue scale) and CRP. Assessments were performed by a single rheumatology research nurse in each centre, independent of the ultrasound

examinations. Each study nurse attended a DAS28 standardization training course within the preceding year of the study start.

5.4.2 Composite Endpoint

Exploratory analyses carried out on data from Panel A identified a composite of the PDUS and DAS28 component endpoints which improved precision for discrimination of active treatment at the 15 mg dose from placebo; the composite endpoint was the average of the standardized z-scores across the DAS28(CRP), 2D Trans VASCi and 2D Long STA endpoints. Analysis for this composite endpoint were performed also in a similar manner to the one for the primary and secondary endpoints.

5.5 Statistical Analysis

The primary hypothesis for both panels was that prednisone (15 mg or 7.5 mg) would have a greater change from baseline in 10MCP Trans PDA (the primary endpoint) after 15 days of treatment. The analysis was performed using an analysis of covariance model with panel and treatment nested within panel as factors, and baseline value included as a covariate. Only observed data were analyzed; missing data were not imputed. The analyses were carried out for change from baseline at each of Days 15, 8, and 2. Interpretation of p-value testing for each endpoint was made in a step-down fashion, in that order, at $\alpha = 0.05$ (1-sided) for the primary endpoint. For Panel A Days 1 and 15, the first scan set acquired and read by the ultrasonographer-reader associated with the clinical site was used for analysis of treatment effects and for correlation with other endpoints; there was one scan set per visit for all other study time points.

For the interim analysis following Panel A, if the true underlying effect size for the primary endpoint was 1.0, the overall power, accounting for the interim and a potential final analysis if the study continued as originally planned, was ~88% for n=18 subjects per treatment, and ~83% for 15 subjects per treatment. The probability of stopping at the interim analysis was ~63%. These computations employ the Hwang, Shih, deCani gamma=1 stopping criteria which yields α=0.03, 1-sided at the

interim and, if applicable, final analyses. This controls the overall α level at 0.05, 1-sided. If the study continued after the interim analysis, a sample size of 15 subjects per group had 80% power to detect a statistically significant (α = 0.05, 1-tailed) difference between prednisone and placebo assuming an effect size of 0.93.

Significance for the effect of the secondary imaging endpoints and DAS28(CRP) was not error-protected from chance significance associated with multiple comparisons. Rationale for this choice is to minimize the chances of false negatives because of the exploratory nature of these secondary endpoint analyses. Thus, they are viewed as hypothesis generating rather than conclusive.

Pearson correlation coefficients were computed among pairs of endpoints, including DAS components, with ultrasound endpoints, to assess association among them.

For the analysis of creating a composite PDUS and DAS28 endpoint, precision was measured by effect size (average effect of the 15 mg and 7.5 mg prednisone effects minus placebo divided by pooled standard deviation) using a model with panel and treatment nested within panel as factors. The method for building composites was the O'Brien global statistic which is the average of the standard z-scores across the endpoints. All tests were performed one-sided at level 0.05.

5.6 Results - Panel A

5.6.1 Patients

Baseline subject and disease characteristics are shown in table 5-2. There were no significant differences between subjects baseline characteristics between those in each treatment assignment in Panel A. All treatments were generally well-tolerated.

Demographics

The baseline demographic characteristics for the study population are summarized below in Table 5-2. An error in the randomization code yielded uneven patient allocation in this study with 10 patients allocated to placebo and 8 to treatment

Table 5.2: Demographics of patient treatment groups by Age and Gender (Panel A)

Treatment	N (%)
Placebo	10 (55.6)
Prednisone 15 mg	8 (44.4)
Gender	N (%)
Female	11 (61.1)
Male	7 (38.9)
Age (years)	Mean (SD)
45 to 86	60 (10.3)

Mean (or median) baseline values for DAS28(CRP), number of tender joints, number of swollen joints, CRP and rheumatoid factor are given in table 5.3. There was no significant difference in the baseline demographics in each of the two randomized groups.

Table 5.3: Description of baseline CRP, Rheumatoid factor and DAS28 with its components (Panel A).

Description of baseline CRP, Rheumatoid factor and DAS28 with its components. With 90% CI expressed in brackets. † Median and quartiles are reported for CRP and Rheumatoid factor

	Placebo	**Prednisone 15 mg**	**Combined**
DAS28(CRP)	5.5 (+/-1.6)	5.2 (+/- 1.3)	5.3 (+/- 1.5)
Number of Tender Joints	13 (+/- 4.1)	10.9 (+/- 3.4)	12 (+/- 3.8)
Number of Swollen Joints	12.5 (+/- 5.7)	10.1 (+/- 4.4)	11 (+/- 5.4)
CRP (mg/L)†	14.0 (3.5-37.2)	8.4 (4.2-25.3)	9.8 (3.8-32)
Rheumatoid Factor(KU/L)†	241 (63-305)	186 (71-234)	220 (67-290)

5.6.2 Endpoint Responsiveness

2D US endpoints

The comparison between prednisone 15 mg daily and placebo after 15 days of dosing using Panel A yielded a statistically significant treatment effect (effect size = 1.17, P=0.013) for the primary endpoint of change from baseline in the transverse Power Doppler Area summed over 10 MCPs (10 MCP 2D Trans PDA); no statistically significant treatment effect was detected after 8 days or 1 day post baseline on this endpoint (Figure 5-4). The effect sizes for 7 other secondary imaging endpoints at 1, 8 and 15 days from baseline are in Figure 5-4. A significant treatment effect for 15 mg prednisone after 14 days was observed for all endpoints with the exception of the transverse synovial thickness index, STi. Significant treatment effects after 7 days after baseline were detected by the longitudinal and transverse Synovial Thickness Areas (STA) and the transverse Vascular Index, VASCi. Significant treatment effects were seen at 1 day after baseline for the longitudinal but not transverse STA. The 90% CI for the effect sizes of the DAS28(CRP) and the imaging endpoints all overlap.

A significant effect of prednisone 15 mg was also observed for the secondary endpoint of DAS28(CRP). Compared with placebo, prednisone 15 mg showed an effect size of 0.95 14 days after baseline for DAS28(CRP); no statistically significant effect was detected 7 days or 1 days after baseline on this endpoint. In this study the placebo group had relatively stable DAS28(CRP) score across the two week treatment period. Analysis of the CRP component of the DAS28(CRP) shows a significant difference between the 2 treatment groups in CRP at Days 14, 7, and 1. There was a borderline difference in VAS score at Days 14, 7, and 1. There was also no significant difference between the Placebo and Prednisone groups in the number of swollen joints or in the number of tender joints at Day 14.

Figure 5-3: Kinetics of US, DAS28 and its components response to Prednisone and Placebo (Panel A)

A: 10MCP 2D Trans PDA; Baseline, Day 1, 7, and 14 after start of treatment **B:** DAS28(CRP) (Score) **C:** CRP (mg/L) (Back-transformed from logarithm) **D:** Number of Swollen Joints **E:** Number of Tender Joints **F:** VAS Score.

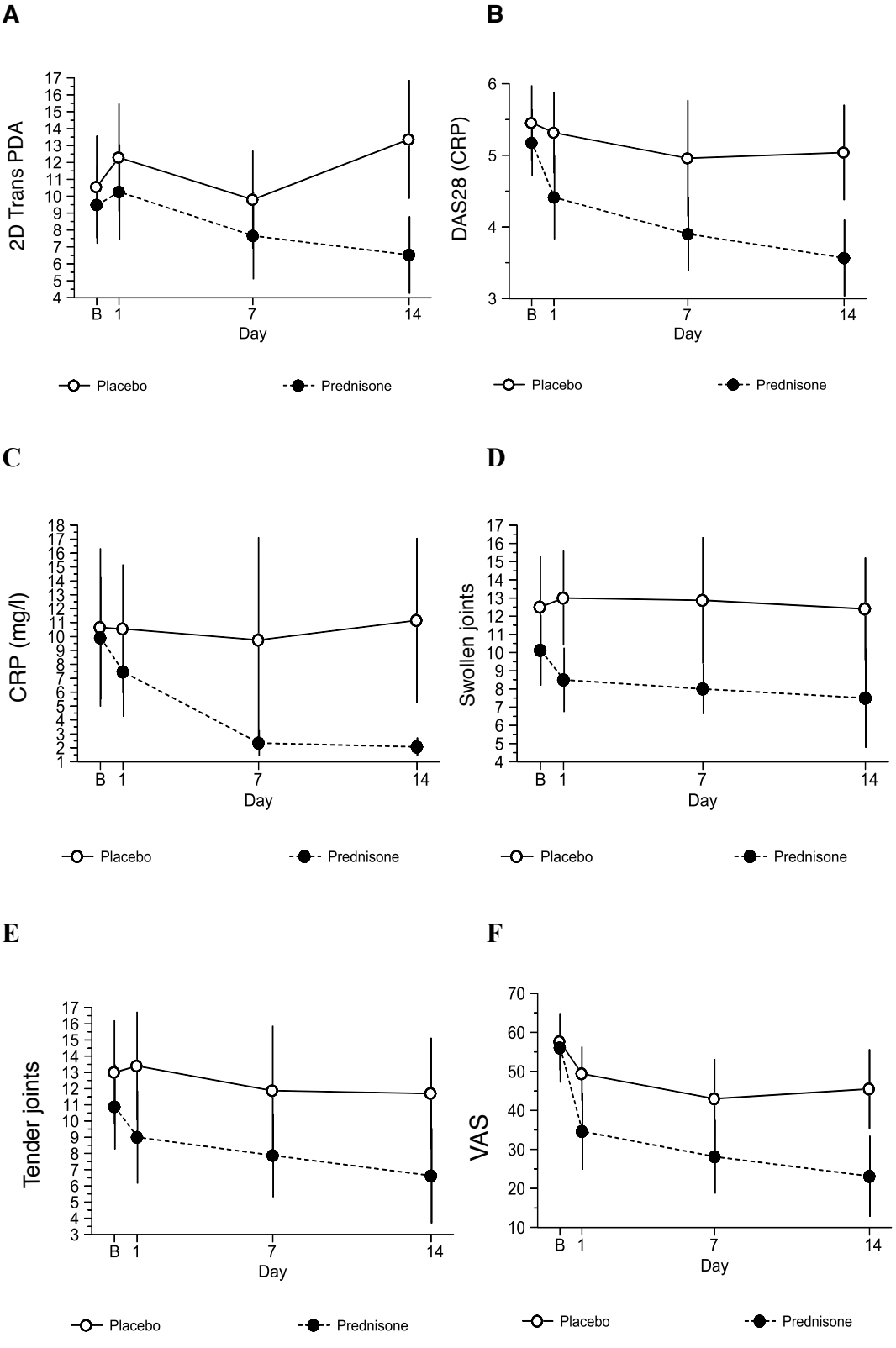

Figure 5-4: Forrest plot of the effect size for all US parameters - Day 1, Day 8, Day 15 for Panel A only

Day 1

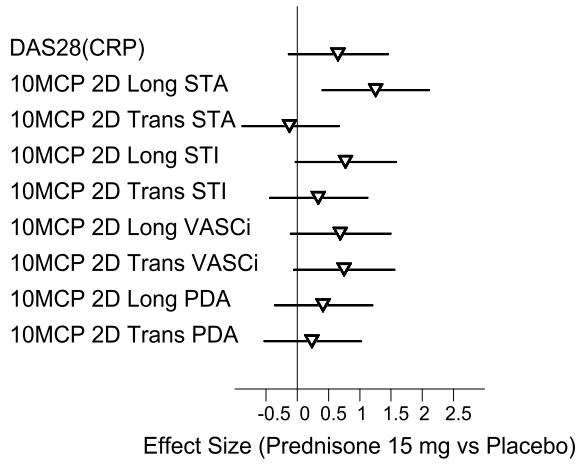

Day 8

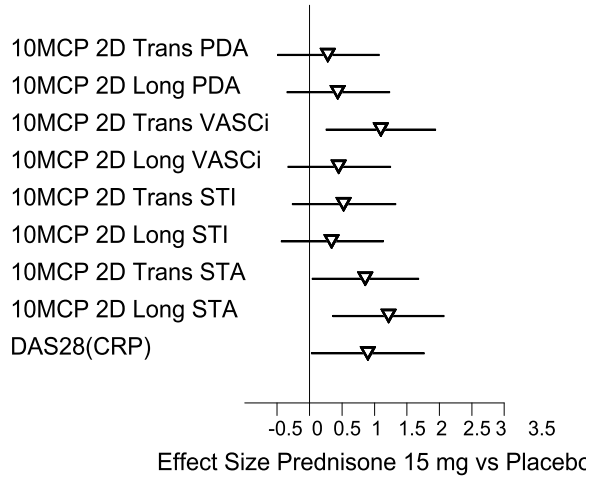

Day 15

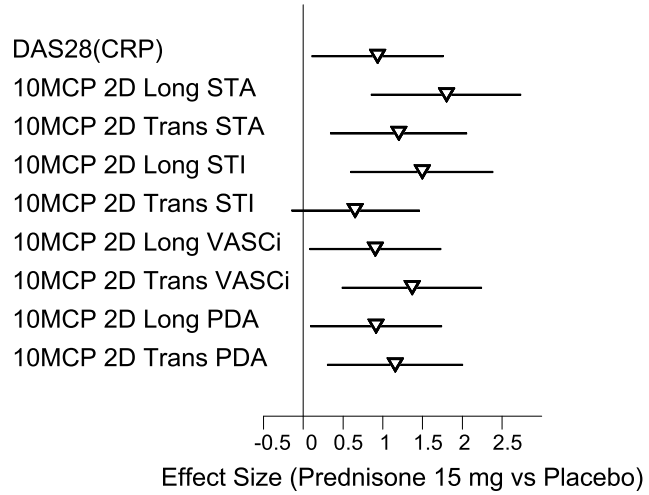

3D US endpoints

The effect size of prednisone 15 mg daily on 3D PDUS endpoints (3D VASCi, 3D PD Vol, 3D VFI) was numerically smaller than the effect size on the 2D endpoints (figure 5-6). None of the endpoints showed treatment was statistically significantly different from placebo at any of the time points assessed in this study.

Figure 5-5: 3D VASCi kinetics of response to 15mg of oral Prednisone or Placebo.

A : 3D VASCi Baseline, Day 1, 7, and 14 after start of treatment **B:** 3D PD Vol, Panel A **C:** Effect size of all power Doppler 3D endpoints at Day 14.

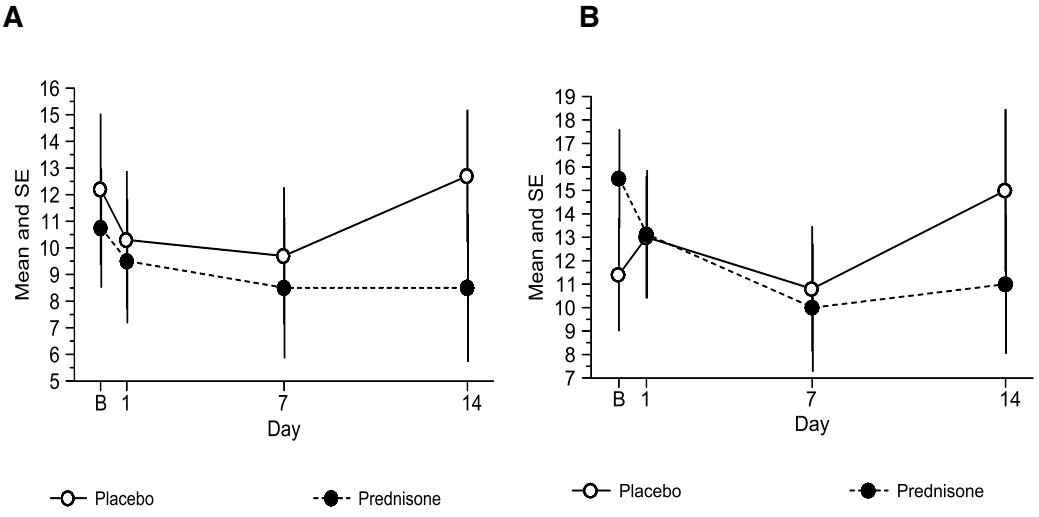

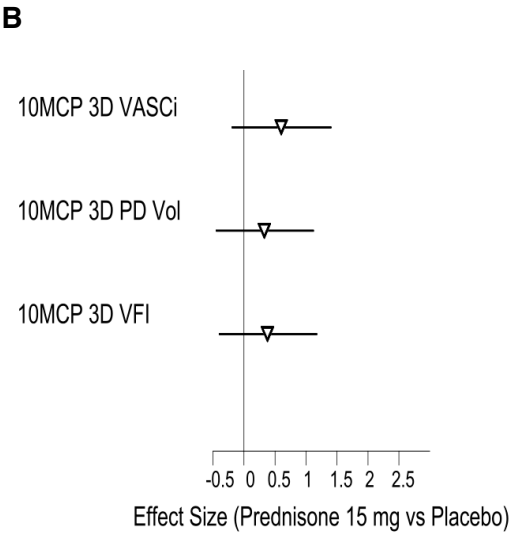

5.6.3 Correlation of 2D and 3D VASCi

There was good correlation of the baseline 2D longitudinal and baseline with the 3D data sets. The correlation with the 2D LONG data set was superior with a Pearson's correlation coefficient of 0.91 (figure 5-6). This correlation seems to hold at Day 15 but the effect size of the 3D VASCi endpoint was not significant .

Figure 5-6: Panel A baseline and Day 15 correlation for 2D and 3D endpoints

A: Panel A: 3D VASCi against 2D TRANS VASCi at baseline. Pearson r 0.75 (0.43 to 0.90) P value 0.0003 **B:** Panel A: 3D VASCi against 2D LONG VASCi at baseline. Pearson r 0.91 (0.78 to 0.96) P value < 0.0001 **C**: 3D VASCi against 2D TRANS VASCi at Day 15 . Pearson r 0.87 (0.67 to 0.95) P value < 0.0001 **D:** 3D VASCi against 2D LONG VASCi at Day 15. Pearson r 0.95 (0.87 to 0.98) P value < 0.0001

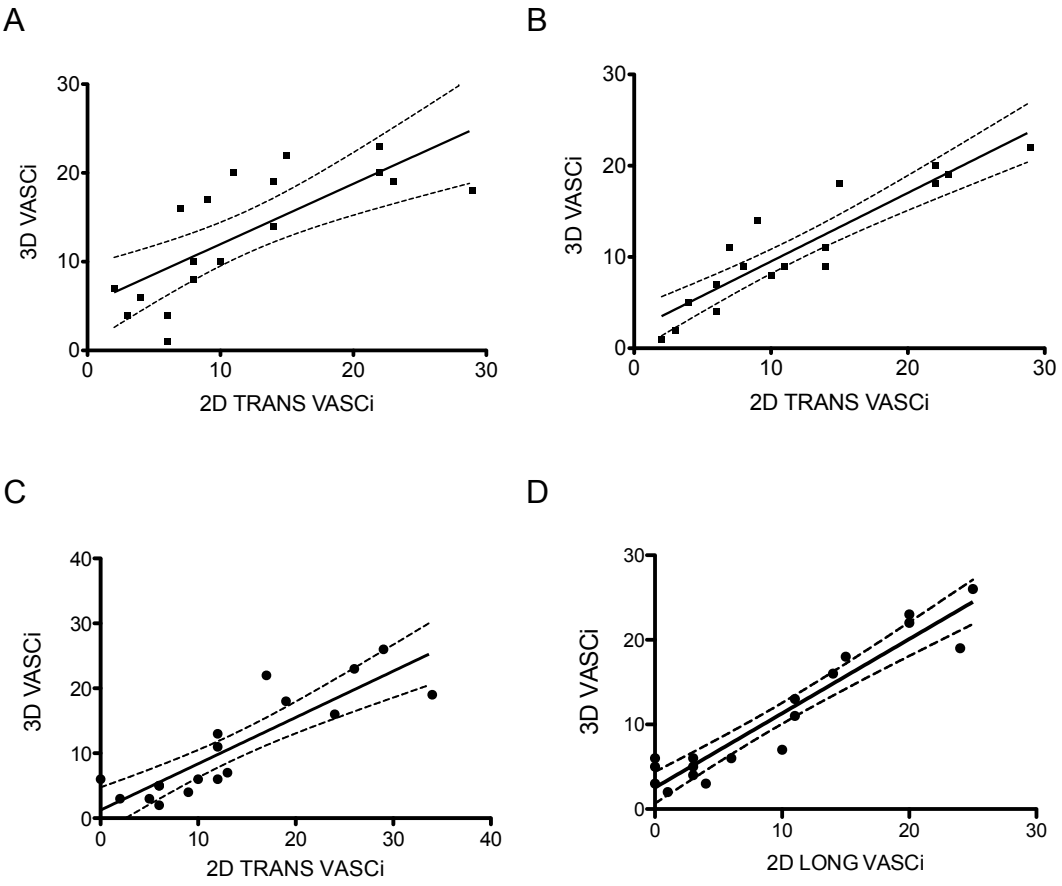

5.6.4 Correlations Between DAS28(CRP) and US endpoints

Table 5-4: Baseline correlation's of 2D US outcome measures with DAS28(CRP).

Correlation matrix showing the relationship of all baseline US outcome measures with baseline DAS28(CRP). 2D Long VASCi performs best with a Pearsons correlation coefficient r = 0.68 ($p<0.001$). (n=18)

2D Trans PDA (90%CI)	**2D Long PDA** (90%CI)	**2D Trans VASCi** (90%CI)	**2D Long VASCi** (90%CI)
0.62 (0.29, 0.82)	0.55 (0.19, 0.78)	0.64 (0.32, 0.85)	0.68 (0.38, 0.85)
2D Trans STA (90%CI)	**2D Long STA** (90%CI)	**2D Trans STi** (90%CI)	**2D Long STi** (90%CI)
0.66 (0.36; 0.84)	0.59 (0.25; 0.80)	0.59 (.25,0.80)	0.52 (.14, 0.76)

5.7 Results - Panel B

Two thirds of patients recruited to Panel B were placed in the treatment group. There was no significant difference any of the baseline characteristics again between each allocated group.

Table 5-5: Demographics of patient treatment groups by Age and Gender (Panel B)

Treatment	**N (%)**
Placebo	9 (33.3)
Prednisone 7.5 mg	18 (66.7)
Gender	**N (%)**
Female	18 (66.7)
Male	9 (33.3)
Age (years)	**Mean (SD)**
32 to 81	60 (13.0)

Mean baseline values for DAS28(CRP), number of tender joints, number of swollen joints, CRP and rheumatoid factor are given in Table 5-5. There is no significant

difference between enrollment criteria between Panel A and Panel B, nor within Panel B for patients allocated to different treatments Table 5-6.

Table 5-6: Description of baseline CRP, Rheumatoid factor and DAS28 with its components (Panel B).

Description of baseline CRP, Rheumatoid factor and DAS28 with its components. With 95% CI expressed in brackets. † Median and quartiles are reported for CRP and Rheumatoid factor

PANEL B	Placebo	Prednisone 7.5 mg	Combined
DAS28(CRP)	5.6 (+/- 1.8)	5.3 (+/- 1.2)	5.4 (+/- 1.4)
Number of Tender Joints	18.4 (+/- 10.1)	13.6 (+/- 8.6)	15.2(+/- 9.2)
Number of Swollen Joints	16.3 (+/- 8.6)	11.3 (+/- 5.6)	13.0(+/- 7.0)
CRP (mg/L)†	3.7(0.7 -11.4)	6.9 (1.7 -14.6)	6.3 (1.6 -14.6)
Rheumatoid Factor(KU/L)†	178 (82-298)	210 (129 - 288)	186 (84-299)

5.7.1 Endpoint Responsiveness

2D US endpoints

Panel B failed to demonstrate treatment effects on the primary ultrasound endpoint (10 MCP 2D Trans PDA) or the secondary clinical endpoint - DAS28 (CRP). There were however significant differences on numerous secondary imaging endpoints at Day 8 and 15. Day 7 showed significant effect size for all the 2D US endpoints except for 2D Trans STi (figure 5-8). At Day 15, the treatment effects assessed by the endpoints 2D Trans VASCi, 2D Long STi and 2D Long STA were statistically significant with effect sizes ranging from 0.93 to 2.23.

Figure 5-7: Kinetics of 2D Trans PDA and DAS28 response to Prednisone and Placebo (Panel B)

A: 10MCP 2D Trans PDA; Baseline, Day 1, 7, and 14 after start of treatment **B:** DAS28(CRP) - Panel B patients randomised to either 7.5mg Prednisone or Placebo

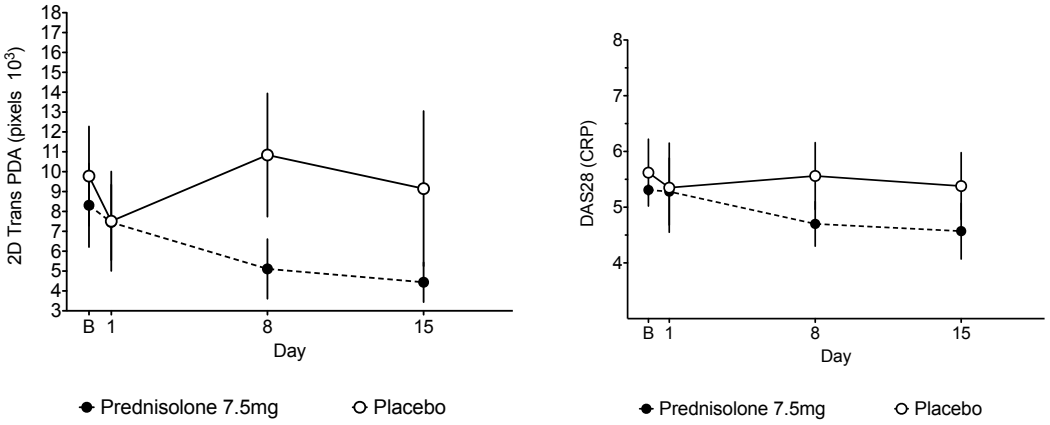

Figure 5-8: Forrest plot of the effect size for all US parameters - Day 1, Day 8, Day 15 for Panel B only

Day 1

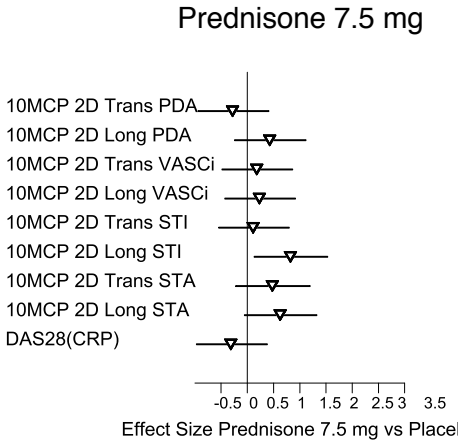

Day 7

Prednisone 7.5 mg

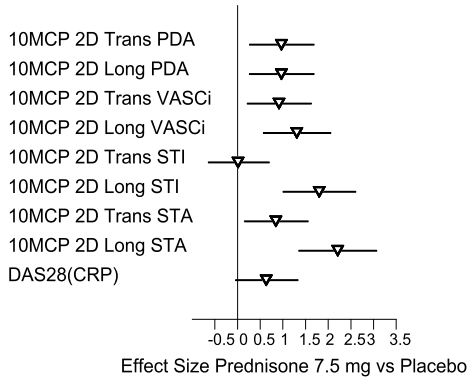

Day 14

Prednisone 7.5 mg

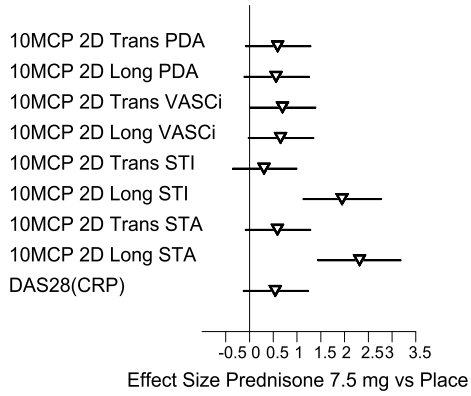

5.8 Exploratory composite endpoint responsiveness

Each composite endpoint is a simple sum of the standardized score corresponding to the DAS28(CRP) and two US endpoints, each summed across 10 MCPJs. The composite endpoint of interest had been pre-specified as the DAS28(CRP), the 2D Trans VASCi and the 2D Long STA. In addition we explored the effect sizes at Days 15, 8 and 2 for a number of composite endpoints constructed using the DAS28(CRP) and either Trans PDA/VASCi or Long STA/STi. These results from Panel A displayed in table 5-7. These were selected as they generally had the largest

effect sizes at the three post-treatment time points. All four composite endpoints demonstrated statistical significance after only a single day of dosing i.e. at Day 2. DAS28(CRP) is recorded for each of the 3 time points as a comparison. This exercise was repeated using both the first scan performed at baseline and Day 15 and the second US scan. This shows similar effect size and significance.

The effect of prednisone 7.5 mg, Panel B, on the relatively easy-to-score pre-defined composite endpoint taken from the analysis of Panel A, Z-score (DAS28+Trans VASCi+Long STi), was significant at Days 15 and Day 8 (effect sizes 1.84 and 1.80 respectively). No composite endpoint could detect a significant difference between doses at each time point for Panel B -- Day 14, Day 7 and Day 1. A significant difference between doses at Day 1 is detected in most of the composites in Panel A, driven by the difference in the DAS28(CRP) endpoint. The effect size of the between-dose difference at Day 1 was numerically higher in the pre-defined sum of DAS28(CRP), 2D Trans VASCi and 2D Long STA compared to the effect size of the DAS28 (CRP), see table 5-8.

Subgroup Analyses

Post-hoc analyses including subjects with DAS28(CRP) scores less than the median were performed to assess the treatment effect on this less severe subgroup population. Treatment effect was assessed using the 'best' composite endpoints defined in section D4. above e.g. the sum of the standardized score of DAS28, Trans VASCi, Long STi; the sum of the standardized score of DAS28, Trans VASCi, Long STi , the sum of the standardized score of DAS28, Trans VASCi, Long STA, the sum of the standardized score of DAS28, Trans PDA, Long STi, or the sum of the standardized score of DAS28, Trans PDA, Long STA.

Based on theses endpoints, effect sizes for the subgroup of subjects with DAS28(CRP) < 5.65 at baseline, were approximately equal to 1 at Days 1 and 7, and between 1 and 1.4 at day 14.Table 10

Table 5-7: Effect Size for Composite Endpoints (Panel A) Day 14, Day 7 and Day 1

§ Significant treatment effect compared to placebo

Endpoint (Z score)	Scan	Day 15	Day 8	Day 2
DAS28+Trans VASCi+Long STi	1	1.96 (0.97; 2.90)§	1.41 (0.46; 2.32)§	1.28 (0.40; 2.13)§
DAS28+Trans VASCi+Long STA	1	2.05 (1.05; 3.01)§	1.53 (0.56; 2.46)§	1.14 (0.28; 1.98)§
DAS28+Long STA+Trans PDA	1	2.14 (1.12; 3.10)§	1.17 (0.25; 2.05)§	1.14 (0.28; 1.98)§
DAS28+Long STi+Trans PDA	1	1.93 (0.95; 2.87)§	0.98 (0.09; 1.84)§	0.95 (0.11; 1.76)§
DAS28+Trans VASCi+Long STi	2	1.78 (0.82; 2.69)§	0.89 (0.01; 1.74)§	0.73 (-0.09; 1.53)§
DAS28+Trans VASCi+Long STA	2	1.86 (0.89; 2.79)§	0.98 (0.09; 1.84)	0.90 (0.07; 1.71)§
DAS28+Long STA+Trans PDA	2	1.39 (0.49; 2.25)§	1.10 (0.19; 1.97)§	1.25 (0.37; 2.09)§
DAS28+Long STi+Trans PDA	2	1.35 (0.46; 2.21)§	0.91 (0.03; 1.77)§	1.01 (0.16; 1.83)§
DAS28(CRP)	-	1.19 (0.11; 1.76)§	0.95 (-0.12; 1.59)§	0.37 (-0.15; 1.46)

Figure 5-9: Kinetics of composite endpoint response and effect size (z- scores) for Panel A and Panel B

A: Mean change in composite endpoint: (DAS28(CRP), 2D Trans VASCi and 2D Long STA) at baseline, Day 1, 7, and 14 after start of treatment for Panel A and B **B:** Z-score (DAS28(CRP) 2D Trans VASCi and 2D Long STA) Effect Size and 90% CI Within-panel Comparisons, Day 1 Prednisone 15 mg and **C:** Prednisone 7.5mg

A

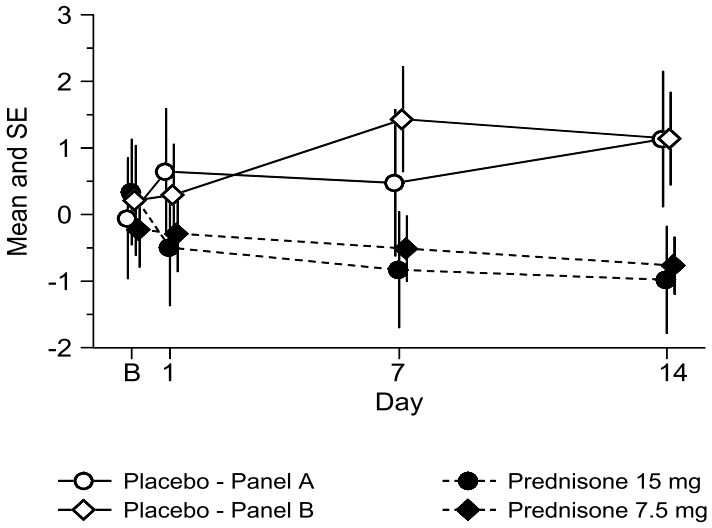

B

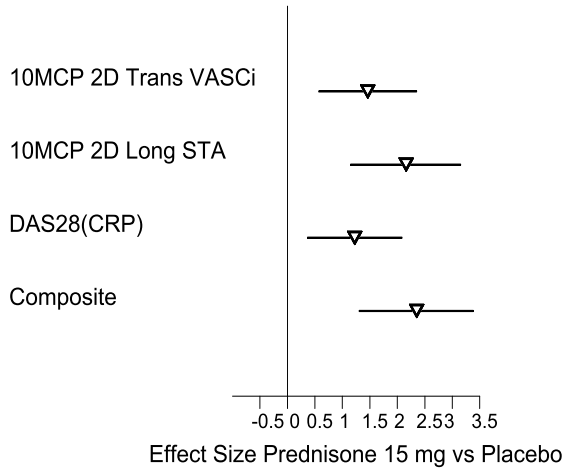

C

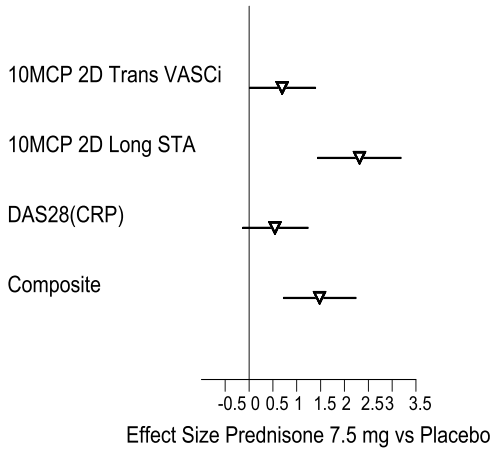

Table 5-8: Effect size for various composite endpoints using DAS28 and alternative US endpoint pairings.

Effect size of selected composite Endpoints, subgroup of subjects with baseline DAS28(CRP) < median (5.65), 5 Placebo and 4 Prednisone Subjects - Day 14, Day 7 and Day 1 Effect Size (90% CI)

Endpoint	Day 14	Day 8	Day 1
DAS28+Trans PDA+Long STA	1.09 (-0.15; 2.25)	0.88 (-0.39; 2.08)	0.91 (-0.29; 2.05)
DAS28+Trans VASCi+Long STA	1.12 (-0.12; 2.29)	1.05 (-0.25; 2.27)	1.01 (-0.21; 2.17)
DAS28+Trans PDA +Long STi	1.35 (0.06; 2.56)	1.83 (0.33; 3.21)	1.23 (-0.03; 2.42)
DAS28+Trans VASCi+Long STi	1.40 (0.10; 2.62)	2.03 (0.47; 3.46)	1.38 (0.08; 2.59)
DAS28(CRP)	0.62 (-0.23; 2.43)	0.41 (-0.32; 2.76)	0.33 (-0.48; 2.59)

5.9 Discussion

We have demonstrated that a wide range of grey scale US measures of synovial thickness and PDUS measures of synovial vascularity at the MCPJs are reproducible and capable of detecting treatment effects of oral prednisone (15 mg and 7.5mg daily) after a week, and two US measures after only one day, in small panels of subjects (n=18 and n=27 respectively) with moderate to severely active RA. DAS28(CRP) was only able to detect a significant treatment effect after two weeks in the 15 mg cohort. Ultrasound may therefore be a leading indicator of therapy response occurring before a clinical response. At present, over 50% of drugs tested fail at phase III and the expense of the traditional drug development pathway has become prohibitive for numerous novel compounds developed to selectively inhibit a range of potential therapeutic targets that have been identified for RA . This study has extensively investigated the sensitivity of a diverse range of 2-dimensional ultrasonographic endpoints at the metacarpophalageal joints and their potential as tools to provide an early and objective indication of a therapeutic response to treatment intervention in rheumatoid arthritis. We have confirmed that

ultrasonography of metacarpophalageal joints is an early, reliable indicator of therapeutic response in RA and it thus has the potential to reduce patient numbers required as well as the duration of clinical trials designed to give a preliminary indication of efficacy. Such an approach to early drug development in RA might enrich for the chances of success in later phase studies designed to meet the regulatory endpoints that are required to achieve approval.

In the present study, correlations between the majority of different US endpoints and DAS28(CRP) at base line showed only moderate correlation. On treatment, there was some improvement in the correlation coefficient between DAS28(CRP) and mainly the vascular US endpoints whilst other endpoints were less well correlated. This may suggest that they measure somewhat different constructs. Combining US endpoints with DAS28(CRP) increased effect sizes at all time points and identified treatment effects earlier. Composite endpoints increased the endpoint sensitivity for 15 mg in Panel A. The DAS28(CRP) had an effect size of about 1.0, which would take 13 subjects per group to identify a treatment difference (α 0.1; 80% power). In combination with an ultrasound endpoint with combined effect size of ~1.5 the sample number drops to six per group. Some combinations of ultrasound endpoints with effect sizes of ~2.0 would require four subjects per group. Likewise, single dose effects of 15 mg prednisone were identifiable with some combinations of endpoints. These findings strongly suggest a potential value in employing such composite endpoints in future prospective small studies designed to establish an early indication of efficacy. Composite endpoints were selected from Panel A on how well they performed. They were tested in Panel B in a in a predefined way but in a limited capacity. These composite endpoints need to be tested in future studies to confirm their utility.

15 mg and 7.5 mg prednisone both represent relatively low corticosteroid doses and it would be notable if an endpoint could differentiate their effect. Overall there was a trend towards a dose-response. Greater numbers of subjects may have discriminated the two doses. Other factors that may have decreased the study's

ability to differentiate the two doses include the fact that there were two centres, the scanning rooms of which for example may have been at different temperatures, and there were two ultrasonographers, the first scans of each in their respective centres were used to determine treatment effect.

For Panel B the 10MCP Trans PDA demonstrated a significant treatment effect earlier than in Panel A. This may be because there were more subjects in Panel B who received active treatment, albeit at a lower dose. To support this, at Day 8 more US endpoints registered a significant treatment effect for Panel B than Panel A.

For Panel A, 7 out of 8 US endpoints demonstrated a consistent time-response to 15mg of Prednisone. Within Panel B more US endpoints registered a significant effect size at Day 8 in comparison with Day 15 perhaps due to waning of therapeutic response to low dose corticosteroid in some subjects. The observed transient response of the US endpoints to 7.5 mg of prednisone was mirrored in the effect sizes of the DAS28(CRP) even though this latter endpoint did not show significance at any time point. We postulate that for some subjects in Panel B, 7.5mg of Prednisone may be just below the threshold dose for a sustained anti-inflammatory effect. The biological response to prednisone at low doses (≤ 7.5 mg/day prednisone or equivalent), is not necessarily predictable in inducing and sustaining an anti-inflammatory effect in RA [29]. If we had used larger doses of prednisone in the study e.g. 40mg we would have undoubtedly seen more consistent time-responses but this would have weakened the impact of the study as it would not have permitted a demonstration of the sensitivity of US to detect change.

The Long STA endpoint performed especially well in the current study. Previous investigations of gray-scale synovial thickness have shown inferiority to power Doppler vascularity in detecting a treatment effect; with respect to the kinetic and the extent of change. However, those studies measured synovial thickness semi-quantitatively in the transverse plane only. Semi-quantitative indices may constrain the detection of change in joints if synovial thickening greatly exceeds the largest score by delivering static scores when genuine reduction in synovial thickening can

be detected quantitatively. The greater area afforded by the longitudinal view versus the transverse may have also benefited the registration of a treatment effect by the Long STA endpoint. The data in the current study support these theories: semi-quantitative measures of synovial thickening had smaller effect sizes than quantitative measures (only exception was Day 2, panel B); transverse measures of synovial thickness had smaller effect sizes than longitudinal measures (only exception was Day 2, Panel A) [Figure 2]. Treatment effect was less at Day 2 and therefore these factors would have had less influence at this early time point.

Due to the time constraints of scanning we restricted our US evaluation to the dorsum of the MCPJs. It may have been valuable to have assessed endpoints derived from imaging over the palmar surface also.

5.10 Conclusions

Our study confirms that ultrasonographic imaging of MCPJs could be used as an early and reliable indicator of a therapeutic response to a new treatment intervention in RA early phase clinical trials with small patient cohorts over a 2 week test period and decrease the time-to-decision for progressing clinical development. By addressing the issues surrounding the reliability of US to objectively measure synovitis this study brings us closer to approving this tool as a recognised endpoint for confirming treatment effect in RA clinical trials. The semi-quantitative US endpoints demonstrated in this study, whether used alone or together with clinical measures as composite endpoints, could be used in centres not possessing quantitative analysis tools. The study also illustrates the potential utility of US to stratify patient selection by detecting those with potentially reversible baseline joint inflammation, an important consideration given concerns about bias introduced in trials by recruitment of patients with equivocal clinical swelling. Moreover, composite endpoints have the potential to further reduce patient numbers and study duration in early phase trials.

6. Safety and tolerability of US guided synovial biopsies

6.1 Introduction

Joint synovium is a clear focal point for the inflammatory process in Rheumatoid Arthritis. Despite significant progress in our understanding of the mechanisms controlling the inflammatory pathway, harvesting of synovial tissue is currently not routinely performed in clinical practice. However, there is great interest in retrieving synovial tissue for research purposes and early phase drug development studies[221 391 392].

The ability to successfully harvest good quality synovial tissue must be in the context of a well tolerated and safe procedure. Historically, synovial biopsies have been performed by a blind needle approach or conventional arthroscopy. Blind needle biopsies are well tolerated and relatively simple to perform[217 225 393]. Arthroscopic biopsies are technically more complicated and require theatre time but have significant advantages in being able to harvest tissue under direct visualization. This procedure has been extensively validated with respect to tissue quality in therapeutic studies making it the accepted gold standard for synovial tissue acquisition [221 265 391 394 395]. This has led to the emergence of relatively small number, proof of concept studies affording an early go/no go decision in drug development. Once again, this technique tends to be performed in larger joints (knee and ankle) limiting recruitment of patients with suitably involved joints.

More recently, advances in ultrasound (US) imaging have facilitated the development of a minimally invasive ultrasound guided synovial biopsy technique[222-224]. A similar technique has previously been described in a small case series using a single portal and forceps approach in 9 patients with established RA[224]. The authors concluded that tissue harvested form small joints using this technique represented a reliable approach for good quality tissue. There is a need to replicate these findings in a much larger cohort of patients and show that it has an acceptable safety and tolerability profile. If proven, the ability to reliably sample synovial tissue from both

large and small joints would have an impact on recruitment for early phase therapeutic studies and broaden the usefulness of synovial biopsies if clinical utility is shown with respect to disease classification or therapeutic drug selection.

6.2 Objectives

The main aim of this study was to determine the tolerability, safety and yield of synovial tissue in ninety three consecutive minimally invasive ultrasound guided synovial biopsies of both small, medium and large joints using an US guided technique in an early arthritis cohort.

6.3 Materials and methods

6.3.1 Patients

93 sequential ultrasound guided synovial biopsy procedures were included in the study. All patients were recruited as part of the Pathobiology of Early Arthritis Cohort (PEAC: www.peac-mrc.mds.qmul.ac.uk) within the department of rheumatology at Barts Health NHS Trust. PEAC is a prospective multicenter study and recruits treatment naive patients with early arthritis (<1 year duration) with at least one clinically swollen joint for a baseline and 6 month follow up synovial biopsy, along with the collection of a number of radiographic and clinical parameters. Data was available from 57 patients undergoing baseline synovial biopsy, 36 of these patients had received a second biopsy procedure performed at a 6 month follow up visit during this period. All procedures were performed following written informed consent and were approved by the hospitals ethics committee (REC 05/Q0703/198).

6.3.2 Ultrasound Guided Synovial Biopsy Technique

US guided synovial biopsy was performed using a GE Logiq 9 ultrasound machine with a 2-dimensional M12L transducer. Three operators (SK, FH and NN) performed all 93 biopsies . Pre-βiopsy standard longitudinal ultrasound images of each biopsied

joint were recorded with power Doppler switched on and off. Synovial tissue was defined as hypoechoic non-compressible intra-αrticular tissue. Power Doppler settings were adjusted to the lowest permissible pulse repetition frequency to maximise sensitivity. Maximum colour gain was used without creating artifactual noise. Each procedure follows a similar routine with 1-3 mls of local anaesthetic injected into the soft tissues up to the joint capsule, visualized under US guidance. A further 2-5mls of local anaesthetic (1% lignocaine) is instilled into small joints, 10-15mls for large joints. For larger joints a suitable coaxial outer needle may be used in addition to the Quick-Core® Biopsy Needle (Cook medical, Limerick, Ireland), placed within the joint capsule - 16 / 14G (Figure 1A). A longitudinal US image is used to detect the needle and guide it to an appropriate pre-determined site for biopsy. For smaller joints a Quick-Core® biopsy Needle (16G, throw length 10mm) was used without a coaxial sheath. The maximum tolerated number of biopsies per joint was attempted with the aim for a minimum of 12 biopsies were aimed to be retrieved per procedure. Six to eight biopsies were immediately fixed in 4% paraformaldehyde for paraffin embedding and a further six immersed in 10:1 v:v of RNA-Later (Ambion) for later RNA extraction. Following the procedure, a small sterile dressing was placed over the site of the needle insertion (online video - www.synovialbiopsy.com).

A standard questionnaire was administered to all patients immediately pre and post biopsy and at their post-βiopsy clinic review (3-7 days). Patients indicated pain, swelling and stiffness of the biopsied joint pre and post procedure using a visual analogue score with tolerability being assessed using a 5-point Likert scale. At their post-βiopsy clinic review patients were also asked to record how likely they were to consider a repeat biopsy in the future using a scale of highly likely, somewhat likely, unsure, somewhat unlikely and highly unlikely.

6.3.3 Ultrasound synovitis score

Standard longitudinal images of individual joints prior to the ultrasound guided procedure were viewed by an observer blinded to patient data. Synovial thickening and degree of power Doppler signal was scored using a previously reported semi-quantitative score (0-3)[396].

6.3.4 Synovial Histopathological Assessment

From each paraffin embedded block of synovial tissue 3µm thick sections obtained from three different cutting levels 50μm apart underwent routine staining with haematoxylin and eosin. Sections were considered valid for further histological scoring only if an intact cell lining layer was visible. A synovitis score was then assigned to each valid tissue section according to a previously described scoring system[145]. Each section underwent semi quantitative assessment for three synovial membrane features; i) thickness of the synovial lining cell layer, ii) stroma cell density and iii) inflammatory cell infiltrate using a scale of 0-3 (Figure 1B). A composite score integrating these three features was then determined and samples categorized as no synovitis (0-1 points), low-grade synovitis (2-4 points) and high grade synovitis (5-9 points).

6.3.5 RNA extraction

RNA was extracted from synovial tissues biopsies using a Trizol separation protocol. A minimum of 10mg of synovial tissue was homogenised in cold Trizol reagent (Life Technologies, Invitrogen Division, UK). Chloroform was mixed with the lysate and following centrifugation the aqueous RNA layer was transferred to a new microcentrifuge tube. Pre-chilled isopropanol was then mixed with the RNA layer. Following incubation and centrifugation, the isopropanol was removed and the RNA pellet washed with 70% ethanol. The pellet was re-dissolved in RNase-free water. The concentration/purity of the RNA sample(s) were measured using the NanoDrop 2000C (Lab Tech, UK) and the quality (RIN) was assessed using the Agilent 2100 Bioanalyser (Agilent Technologies, UK) (Figure 1B).

6.4 Statistical analyses

Demographic characteristics of patients, safety and tolerability data were described with mean (+/-Standard Deviation [SD]) values or relative frequencies. As RNA yield was a non-parametric variable, median (interquartile range=IQR) or relative frequencies were used for descriptive analyses for the tissue quality data. Univariate analyses were performed using Fisher's test, Mann Whitney U and Kruskal-Wallis when appropriate. Multiple linear regressions were performed to model the percentage of graded biopsies and the quantity of RNA yield (log transformed) according to the ultrasonography score of synovial thickening (from 1 to 3), the biopsy site (small, medium or large) and the biopsy rank. P values <0.05 were taken as statistically significant.

All statistical analyses were performed using GraphpadPrism version 3.03 (Graph pad software for mac version 5.0).

6.5 Results

Characteristics of the study patients

Demographic and clinical features of the 57 patients included within the study are shown in Table 1. Of these patients 36 had undergone a second biopsy. 5 different joint sites were biopsied (Table 1), with the knee (34.5%) and wrist 44.1%) most frequently biopsied.

6.5.1 US guided synovial biopsy is safe and is well tolerated by patients

Of the 93 ultrasound guided procedures performed the only reported complication was 3 patients feeling faint during the procedure however after a suitable period of time all 3 allowed the procedure to be completed. Potential complications assessed at the post-procedure follow up visit were infection, haemarthrosis, deep venous thrombosis, thrombophlebitis, post procedure arthralgia and flare of the underlying disease. Importantly there were no reported cases of wound or joint infection and no evidence of a flare of the underlying disease. At the post-procedure follow up visit 18 patients (19.4%) reported mild arthralgia following the procedure, however this

resolved within 24hrs with simple analgesia. Patients were also asked to indicate the tolerability of the procedure using a 5-point likert scale ranging from no discomfort to severe pain (Table 2). There was a significant difference in the number of patients reporting discomfort during biopsy of a large joints (elbow, knee) compared to small and medium sized joints (Wrist, MCP and PIP) (Fisher exact test p = 0.03). There were no significant differences between any of the other patient reported outcomes. Only 1 patient described mild pain during the biopsy and his was attributed to a prolonged procedure.

Patients were asked to complete pre and post procedure VAS assessments of pain, stiffness and swelling. While there was a small trend to reduction in all post procedure assessments this did not reach statistical significance (Figure 2A).

The majority of patients were agreeable to having a subsequent US guided synovial biopsy at a later date with 81.7% of patients either 'very likely' or 'somewhat likely' to have a repeat procedure (Figure 2B). However in practice, 54 of the 57 patients surveyed following their first biopsy have subsequently consented to a second biopsy as part of the PEAC study, representing more than 95% compliance with two US guided synovial biopsies at baseline and at 6 months follow up.

6.5.2 US guided synovial biopsy yields high quality synovial tissue suitable for histopathological characterisation

A median of 14 biopsies samples were retrieved from each procedure (range 4-32). Three H and E stained sections 50μm apart from each synovial biopsy were examined at x40 magnification and sections with a visible lining layer underwent semi-quantitiative assessment for degree of synovitis (scale 0-9)[145]. Of all 93 procedures performed 85 (91.3%) procedures yielded synovial tissue suitable for undergoing further histopathological classification for synovitis, these are subsequently referred to as "graded biopsies". Patients were classified as high grade, low grade or uninflamed dependent on the predominant synovitis score

between tissue sections. 43% of procedures yielded tissue classified as low grade synovitis and 34% high grade synovitis, 9% of patients were classified as uninflamed. A median number of 15, 14 and 13 samples were taken respectively from small joints (MCP / PIP / MTP), medium joints (wrists) and large joints (knees and elbows). In order to determine whether yield of graded synovial tissue was dependent on size of joint biopsied procedures were then classified into those performed on small (MCP, PIP and MTP), medium (wrist) and large (elbow and knee) joints. For each group, the mean percentage of graded tissues was reported (Figure 3A). Although there was a trend for small joint biopsies to yield a smaller percentage of graded biopsies (40%) versus medium (51%) and large (58%) this did not reach statistical significance.

6.5.3 US guided synovial biopsy yields tissue sufficient for high quality RNA extraction

In order to determine whether us-guided synovial biopsy yielded sufficient quantity and quality of synovial tissue for RNA extraction synovial tissue stored in RNA-Later underwent processing for extraction of RNA (need MB to word this correctly not sure which method they used). Quality of RNA was determined via the RNA integrity score (Figure 1B) (RIN) and quantity of RNA determined per us-guided biopsy procedure. The median RNA yield for each joint varied according to joint size (large - 0.89 µg/10 mg tissue, medium - 0.69µg/10 mg tissue, small - 0.54 µg/10 mg tissue), however no statistical difference was demonstrated between total RNA yield in each group joint size despite a tendency for smaller joints to provide a lower yield (p=0.22) (Figure 3B).

Tissue quality and RNA yield is maintained in subsequent biopsies

Thirty-six patients within this study were patients undergoing a second synovial biopsy at 6 months post recruitment to the PEAC study. As the second us-guided synovial biopsy was performed in all cases on the same joint biopsied at baseline, a

comparison of tissue quality between procedures was feasible. Similar numbers of samples were taken at both first and second biopsies (median of 14 [range 6-32] and 14 [range 4-24] samples respectively). When number of procedures yielding graded synovial tissue per total procedures performed following first biopsy (93%) and second biopsy was compared (88.9%), no significant difference was seen (p=0.70). Additionally, although total RNA yield varied from first to second biopsy this did not reach statistical significance, 1st biopsy - 1.14µg/10mg tissue (IQR: 0.46; 2.07), 2nd biopsy 0.61 µg/10mg tissue(0.26 - 0.89) (p=0.08), (figure 3C).

6.5.4 Synovial tissue quality varies with pre-βiopsy ultrasound assessment of synovial thickening

In order to determine whether pre-βiopsy US assessment of synovitis determined yield of either graded synovial tissue or RNA quantity us-guided biopsy procedures were segregated according to the pre-βiopsy US grey scale synovial thickness and power Doppler score (semi-quantitative 0-3). Differences in yield of graded synovial tissue per total procedures performed and mean yield of RNA (ug/mg) were then examined within each US-GS group. There was a significantly higher yield of graded synovial tissue in those with grade 3 synovial thickening versus grade 2 and grade 1 ($p<0.01$) (figure 4A). Similar results were seen when RNA yield was examined with grade 3 synovial thickening associating with a significantly higher RNA yield than grade 2 and grade 1 (Figure 4B). A similar analysis was performed when segregating procedures according to pre biopsy power Doppler signal but no significant differences in either graded synovial tissue or RNA yield were seen (results not shown).

Using synovial thickness score, power doppler score and and joint size as variables, the degree of US detected synovial thickening was the only independent predictor of tissue RNA extraction and grading using multi variant analysis (Figure 4A and 4B). A

single MCP joint of US synovial thickness grade 3 was biopsied and thus excluded from the analysis.

6.6 Discussion

Harvesting of good quality synovial tissue is an important step along the path of understanding the pathogenesis and disease evolution of Rheumatoid Arthritis. To date the most convenient method for tissue collection has been either at the point of joint replacement surgery or by arthroscopic intervention. By definition, joint replacement surgery is usually required in established disease with clinical manifestation of inflammatory joint pathology for many years. The ability to retrieve synovial tissue of good quality, by a safe and tolerable method, at the initial onset of inflammatory joint disease will help dissect the pathological process evolving in our patients. Additionally, the ability to harvest good quality tissue from smaller joints, such as wrist and MCP joints, may improve recruitment to small proof of concept studies in context of early drug development.

In this paper we have demonstrated that a minimally invasive approach to synovial tissue harvesting using US guided approach can be both safe and tolerable to patients. Tolerability appears to be better in small and medium sized joints (MCP/ PIP / Wrists) which is likely to represent the relationship of joint size to local anesthetic instilled. PIP joints are often biopsied using a ‘ring block’ technique providing total anesthesia to the digit. Tissue quality appears to be preserved in subsequent biopsies following therapeutic intervention as shown by the 36 patients in our cohort who received a second synovial biopsy. This is an important finding in the context of using such a technique to monitor changes in synovial biomarkers with response to therapy. While we did not demonstrate a statistical difference in terms of joint size and tissue quality, there is a suggestion that smaller joints such as MCP or PIP joints may yield less graded tissue with a lower total RNA yield extracted. This is likely to reflect the technical difficulties in performing the biopsy at this level but

encouragingly at least 40% of all tissue samples are graded with sufficient RNA extracted for laboratory analysis.

Ultrasound as a pre-αssessment tool appears to improve tissue yield with joints demonstrating greater synovial thickening performing better on tissue grading and total RNA yield. Once again this is likely to reflect the mechanics of sampling joints with small amounts of ultrasound detectable synovial thickening regardless of joint size. Therefore, to inform the choice of joint to be biopsied and maximise tissue quality we suggest a decision tree based upon our findings (figure 5).

Our overall success rate of 92.5% patients with graded synovial tissue seems to compare favorably with similar invasive diagnostic procedures. Renal biopsies are performed routinely as part of the diagnostic work up with a variable success rate. Suitable tissue for analysis being harvested in 83% - 97% of case series reported[397-401]. A similar results are seen in the context of liver biopsies with adequate or diagnostic liver tissue obtained in 81% - 97% of cases[402]. In addition, major complications of renal biopsies have been quoted as between 18% and 28 % in these series. Arthroscopic procedures performed by Rheumatologists or Orthopaedic surgeons reportedly runs approximately 1% risk of a significant port - procedure complication[218]. Our data compares favorably to this with no patients presently reporting a significant complication following this minimally invasive ultrasound guided biopsy technique, however 3 patients did report feeling faint during the procedure. While 93 biopsy procedures represents the largest published cohort of patients undergoing this procedure to date, we are aware that as a developing technique, safety remains an important outcome to be monitored and reported. Importantly, this report refers to a single units experience of this procedure. Further work is needed to confirm these finding in different sites, specifically confirming the safety and quality of harvested tissue.

Table 6-1: Summary of patient demographics undergoing synovial biopsy.

Clinical characteristics of 57 patients were recruited to the study

	N (%)
Gender - Female - Male	 36 (63.2) 21 (37.8)
Age (years) mean+/- SD	50.7 +/- 7.9
Disease duration (months) mean +/-SD	7.2 +/- 1.3
Clinical diagnosis - Rheumatoid arthritis - Psoriatic arthritis - Undifferenciated arthritis - Monoarthritis	 40 (70.2) 6 (10.5) 10 (17.6) 1 (1.7)
Serology - Rheumatoid factor - Anti-CCP	 19 (33.3) 14 (24.6)
Biopsied joint Large -- Knee -- Elbow Medium --Wrist Small -- PIP -- MCP	 33 (35.5) -- 32 (34.4) -- 1 (1.1) 41 (44.1) -- 41 (44.1) 19 (20.4) -- 2 (2.2) -- 17 (18.3)

Table 6-2: Patient reported pain / discomfort during the ultrasound guided synovial biopsy.

Percentages in each group are noted in brackets.

	None (%)	Mild discomfort (%)	Moderate discomfort (%)	Mild pain (%)	Severe pain (%)
All biopsies	72 (77.7)	14 (15.1)	6 (6.5)	1 (1.1)	0 (0)
Small Joints	18 (81.8)	1 (4.5)	3 (13.6)	0 (0)	0 (0)
Medium Joints	35 (87.5)	4 (10)	0 (0)	1 (2.5)	0 (0)
Large Joints	19 (61.3)	9 (29)	3 (9.7)	0 (0)	0 (0)

Figure 6-1: Histopathological scoring of synovial tissue acquired during us-guided synovial biopsy

A. Image illustrative of patient undergoing ultrasound guided synovial biopsy of right wrist with needle placement at the scaphoid lunate junction **B**. Representative images of synovial tissue sections x4 magnification from ultrasound-guided synovial biopsy procedures of patients biopsied within this study cohort. 3µm sections underwent routine staining with haematoylin and eosin and were semi-quantitatively assessed using a previously validated synovitis score[145]. A composite score of 0-9 was determined following assessment of increasing lining layer thickness (panels A,D and G), density of the resident sublining cellular infiltrate (fibroblasts, endothelial cells and macrophages)(B, E and H) and sublining inflammatory cell infiltrate (lymphocytes and plasma cells), (C, F and I). IHC performed by Dr. B. Hands (Experimental Medicine and Rheumatology, William Harvery Research Institute).

A

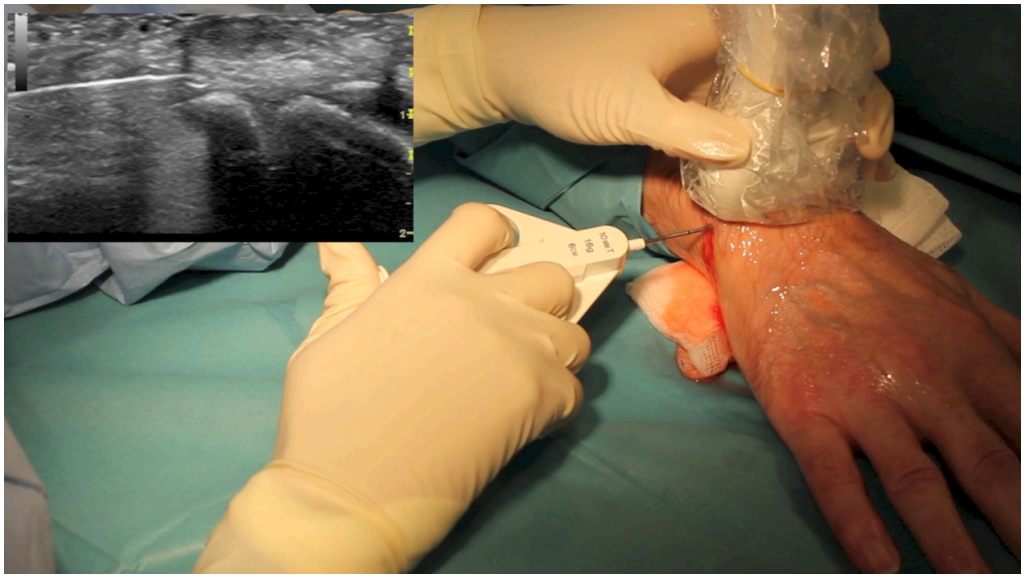

B

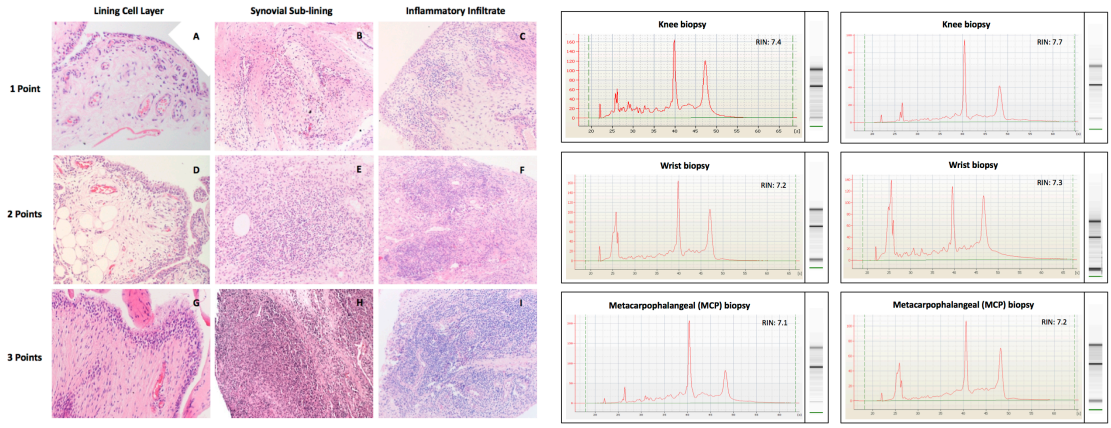

Figure 6-2: US-guided synovial biopsy is a safe and well tolerated procedure.

A. Patients were also asked to complete a Visual analogue score (VAS) assessing immediately prior to and following the procedure, joint pain, stiffness and swelling. No significant differences in any of the 3 variables pre and post procedure was reported (n=93). **B:** At their post procedure clinic visit 3-7 days following the synovial biopsy patients were also asked to record the how agreeable they were to having a subsequent synovial biopsy: Very likely (VL), Somewhat likely (SL), Not sure (NS), Somewhat unlikely (SU), Very unlikely (VU). Results are expressed as percentage of total patients (n=93). **C**: Patient reported discomfort during the biopsy procedure

A

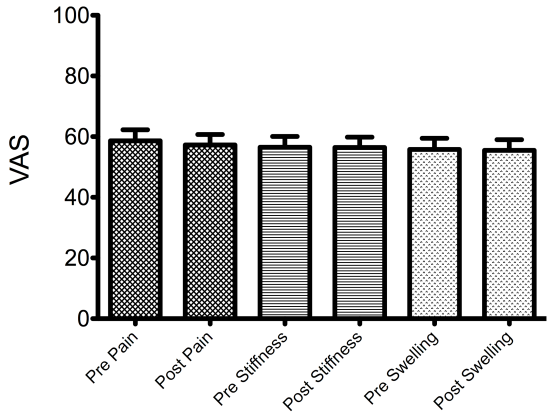

B

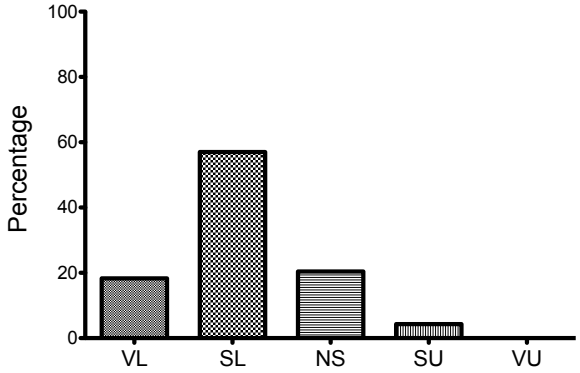

C

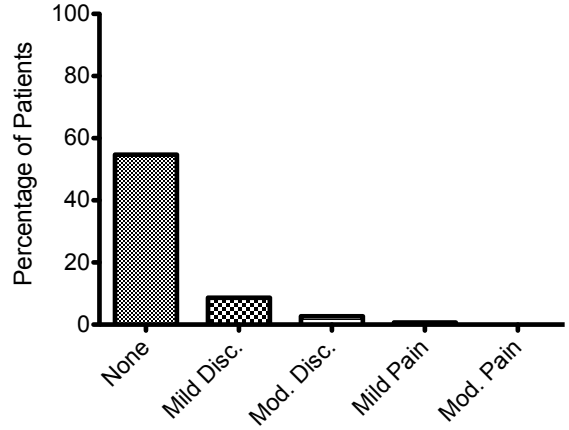

Figure 6-3: Percentage of gradable tissue and RNA yield from small medium and large joints

A: Percentage of graded synovial tissue within each procedure by joint size, **B**: Total yield of RNA from biopsy samples by joint size, **C**: Average total RNA yield of per biopsy procedure of 1st and 2nd biopsy procedures

A

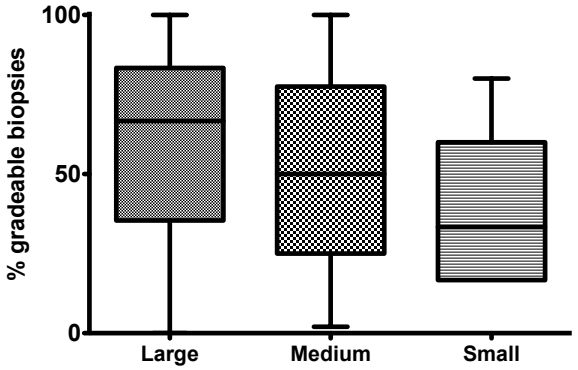

B

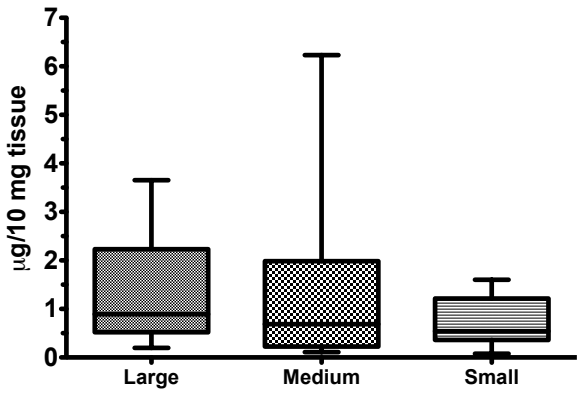

C

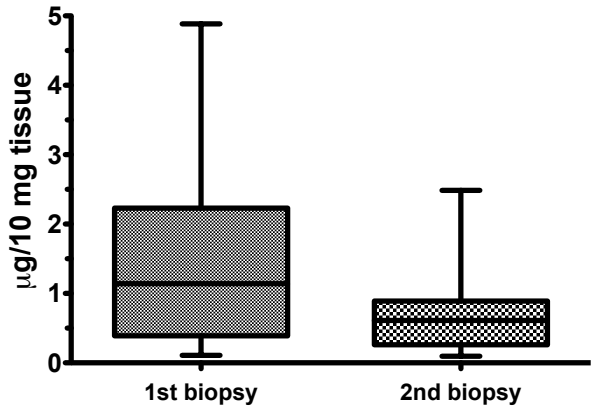

Figure 6-4: Synovial tissue quality varies with pre-βiopsy ultrasound assessment of synovial thickening

A: Tissue gradability by pre-βiopsy US grey scale (US-GS 1-3) synovial thickening assessment. **B**: Average total RNA yield by pre-βiopsy US grey scale synovial thickening assessment.

A

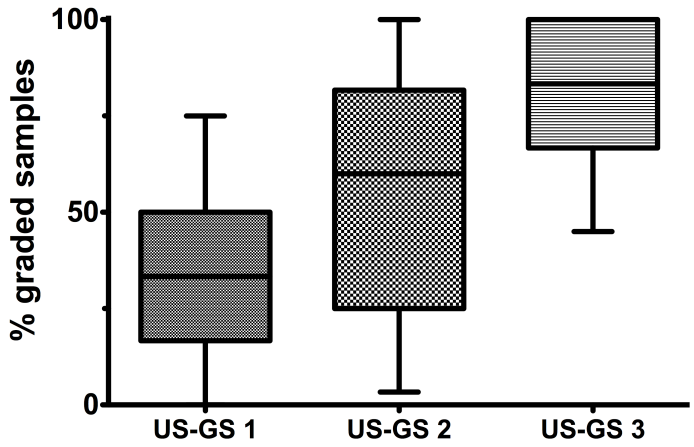

B

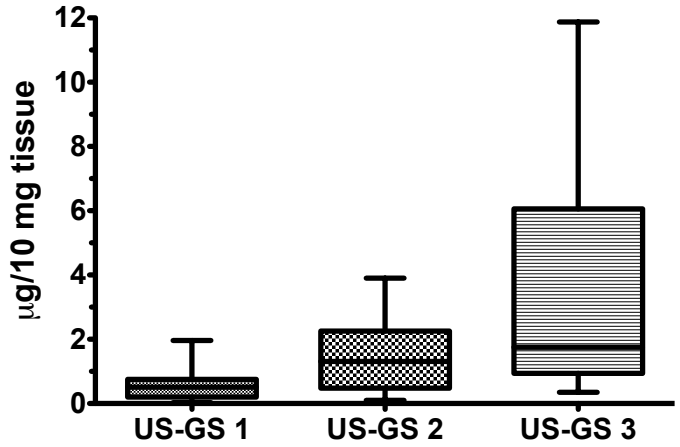

Figure 6-5: variation of tissue grading and RNA yield by joint size and US determined synovial thickness

A: Variation of graded tissue as demonstrated by joint size and US grey scale synovial thickness score. **B:** Variation of average total RNA yield as demonstrated by joint size and US grey scale synovial thickness score. L - Large joint, M - medium joint, S - Small joint. US GS synovial thickness grade 1 - 3 e.g. M2 - medium joint with US grade 2 synovial thickness

A

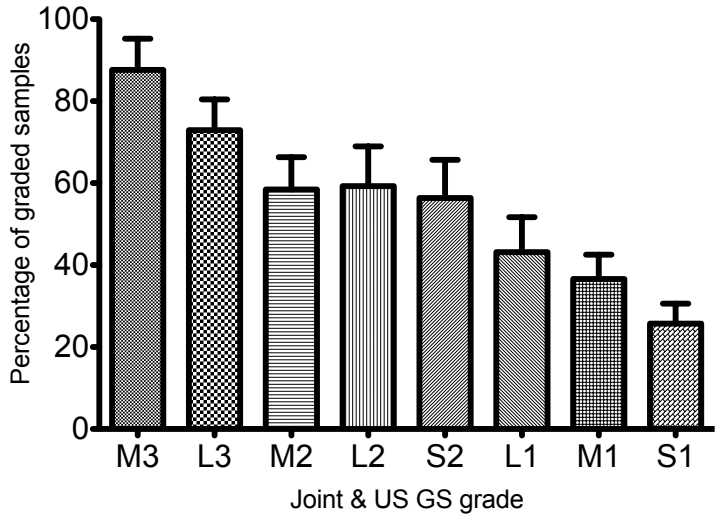

B

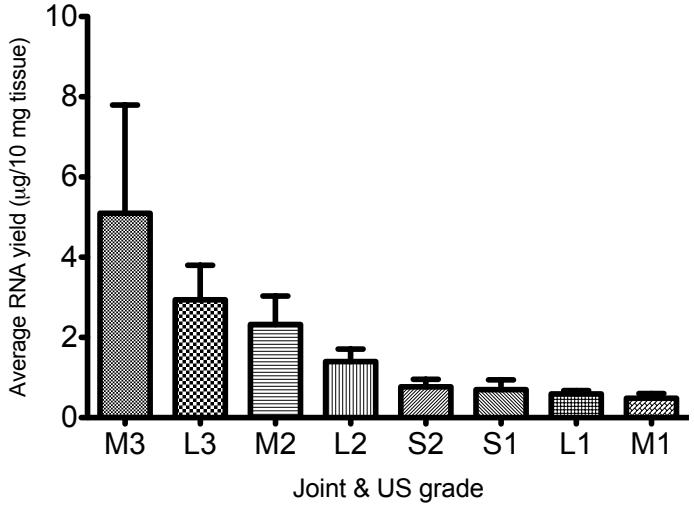

Figure 6-5: Suggested decision tree for guiding joint selection for US guided synovial biopsies and MCP, Wrist and Knee grading atlas

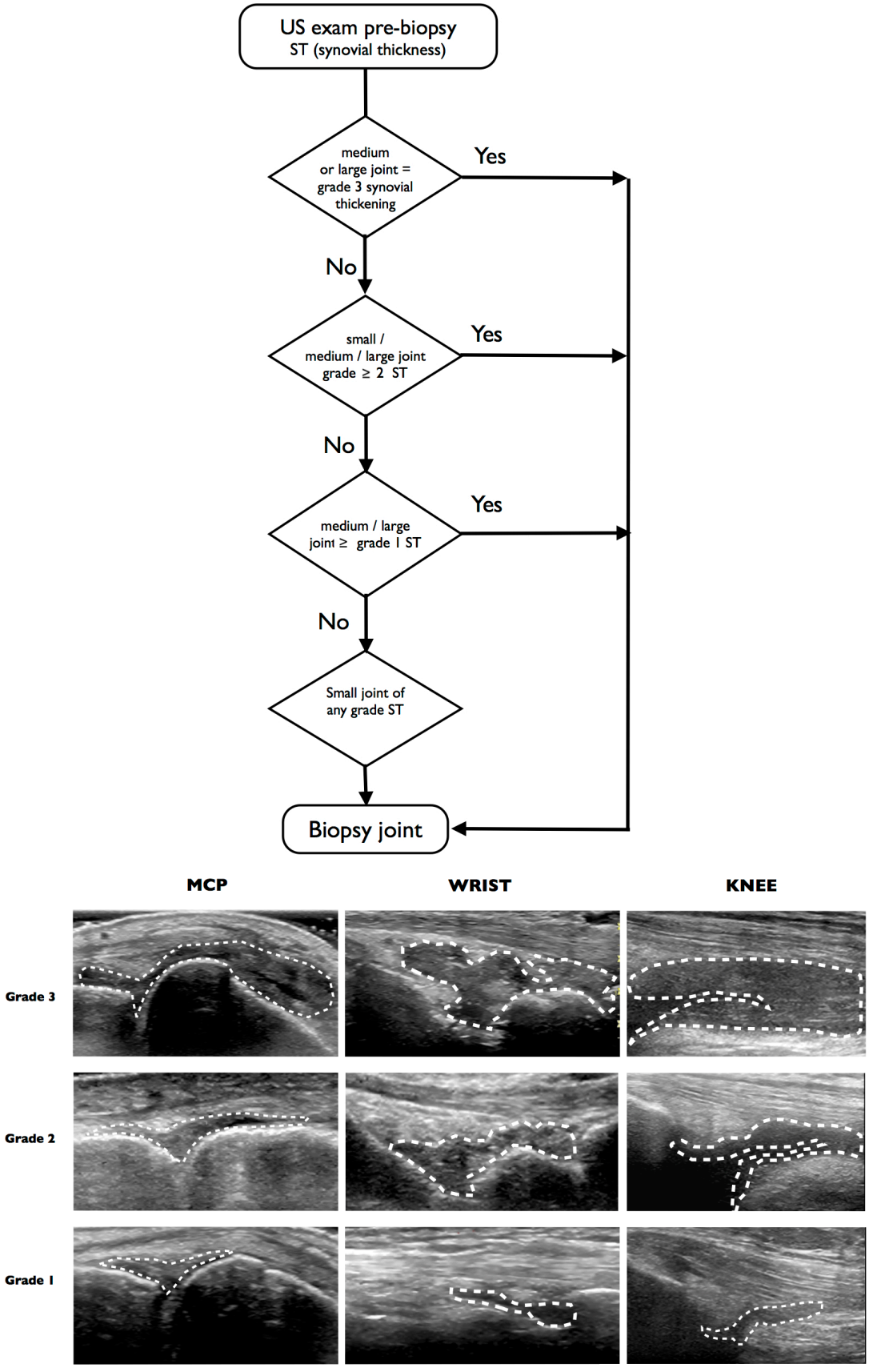

7. The relationship of ultrasound imaging to small joint synovial histopathology in patients with active Rheumatoid arthritis

7.1 Introduction

The assessment of synovial inflammation in patients with inflammatory arthritis is a critical aspect of everyday, routine clinical care. This assessment may take the form of a simple clinical examination of tender or swollen joints but more frequently Rheumatologists are employing other modalities, such as MRI or Ultrasound (US), to better define the presence of on going synovial inflammation. The most convincing comparator or gold standard for any assessment of joint inflammation is microscopic or macroscopic pathologic evidence of synovial inflammation. This is not a feasible routine investigation and as such, surrogate markers are required to provide physicians with the tools to classify patients and monitor response to interventions. One of the simplest surrogates employed by Rheumatologists is the assessment of joints by clinical examination. Swollen, tender, warm metacarpal-phalengeal (MCP) joints reflecting underlying synovial inflammation does have an inherent appeal with considerable face validity. The inclusion of the tender and swollen joint count as a component of the DAS28, a validated clinically relevant disease activity measure, does confirm its function as an important bedside assessment tool. Despite the considerable validation of DAS28 as a useful tool to monitor RA disease activity and guide therapeutic decisions, it has become clear that it has many deficiencies. Joint tenderness is very subjective and the physicians assessment may vary with the patients threshold for pain and on the examiners force of palpation. Swelling is often impossible to assess in larger patients or where joint inflammation in minimal.

The introduction of MRI and US as additional assessment tools has provided greater options for the Rheumatologist when determining the degree of disease activity and response to therapy. Despite the additional information afforded to Rheumatologists, there is still much work to be done to provide a suitable framework of integration for these imaging modalities. Many investigators have examined the use of US in

inflammatory arthritis and shown it to be a sensitive assessment tool which is responsive to therapeutic intervention and predictive of disease outcome in early arthritis. Few, however have addressed the validity of US imaging with respect to underlying histological features of synovial inflammation. Synovial vascularity was investigated by Walther et al., who found a good correlation between histological vascularity and visual grades of PDU signal in the synovium of both knee and hip joints in patients undergoing arthroplasty (r - 0.81 p <0.001). Schmidt et al. found good agreement between presence of colour Doppler signal and histologically verified pannus tissue in knee joints of RA and osteoarthritis patients undergoing joint replacement surgery. Pannus in this study was histologically defined as 'synovial proliferation with invasive destruction of cartilage and bone'. A study by Fiocco et al. found a significant correlation between B-mode US synovial thickness and arthroscopic grade of synovitis in arthritic knee joints.

Koski et. al. have provided the most extensive assessment to date of ultrasound and synovial histopathology. This study examined the relationship of ultrasound parameters and synovial histological findings in patients undergoing a percutaneous synovial biopsy of the designated site. Forty-four patients with either monarthritis or polyarthritis were recruited with a majority of knees (25 /44) being biopsied. In this study a robust assessment of the synovial tissue was made with only sections with an intact synovial lining layer being assessed. Seven histological parameters of each specimen was scored (multiplication of synovial lining, villous hypertrophy of the synovial surface, surface fibrin deposition, sub-synovial infiltration of polymorphonuclear leucocytes, sub-synovial infiltration of mononuclear leucocytes, proliferation of blood vessels and fibrosis). Each histopathological and ultrasound parameter was graded on a semiquantitative scale, with the 7 histological parameters summed to provide an overall score for the biopsied tissue. Grey-scale ultrasound showed synovial proliferation in 39 of 44 (89%) the patients however no significant correlation was found between the degree of synovial proliferation detected with ultrasound, and the overall histopathological score (r=0.222, p=NS). A

positive Doppler signal was detected in 34 of 44 (77%) of the patients and once again no significant correlation was found between the amount of the power Doppler signal in the synovium and the overall histopathological score ($r=0.239$, $p=NS$). The amounts of sub-synovial infiltration of polymorphonuclear leucocytes did correlate with the amount of power Doppler signal (0.328, $p<0.05$). Whilst this study makes a more detailed histological assessment of the synovium there is a lack of homogeneity of patients and joints sampled. A standarised assessment of each joint was not described but significant doppler sensitivities are likely to have arisen between knee, wrist and tendon PDS assessment. The use of a 8MHz probe may also have diminished the US sensitivity and contributed to the lack of correlation.

Characteristic features of RA synovitis include hypertrophy of the lining layer, neo-αngiogenesis and infiltration of immune-cells of both the innate and adaptive immune system. Immune-cells can be found either randomly distributed within the synovial sublining or spatially grouped into follicular structures (25). These structures may acquired features of secondary-lymphoid-organs-(SLO) to include high-endothelial venules (HEV), T/B-cell segregation, follicular-dendritic-cells networks and are defined as ectopic/tertiary lymphoid-like structures (ELS/TLS).

A number of histologically determined synovitis scores have been proposed in patients with Rheumatoid Arthritis. The Rooney score assesses 6 histological features of the synovial membrane and was assessed in a prospective RA population. Unfortunately, no correlation with joint damage was demonstrated over a 2-year period in a cohort of 60 RA patients. Koizumi et al. described a synovitis score which was aimed at allowing reliable differentiation of RA and OA synovium. To this end it was successful and additionally having showed a moderate correlation with the degree of erosive damage and levels of CRP but was based on a purely cross-sectional population with no prospective validation performed to date with regards to disease activity and sensitivity to change. Krenn et. al. described a 9 point synovitis score based upon lining layer hypertrophy, synovial stroma cell density and the degree of organisation of the infiltrate. These components are scored 0-3 and

summed to achieve the overall score. This score was described in a study attempting to differentiate inflammatory and non-inflammatory joint pathology. A high-grade synovitis on the Krenn score was strongly associated with rheumatic joint diseases ($P<0.001$) as a-posed to OA synovium. These 2 scoring systems described above for have not been examined in a prospective fashion and there is no indication if they respond significantly to treatment.

A number of inflammatory cells can be seen within the synovium of patients with active RA (CD3 - T cells, CD20 - B cells, CD138 - Plasma cells CD68 - macrophages). Sub-lining CD68+ macrophages (CD68SL) were shown by Tak et. al. to be a correlated with disease response to active therapy and importantly minimize the placebo effect in a randomised controlled trials. A number of placebo controlled studies have confirmed the relationship of change in DAS28 and change in CD68SL macrophage numbers. In a small prospective study in patients with early inflammatory arthritis, the number of synovial sub-lining layer macrophages at baseline was associated with the number of new erosions on radiographs of the hands and feet at 1 year later ($P = 0.002$). A similar finding in established RA was also demonstrated. In addition, the histological processing and assessment of this particular synovial biomarker seems to be reliable and reproducible as determined in a multi-site examination of the technique. This measurement of synovial inflammation has come to be regarded as the optimal synovial characteristic in describing synovial disease activity and detecting response to therapy in patients with RA and as such is often used in the context of early phase drug development.

It is therefore within two cohort of patients we seek to examine the relationship of ultrasound measures of synovitis with histological and clinical parameters prior to treatment. An Early RA population was recruited (treatment naive) in addition to an established cohort (DMARD inadequate response). In addition, we will attempt elicit any favorable baseline characteristics which predict patients response to therapy within each cohort. Additionally, I will describe a wrist ultrasound score and its

relationship to synovial markers of inflammation, facilitating its incorporation into a limited US joint data set.

7.2 Aims

Within a cohort of patients, naive to treatment and with inadequate response to DMARDs I wished to examine:

i) The variation of ultrasound parameters (grey scale and power doppler synovitis) within a single wrist joint and determine the optimal assessment of US synovitis in relation to synovial histology.

ii) The relationship of histologically defined synovial inflammation, and in particular CD68SL macrophage and Krenn score, to a single joint and limited US joint data set.

iii) Whether patients' clinical, ultrasound or synovial histomorphology parameters correlate with the mean change in DAS28 and identify any baseline predictors of response.

7.3 Methods

7.3.1 Patient selection

Early Arthritis Cohort: 20 patients with a new diagnosis of RA (ACR 1998 criteria) were recruited to an on going early inflammatory arthritis study (PEAC; Pathobiology of Early Arthritis Cohort, REC ref: 05/Q0703/198) in which patients were assessed clinically and with ultrasound imaging at baseline and at 6 months from recruitment. Patients also received an ultrasound guided synovial biopsy as previously described at baseline prior to treatment and at 6 months. All patients recruited has inflammatory joint symptoms for 3 - 12 months prior to recruitment and had at least one suitable joint for biopsy.

All patients with RA were treated with combination therapy of Methotrexate and sulphasalazine and low dose prednisolone 7.5mg. Patients were eligible for anti-TNF therapy at 6 months if they fulfilled NICE guidelines.

Established RA: 20 patients with RA (1987 revised ACR classification criteria) who fulfilled the NICE guidelines for TNF Blocking therapy were recruited to a synovial biopsy based study. All subjects were receiving MTX for at least 4 months, with a stable dose of 7.5-25 mg/week for a minimum of 4 weeks. In addition, all patients were on a stable doses of oral steroids (prednisone ≤10 mg/day, or equivalent corticosteroid) for 4 weeks prior to recruitment. All patients received screening for TB, Hepatitis and HIV prior to anti-TNF therapy initiation as per normal NHS guidelines and were excluded if they failed any of these screening tests. A synvoial biopsy was taken at baseline and after 3 months.

7.3.2 Clinical Disease Activity assessment

The primary measure of disease activity in this study was the DAS28(CRP). The components of the DAS28(CRP) are the number of tender joints (28 joint count), the number of swollen joints (28 joint count), a Global Health index (100 mm VAS), and the CRP (in mg/L). The formula for determining the DAS28(CRP) is as follows:

$$DAS28(CRP) = 0.56*\sqrt{(TJC28)} + 0.28*\sqrt{(SJC28)} + 0.36*\ln(CRP+1) + 0.014*GH(VAS) + 0.96$$

DAS 28 Response criteria

Non-responders – patients were designated non-responders if their DAS28 has not improved by > 1.2 from baseline six months after treatment;

Partial responders – patients will be designated partial responders if their DAS28 improves by >1.2 from baseline but remains >3.2.

Good responders – patients will be designated good responders if their DAS28 falls by >1.2 to a level <3.2 (i.e. into a 'low disease activity state' [LDAS])

Remission – patients will be designated as in remission if their DAS28 falls to <2.6.

Health assessment questionnaire (HAQ)

The HAQ was self-αdministered at study baseline. The Disability Index consists of eight categories assessed by the Disability Index are 1) dressing and grooming, 2) arising, 3) eating, 4) walking, 5) hygiene, 6) reach, 7) grip, and 8) common daily activities. For each of these categories, patients report the amount of difficulty they have in performing two or three specific activities.

7.3.3 Ultrasound Assessment

Patients received a baseline US assessment of the biopsied joint and in addition a limited US joint set using a GE logiq 9, ultrasound system and the 2D M12L Probe. The limited US set consisted of MCP 1-5 (Left and Right), Wrists (Left and Right). The MCP examinations were performed in both longitudinal and transverse orientations as described in the appendix. Wrist assessment was in a longitudinal direction from 3 pre-defined regions of interest:

1. Midline: encompassing the distal radius, Lunate and Capitate bones and common extensor tendons.
2. Radial: Encompassing the distal radius, Scaphoid, Trapezium and 1st carpal-metacarpal joint (CMC).
3. Ulna: encompassing the distal ulna, Pisiform, Hamate and the 5th CMC joint.

A summed 10 joint US score (10 MCP joints) and a 12 joint US score (10 MCP + 2 Wrists) were derived form the available US data.

The grey scale and power doppler images images were stored on the Logiq 9 US system and transferred to a suitable repository. Images were analysed both qualitatively and quantitatively as described in the appendix. Definitions of US parameters are given in chapter 2. To facilitate correlation of a categorical score for the histological parameters the continuous variables of synovial thickness area (STA) and PDA (power doppler area) were subdivided. This was modeled on the published

data by Walther et. al. who categorized the doppler signal in his study to facilitate correlation with a semi-quantitative 0-4 vascular histology score. Table 7-1 shows the PDA and STA scales and corresponding categorical values.

Current experience would dictate that in normal individuals , with no evidence of inflammatory arthritis, no doppler signal should be detectable on US imaging. Therefore the lowest category, score '0', relates to 0 PD pixels on the continuous variable.

The same cannot be assumed for the STA. Many normal joint have small amounts of synovial thickening which is deemed within normal limits for the purposes of differentiating between normality and pathology at a single joint level. Therefore an examination of 92 single MCP joints were undertaken and a threshold for normal quantitative assessment of was derived. The mean area of synovial thickening was 5.8 $x10^3$ (S.D. $1.6x10^3$). A threshold was therefore determined as mean + 2.5 x S.D. (10,000 pixels).

Figure 7-1: Histogram showing the distribution of quantitative assessment of synovial thickening within normal joints.

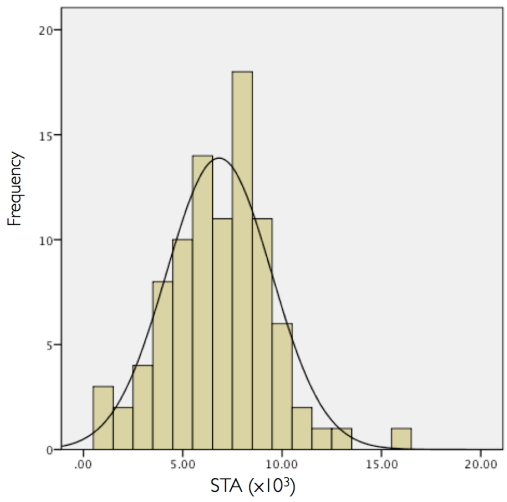

Table 7-1: Ordinal reference ranges for continuous variables of STA and PDA.

STA - Synovial thickness area, PDA - Power Doppler Area

Ordinal scale	STA	PDA
0	0-10000	0
1	10,000 - 20,000	1- 500
2	20,001 - 30,000	501- 1000
3	30,001 - 40,000	1001 - 1500
4	> 40,000	> 1500

7.3.4 Synovial biopsy

An ultrasound guided synovial biopsy was performed on patients prior to the commencement of therapy as described in chapter 2. Early RA patients received a synovial biopsy prior to the initiation of any therapy including corticosteroids and again after 6 months. The established cohort of RA patients received their ultrasound guided synovial biopsy prior to receiving anti-TNF therapy and after 3 months.

7.3.5 Histopathological processing of synovial tissue

Tissue processing

Synovial tissue biopsy samples were fixed in 4% formalin overnight and processed on an automated vacuum TP1050 tissue processor (Leica) the following on a routine overnight cycle. The processed biopsy specimens were transferred to an SLEE tissue embedding centre and were embedded in paraffin wax blocks (FFPE tissue blocks).

FFPE tissue blocks were sectioned on a Leica RM1235 microtome. Sections were cut at a thickness of 3µm and mounted on to Superfrost plus (+) slides. Sections were cut for subsequent Haematoxylin and Eosin (H&E) staining/assessment as well as IHC staining. Sections for immediate use were left to dry in a slide rack at room temperature for 30 minutes and then transferred to a heating plate (60ºC) for a

minimum of 30 minutes prior to staining. Tissue sections were H&E stained for initial grading and synovitis scoring and viewed/imaged using an Olympus BX61 microscope.

Histological Assessment

H&E-stained specimens

The aggregational phases of the synovial lymphoid tissue were defined using an in-house grading score. All specimens that exhibited a synovial cell lining layer were graded and synovitis scored. Cell aggregates are initially categorised into three groups according to the radial cell count. The radial cell count was determined by counting the number of cells from the centre of an aggregate to the identifiable edge. The determination was made at the point of widest infiltration. Cell aggregates with a radial cell count between 2 -5 cells are classified as Grade 1. Grade 2 specimens have a radial count of 6 -10 cells, while Grade 3 specimens have a radial count of more than 10 cells.

In conjunction with the grading, an inflammatory score (synovitis score) was also assigned according to the three synovial membrane features (thickness of the synovial lining cell layer, stroma cell density and inflammatory infiltrate). The ranking of alterations is on a scale from none (0), slight (1) and moderate (2) to strong (3) for each feature. The values of the parameters are summarised and interpreted as follows: 0–1, no synovitis; 2–4, low grade synovitis; and 5–9, high-grade synovitis (Krenn et al., 2006).

Scoring of IHC-stained Specimens

IHC-stained specimens for T-cells, macrophages and plasma cells (CD3, CD68 & CD138 respectively) are scored on a 5 point scale: 0-4 depending on the increasing number of positively stained cells calibrated against a standardised atlas (minimal infiltration = 0 and infiltration by numerous inflammatory cells = 4 (Tak et al., 1997). The level of B cell infiltration (CD20) was categorised as B Cell Poor (0-1), B Cell

Rich (2-3) and Germinal Centre (GC) Rich (4). Accordingly, where B cell aggregates were observed for CD20, synovial biopsies were IHC-stained for CD21 to for the presence of GC (CD21 positive follicular dendritic cells (FDC) networks).

Figure 7-2: Image Atlas of synovium stained by Immunohistochemistry for CD3, CD20, CD68 and CD138

RA synovium stained by Immunohistochemistry for CD3, CD20, CD68 and CD138. A qualitative 0-4 score is demonstrated with typical reference image atlas below. IHC performed by Dr. B. Hands (Experimental Medicine and Rheumatology, William Harvery Research Institute).

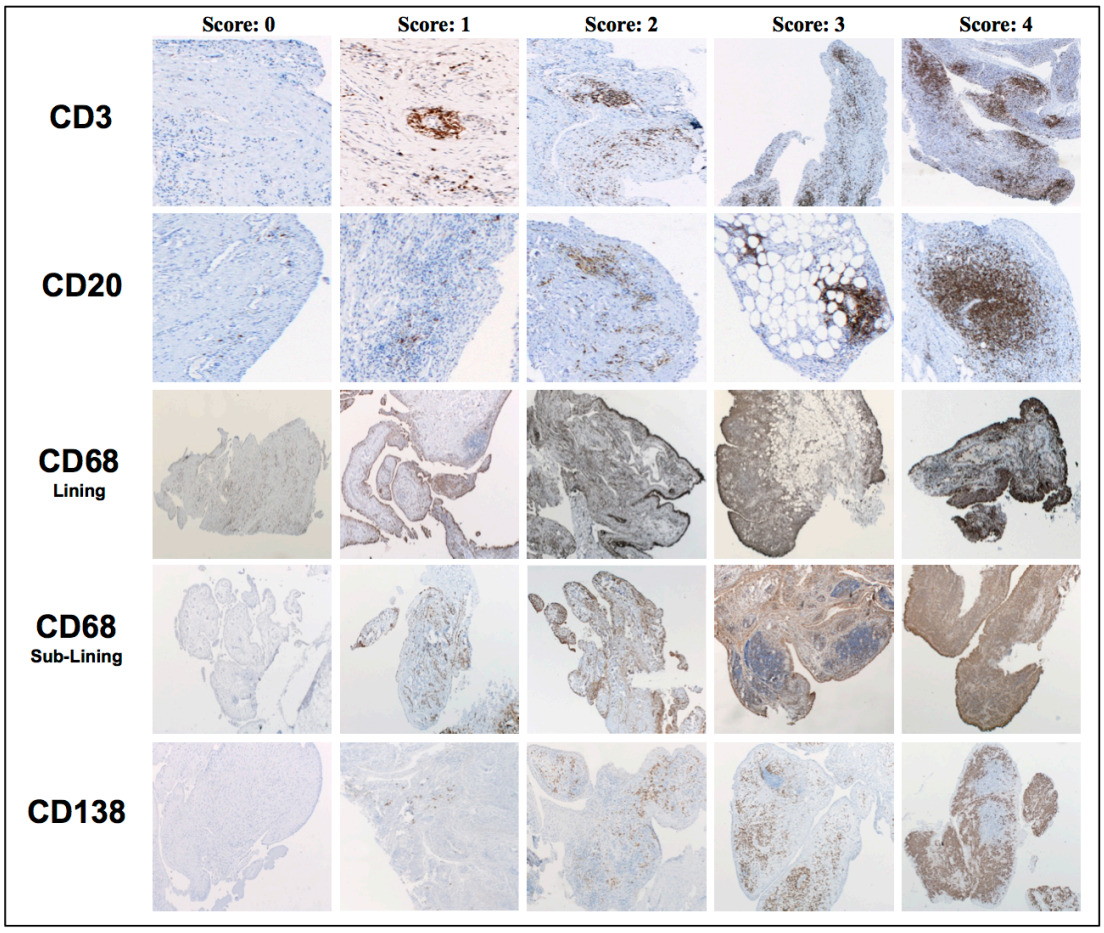

7.4 Results

7.4.1 Patient demographics

Table 5-2 gives an overview of the patient demographics for both cohorts. No significant difference was detected for age, sex inflammatory markers or DAS28. Reflecting the inclusion criteria for each cohort, a significant difference was seen for the duration of symptoms with the treatment naive cohort having a mean of 0.51 years as expected.

Table 7-2: Patient demographics of recruited patients to both treatment naive and DMARD inadequate response arms.

	Treatment Naive (S.D.)	DMARD IR (S.D.)	P value
Female : Male	15 : 5	14 : 6	0.4
Previous DMARDs	0	1.6 (0.5)	-
Age	51.2 (21)	50.8 (12.1)	0.61
Duration (years)	0.51 (0.24)	6.9 (6.1)	< 0.0001
ESR	40 (23)	29.2 (22)	0.09
CRP	21 (18)	13.6 (14.4)	0.18
RF	119 (145)	49.8 (58)	0.12
CCP	234 (258)	241 (261)	0.53
Pain (VAS)	58 (29)	63 (18)	0.58
Global Health (VAS)	64 (28)	65 (21)	0.61
Tender Joint	11 (7.3)	13 (5.2)	0.47
Swollen Joints	7.9 (5.4)	9.1 (6.3)	0.32
DAS28 (CRP)	5.8 (S.D. 1.3)	6.4 (0.9)	0.41
HAQ	1.3 (0.7)	1.6 (0.7)	0.29

7.4.2 Reliability of qualitative synovial immunohistochemistry score

BH and SR scored all immunohistochemistry slides. Each reader was blinded to the others result and to the clinical and ultrasound data. Inter class correlation co-efficient were calculated for consistency. Each parameter was scored individually and ICC scores tabulated. Excellent agreement was seen between both readers for all qualitative scores table 7-3.

Table 7-3: ICC results for immunohistochemistry markers scored according to the standard image atlas.

	Krenn score	CD3	CD20	CD68L	CD68SL	CD138
ICC (95% CI)	0.87 (0.82-0.94)	0.94 (0.83-0.98)	0.99 (0.97-0.99)	0.95 (0.82-0.98)	0.98 (0.93-0.99)	0.98 (0.94-0.99)

7.4.3 Wrist joint score

Of the 40 patients recruited, 32 received a wrist synovial biopsy. The three regions imaged for the wrist joint were compared for the degree of synovial thickening and power doppler signal (qualitative and quantitative). There was a significantly great score for both VASCi and STi scores when comparing the midline versus radial or ulnar regions (repeated measures anova; $p = 0.001$, $p= 0.003$ respectively) figure 7-3. This was also reproduced for qualitative assessments for STA and PDA (repeated measures anova; $p = 0.002$, $p= 0.001$ respectively). When each cohort was treated separately, a similar significant difference was detected between regions.

Figure 7-3: Bar chart of ultrasound scores for each region of interest within the wrist joint (Average score, SEM)

A: Ultrasound vascular index score (VASCi) for each region of interest. B: Ultrasound synovial thickness index (STi) for each region of interest.

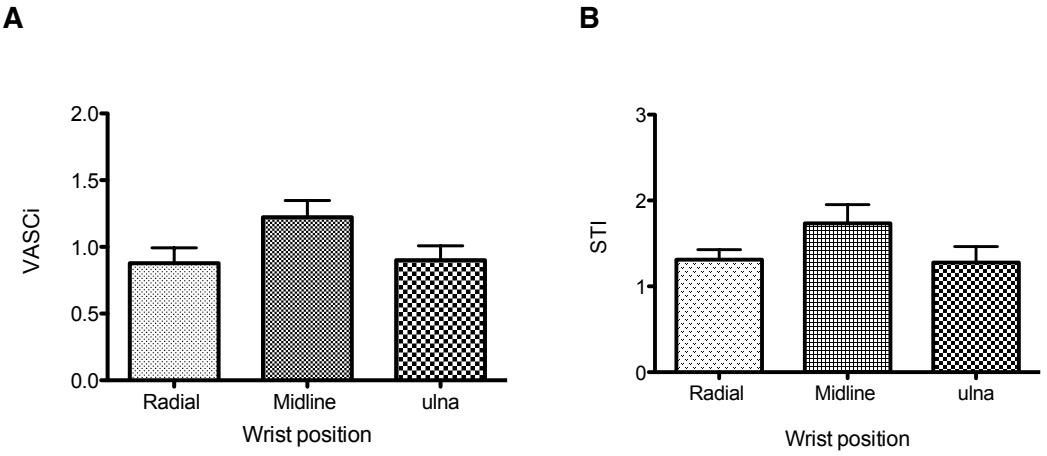

Histological parameters were correlated with both quantitative and qualitative ultrasound scores. The correlation was performed using a summed score for all three wrist regions for both synovial thickness and power doppler. In addition, the histological correlation was also run using only the midline wrist US scan. A summary of the correlation data can be seen in table 7-4. All correlations were performed using Spearman rank as all variables represented ordinal scores.

Table 7-4: Correlation matrix of histological and ultrasound parameters for wrist joints only

Table showing the correlation of synovial histological parameters as determined by immunohistochemistry and ultrasound assessment of the wrist. Spearmans rank correction. Total scores represent a summed result for 3 regions of interest within the wrist (radial, midline and ulna). Midline scores refer to the midline wrist image only. Asterix (*) denotes statistically significant result.

Histology variable	STi (total)	VASCi (total)	STA (total)	PDA (total)	STi (Midline)	VASCi (Midline)	STA (Midline)	PDA (Midline)
Krenn score	0.67*	0.69*	0.67*	0.71*	0.63*	0.68*	0.78*	0.69*
CD3	0.46*	0.55*	0.31	0.43	0.31	0.52*	0.52*	0.55*
CD20	0.62*	0.73*	0.53	0.7*	0.53*	0.71*	0.69*	0.76*
CD68L	0.71*	0.74	0.71*	0.75*	0.63*	0.74*	0.63*	0.75*
CD68SL	0.83*	0.81*	0.82*	0.84*	0.73*	0.69*	0.72*	0.8*
CD138	0.58*	0.71*	0.62*	0.74*	0.67*	0.8*	0.65*	0.72*

Figure 7-4: Correlation of wrist VASCi (total) score and qualitative CD6SL macrophage score

Correlation of total wrist VASCi score and qualitative CD6SL macrophage score in 32 wrist joints form patients with active inflammation. Spearmans rank correction r = 0.81, $p<0.001$.

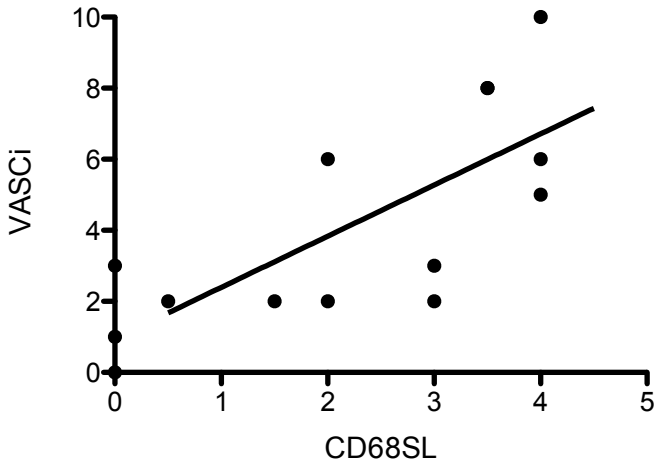

A significant association was seen both qualitative and quantitative US parameters and the CD68SL macrophage with the STi and VASCi both showing a strong correlation (0.83; $p < 0.001$and 0.81; $p < 0.005$ respectively). The midline US scan also correlated with the CD68SL score but only moderately (STi 0.73; $p < 0.012$, VASCi 0.69 $p<0.004$). The majority of all other immunohistochemistry variables correlated with the ultrasound parameters except for the CD3 score which showed only a moderate correlation with STi and VASCi (total). The 3 variable, 'Krenn score', also correlated with all ultrasound parameters but to a lesser extent than the CD68SL score.

7.4.4 US parameters predict synovial CD68SL macrophage score.

To calculate the positive and negative predictive value for both STi and VASCi a binary separation of the data was required. All wrist joints were assessed using a summed VASCi and STi score. A significant VASCi was considered a score of 1 or more. A score of grade 1 in each wrist region was permitted (total score of 3 or more) when separating the STi score into binary categories. The sensitivity of the VASCi score in the wrist was 0.96 with a specificity of 0.8 (Fisher exact $P = 0.0007$). The positive predictive value for the presence of CD68SL macrophages in patients with a significant VASCi score was 0.96 with a negative predictive value of 0.8 if the VASCi was 0. Similarly, the sensitivity and specificity of STi in reflecting the presence of CD68SL macrophages within the synovium was 1.0 and 0.6 with a positive predictive value of 0.93 and negative predictive value 1.0.

Table 7-5: Chi squared (2x2) table showing the number of patients with Doppler signal present on US examination and presences or absences of synovial CD68 SL macrophages.

A: 2x2 table of patients with VASCi / no VASCi and presence / absence of CD68SL macrophages within the synovium. **B:** 2x2 table of patients with STi / no STi and presence / absence of CD68SL macrophages within the synovium. CD68SL+ presence of CD68+ macrophages in sublinig, CD68SL- no CD68+ macrophages seen in sublining.

A

	VASCi +	VASCi -
CD68SL+	25	2
CD68SL -	1	4

B

	STi +	STi -
CD68SL+	26	1
CD68SL -	0	5

7.4.5 Correlation of a limited US data set with synovial and clinical parameters of disease activity.

A limited 10 joint US data set (10 MCPs) was correlated with synovial histological parameters in both the early RA and established RA cohorts. The US data set was calculated using transverse and longitudinal images for both cohorts and presented in table 7-6. A moderate correlation was seen with CD68SL and all of the 10 joint *longitudinal* US data sets in both cohorts with the Early RA - 10 long STi performing best (correlation coefficient of 0.58; $p < 0.001$). In both cohorts, only the STi and STA US scores of the 10 joint longitudinal data set correlated with the Krenn score (0.52; $p < 0.01$ and 0.57 $p < 0.02$ respectively).

Within both cohorts, the 10 joint *transverse* US scores correlated with CD68SL expect for 10 Trans Sti (0.41 $p = 0.23$). Similarly, only STi and STA scores correlated

with the Krenn score using the transverse data set. Overall, the longitudinal US data sets typically out perform the corresponding transverse data set in both established and early disease.

Extending the US joint set to include both wrists provided a 12 joint US data set. The relationship of this extended US data set to histological parameters was examined. The US parameters for this summed data set were based upon the MCP joints longitudinal data.

Two variations of this score were used:

1. 12 Joint score (weighted wrist): 10MCPs + Left Wrist (ulna + midline + radial score) + Right Wrist (ulna + midline + radial score)

Effectively the wrist is weighted x3 compared to a single MCP joints

2. 12 joint score (average wrist): 10 MCPs + Left Wrist ([ulna + midline + radial score] / 3) + Right Wrist ([ulna + midline + radial score] / 3).

The wrist score is averaged and weighted x1 compared to a single MCP joints

Table 7-6: Correlation of Longitudinal and Transverse VASCi and STA scores with histological parameters in an early and established RA cohort.

A: Early Arthritis Cohort; 10 joint US data set (longitudinal images only) correlated to the Krenn score and CD68SL macrophage score (Spearman rank). B: *Early Arthritis Cohort;* 10 joint US data set (transverse images only) correlated to the Krenn score and CD68SL macrophage score (Spearman rank). Asterix (*) denotes statistically,significant result.

A

Early Arthritis Cohort	10 long STi	10 long VASCi	10 long STA	10 long PDA
Krenn score	0.56*	0.31	0.62*	0.36
CD68SL	0.61*	0.62*	0.6*	0.68*
Early Arthritis Cohort	10 Trans STi	10 Trans VASCi	10 Trans STA	10 Trans PDA
Krenn score	0.35	0.20	0.53*	0.27
CD68SL	0.4*	0.46*	0.43*	0.5*

B

Established RA	10 long STi	10 long VASCi	10 long STA	10 long PDA
Krenn score	0.4*	0.23	0.5*	0.20
CD68SL	0.41*	0.49*	0.43*	0.48*
Established RA	10 Trans STi	10 Trans VASCi	10 Trans STA	10 Trans PDA
Krenn score	0.42*	0.25	0.46*	0.21
CD68SL	0.29	0.4*	0.47*	0.42*

Table 7-7: Correlation of 12 joint VASCi and STA scores (averaged and weighted wrists scores) and histological parameters in an early and established RA cohort.

A: Early Arthritis Cohort; 12 joint US data set (total wrist score) correlated to the Krenn score and CD68SL macrophage score (Spearman rank). B: *Established cohort*; 12 joint US data set (Average wrist score) correlated to the Krenn score and CD68SL macrophage score (Spearman rank). Asterix (*) denotes statisticallysignificant result.

A

Early Arthritis Cohort	12 joint STi (weighted wrist)	12 joint VASCi (weighted wrist)	12 joint STA (weighted wrist)	12 joint PDA (weighted wrist)
Krenn score	0.74*	0.60*	0.82*	0.60*
CD68SL	0.70*	0.66*	0.64*	0.57*
Early Arthritis Cohort	12 joint STi (average wrist)	12 joint VASCi (average wrist)	12 joint STA (average wrist)	12 joint PDA (average wrist)
Krenn score	0.59*	0.32	0.57*	0.19
CD68SL	0.62*	0.58*	0.50*	0.42*

B

Established RA	12 joint STi (weighted wrist)	12 joint VASCi (weighted wrist)	12 joint STA (weighted wrist)	12 joint PDA (weighted wrist)
Krenn score	0.46*	0.53*	0.58*	0.49*
CD68SL	0.21	0.47*	0.39	0.51*
Established RA	12 joint STi (average wrist)	12 joint VASCi (average wrist)	12 joint STA (average wrist)	12 joint PDA (average wrist)
Krenn score	0.31	0.12	0.35	0.27
CD68SL	0.34	0.42*	0.31	0.39

A significant correlation was found more frequently using a 12 joint data set involving a weighted wrist sum for both CD68SL and Krenn score in both early and established populations. The 12 joint STA (weighted) score performed best (0.81; $p < 0.01$) within both early and established RA cohorts (Early RA 0.81; $p < 0.01$, Established 0.58; $p< 0.02$). Within the established RA cohort of patients the 12 joint US scores (averaged wrist) did not perform well and was only significantly correlated to the 12 joint VASCi and PDA scores (0.42 $p<0.03$, 0.39 $p<0.045$ respectfully).

None of the histological or US scores correlated with either the baseline DAS28 or HAQ score within the Early RA population. No correlation was detected with any of its components including ESR, tender joint, swollen joint or patient global. Within the Established RA cohort, a significant correlation was seen between the DAS28 score and the 10 joint VASCi (long), 12 joint VASCi (weighted wrist) and 12 joint VASCi (averaged wrist), (0.45, $p < 0.015$; 0.61, $p < 0.03$; 0.48, $p < 0.025$ respectfully). None of US scores for synovial thickness were significantly correlated with the DAS28. Once again the HAQ at baseline did not correlate with any of the histological or imaging scores.

7.4.6 Change in DAS28 correlates with the change in US parameters and histological scores.

All clinical, ultrasound and histological parameters showed a significant mean change from baseline in both the early and established patient cohorts (Paired t-test $P<0.001$).

Figure 7-5: Mean score for all histological parameters at first and second synovial biopsy

A: Mean score for all histological parameters at first (1) and second (2) biopsy (Krenn score, CD3, CD20, CD68L, CD68SL, CD138) - Early RA cohort **B**: Mean score for all histological parameters at first (1) and second (2) biopsy (Krenn score, CD3, CD20, CD68L, CD68SL, CD138) - Established RA cohort

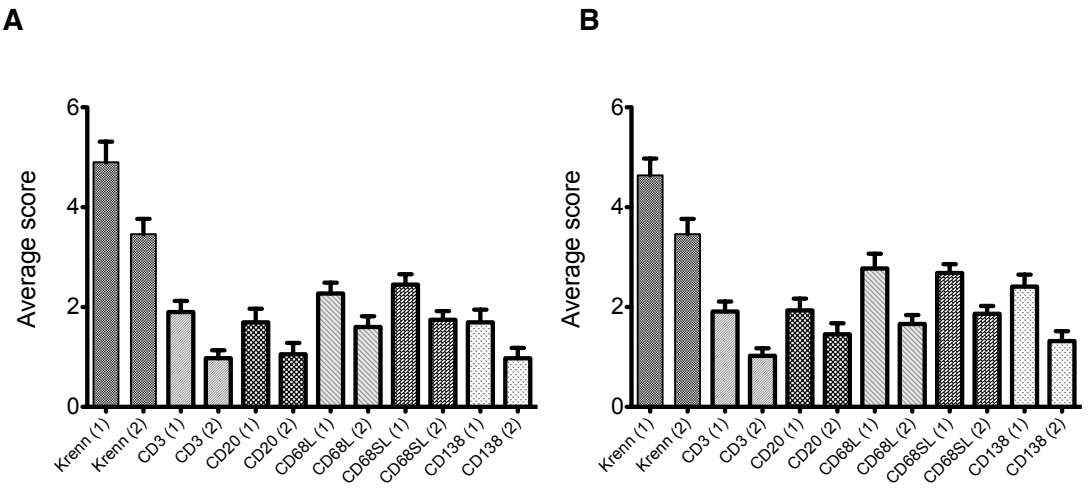

In both cohorts the mean change in DAS28 was significantly correlated with the mean change in both US and histologic parameters. A table below describes the signifiant correlations with the mean change in DAS28. Within both cohorts the 12 Joint VASCi (weighted wrist) performed well when correlated with DAS28 (*Early RA*, r = 0.56; P < 0.003, *Established RA* r = 0.48; P <0.01). Within the Early RA cohort the histological parameter which correlated best was the change in the synovial CD3 score (r = 0.43: P < 0.031) however, within the Established cohort CD68SL appeared to correlate best (r = 0.39; P < 0.011).

Table 7-8: Correlation matrix of mean change in DAS 28 with US and histological parameters

Table showing the correlation of the mean change in ultrasound and histological parameters with the mean change in DAS28. Asterix (*) denotes statistically,significant result.

	Early RA	Established RA
US data sets	Delta DAS	Delta DAS
12 Jt VASCi (weighted wrist)	0.56*	0.48*
12 Jt STi (weighted wrist)	0.42*	0.39*
10 Long VASCi	0.44*	0.41*
10 Long STi	0.38*	*0.4
Histology		
Krenn score	0.39*	0.33*
CD3	0.43*	0.38*
CD20	0.27	0.31
CD68L	0.41*	0.32*
CD68SL	0.38*	0.39*
CD138	0.32	0.38*

7.5 Relationship of clinical response to synovial histology, ultrasound and baseline clinical parameters

Linear regression modeling was used to predict the change in DAS28 at 6 months following treatment with baseline characteristics of patients. 38 out of 40 patient had a DAS28 available at 6 months for analysis (20 Established RA, 18 Early RA). The analysis was run separately for early and established RA cohorts. The model generated from the early RA cohort was tested in the established RA group. Histological parameters (Krenn score, CD3, CD20, CD68DSL and CD138) and Ultrasound scores (10 joint STi and VASCi long,12 joint STi and VASCi [weighted

wrists]) and clinical parameters (CRP, ESR, DAS28, Rheumatoid factor, anti-CCP antibodies) were used as variables.

Within the Early RA cohort, synovial CD3 score and 12 joint VASCi were both significantly associated with the change in DAS28 (r^2 - 0.45, $p< 0.02$ and 0.39, $p<0.04$ respectfully). This provided a predictive model with a value of 76.7%.

Testing the same model within the established RA cohort resulted in a reduction in the models ability to predict the change in DAS28 (value 38.9%).

An independent model generated from the Established RA cohort subsequently treated with anti-TNF therapy suggested that the baseline 12 joint STi (weighted wrist), CD68SL and CRP (r^2 - 0.35, $p< 0.001$, r^2 - 0.29, $p<0.03$ and r^2- 0.31 $p<0.01$ respectfully) levels were independently related to the mean change in DAS28. This model suggested a predictive value of 73.2%.

7.5.1 Histomophological segregation of synovial tissue suggests a dichotomous population

Using the histomorphological phenotype of the synovial tissue to segregate the patients, US and histological parameters of patients shows evidence of a dichotomous population. Significant differences were seen with the Krenn score, CD68SL macrophage score with a G2/G3 phenotype predominant in the patients with high synovial inflammatory scores (Chi Squares test $p = 0.003$ and $p= 0.002$ respectfully). Likewise, a G2/G3 histomorphological phenotype seems to be associated with a high VASCi and STi score at an individual joint level (Chi Squares test $p = 0.0018$ and $p= 0.0029$ respectfully) Table 5-9.

Table 7-9: Table showing ultrasound and parameters according to the synovial histomorphology.

Table showing ultrasound and parameters according to the synovial histomorphology. There is a significant difference in the Diffuse, G1 group compared with the G2,G3 grouping (chi sq) for histological and US parameters as well as RF.

	Diffuse, G1	G2, G3	Chi Sq, p value
Krenn score < = 3 > 3	 13 5	 1 21	p = 0.003
CD68 SL 0 - 2 3 - 4	 15 3	 4 18	p = 0.002
STi 0 - 2 3 - 4	 14 4	 6 16	p = 0.0029
VASCi 0 - 2 3 - 4	 13 5	 3 19	p = 0.0018
RF (%)	6 (33%)	17 (78%)	p = 0.0029

7.6 Discussion

This study examines a number of aspects of the relationship of ultrasound imaging to synovial histological parameters both at a single joint level and using an extended US joint data set. All patients had a high disease activity score on recruitment, prior to receiving a synovial biopsy, which inevitably limits correlation with clinical disease activity parameters. However, both cohorts of patients represent clear clinical scenarios in which the use of ultrasound imaging is used frequently to characterise patients and influence management decisions.

The wrist is a frequently involved joint in RA. The wrist joint poses a particular problem for ultrasonographers due to the multiple synovial articulations present within a ‘single joint’. The score derived from such a complex joint is likely to require the assessment of more than 1 single region of interest. My results demonstrate a difference in ultrasound parameters between three regions of the wrist joint, examined from the dorsal aspect. The midline scan of the wrist encompassing the

distal radius, lunate and capitate demonstrated greater synovial thickness and vascular scores compared to the radial or ulnar regions. Despite this, it is interesting to note that whist a single midline image for STi and VASCi correlated with the CD68SL macrophage qualitative score, the VASCi score encompassing three regions of interest was superior. A similar result was not seen by using the Krenn score, CD20 or CD3 for either US wrist scores. In addition, the integration of the wrist US score into a 12 joint US data set performed better in terms of histological correlation, but more importantly was shown to be an indicator of a change in DAS28 at 6 months. When an averaged score or single midline image was used no association was demonstrated. Therefore the scoring of the wrist joint, either singly or as part of an extended joint data set, would argue for it being weighted in favour of a summed score of a radial, midline and ulnar regions of interest. Further work is required to determine if a summed score for the wrist performs well as an indicator of therapeutic response, if the histological correlations remain consistent following treatment and whether it parallels clinical disease activity over time.

Both qualitative and quantitative scores performed similarly at a single joint level. The artificial categorisation of the continuous vascular and synovial thickness scores (PDA and STA) was necessary to correlate with these parameters with the ordinal scale used for the histological variables. There is an assumption in using an ordinal scale that the difference between values remains relatively constant whether transitioning form 1 to 2, or form 3 - 4. With this in mind, the categorisation of the continuous variables was undertaken. In practical terms, this has the potential to underestimate the relative value of PDA or STA at the limits of the scale. Ideally, a continuous variable should be generated for the histological scores using digital imaging analysis which would facilitate a more meaningful correlation. Despite these limitations the quantitative score performed well at the single joint level although only the the VASCi appeared to be predictive of a change in DAS28 over time.

The positive predictive value of ultrasound imaging was explored in all patients with a high DAS28 score undergoing wrist synovial biopsies at baseline. The presence of a

VASCi score of 1 or more had a high positive predictive value - 0.96, for the presence of CD68SL macrophages whereas a STi score of 1 or less for the wrist had a negative predictive value of 1.0. This result may have significant implication on the interpretation of ultrasound findings in a clinical and research context. 32 wrist joints represents a reasonable sample size for this dichotomous distinction, however as all patients were deemed clinically to have active disease there is typically a small number of patients with an absence of CD68SL histologically with a predominance of CD68SL +, VASCi + individuals. It will be important to explore this relationship in a more diffuse RA population at varying degrees of clinically assessed disease activity. Whilst a high negative predictive value is seen in this model for the absence of significant STi, it may not be as robust in the context of low disease activity.

There has been much interest in establishing a representative, limited US joint data set for use in the context of routine clinical care and clinical trial setting which provides further information on RA disease activity. A number of data sets have been examined in the literature and been shown to be response to to change with varying degrees of reliability. In Chapter 5, I demonstrate the responsiveness of a limited US data set (10 MCP joints) in a randomised controlled clinical trial. The implication form these studies is that US assessment of joint synovitis is a surrogate biomarker for synovial inflammation. I have already discussed the excellent correlation between synovial biomarkers and the ultrasound grey scale and doppler scores, however a valid, representative US data set would also be expected to correlate with histologically defined synovial inflammation. This study examined a number of US data sets and their relationship to synovial inflammation. A limited joint data set of 10 MCPs were examined with US images being collected form a longitudinal or transverse orientation as described in appendix 1. For all parameters the longitudinal 10 MCP score preformed better than the corresponding transverse score although all scores were significantly correlated with CD68SL macrophage score except for the 10 MCP Transverse score in the established RA cohort. Given the superior performance of the longitudinal imaging for the MCP joints the 12 joint data set

utilised only these images whilst including both wrists. The 12 joint data set was analysed using 2 wrist scoring methods; 1) summed score for the wrist and 2) averaged score for the 3 compartments. Using a summed score for the wrist based on 3 regions of interest effectively weights the wrist contribution of this data set. An average score only equates the wrist with a single MCP joint. The correlation co-efficients demonstrate a closer relationship for the synovial biomarkers and the weighted 12 joint US scores. Both 12 joint STi (total) and 12 joint VASCi (total) scores demonstrated a good correlation with CD68SL macrophages in the early RA cohort (0.7, $p<0.001$; 0.66 $P<0.001$ respectfully) with all histological parameters recording a significant correlation.

Comparing the relationships of US synovial thickness and vascularity measurements, a distinct difference can be seen on inspection of the correlation matrix between the early and established RA cohorts. The correlations are generally weaker in the established cohort with no significant correlation seen with CD68SL macrophages and either the qualitative or quantitative assessments of synovial thickness. The correlations are preserved for the vascular assessments albeit at a moderate level. The disease duration is significantly longer in the established cohort compared to the early RA patients (0.51 years and 6.9 years respectfully). This may suggest that, over time, grey scale synovial thickening may be a less effective surrogate of synovial inflammation. Certainly, a chronic inflammatory process predisposes to fibrosis and scaring which may be in part responsible for the synovial thickening seen bot on US examination and clinically. The potential uncoupling of the relationship of grey scale synovial thickening with synovial inflammation is an important finding and warrants further examination. These two cohorts of patients represent cross-sectional data, therefore a prospective follow up of an early RA cohort over time may address this question if paired with serial synovial biopsies. In addition to the duration of disease, all of the established cohort have received DMARD therapy. Consequently I must also consider the possibility that treatment has a role to play in altering this dynamic.

The relationship of US and histological parameters to disease activity was examined using linear regression and subsequent modeling of DAS28 response form baseline characteristics. Within the early RA cohort, all of the synovial biomarkers and Krenn score had a positive relationship with both qualitative and quantitative US outcome measures. The linear regression model isolated CD3 and the 12 joint VACSi score as contributing significantly in a predictive model (Predictive value 76.7% of DAS28 change at 3 months following therapy) with CD3 contributing 82.3% to the model compared to 17.7% for the 12 joint VASCi. Using this model in the established RA cohort provided little predictive value (37.9%). There are a number of limitations of this model. The DAS response for methotrexate is likely to be better assessed at 6 months rather than 3. This may under weight a number of the variables in the model. In additon, both cohorts received different treatment regimes with the established RA population going on to have anti-TNF therapy. It is conceivable that different synovial and US signatures may predict response to different DMARDS and biological agents. This is a major limitation of the model and thus a separate model was constructed from the same baseline parameters within the established RA cohort. This revealed a CD68SL macrophages, 12 Joint VASCi and CRP as significant predictors of DAS28 response (Predictive value 73.2% of DAS28 change at 3 months following therapy). To register in a predictive linear model in such a small cohort of patients, these significant parameters would suggest a large effect. Despite this, both models only predict approximately 75% of the overall DAS28 response to treatment. This would suggest that whilst synovial histology and US data have a role to play in predicting response to treatment other factors are certainly relevant and influencing patient response.

7.7 Conclusion

To summarise, this study examined a number of histological and ultrasound parameters in two distinct cohorts of patients. The use of a limited US data set including the wrist performs better when weighted. The correlation between synovial

histological markers of inflammation, including CD68SL, and US parameters appears to differ in the two populations with an excellent correlation seen with in the early RA cohort and a moderate correlation in the established cohort. The lack of synovial thickness assessments to correlated with any of the synovial biomarkers in the established cohort may have implications for the use of this parameter in clinical studies. A clinical predictive model base upon baseline clinical, ultrasound and histological data was only moderately successful at predicting response but did confirm both imaging and synovial histology as important contributors in the change of DAS28 following 3 months of treatment.

8. The relationship of ultrasound and synovial neoangiogenesis within the Knee joint.

8.1 Introduction

Neovascularization is the development of new blood vessels from the existing microvascular bed. It involves a number of steps including endothelial cell division, selective degradation of vascular basement membranes and the surrounding extracellular matrix, and endothelial cell migration. In addition, up-regulation of angiogenesis promoters and down-regulation of inhibitors an be detected. This is a early, critical aspect to synovial pannus formation and facilitates the perpetuation of the inflammatory process within synovial joints.

Ultrasound imaging of synovial joints provides information regarding synovial hypertrophy (referred to as grey scale synovitis) and vascular flow within the synovium (Doppler ultrasound). Doppler ultrasound is of particular importance to the assessment of synovial vascularity. Power Doppler ultrasound differs from colour doppler by negating the directional information by summation of the positive and negative waveforms generated, providing a greater signal to noise ratio. This facilitates the detection of flow at low velocities commonly encountered within the synovium. Previous authors have shown correlation of PDU and synovial vascularity. Walther et. al. showed that in patients undergoing knee joint arthroplasty (OA and RA), qualitative histological synovial vascularity scores correlated with qualitative PD ultrasound of the supra-patella pouch. Others have confirmed a relationship between synovial inflammation and ultrasound PD. Schmidt et al. found good agreement between presence of colour Doppler signal and histologically verified pannus tissue in knee joints of RA and osteoarthritis patients, whereas Fiocco et al. found a significant correlation between B-mode US synovial thickness and arthroscopic grade of synovitis in arthritic knee joints.

There are number of factors which drive new vessel formation within the synovium. Tissue hypoxia is certainly a factor with an expanding hyper-cellular, metabolically

active synovium. Lund-Olesen et. al. demonstrated that synovial fluid pO2 in RA knee joints had a partial pressure as low as 27 mm Hg compared with 43 mm Hg in patients with osteoarthritis and 63 mm Hg in patients with a traumatic effusions. Some studies have suggested the partial pressure could be as low as 15 mm Hg. This is a profound driver of neovascularisation. Hypoxia inhibits the constitutional degradation of HIF-1a allowing it to bind to its constitutively expressed partner, HIF-1b. This stable complex translocates to the nucleus, where it upregulating angiogenesis related genes. VEGF, HIF-1, HIF-2, Ang1, Tie2 are all expressed in the synovium of patients with Rheumatoid Arthritis. VEGF and angiopoietin-1 (Ang1)/ Tie-2 interaction is critical for the stabilization of newly formed blood vessels within the rheumatoid synovium. In contrast, Ang2 antagonizes Ang1 and thus inhibits vessel maturation. VEGF may also act in a HIF-independent fashion.

In addition, other soluble and cell surface-βound mediators are important. Vascular endothelial growth factor (VEGF) and hypoxia-inducible factors (HIFs), pro-inflammatory cytokines (TNF-α, IL-1, IL-6), chemokines (IL-8/CXCL8, ENA-78/ CXCL5) and adhesion molecules (β1 and β3 integrins, E-selectin, VCAM-1, ICAM-2) play an important roll in stimulating new vessel formation as a consequence of tissue inflammation.

Pro-inflammatory cytokines can have a direct influence on new vessel formation within the synovium or act via VEGF-dependent pathways. TNF-α, IL-1, IL-6, IL-8, IL-15, macrophage migration inhibitory factor (MIF), granulocyte (G-CSF) and granulocyte-macrophage colony-stimulating factors (GM-CSF) are involved in angiogenesis. There is therefore a concert of angiogenic factors at work with the rheumatoid synovium to promote new vessel formation and stabalisation. Whilst a number of mechanisms exist, a common end result is seen in the patient with a perfused synovial tissue which is allowed to expand with a suitable vascular supply network. Imaging of this network of new vessels provides indirect evidence of tissue inflammation however the relationship of US measures of synovitis and synovial tissue angiogenic factors and vessel density has not been previously explored.

8.2 Aims

1. To explore the relationship of ultrasonographic measures of synovitis (GS-synovitis and PDU) and synovial vascularity within the knee joint of patients with early Rheumatoid Arthritis.
2. To correlate the synovial tissue expression of vascular mediators an pro-inflammatory cytokines, such as IL-6 and TNF-α, to US measures of synovitis.
3. To examine the variability of US parameters, synovial vascular density and inflammatory mediators within the knee joint.

8.3 Methods

Patients and samples

12 patients with early Rheumatoid Arthritis were recruited as part of an ongoing study in patients with early inflammatory arthritis (Pathobiology of Early Arthritis Cohort). All patients were recruited from the Early Arthritis Clinic (EAC) within the department of rheumatology at Barts Health NHS Trust. All patients had a knee joint clinically involved and fulfilled the ACR diagnostic criteria (1987) for Rheumatoid Arthritis.

Patients were treatment naive prior to all baseline assessment. Following written informed consent, patients received a clinical assessment, ultrasound examination and ultrasound guided synovial biopsy from the supra-patella pouch.

Synovial tissue processing

Each synovial specimen was divided into two parts: one was formalin fixed and paraffin embedded for immunohistologic analysis and the second was stored in RNA later (AMBION) at -80°C until RNA extraction and QT.PCR analysis.

Immunohistochemistry

Paraffin embedded tissue specimens were cut in consecutive 3μm-thick sections. The sections were then deparaffinized and rehydrated through graded ethanols. A haematoxylin and eosin stain was performed to ensure tissue morphology was

preserved: only tissue sections with an intact lining layer were used. To quantify vascular density in the synovial tissue in terms of both number and size of vessels profiles, a double immunofluorescent staining for factor VIII and α-SMA was used.

The following primary antibodies were used for immunofluorescence analysis: mouse anti human factor VIII (clone F8/86; Dako, Glostrup, Denmark), Cy3 conjugated mouse anti human α-SMA (clone 1A4; Sigma, Missouri, USA). The appropriate secondary antibody for Factor VIII was obtained from Invitrogen, Paisley, UK. As negative control irrelevant isotype –matched antibodies (Dako, Glostrup, Denmark) were used.

Briefly, antigen retrieval was performed by heating for 35 minutes at 95°C in Dako Target Retrieval Solution. Sections when then washed in Tris Buffered saline, incubated with protein block (Dako, Glostrup, Denmark) and then in the first primary antibody for one hour (mouse anti human factor-VIII using antibody dilution of 1:50). After washing, the appropriate Alexa-488 conjugated secondary antibody was applied for 30 minutes; sections were then washed and the directly conjugated second primary antibody, α-SMA, was added at dilution of 1:200.Synovial tissue was counterstained with 4'-6-diamidino-2-phenylindole (DAPI) and mounted with anti fade mounting medium.

Aimed to obtain a more representative assessment of synovial vascularity all available synovial specimens were cut and stained at two different cutting levels, 50μm apart.

Digital image analysis for synovial vascularity evaluation

One observer blinded for order, patients and clinical data, performed both image acquisition and subsequent image analysis for all the sections.

Digital images of immunofluorescent stained synovial blood vessels, were acquired at 20X magnification on a fully automated Olympus BX60 microscope, captured using a video camera (figure 8-1) and then digitized using Cell P image analysis software.

For the most extended synovial tissue, more than a single picture was obtained to capture all the part of the samples.

Each acquisition was performed in one single session for each vascular marker, factor-VIII and α-SMA, respectively, with fixed variable as derived from the calibration.

The obtained factor-VIII and α-SMA stained images were saved in jpeg format and used for the subsequent digital images analysis.

The images were first manually processed and, using the drawing method, a selected area was defined as the region of interest (ROI) for both blood vessel density evaluation and digital vessel size analysis.

The ROI was then use to generate a “tissue mask” by thresholding through a value separating the background (DAPI staining) of histological slides from the stained vessels, resulting in binary black and white signal images.

Since both factor-VIII and α-SMA signals were used to count and analyze blood vessels within synovium, both their green and red fluorescent color, respectively, were converted into solid white color for binary bitmap images. This conversion step was adjusted to achieve selection of vascular structures without fragmentation or fusion of vessels. The vascular objects greater than 10μm in diameter were quantified within the selected ROI, using Cell P analysis software and expressed as blood vessel numerical density (number of vessel per square millimeter) and blood vessel fractional area (area enclosed within and including vascular endothelium expressed as a percentage of the selected ROI), respectively.

Using the same digital analysis system synovial blood vessels were additionally divided into classes based on blood vessel surface area and each area-class was visualized using a unique color. Larger vessels, exceeding the maximum range of the blood vessel area considered, served as positive control both for immunohistology and for digital analysis.

Using the above detailed algorithm for blood vessel density and size evaluation we analyzed synovium vascularity specifically in the previously described three different

tissue sampling sites (the midline supra- patella, the medial supra-patella and the lateral supra-patella areas).

QT-PCR OF ENDOTHELIAL SPECIFIC GENES

Total RNA was extracted from the remaining portion of synovial tissue stored in RNA later, using the RNeasy Mini Kit (Qiagen, Chatsworth, CA)), with on column DNase I digestion to avoid genomic DNA contamination.

cDNA was generated from 1 ug of RNA using the Thermoscript RT-PCR System (Invitrogen, San Diego, CA).

QT-PCR was performed to detect mRNAexpression levels of Ang-1, Ang 2, VEGF-α, VEGF-C Tie-2 and VEGFR2 using specific primers and probes (detaliled in Table….). The RT-PCR was run in triplicate with an equal loading of 20 ng of cDNA/well. Results were analysed after 40cycles of amplification using the ABI PRISM 7900HT Sequence Detection System Version 3. Relative quantification was measured using the Comparative Ct (Threshold Cycle) Method. cDNA from human placenta was used as a positive control. Placenta is a very good positive control tissue for several techniques (IHC, gene expression) as it expresses many angiogenic factors. It has vascular, epithelial, stromal and hematopoietic components in the different parts of the placenta. In particular, in terms of vasculature it is very rich in new blood vessels with up regulation of most angiogenic factors and endothelial proteins expressed.

Figure 8-1: synovial tissue stained with Factor VIII demonstrating vessels and gated digital analysis for different sized vessels.

High powered field of synovial tissue with factor VIII staining indicating vessel wall fluorescence. Division of vessel size using digital imaging analysis can be performed based on automatic generated gates with colour differentiation. IHC performed by Dr. B. Hands (Experimental Medicine and Rheumatology, William Harvery Research Institute).

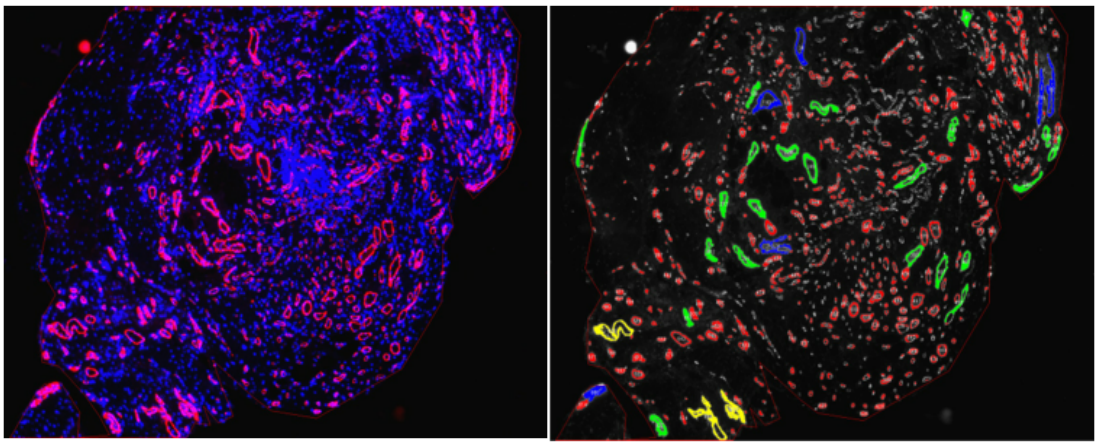

Ultrasound Guided Synovial Biopsy Technique

US guided synovial biopsy and standard US images were performed using a GE Logic 9 ultrasound machine with a 2-dimensional M12L transducer. All synovial biopsies were performed by the same individual. Knee synovial biopsies were all carried out from a lateral approach into the supra-patella pouch with the joint in 30 degrees of flexion. Each procedure required 1-3 mls of local anaesthetic(1% lignocaine) injected into the soft tissues up to the joint capsule, visualized under US guidance. A further 10-15mls of local anaesthetic was instilled in to the supra patella space. A 16G or 14G Quick-Core® Biopsy Needle (Cook medical, Limerick, Ireland), placed within the joint capsule under US guidance. A longitudinal US image is used to detect the needle and guide it to an appropriate pre-determined site for biopsy. A minimum of 18 biopsies were aimed to be retrieved per procedure (6 samples for each 3 sites within the supra patella pouch. 12 biopsies were immediately fixed in 4% paraformaldehyde for paraffin embedding and a further 6

immersed in 10:1 v:v of RNA-Later (Ambion) for later RNA extraction. Following the procedure a small sterile dressing was place over the site of insertion .

Ultrasound scoring

Ultrasound images of the knee were recorded and analysed by two independent examiners. Three standardised, 30 second cine loops, were recorded from i) the midline supra patella pouch ii) medial suprapatella pouch iii) lateral supra patella pouch corresponding to region of synovial tissue sampling with the knee in 30 degrees of flexion. All images were acquired by a single sonographer.

Pre-βiopsy, standard longitudinal ultrasound images of each biopsied joint were recorded with power Doppler switched on and off. Synovial tissue was defined as hypoechoic non-compressible intra-αrticular tissue. Power Doppler settings were adjusted to the lowest permissible pulse repetition frequency to maximise sensitivity. Maximum colour gain was used without creating artifactual noise. A standard depth of 3.8cm was used for each image acquisition.

Quantitate analysis of the recorded cine loops were performed using Image J (NIH, http://rsb.info.nih.gov/ij/. 1997-2008) with a customised macro application for pixel area measurement. The cine loop was played and the frame representing the maximum doppler signal selected by the reader. The area measurement was applied by outlining the total grey scale synovial area. Quantitative measurements provided included synovial thickness area (STA), power doppler signal (PDA), doppler signal over a predetermined colour threshold (PDThA) and a ratio of synovial to doppler area (PDA/STA). A qualitative score was applied to both the grey scale synovial thickness (STi) and total power doppler signal (VASCi) for each region of the SPP. Both quantitative (STA, PDA, PDThA) and qualitative scores (VASCi, STi) were performed by two experienced readers and the ICC reported.

8.4 Results

8.4.1 Patient demographics

12 patients were biopsied (9 female, 3 male) with a mean age of 47 (S.D. 5.9). All patients had symptoms of less than 12 months duration with an average of 7 months form symptom onset to recruitment. 5 patients (42%) were seropositive for Rheumatoid factor with 4 patients (33%) being positive for anti-CCP antibodies at presentation. The mean DAS28 score was 5.4 (limits 3.9 - 6.8).

All 12 patients received synovial biopsies from each of the three specific regions of the SPP pouch (medial, middle and lateral) as described above. All samples were graded histologically only if an intact synovial lining was present, identifying the tissue sample as synovial tissue. For 2 patients there was ungraded tissue from the lateral compartment resulting in a total of 34 tissue samples being analysed (12 medial, 12 middle, 10 lateral).

Table 8-1: Patient demographics (n=12)

	N (%)
Gender - Female - Male	 9 (75) 3 (25)
Age (years) mean+/- SD	47 +/- 5.9
Disease duration (months) mean +/-SD	7 +/- 0.8
Serology - Rheumatoid factor - Anti-CCP	 5 (41.6) 4 (33.3)
DAS28	5.4 +/- 0.88
Inflammatory markers - ESR - CRP	 43 +/- 12 23 +/- 5

8.4.2 Interclass correlation co-efficient (ICC) of knee US scores

Ultrasound images for all 36 sites (12 from each region) were analysed for grey scale and power doppler parameters. The ICC values for PDA, VASCi, STA showed good levels of agreement. The STi (ICC 0.68; 0.34-0.89) showed moderate agreement

within the medial and lateral supra patella pouch but good agreement within the middle compartment. Visual interpretation of the Blant-αltman graph did not show any significant deviation of agreement at higher levels in the US score range.

Table 8-2: Table of ICC values for qualitative and quantitative assessment of US parameters from each SPP region.

SPP region of interest	Med	Mid	Lat
VASCi	0.92	0.89	0.95
PDA	0.94	0.95	0.97
STi	0.68	0.84	0.71
STA	0.88	0.88	0.86

8.4.3 Variation of parameters within the SPP

The three areas of the supra patella pouch were analysed for angiogenic gene expression, vascular density and ultrasound parameters as described above (figure 8-2). Within the three regions of interest there was no significant difference in TNF-α expression within the tree regions of interest within the SPP (Kruskal-Wallis; $p = 0.31$), (figure 8-2, A). There was no significant difference found in the gene expression profile for any other angiogenic factors or pro-inflammatory cytokines examined (Angiopoietin 1 / 2, VEGFc, VEGFa, FVIII, Tie2, IL-1 β, IL-6). In addition, there was no significant difference in the vascular area measurement in each region, although there was a tendency for the lateral compartment to have slightly higher area values than the medial and middle compartments (figure 8-2 B).

No difference was detected in the ultrasound parameters within the SPP pouch. However, similarly, higher levels of PDA and VASCi were noted in the lateral compartment along with higher levels of STA and STi (figure 8-2 C and D). The ratio of PDA / STA remained stable throughout the three regions of interest with no significant difference detected between regions (figure 8-2 E).

Figure 8-2: No significant variation of ultrasound, vascular area and gene expression between each region of the supra patella pouch (SPP)

A: TNF α expression by by each region of interest within the SPP. **B:** PDA (pixels) by each region of interest within the SPP. **C:** STA (pixels) by each region of interest within the SPP **D:** Vascular area / mm^2 by by each region of interest within the SPP. **E:** PDA/STA ratio by each region of interest within the SPP.

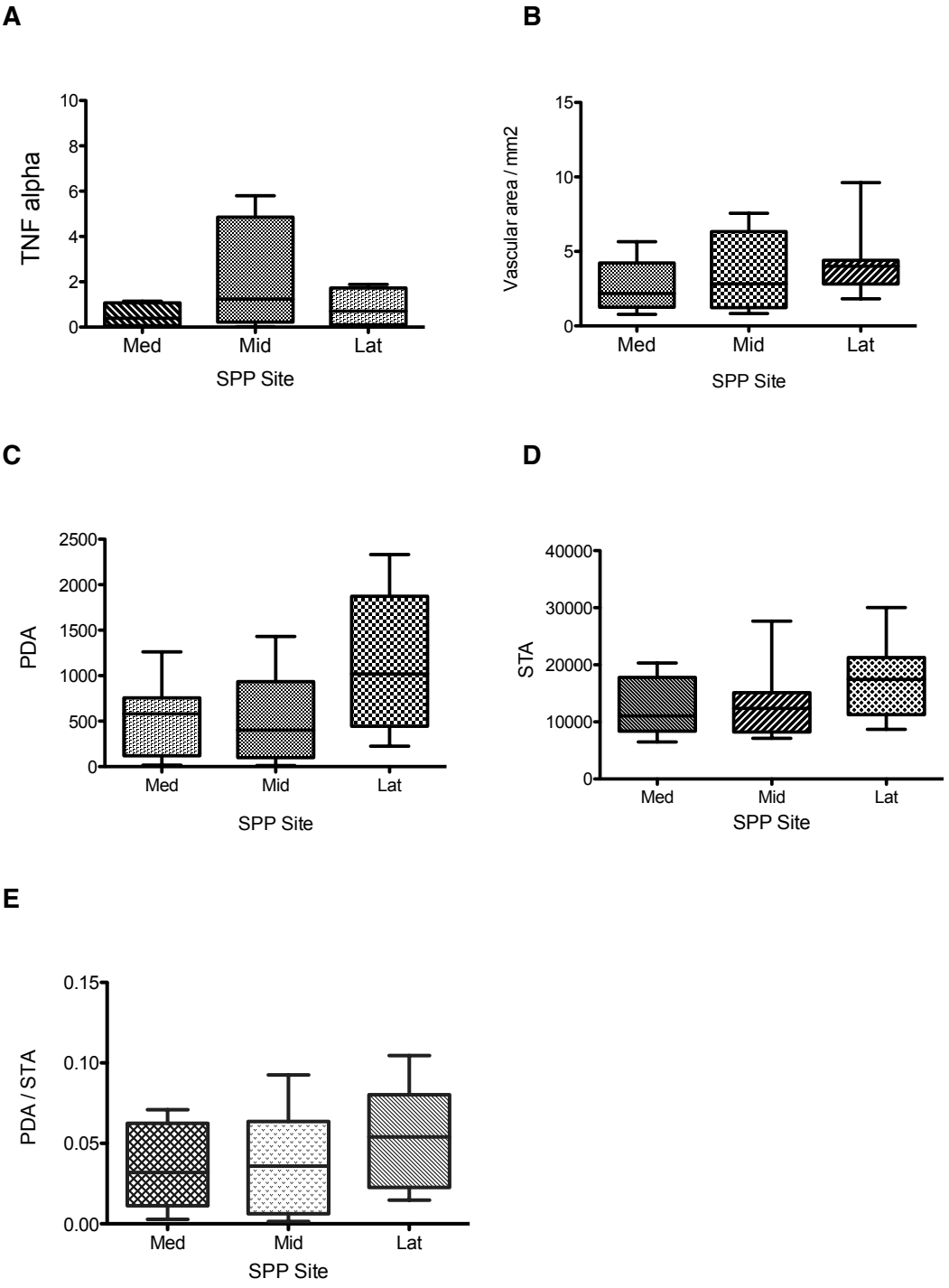

8.4.4 Relationship of synovial vascular area to US variables and angiogenesis factors

The synovial vascular area was calculated for all tissue samples from each site f the supra patella pouch. The histological vascular area was correlated with the ultrasound parameters of synovitis (results shown in table 8-4). All qualitative and quantitative ultrasound parameters correlated with the synovial vascular area / mm2. The PDA vascular index correlated best of the individual parameters (Spearmans rank - 0.73; SD 0.53-0.89). The qualified ratio of PDA / STA also correlated well (Spearmans rank - 0.77; SD 0.59-0.92). Blood vessel number also correlated with PDA, PDThA and PD/STA but not with the STA and VASCi.

The synovial vascular area showed a good correlation with the pro-inflammatory cytokines, IL-1b and TNF-α but not with IL-6. There was also good / moderate correlation with tissue gene expression of pro-αngiogenic factors (VEGFa, angiopoietin-1). Synovial vascular area correlated with VEGFr3 (Spearmans rank - 0.68; SD 0.43-0.88), a lymphogenetic receptor, but not for VEGFc its potential receptor. These correlations held when the data was examined as per each SPP site rather than as a total group.

Table 8-3: Correlation matrix of synovial vascular area and US assessment of PDS and synovial thickness (STA).

All correlation's performed using Spearmans rank, significant if p <0.05

US assessment	VASCi	STA	PDA	PDThA	PD / STA
Synovial vascular area / mm^2	0.64*	0.47*	0.73*	0.66*	0.77*
Blood vessel no. / mm^2	0.38*	0.32	0.53*	0.66*	0.61*

Figure 8-3: Graphical representation of synovial vascular area correlated with US vascular parameters

Synovial Vascular area / mm^2 of synovial tissue correlated with US parameters. **A:** total PDA correated with synovial tissue vascular area / mm2 (Spearmans rank, r = 0.73, p = 0.001), **B:** Ratio of PDA / STA correlated with synovial tissue vascular area / mm^2 (Spearmans rank, r = 0.77, p = 0.001). PDA/STA represents an US equivalent to the synovial tissue vascular area / mm^2.

A

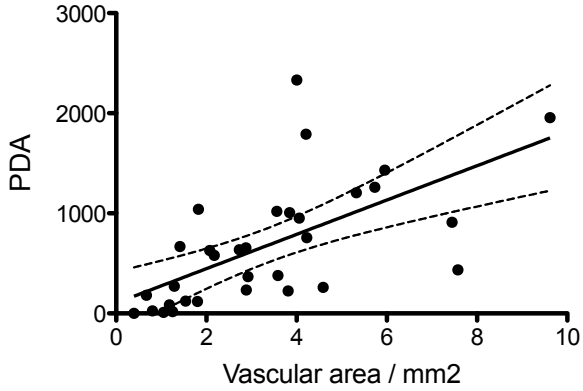

B

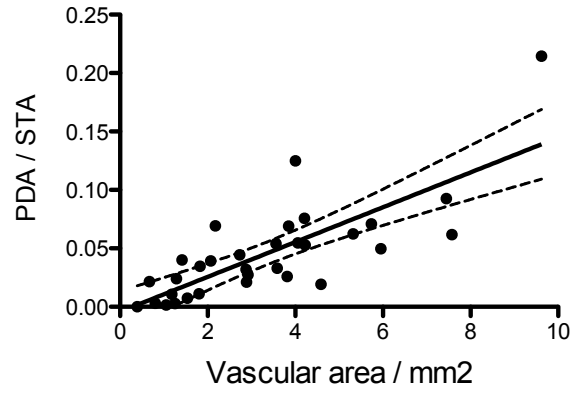

Table 8-4: Correlation matrix of angiogenic factors and US assessment of PDS and Synovial thickness

All correlation's performed using Spearmans rank, significant if p <0.05

Angiogenic factor	Ang 1	Ang 2	VEGFR3	VEGFc	VEGFa	Tie2	IL-1 b	IL-6	TNF - a
Synovial vascular area / mm2	0.24	0.64*	0.68*	0.44	0.60*	0.41	0.61*	0.3	0.58*
Blood vessel no. / mm2	0.30	0.44	0.49	0.45	0.63*	0.22	0.60*	0.4	0.46

Figure 8-4: Graphical representation of angiogenic factors correlated with US vascular parameters

Synovial Vascular area / mm^2 of synovial tissue correlated with angiogenic factors. **A:** VEGFa correlated with synovial tissue vascular area / mm2 (Spearmans rank, r = 0.60, p = 0.005), **B:** Anti-TNFa correlated with synovial tissue vascular area / mm^2 (Spearmans rank, r = 0.58, p = 0.01).

A

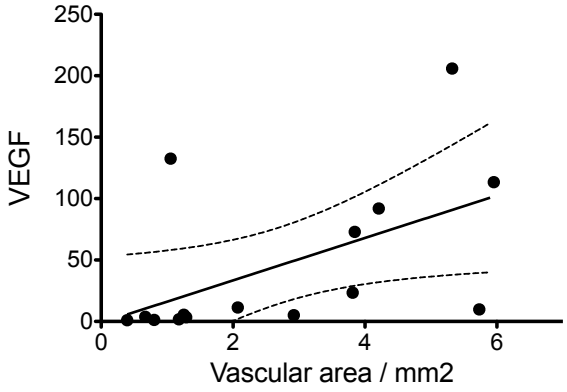

B

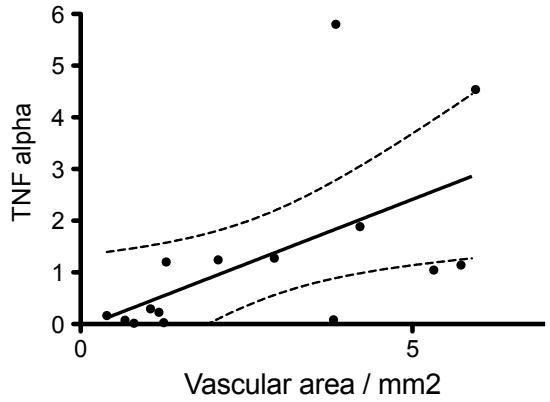

8.4.5 Relationship of ultrasound parameters to angiogenic factors

The US parameters of synovitis assessed in this study have been shown to correlate with the synovial vascular area / mm2. In addition, these parameters were correlated with gene expression for a number of pro-αngiogenic factors and inflammatory cytokines. STA showed a good correlation with all three pro-inflammatory cytokines tested (IL-1b, IL-6 and TNF-α) and moderately with angiogenic factors such as VEGFa, Tie-2 and Angipoietin 2. No significant relationship was seen between STA and Angiopoietin 1. PDA and PDA / STA parameters also correlated with pro-inflammatory cytokines, with only a modest correlation demonstrated between with PDA and IL-6 (Spearmans rank - 0.48; SD 0.12-0.72). The quantitative, thresholded PDA parameter correlated only with IL-1b and TNF-α but not IL-6. PDThA also correlated with VEGFa but none of the other angiogenic factors.

The qualitative, VASCi score, performed poorly when correlated with all the of the angiogentic factors and inflammatory cytokines, showing only an modest relationship to TNF-α expression (Spearmans rank - 0.52; SD 0.23-0.85).

With respect to lymphangiogeneis, VEGFc and its receptor VEGFr3 correlated with both synovial thickness and PDA but not with any of the other US parameters measured. Table 8-4 shows a correlation matrix for US parameters assessed and angio- and lymphoangiogenic factor expression.

Table 8-5: A correlation matrix of ultrasound parameters and angio- and lymphoangiogenic gene expression in 12 patients with newly diagnosed RA. All correlations performed using Spearmans.

US assessment	VASCi	STA	PDA	PDThA	PD / STA
Angiopoietin 1	0.33*	0.37*	0.22*	0.11*	0.20*
Angiopoietin 2	0.44*	0.74	0.61	0.46*	0.55
VEGF-R3	0.51	0.61	0.55	0.36*	0.47*
VEGFc	0.21*	0.62	0.39	0.14*	0.29*
VEGFa	0.3*	0.56	0.52	0.48	0.51
Tie-2	0.33*	0.51	0.46*	0.22*	0.38*
IL-1 β	0.53	0.81	0.68	0.64	0.66
IL-6	0.36*	0.70	0.48	0.46*	0.56
TNF-α	0.52	0.75	0.63	0.63	0.60

Figure 8-5: Graphical representation of PDA correlated with angiogenic factors in 12 patients.

PDA correlated with angiogenic factors in 12 patients.. A: TNFa correlated with Power Doppler Area (Spearmans rank, $r = 0.63$, $p < 0.001$), B: VEGFa correlated with Power Doppler Area (Spearmans rank, $r = 0.52$, $p < 0.001$).

A

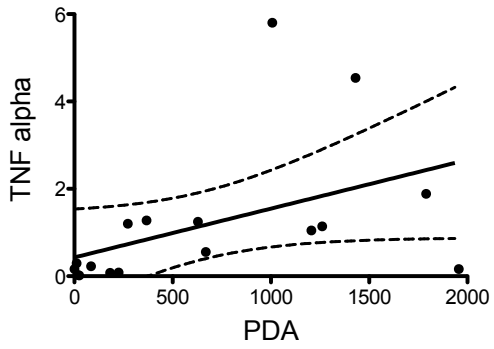

B

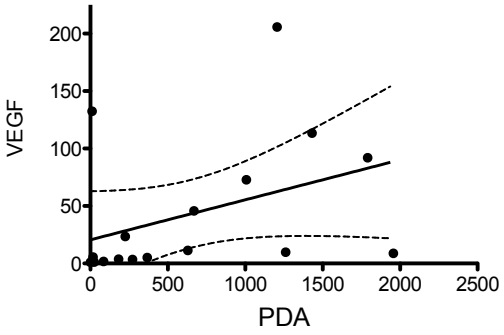

8.4.6 Correlation of US vascular parameters and synovial vessel size

Each synovial tissue specimen was analysed by blood vessel size as describe in section 6.3. Variable gating of the digital image generated form the immunohistochemistry staining allowed for identification of 3 sizes of vessels within each specimen (figure 8-6). Medium sized vessels contributed most to the overall vascular area (79%) within each tissue specimen with small and large vessels contributing on 9.5% and 11.5% respectively.

Figure 8-6: Bar chart showing the relative percentage contribution to the overall histological vessel area made by each vessel size.

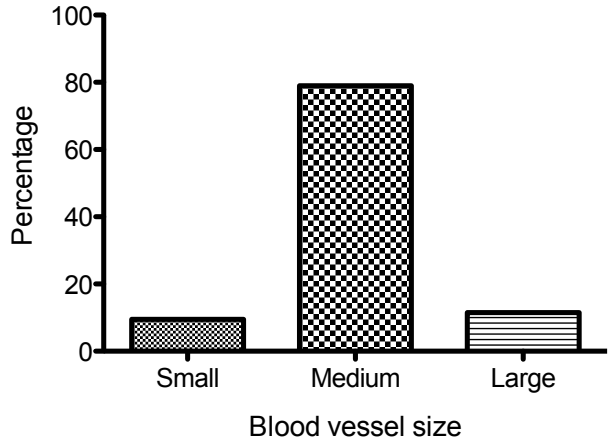

The vascular US parameters were correlated with the vascular area / mm2 denoted by a subdivision of the overall area by vessel area for all 34 samples and table provides an overview of the relationships. Only PDThA significant correlation with the medium vessel size.

Table 8-7: Correlation matrix of synovial vascular indices and synovial vessel size (small, medium and large).

Synovial Vessel size	Small	Medium	Large
VASCi	0.40 (0.08-0.77)	0.38 (-0.08-0.70)	0.36 (-0.10-0.69)
PDA	0.43 (0.19-0.73)	0.34 (-0.11-0.67)	0.16 (-0.29-0.55)
PDA / STA	0.40 (-0.05-0.71)	0.34 (-0.13-0.67)	0.12 (-0.33-0.53)
PDThA	0.03 (-0.41-0.45)	0.56 (0.15-0.80) **§**	0.05 (-0.38-0.47)

8.5 Discussion

This study demonstrates a clear relationship between US imaging, specifically grey scale and doppler assessment of synovitis, and histological synovial vascularity.

All patients within this cohort had active rheumatoid disease with a moderate to high DAS 28 score prior to biopsy and a knee which was clinically involved allowing successful harvesting of synovial tissue. This work parallels previous work by Walther et. al. who similarly examined the relationship of synovial vascularity at the knee and power doppler ultrasound. However, this previous report examined patients with both OA and RA, and severe degenerative arthritis requiring knee joint arthroplasty. This study differs significantly in only including patients with early RA, within 1 year of symptom onset and naive to immunosuppressant therapy. Patients received an US guided synovial biopsy to harvest tissue from the appropriate region of interest previously recorded at the pre-procedure examination. The use of US as both the assessment tool and facilitator of tissue sampling strengthens the legitimacy of correlating synovial tissue and ultrasound assessment at each separate sampling site.

As with previous reports, a significant correlation was found between the synovial vascularity on histological analysis for both the grey scale assessment of synovial thickness and power doppler signal. Previous authors have used a qualitative analysis of tissue sections using a semi-quantitative 0-4 score which was subsequently correlated with US parameters. In this study we favored a quantitative approach to tissue assessment with the vascular area being scored using Digital Imaging Analysis (DIA). This has a number of advantages including scoring standardisation and providing a fractional vascular area assessment. This intuitively provides greater information as to the vessel density within the synovium rather than an absolute area which may vary with tissue size.

Both histological and ultrasound parameters showed no significant difference between regions of interest within each joint. Previous studies have examined the variability of histological markers of synovitis such as sub-lining macrophages (SL-

CD68) within joints and reported that there seems to be a degree of homogeneity. The US STA and PDA did reveal a higher average signal in the lateral compartment of the joint. Whilst this did not reach statistical significance, the small number of patients within this study may be under powered to detect a real difference. These findings should be explored in a larger cohort of patients. Correction for the PDA by STA expressed as a fraction also remains relatively constant thought out the joint and may be a more appropriate measure of synovial blood flow. A similar trend was seen with the histological vascular area measurement but again did not reach statistical significance. The angiogenic factors and pro-inflammatory cytokines did not show and difference when measured in different compartments.

In addition to synovial vascular area, blood vessel number was also assessed with DIA within all compartments. Both these variables correlated well with PDA, PDThA and PDA / STA (0.73, 0.66 and 0.77 respectively). Blood vessel number only showed a moderate correlation with the US vascular parameters and, unlike synovial vascular area, gave no significant correlation with STA or VASCi. The blood vessel size and overall vascular area would appear to be an important factor in synovial expansion rather than the vessel number. Figure xxx, shows the percentage of small medium and large vessels. Medium size vessels clearly make the greatest contribution (79%) to the vascular area score, representing more developed and a relatively stable vasculature. A correlation with a number of angiogenic and pro-inflammatory cytokines was detected (TNF- a, IL-1b, Ang 2, VEGFa and VEGFr3) but not with IL-6 or Ang 1. The positive correlation with VEGFa, Ang2 but not Ang1 with synovial vascular area and PDA may indicate a profile of synovial tissue underoing neovascularisation. In tumors, the over expression of VEGFa and Ang2 has a positive effect of growth whilst Ang1 over expression reduces tumor expansion. Ang 1 has a stabalising effect on new vessels and is required for vascular maturity. Within an inflammed joint, the synovial expansion would require the rapid expansion of a suitable vascular network. Up regulation of VEGFa and Ang2 in this context would appear to be an important factor. It would be important to to examine these

relationships longitudinally and determine if this profile alters in favour of Ang1 expression in a quiescent joint in a patient in remission.

A positive correlation is also seen with US parameters and these mediators. PDA and STA correlate with all factors assessed except for Ang1. STA provided a good correlation with Ang 2, IL-6, IL-1b and TNF-α and moderate correlation with VEGFa, VEGFc and VEGFr3. VEGFc and its receptor VEGFr3 are known to be important lymphogeneic factors and their association with STA and PDA may suggest that this process is seen within an expanding, inflamed synovium. However, a report from Polzer et. al. suggested that lymphangiogenesis was encouraged following treatment of humans with anti-TNF α with a greater expression of lymphatic vessels in synovial tissue when examining pre and post treatment synovial tissue. The expression of of VEGFc and VEGF-R3 were not specifically commented upon in this study.

The relationship of STA and IL-6, IL-1b and TNF-α may have a number of potential explanations. These pro-inflammatory cytokines have a number of functions such as chemoattractants, up-regulating of endothelial adhesion molecules and increasing vascular permeability. STA was previously shown to be a good parameter in chapter 5 with a considerable effect size in detecting response to therapy. Synovium, as imaged by US, consists of a number of components. Hypertrophy of the lining layer and infiltration of the sub-lining can be seen histologically, however complete resolution of these histological finding are insufficient to explain the magnitude of change which can be detected on US examination. In established synovitis, synovium is often necrotic on histological examination, or shows marked fatty infiltration and fibrosis. These components may be susceptible to fluid shifts and a reduction in vascular permeability, lead by a down regulation of pro-inflammatory cytokines expression.

The US assessment of vascularity correlates well with the synovial vascular area and the mediators of angiogenesis. A moderate correlation is seen between PDThA and the synovial vascular area. In addition, PDThA correlated with medium vessel size which in the major contributor to total vascular area. This correlation is also seen with

TNF-α and IL1-β expression which may suggest that the intensity of the doppler signal detected on US examination relates to not only the vascular density of the synovium but also to vasoactive mediators exerting afferent vascular control. Power doppler signal and synovial area measurement changes can be detected within 24hrs of treatment (chapter 5). Neoangiogenesis and vascular regression are processes which are unlikely to contribute significantly to US PDS changes within such a short time frame. A more likely explanation is again the effects of vasoactive mediators and their down regulation. Significant reduction vascular signal can be seen on cooling hands by only a few degrees (chapter 4). Therefore, the earliest change in doppler signal in treated patients is likely to be due to afferent vessel control rather than vessel regression.

8.6 Conclusion

Power doppler ultrasound assessment of synovitis in patients with early RA is a valid measure of synovial vascularity and shows a positive relationship with the expression of pro-inflammatory cytokines and angiogenic factors. Quantitative and qualitative measures (VASCi, PDA) correlate with synovial vascular area. Grey scale US assessment of synovial thickening also has a close relationship to vascular area and angiogenic factors. There is a degree of homogeneity between synovial regions within the supra patella pouch which would suggest that a single region of interest may be representative both histologically and ultrasonographically.

Angiogenic mediators fluctuate during different phases of vessel development and maturation. Inflammatory cytokines, such as TNF-α, vary depending upon the disease activity within the joint. The interplay between these factors and the synovial vasculature is complex with different cytokines having various effects depending upon co-expression of other mediators. Therefore a single snap shot of the angiogenic profile in this context is very difficult to interrupt with certainty. The relationship of synovial vascularity, angiogenic factors and power doppler ultrasound imaging can only be dissected further with serial assessments before and after

therapy. Specifically, the next step is to ask if following effective treatment, PDS reduction occurs independently from vascular remodeling or is directly related to down regulation of cytokine networks.

9. General Summary

Ultrasound imaging has an important role to play in the modern Rheumatology department. Ultrasound is a relatively inexpensive and portable imaging modality which can add important diagnostic and prognostic information for Rheumatologists in daily practice. The initial use of ultrasound imaging in routine care was directed primarily towards soft tissue lesions, muscle pathology and tendonopathy however its use in inflammatory arthritis has grown over the past 20 years along side the technological improvements which have produced high quality images for interpretation. The OMERACT - ultrasound group have made significant steps in validating ultrasound imaging in this context. Despite this many questions remain and require further evaluation. The two central themes of this thesis are the responsiveness of ultrasound imaging and the correlation between ultrasonographic findings and the histomorphological characteristics of the synovial tissue being imaged. In addition, an important on going debate continues over the most appropriate ultrasound data set. Therefore in this thesis I focus on a limited US joint data set to include 10 metacarpal-phalengeal joints (MCPJ) in an attempt to demonstrate that a relatively small data set can provide addition information over currently existing clinical assessment tools such as the DAS28. The incorporation of 3D imaging into a number of the studies reflects the continued technological development with potential benefits for the ultrasonographer.

Whilst an assessment tool can be a valid measure of a particular construct, if it is not consistent or reliable then implementation as a useful clinical test is problematic. Conversely, a reliable tool is not necessarily a valid one. This provides the starting point for this thesis. Previous authors have reported good to excellent agreement in a number of different settings[202-207]. Naredo specifically reported the reliability of US imagining for MCP joint US scoring (Kappa 0.88) and demonstrated that this was superior to clinical assessment in detecting synovitis[112]. However, ultrasound imaging is unusual by having two clear levels of variability - variation when the image is

acquired and when it is read. In order to examine these two aspects to ultrasound reporting myself and colleague (MS) performed multiple US assessments at various stages of a multi centred, randomised controlled clinical trial. All endpoints were examined in 10 MCPJ and included vascular and synovial thickness assessments. Qualitative and quantitative scores were used and agreement calculated using the interclass correlation co-efficient at baseline and at the end of study (DAY 14) with all 2D scans being performed in both a longitudinal and transverse orientation..

I am able to report that:

1. 2D vascular endpoints show excellent within scan inter-reader and parallel scan inter-reader and intra-reader reliability at both baseline and DAY 14.
2. 2D synovial thickness endpoints show good within scan inter-reader parallel scan intra-reader reliability but poor parallel scan inter-reader reliability for the transverse synovial thickness index score.
3. 3D endpoints perform well and are consistent at baseline and at DAY 14 except for the vascular index score parallel scan intra-reader reliability.

This reliability study provides conformation that, as a limited joint US data set, the 10 MCP joints are able to be scored consistently both in 2D and 3D US imaging. The reproduction of this study on 2 sites provides evidence that a well defined US assessment of a limited joint set may be used in the context of a multi centered clinical trial.

My next aim was to establish if this limited data set was responsive to change. To this end I used both a physiological (cryotherapy) and pharmacological (Prednisolone) triggers to initiate this change. Cryotherapy provides a convenient, inexpensive and a relatively safe stimulus causing peripheral vasospasm. This allows many of the vascular US endpoints to be examined in a safe *in vivo* setting. Once again the 10 MCP joints were assessed both by 2D and 3D imaging. I can report that following cryotherapy:

1. All the vascular endpoints (2D and 3D) demonstrated a significant change.

2. There was good correlation between 2D and 3D vascular endpoints including 3D topographical imaging endpoint.
3. 2D US vascular endpoints showed the greatest response to change

All of the endpoints failed to return to pre-cooling levels 15mins after removal of the stimulus which would suggest that thermoregulation in an important factor which should be bourn in mind when integrating US imaging into therapeutic study design. Within this model, the ability of 2D and 3D US parameters to detect change in synovial vascular flow over a relatively short period of time can be demonstrated. The vascular index scores used over 10 MCP joints would seem to be both responsive and reliable.

Having shown that this limited US joint count responds to cryotherapy, I examined the ability of this same data set to detect change in patients with active RA over a 14 day period. Patients were prescribed either Prednisolone or Placebo and ultrasound assessments made at baseline, DAY 1, 7 and 14. This study consisted of two panels. Panel A used Prednisolone at 15mg per day were as Panel B used 7.5mg per day. This attempted to demonstrate a dose response with US endpoints. The qualitative transverse synovial PDS over 10 MCP joints was chosen as the primary endpoint with all other synovial thickness and vascular qualitative and quantitative scores as secondary end points. All patients received a clinical assessment of disease activity (DAS28). Within Panel A:

1. The 10MCP Trans VASCi score showed a significant treatment effect at DAY 14 compared to placebo.
2. All 2D secondary endpoints showed a significant treatment effect compared to placebo at DAY 14 except for transverse synovial thickness index (Trans STi)
3. All of the 3D endpoints produced numerically smaller effect sizes which did not reach significance.

Within Panel B:

1. The primary endpoint demonstrated a statistically significant treatment effect at DAY 7 but not 14.

2. Longitudinal 2D synovial thickness index showed a significant treatment effect at DAY 7 and DAY 14.

Using a composite endpoint consisting of the DAS28(CRP)+Long STi+Trans VASCi a significant effect size was demonstrated in both panel A and B with a suggestion that a dose effect could be demonstrated.

This provides a good evidence that this limited joint US data set is responsive and has utility over and above standard clinical assessments of disease activity. Prednisolone provides a very demonstrable change in disease activity. However, it remains to be proven that similar effect sizes can be reproduced within different clinical settings such as following DMARDS or Biologic agents.

There is good evidence that ultrasound assessment of joints provides greater evidence of pathology than clinical assessment alone. I was also able to show that in this clinical trial the change in US variables were superior to the change in the DAS28(CRP) assessment. Whilst the DAS28 score has demonstrated value in many clinical situations there is evidence that some patients continue to have subclinical inflammation and erosive progression on x-rays despite having a low DAS28 score. This leads to the next aim of my thesis. If US assessment of joint synovitis is much more sensitive than clinical examination, and a more faithfully assessment of synovial inflammation - what are the histopathological correlates with these imaging findings. In order to facilitate this aspect of the thesis I developed a ultrasound guided synovial biopsy technique which would provide tissue for analysis. The use of arthroscopy to harvest synovial tissue is well established however there are limitations with larger joints being more easily accessed, the cost of day surgical office space and relative patient discomfort when performed under local anesthetic. Using a Quick core biopsy needle I was able perform sampling on both small and large joints. In a cohort of 57 patients (93 consecutive biopsies) I examined the safety, tolerability and quality of tissue harvested. I can report:

1. Using an Ultrasound guided synovial biopsy technique for sampling synovial tissue is both safe and well tolerated by patients.

2. There is no significant impact on joint tenderness, swelling or pain following the procedure.
3. Good quality tissue can be harvested form both small and large joints.
4. The quality of the synovial tissue recovered in terms of RNA yield and tissue grading varies according to the pre-βiopsy ultrasound assessment synovial thickness score.

Using regressional analysis I have produced a suggested algorithm to inform the decision process as to choosing the optimal joint for biopsy based upon both size and synovial thickness score on US. The ability to acquire tissue form both small and large joints for suitable immunohistochemical analysis was imperative if I was able to examine the histopathological correlation a a limited small joint US data set.

Using a cohort of patients with both established and early RA (less than 1 year of symptom duration) I performed synovial biopsies prior to treatment initiation and after treatment. The wrist and MCP joints were most often biopsied. Histological assessment of the tissue was based upon a recognized scoring system developed by Krenn and immunohistochemical analysis of known inflammatory cells such as B cells, plasma cells, lymphocytes and macrophages.

At the single joint level a good correlation was seen with many histological variables associated with joint inflammation, such as the CD68+ macrophage sublining cells, CD20 B cells and CD138 plasma cells and CD3+ lymphocytes with both PDS and synovial thickness. CD68+ macrophages appear to correlate best with the quantitative assessment of PDS (Spearmans rank $r=0.84$, $p<0.001$). Using both cohorts I was able to demonstrate that:

1. At a single joint level the positive predictive value for the presence of CD68SL macrophages in patients with a significant PDS was 0.96 with a negative predictive value of 0.8 in the absence of any signal.
2. Both vascular and synovial thickness ultrasound scores in 10 MCP joints correlate with the Krenn synovitis score and CD68+ sublining macrophages in both early and established RA patients.

3. Histomorphological charcterisation by the absence or presence of geminal center like structures within the synovium provides a dichotomous population. Patients with histomorphologically defined Grade 2 / 3 germinal centers have significantly more US PDS and synovial thickening.
4. Using an extend joint count to include 10MCP joints + 2 wrists shows a closer relationship with histological and US variables in both cohorts, than 10MCP joints alone.
5. The change in DAS28 correlates with the change in US PDS and ST scores for both the 10MCP joint limited US data set and 12 joint MCP + 2 Wrists US data set.

This provides concurrent validity of US assessment of synovitis at both a single joint level and for an extended joint count. The 10MCP joint set does correlate with synovial markers of inflammation but an extend joint count does appear to perform better. This is likely to in part reflect a predominance of wrist joints biopsied as the correlation with US parameters was superior when examined at the single joint level. The moderate correlation in the change in DAS28 and US parameters confirms that both assessments are likely to measure different constructs and that there may be additional benefit to incorporating them into a single score.

Given that US parameters correlate with histological defined synovial inflammation, it is important to examine the relationship with synovial vascularity as PDS is the *de facto* result of synovial blood flow. Previous authors have examined this relationship macroscopically with only one report of histologically confirmed synovial vascular area being correlated with US PDS. I proposed, using the minimally invasive US guided synovial biopsy technique, to explore this relationship in more depth. I harvest tissue from 13 knee joints in patients with early RA. Using US guidance I was able to perform the biopsy procedure in 3 distinct areas within the supra-patella pouch (medial, middle and lateral). The synovial tissue was analysed for synovial vascular area and vessel size. In addition gene expression analysis examined the levels of a number of pro-αngiogenic and lymphangiogenic molecules. In this limited cohort of 13 patients I was able to show:

1. There is a close relationship between synovial vascular area and both US PDS and ST area.
2. US PDS and ST correlate with angiogenic and lymphangiogenic gene expression.

This provides further validity to the use of US to access synovial blood flow and that the presence of PDS on US examination reflects an underlying synovial environment in which neoangiogenesis can occur.

Whilst many aspects of US imaging have previously been validated, a discreet US joint data set is a valuable addition to the Rheumatologist in both clinical practice and the research setting. This thesis provides a supportive body of work which would suggest that a limited US data set of 10MCP joints may have utility in particular patient cohorts. The data set is reliable, responsive and correlates with synovial histological markers of neovascularisation and inflammation. Further work is required to address whether this data set has prognostic significance in terms of patients function and joint damage. Whether it shows the same responsiveness with different pharmacotherapies, including biologics, remains to be seen. Perhaps more importantly is whether such a US joint data set can be incorporated easily into the routine clinical care of patients with RA. Provided the information gleaned from this assessment is robust and meaningful then it is likely that such an investigation will slowly be incorporated in to the routine care of patients with RA. The use of this tool in other inflammatory arthropathies and patients presenting with an undifferentiated arthritis remains to be seen.

Ultrasound manual

MCP, Wrist and knee joint assessment©

US System and Probes

System: GE Logiq 9

Probes: 4D16L / 2D M12L

For the purposes of this study, all patients will be imaged using the GE logiq 9, ultrasound system and the 4D16L / 2D M12L Probes, which will allow both 2D and 3D image collection. Software version 7.05.

Figure 1: GE Logiq 9 - software version 7.05 / 4D16L Probe / 2D M12L Probe

The the 2D M12L Probe will be used to collect 2D images of both the MCP and wrist joints. The 4D16L Probe will be used for collection of 3D images from MCP and wrist joints.

Data Input

Data required for registration of patient details for the study prior to scanning.

- Centre and study name is pre-entered
- **BLT -Mile End** (St Barts and The Royal London - Mile End Hospital) / **Study - xxxxxxx**
- Operator initials - SK (Stephen Kelly) - pre-entered
- Date of Birth - DD/MM/YYYY
- Unique number - This will consist of the date and time of examination as shown e.g. 10th November 2008 at 14:30 (101108-1430)
- Study number

When complete the data can be stored by pressing Register. To commence scanning, press the freeze button

Imaged joints - 2D assessment

2D M12L Probe settings will be pre-set and activated when the M12L Probe is selected in the touch screen menu. Still Grey scale images and cine clip Power Doppler signal images will be recorded for each scanning position and joint.

Labelling

Labeling for 2D images - MCP / Wrist joints/ Supra patella pouch (SPP)/ knee joint line (Jt line)

Med - Medial, Lat- Lateral, Mid - middle

Lateralising	Joint	Digit Number or location	Plane
RT	MCP	1-5	LONG (Longitudinal)
LT	Wrist	Mid	TRAN (Transverse)
	Knee SPP	Med	
	Knee Jt line	Lat	

Example:
RT MCP 2 LONG
RT Knee SPP Mid
LT Wrist Mid

Recording Grey scale still images and PDS cine loops

Grey scale images will be recorded by:

Select the appropriate Pre-Set for either MCP or Wrist

Acquire the desired image using the 2D M12L Probe

Label the image appropriately

Whilst settled on this image Press Freeze

Press P1

Image will be stored to the machine hard drive

PDS cine clip will be recorded by:

Select the appropriate Pre-Set for either MCP or Wrist

Acquire the desired image using the 2D M12L Probe.

Label the image appropriately

Activate the PDS mode by pressing the PDS button. This should provide a region of interest the size of the monitor window.

Whilst settled on this image for 3 seconds, Press P1

The cine loop of 3 seconds will be stored to the machine hard drive

Probe positions - 2D

Metacarpal-phalengeal Joints (MCPJ) - This assessment will be performed in both Longitudinal and Transverse planes from the dorsal aspect of the joint.

MCP joints will be imaged within a molded splint to restrict movement. Longitudinal images will require the extensor tendon to be present and should bisect the joint. Transverse images will require the joint margin to be seen within the middle of the US image.

Figure 2: Longitudinal position for MCP joints

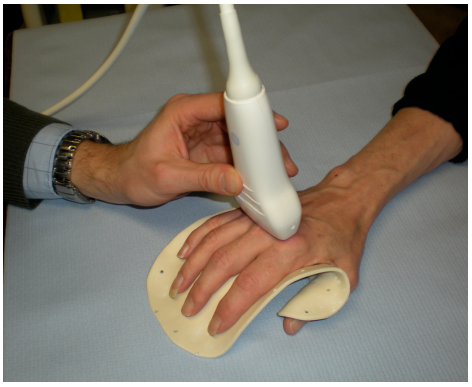

Figure 3: Transverse view for MCP joints

Wrist - The wrist images are acquired in 3 positions. The radial and ulnar aspects of the joint are imaged in a longitudinal plane. A mid position is chosen to include the distal radius, lunate, capitate and metacarpal bone. There are 2 synovial recesses which are often apparent in these positions.

Knee - Positioning of the patient: the patient should be placed on the bed with the knee in 30o of flexion. A pillow may be used to support the patient's knee in this position. Use the coupling gel at 20oC. Imagine supra-patella pouch / medial and lateral joint lines as describe below. A single Grey scale and PDU cine loop will be recorded for each position.

Probe position:

Fig 4: Probe position for imaging the supra-patella pouch in longitudinal section

Medial and lateral joint line

Probe position: the probe should be placed transversely across the joint line a

Probe position:

Fig 5: Transverse probe position for medial joint line

Fig 6: Transverse probe position for lateral joint line

Imaged joints - 3D assessment

A 3-dimensional image will be generated for MCP and wrist joints. A total of 12 images will be acquired at each visit. These will be used to explore the response to change and quantify erosions volumetrically. To reconstruct a 3D vascular signal from the probe sweep the PDS will have to be selected in conjunction with the 3D settings.

Labeling

There is no requirement for directional information in the labeling of these images. The convention below should be followed

Right or Left	Joint	Digit Number if applicable
LT	MCP	1-5
RT	WRIST	

Example: LT MCP 5

Recording a 3D images of MCP and Wrist joints

Recording 3D images - MCP joints

Select the 4D16L Probe on the touch screen menu

Select 3DMCP on the PRESET menu

Select the PDU button

Select 3D/4D button

Label the probe appropriately

Position the probe transversely across the MCP joint as seen in figure 7.

Press the left view button and hold the probe steady.

Once the 10 second probe sweep has finished review the image and press P1 to save.

Recording 3D images - Wrist joints

Select the 4D16L Probe on the touch screen menu

Select 3D wrist on the PRESET menu

Select the PDU button

Select 3D/4D button

Position the probe transversely across the wrist.

Press the left view button and hold the probe steady.

Once the 10 second probe sweep has finished review the image and press P1 to save.

Probe positions - 3D

Metacarpal-phalengeal Joints (MCPJ) - This assessment was performed in a Transverse plane.

MCP joints will be imaged within a molded splint to restrict movement. The Probe will be orientated transversely and the internal sweep passing distal to proximal.

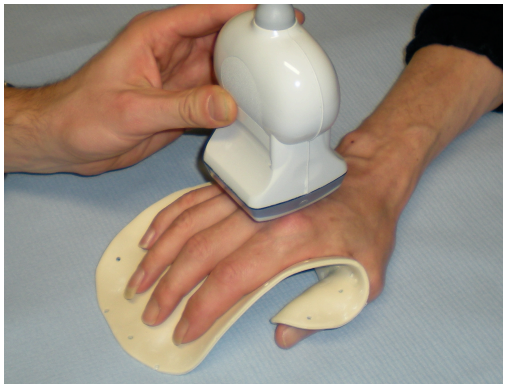

Figure 7. Positioning of probe for 3D imaging (MCP) reconstruction

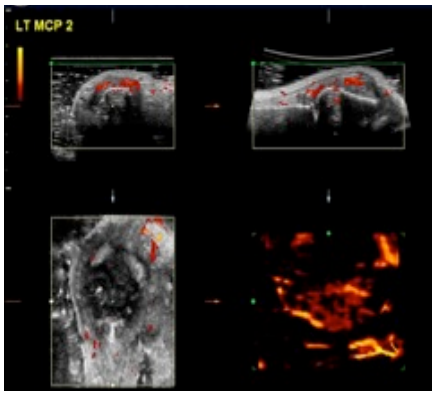

Figure 8. Quad view of 3D image

Wrists - This assessment will be performed in a transverse plane

The Wrist joint will be imaged with the hand in prone position and the elbow leaning on the table for stability. The Probe will be orientated transversely and the internal sweep passing distal to proximal. The mid line starting position should be at the scaphoid lunate junction.

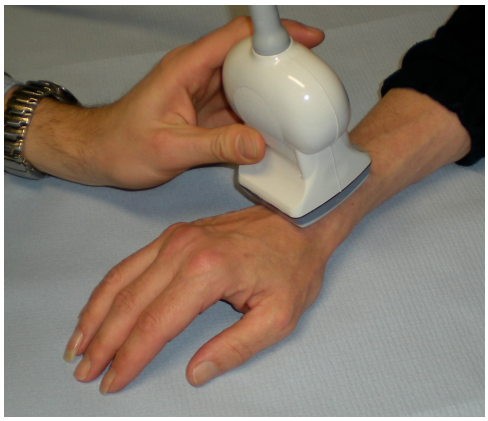

Figure 9. Positioning of probe for 3D imaging (Wrist)

Scoring US images

MCP Synovial Thickness index - STi

Synovial thickness will be scored on a 5 point score (0-4). This assessment will be based upon standard images below for both Longitudinal and Transverse images.

0= normal, 1= minimal, 2= mild , 3= moderate, 4= severe

Longitudinal STi

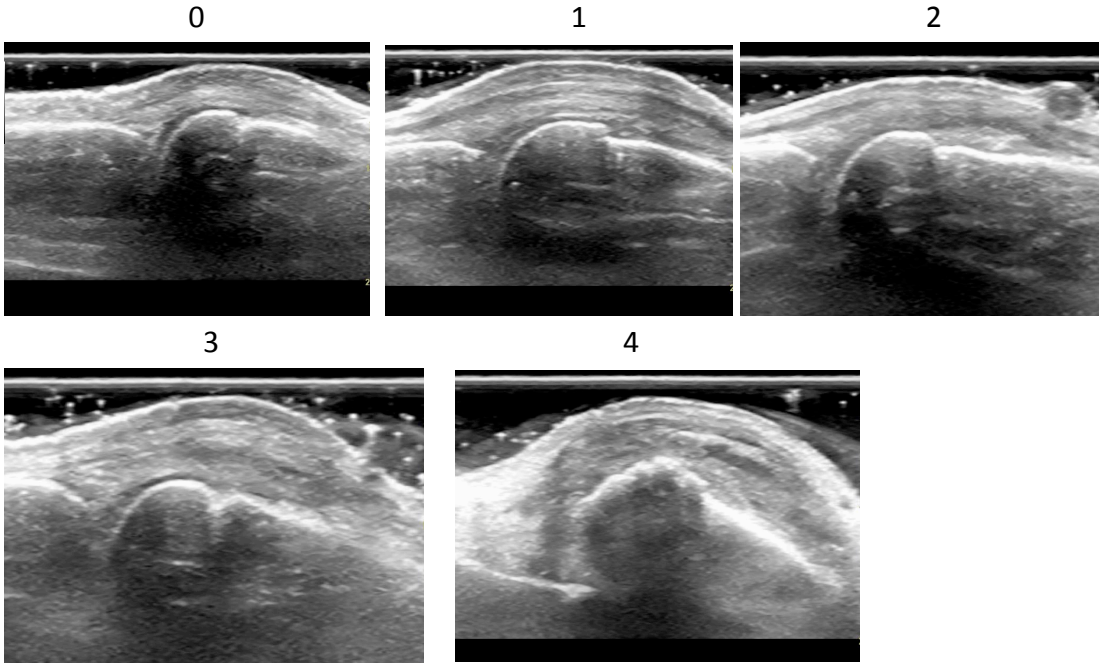

Transverse STi

0

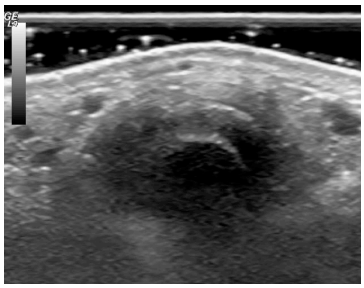

1

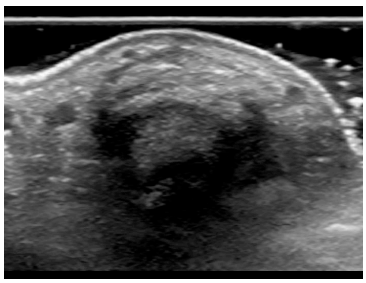

2

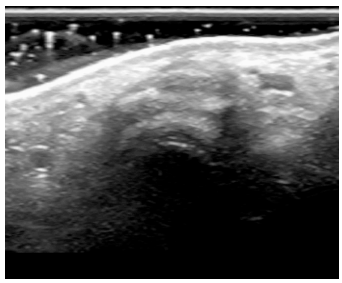

3

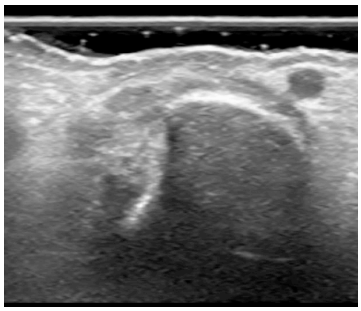

4

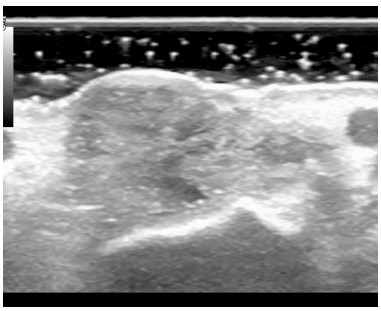

MCP Vascular index - VASCi

Synovial vascularity will be scored on a 5 point score (0-4). This assessment will be based upon standard images below for both Longitudinal and Transverse images.

0= normal, 1= minimal, 2= mild , 3= moderate, 4= severe

Longitudinal VASCi

0

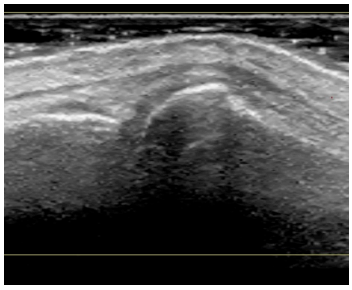

1

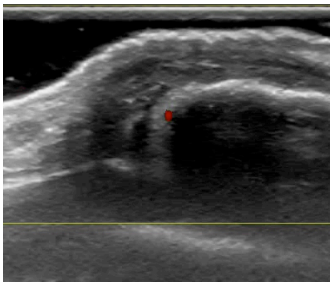

2

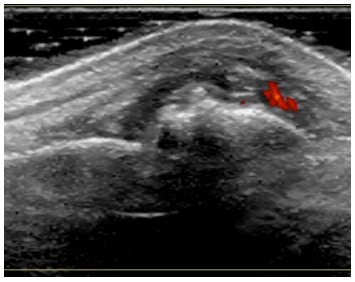

3

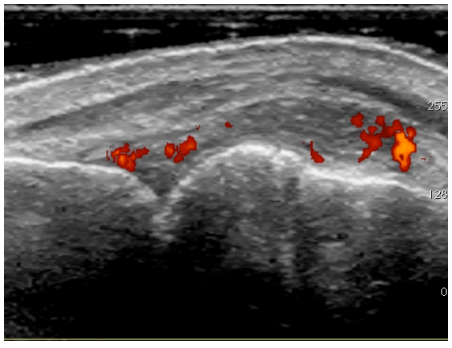

4

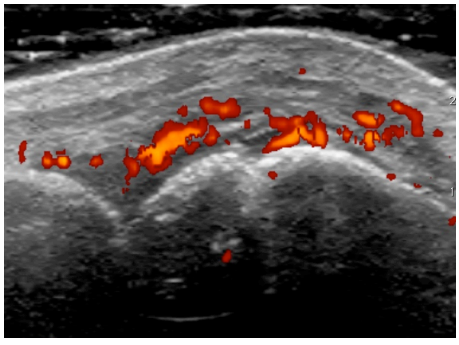

Transverse VASCi

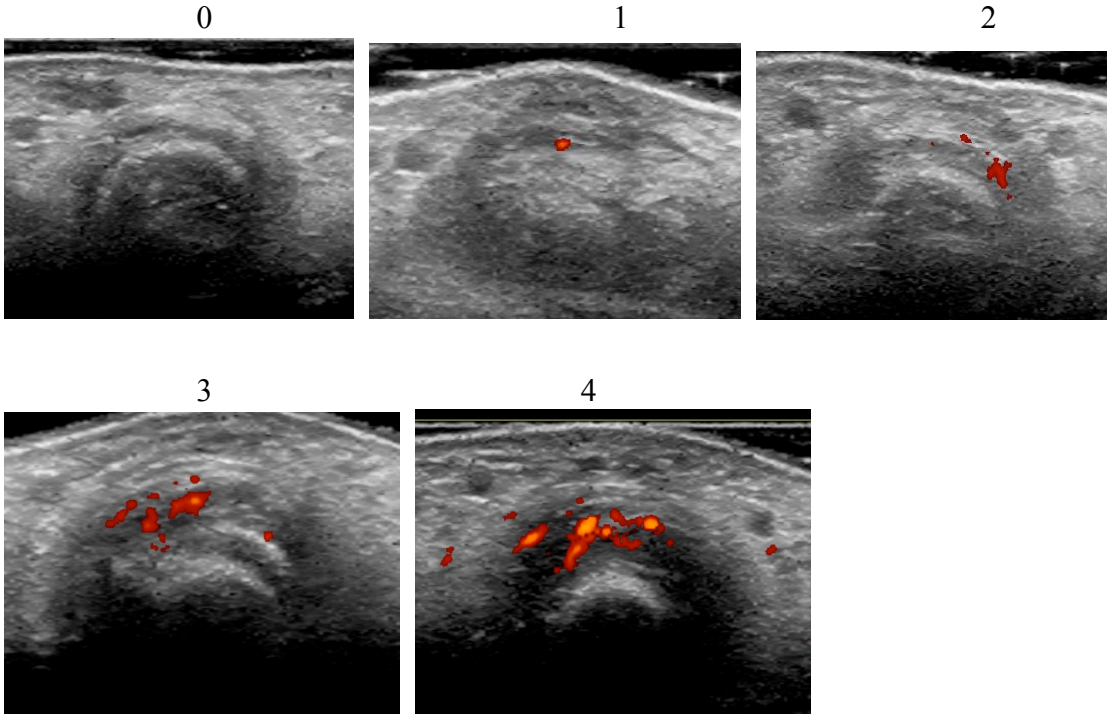

Quantitative assessment of 2D PDS

Each 2D Power Doppler image will be analysed using Image J software[403]. This allows the identification of the maximal signal intensity of the 2D cine clip and by binary thresholding the Doppler signal against the grey scale background its is possible to calculate the pixel number on each slice. This data will be recorded in an excel spreadsheet for analysis.

Out-put measures:

Pixel Number

Synovial Area

Pixel Intensity

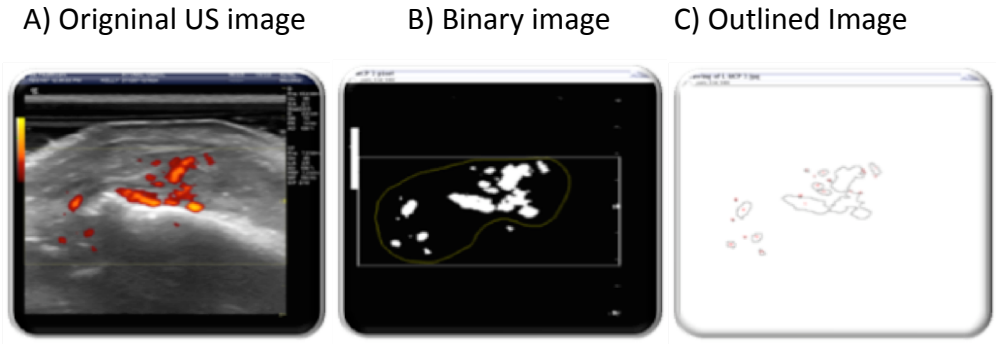

Figure 12 showing the A) original, B) binary and C) outlined images produced from the Image J analysis software

3D MCP VASCi

Three dimensional synovial vascularity will be scored on a 5 point score (0-4). This assessment will be based upon standard images below for both Longitudinal and Transverse images.

0= normal, 1= minimal, 2= mild , 3= moderate, 4= severe

0

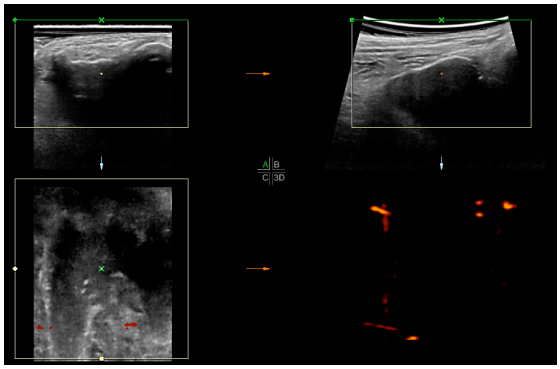

1

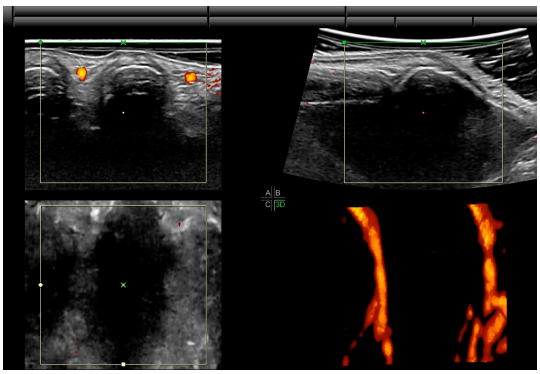

2

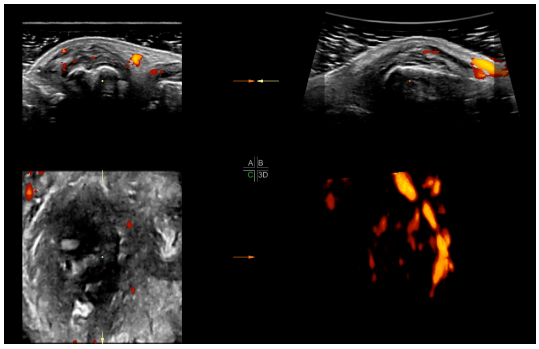

3

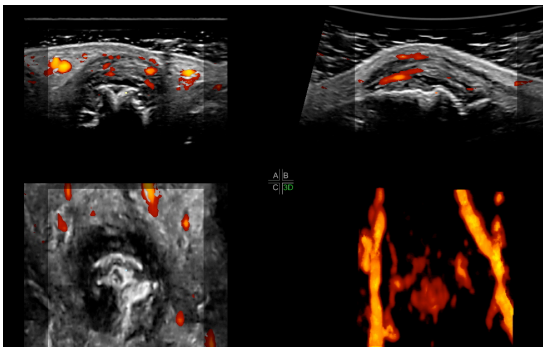

4

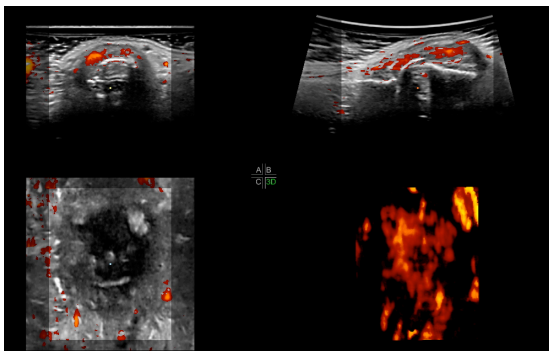

Probe settings

Theses are the settings for both M12L and 16L probes. These are pre- recorded and stored in the Logiq 9. They can be retrieved by selecting the appropriate setting on the touch screen display after selecting the preset icon on the top right of the display.

2D M12L 2D settings (Wrist and MCP)

Gray Scale

Frequency 12MHz
Gain 50
Depth 2.0cm
Frame Rate 24
CrossBeam# - Low
Virtual Convex
SRI HD – 2
Rejection – 0
Edge Enhance – 2
Frame Average – 1
Colorize – Tint Map D
Gray Map – Gray Map D
Rotation – Up
Frequency – 14 MHz
Line Density – 3
Dynamic Range – 66 dB

Power Doppler mode

Frequency 7.5 MHz
Gain 45
PRF 1.4kHz
WF 127Hz
S/P 1/14
L/A 3/5
Acoustic Output 100%
Cross Beam Off
Middle Focus Position
Flash suppression 1

2D probe (M12L) settings: KNEE

Gray scale
Frequency 14MHz
Gain 50
Depth 3.5cm
Frame Rate 24

Power Doppler mode
Frequency 7.5 MHz
Gain 46
PRF 1.4kHz
WF 127Hz
S/P 1/14
L/A 3/5
Acoustic Output 100%
Cross Beam Off
Middle Focus Position
Flash suppression 1

4D16L Probe 3D Settings

Gray Scale

CrossBeam# - Low
Virtual Convex
SRI HD – 2
Rejection – 0
Edge Enhance – 2
Frame Average – 1
Colorize – Tint Map D
Gray Map – Gray Map D
Rotation – Up
Frequency – 15 MHz
Line Density – 4
Dynamic Range – 66 dB
Frequency 15MHz
Gain 50
Depth 2.0cm
Frame Rate 26

Power Doppler Mode

Frequency 7.5 MHz
Gain 45
PRF 0.9 kHz
WF= 110Hz
S/P 1/14
L/A 2/5
Acoustic Output 100%
Cross Beam On
Power DI Off
Frame average= 5
Flash suppression = 2
Quality Hi 2
Volume Angle 19

Bibliography

1. Silman AJ. Epidemiology of rheumatoid arthritis. *Apmis* 1994;102(10):721-8.
2. Scott DL, Symmons DP, Coulton BL, Popert AJ. Long-term outcome of treating rheumatoid arthritis: results after 20 years. *Lancet* 1987;1(8542): 1108-11.
3. Alessandri C, Priori R, Modesti M, Mancini R, Valesini G. The role of anti-cyclic cytrullinate antibodies testing in rheumatoid arthritis. *Clin Rev Allergy Immunol* 2008;34(1):45-9.
4. Vane JR. The fight against rheumatism: from willow bark to COX-1 sparing drugs. *J Physiol Pharmacol* 2000;51(4 Pt 1):573-86.
5. Pasero G. The treatment of rheumatoid arthritis in this century: from spas to monoclonal antibodies. *Clinical and experimental rheumatology* 1997;15 Suppl 17:S67-70.
6. Boers M. The COBRA trial 20 years later. *Clin Exp Rheumatol* 2011;29(5 Suppl 68):S46-51.
7. Mottonen TT, Hannonen PJ, Boers M. Combination DMARD therapy including corticosteroids in early rheumatoid arthritis. *Clinical and experimental rheumatology* 1999;17(6 Suppl 18):S59-65.
8. Bakker MF, Jacobs JW, Verstappen SM, Bijlsma JW. Tight control in the treatment of rheumatoid arthritis: efficacy and feasibility. *Annals of the rheumatic diseases* 2007;66 Suppl 3:iii56-60.
9. Goekoop-Ruiterman YP, de Vries-Bouwstra JK, Allaart CF, van Zeben D, Kerstens PJ, Hazes JM, et al. Clinical and radiographic outcomes of four different treatment strategies in patients with early rheumatoid arthritis (the BeSt study): A randomized, controlled trial. *Arthritis Rheum* 2008;58(2 Suppl):S126-35.
10. Mottonen T, Hannonen P, Leirisalo-Repo M, Nissila M, Kautiainen H, Korpela M, et al. Comparison of combination therapy with single-drug therapy in early rheumatoid arthritis: a randomised trial. FIN-RACo trial group. *Lancet* 1999;353(9164):1568-73.
11. Verstappen SM, Jacobs JW, van der Veen MJ, Heurkens AH, Schenk Y, ter Borg EJ, et al. Intensive treatment with methotrexate in early rheumatoid arthritis: aiming for remission. Computer Assisted Management in Early Rheumatoid Arthritis (CAMERA, an open-label strategy trial). *Annals of the rheumatic diseases* 2007;66(11):1443-9.
12. Caporali R, Pallavicini FB, Filippini M, Gorla R, Marchesoni A, Favalli EG, et al. Treatment of rheumatoid arthritis with anti-TNF-alpha agents: A reappraisal. *Autoimmun Rev* 2008.
13. Makinen H, Kautiainen H, Hannonen P, Mottonen T, Leirisalo-Repo M, Laasonen L, et al. Sustained remission and reduced radiographic progression with combination disease modifying antirheumatic drugs in early rheumatoid arthritis. *The Journal of rheumatology* 2007;34(2):316-21.
14. Allaart CF, Goekoop-Ruiterman YP, de Vries-Bouwstra JK, Breedveld FC, Dijkmans BA. Aiming at low disease activity in rheumatoid arthritis with initial combination therapy or initial monotherapy strategies: the BeSt study. *Clinical and experimental rheumatology* 2006;24(6 Suppl 43):S-77-82.
15. Korpela M, Laasonen L, Hannonen P, Kautiainen H, Leirisalo-Repo M, Hakala M, et al. Retardation of joint damage in patients with early rheumatoid arthritis by initial aggressive treatment with disease-modifying antirheumatic drugs: five-year experience from the FIN-RACo study. *Arthritis and rheumatism* 2004;50(7):2072-81.
16. Borg G, Allander E, Berg E, Brodin U, From A, Trang L. Auranofin treatment in early rheumatoid arthritis may postpone early retirement. Results from a 2-year double blind trial. *The Journal of rheumatology* 1991;18(7):1015-20.

17. March L, Lapsley H. What are the costs to society and the potential benefits from the effective management of early rheumatoid arthritis? *Best practice & research* 2001;15(1):171-85.
18. Young A, Dixey J, Cox N, Davies P, Devlin J, Emery P, et al. How does functional disability in early rheumatoid arthritis (RA) affect patients and their lives? Results of 5 years of follow-up in 732 patients from the Early RA Study (ERAS). *Rheumatology (Oxford, England)* 2000;39(6):603-11.
19. Visser H, le Cessie S, Vos K, Breedveld FC, Hazes JM. How to diagnose rheumatoid arthritis early: a prediction model for persistent (erosive) arthritis. *Arthritis and rheumatism* 2002;46(2):357-65.
20. Schumacher HR, Pessler F, Chen LX. Diagnosing early rheumatoid arthritis (RA). What are the problems and opportunities? *Clinical and experimental rheumatology* 2003;21(5 Suppl 31):S15-9.
21. Visser K, Goekoop-Ruiterman YP, de Vries-Bouwstra JK, Ronday HK, Seys PE, Kerstens PJ, et al. A matrix risk model for the prediction of rapid radiographic progression in patients with rheumatoid arthritis receiving different dynamic treatment strategies: post hoc analyses from the BeSt study. *Annals of the rheumatic diseases* 2010;69(7):1333-7.
22. Tunn EJ, Bacon PA. Differentiating persistent from self-limiting symmetrical synovitis in an early arthritis clinic. *British journal of rheumatology* 1993;32(2): 97-103.
23. Wolfe F, Ross K, Hawley DJ, Roberts FK, Cathey MA. The prognosis of rheumatoid arthritis and undifferentiated polyarthritis syndrome in the clinic: a study of 1141 patients. *The Journal of rheumatology* 1993;20(12):2005-9.
24. Symmons D, Harrison B. Early inflammatory polyarthritis: results from the norfolk arthritis register with a review of the literature. I. Risk factors for the development of inflammatory polyarthritis and rheumatoid arthritis. *Rheumatology (Oxford, England)* 2000;39(8):835-43.
25. El Miedany Y, Youssef S, Mehanna AN, El Gaafary M. Development of a scoring system for assessment of outcome of early undifferentiated inflammatory synovitis. *Joint Bone Spine* 2008;75(2):155-62.
26. Raza K, Buckley CE, Salmon M, Buckley CD. Treating very early rheumatoid arthritis. *Best practice & research* 2006;20(5):849-63.
27. Bunn DK, Shepstone L, Galpin LM, Wiles NJ, Symmons DP. The NOAR Damaged Joint Count (NOAR-DJC): a clinical measure for assessing articular damage in patients with early inflammatory polyarthritis including rheumatoid arthritis. *Rheumatology (Oxford, England)* 2004;43(12):1519-25.
28. van der Helm-Vanmil AH, le Cessie S, van Dongen H, Breedveld FC, Toes RE, Huizinga TW. A prediction rule for disease outcome in patients with recent-onset undifferentiated arthritis: how to guide individual treatment decisions. *Arthritis and rheumatism* 2007;56(2):433-40.
29. Panchagnula R, Rajiv SR, Prakash J, Chandrashekara S, Suresh KP. Role of anticyclic citrullinated peptide in the diagnosis of early rheumatoid factor-negative suspected rheumatoid arthritis: is it worthwhile to order the test? *J Clin Rheumatol* 2006;12(4):172-5.
30. Matsui T, Shimada K, Ozawa N, Hayakawa H, Hagiwara F, Nakayama H, et al. Diagnostic utility of anti-cyclic citrullinated peptide antibodies for very early rheumatoid arthritis. *The Journal of rheumatology* 2006;33(12):2390-7.
31. Schellekens GA, Visser H, de Jong BA, van den Hoogen FH, Hazes JM, Breedveld FC, et al. The diagnostic properties of rheumatoid arthritis antibodies recognizing a cyclic citrullinated peptide. *Arthritis and rheumatism* 2000;43(1):155-63.
32. Agrawal S, Misra R, Aggarwal A. Autoantibodies in rheumatoid arthritis: association with severity of disease in established RA. *Clinical rheumatology* 2007;26(2):201-4.

33. Machold KP, Stamm TA, Eberl GJ, Nell VK, Dunky A, Uffmann M, et al. Very recent onset arthritis--clinical, laboratory, and radiological findings during the first year of disease. *The Journal of rheumatology* 2002;29(11):2278-87.
34. Mewar D, Coote A, Moore DJ, Marinou I, Keyworth J, Dickson MC, et al. Independent associations of anti-cyclic citrullinated peptide antibodies and rheumatoid factor with radiographic severity of rheumatoid arthritis. *Arthritis Res Ther* 2006;8(4):R128.
35. Ates A, Karaaslan Y, Aksaray S. Predictive value of antibodies to cyclic citrullinated peptide in patients with early arthritis. *Clinical rheumatology* 2007;26(4):499-504.
36. Jansen LM, van Schaardenburg D, van der Horst-Bruinsma I, van der Stadt RJ, de Koning MH, Dijkmans BA. The predictive value of anti-cyclic citrullinated peptide antibodies in early arthritis. *The Journal of rheumatology* 2003;30(8):1691-5.
37. Raza K, Breese M, Nightingale P, Kumar K, Potter T, Carruthers DM, et al. Predictive value of antibodies to cyclic citrullinated peptide in patients with very early inflammatory arthritis. *The Journal of rheumatology* 2005;32(2): 231-8.
38. Harle P, Bongartz T, Scholmerich J, Muller-Ladner U, Straub RH. Predictive and potentially predictive factors in early arthritis: a multidisciplinary approach. *Rheumatology (Oxford, England)* 2005;44(4):426-33.
39. Filer A, de Pablo P, Allen G, Nightingale P, Jordan A, Jobanputra P, et al. Utility of ultrasound joint counts in the prediction of rheumatoid arthritis in patients with very early synovitis. *Annals of the rheumatic diseases* 2011;70(3):500-7.
40. van der Heijde DM, van Riel PL, van Leeuwen MA, van 't Hof MA, van Rijswijk MH, van de Putte LB. Prognostic factors for radiographic damage and physical disability in early rheumatoid arthritis. A prospective follow-up study of 147 patients. *British journal of rheumatology* 1992;31(8):519-25.
41. van der Heijde DM, van Riel PL, van Rijswijk MH, van de Putte LB. Influence of prognostic features on the final outcome in rheumatoid arthritis: a review of the literature. *Seminars in arthritis and rheumatism* 1988;17(4):284-92.
42. Ransohoff DF, Feinstein AR. Problems of spectrum and bias in evaluating the efficacy of diagnostic tests. *The New England journal of medicine* 1978;299(17):926-30.
43. van der Heijde DM, van 't Hof M, van Riel PL, van de Putte LB. Development of a disease activity score based on judgment in clinical practice by rheumatologists. *The Journal of rheumatology* 1993;20(3):579-81.
44. van der Heijde DM, van 't Hof M, van Riel PL, van de Putte LB. Validity of single variables and indices to measure disease activity in rheumatoid arthritis. *The Journal of rheumatology* 1993;20(3):538-41.
45. van Gestel AM, Prevoo ML, van 't Hof MA, van Rijswijk MH, van de Putte LB, van Riel PL. Development and validation of the European League Against Rheumatism response criteria for rheumatoid arthritis. Comparison with the preliminary American College of Rheumatology and the World Health Organization/International League Against Rheumatism Criteria. *Arthritis and rheumatism* 1996;39(1):34-40.
46. Prevoo ML, van 't Hof MA, Kuper HH, van Leeuwen MA, van de Putte LB, van Riel PL. Modified disease activity scores that include twenty-eight-joint counts. Development and validation in a prospective longitudinal study of patients with rheumatoid arthritis. *Arthritis and rheumatism* 1995;38(1):44-8.
47. Kuper HH, van Leeuwen MA, van Riel PL, Prevoo ML, Houtman PM, Lolkema WF, et al. Radiographic damage in large joints in early rheumatoid arthritis: relationship with radiographic damage in hands and feet, disease activity, and physical disability. *Br J Rheumatol* 1997;36(8):855-60.
48. Fransen J, van Riel PL. The Disease Activity Score and the EULAR response criteria. *Clinical and experimental rheumatology* 2005;23(5 Suppl 39):S93-9.

49. Fransen J, van Riel PL. DAS remission cut points. *Clinical and experimental rheumatology* 2006;24(6 Suppl 43):S-29-32.
50. Fransen J, van Riel PL. Outcome measures in inflammatory rheumatic diseases. *Arthritis research & therapy* 2009;11(5):244.
51. Fries JF, Spitz P, Kraines RG, Holman HR. Measurement of patient outcome in arthritis. *Arthritis and rheumatism* 1980;23(2):137-45.
52. Linde L, Sorensen J, Ostergaard M, Horslev-Petersen K, Hetland ML. Health-related quality of life: validity, reliability, and responsiveness of SF-36, 15D, EQ-5D [corrected] RAQoL, and HAQ in patients with rheumatoid arthritis. *The Journal of rheumatology* 2008;35(8):1528-37.
53. Esteve-Vives J, Batlle-Gualda E, Reig A. Spanish version of the Health Assessment Questionnaire: reliability, validity and transcultural equivalency. Grupo para la Adaptacion del HAQ a la Poblacion Espanola. *The Journal of rheumatology* 1993;20(12):2116-22.
54. Hewlett S, Smith AP, Kirwan JR. Measuring the meaning of disability in rheumatoid arthritis: the Personal Impact Health Assessment Questionnaire (PI HAQ). *Annals of the rheumatic diseases* 2002;61(11):986-93.
55. Thorsen H, Hansen TM, McKenna SP, Sorensen SF, Whalley D. Adaptation into Danish of the Stanford Health Assessment Questionnaire (HAQ) and the Rheumatoid Arthritis Quality of Life Scale (RAQoL). *Scand J Rheumatol* 2001;30(2):103-9.
56. van der Heijde DM, van Riel PL, van de Putte LB. Sensitivity of a Dutch Health Assessment Questionnaire in a trial comparing hydroxychloroquine vs. sulphasalazine. *Scand J Rheumatol* 1990;19(6):407-12.
57. Taccari E, Spadaro A, Rinaldi T, Riccieri V, Sensi F. Comparison of the Health Assessment Questionnaire and Arthritis Impact Measurement Scale in patients with psoriatic arthritis. *Rev Rhum Engl Ed* 1998;65(12):751-8.
58. Archenholtz B, Bjelle A. Reliability, validity, and sensitivity of a Swedish version of the revised and expanded Arthritis Impact Measurement Scales (AIMS2). *The Journal of rheumatology* 1997;24(7):1370-7.
59. Soderlin MK, Hakala M, Nieminen P. Anxiety and depression in a community-based rheumatoid arthritis population. *Scand J Rheumatol* 2000;29(3):177-83.
60. Peck JR, Smith TW, Ward JR, Milano R. Disability and depression in rheumatoid arthritis. A multi-trait, multi-method investigation. *Arthritis and rheumatism* 1989;32(9):1100-6.
61. Houssien DA, McKenna SP, Scott DL. The Nottingham Health Profile as a measure of disease activity and outcome in rheumatoid arthritis. *British journal of rheumatology* 1997;36(1):69-73.
62. Wolfe F, Kong SX. Rasch analysis of the Western Ontario MacMaster questionnaire (WOMAC) in 2205 patients with osteoarthritis, rheumatoid arthritis, and fibromyalgia. *Annals of the rheumatic diseases* 1999;58(9): 563-8.
63. Hakkinen A, Kautiainen H, Hannonen P, Ylinen J, Arkela-Kautiainen M, Sokka T. Pain and joint mobility explain individual subdimensions of the health assessment questionnaire (HAQ) disability index in patients with rheumatoid arthritis. *Annals of the rheumatic diseases* 2005;64(1):59-63.
64. Sokka T, Kankainen A, Hannonen P. Scores for functional disability in patients with rheumatoid arthritis are correlated at higher levels with pain scores than with radiographic scores. *Arthritis Rheum* 2000;43(2):386-9.
65. Barrett EM, Scott DG, Wiles NJ, Symmons DP. The impact of rheumatoid arthritis on employment status in the early years of disease: a UK community-based study. *Rheumatology (Oxford, England)* 2000;39(12):1403-9.
66. Fex E, Larsson BM, Nived K, Eberhardt K. Effect of rheumatoid arthritis on work status and social and leisure time activities in patients followed 8 years from onset. *The Journal of rheumatology* 1998;25(1):44-50.

67. Gillen M, Jewell SA, Faucett JA, Yelin E. Functional limitations and well-being in injured municipal workers: a longitudinal study. *J Occup Rehabil* 2004;14(2):89-105.
68. Rodgers M ED, Bojke L, et al. Southampton (UK): NIHR Evaluation, Trials and Studies Coordinating Centre (UK); http://www.hta.ac.uk/research/HTAjournal. 2011.
69. Larsen A, Dale K, Eek M. Radiographic evaluation of rheumatoid arthritis and related conditions by standard reference films. *Acta Radiol Diagn (Stockh)* 1977;18(4):481-91.
70. Sharp JT, Lidsky MD, Collins LC, Moreland J. Methods of scoring the progression of radiologic changes in rheumatoid arthritis. Correlation of radiologic, clinical and laboratory abnormalities. *Arthritis and rheumatism* 1971;14(6):706-20.
71. van der Heijde D. How to read radiographs according to the Sharp/van der Heijde method. *J Rheumatol* 1999;26(3):743-5.
72. Landewe R, van der Heijde D. Radiographic progression in rheumatoid arthritis. *Clinical and experimental rheumatology* 2005;23(5 Suppl 39):S63-8.
73. Bruynesteyn K, Boers M, Kostense P, van der Linden S, van der Heijde D. Deciding on progression of joint damage in paired films of individual patients: smallest detectable difference or change. *Annals of the rheumatic diseases* 2005;64(2):179-82.
74. Eder L, Chandran V, Gladman DD. Repair of Radiographic Joint Damage Following Treatment with Etanercept in Psoriatic Arthritis Is Demonstrable by 3 Radiographic Methods. *The Journal of rheumatology* 2011.
75. van der Heijde D, Landewe R. Imaging: do erosions heal? *Annals of the rheumatic diseases* 2003;62 Suppl 2:ii10-2.
76. van Leeuwen MA, van der Heijde DM, van Rijswijk MH, Houtman PM, van Riel PL, van de Putte LB, et al. Interrelationship of outcome measures and process variables in early rheumatoid arthritis. A comparison of radiologic damage, physical disability, joint counts, and acute phase reactants. *The Journal of rheumatology* 1994;21(3):425-9.
77. van Leeuwen MA, van Rijswijk MH, Sluiter WJ, van Riel PL, Kuper IH, van de Putte LB, et al. Individual relationship between progression of radiological damage and the acute phase response in early rheumatoid arthritis. Towards development of a decision support system. *The Journal of rheumatology* 1997;24(1):20-7.
78. Welsing PM, Landewe RB, van Riel PL, Boers M, van Gestel AM, van der Linden S, et al. The relationship between disease activity and radiologic progression in patients with rheumatoid arthritis: a longitudinal analysis. *Arthritis and rheumatism* 2004;50(7):2082-93.
79. Welsing PM, van Gestel AM, Swinkels HL, Kiemeney LA, van Riel PL. The relationship between disease activity, joint destruction, and functional capacity over the course of rheumatoid arthritis. *Arthritis and rheumatism* 2001;44(9):2009-17.
80. Drossaers-Bakker KW, Zwinderman AH, Vliet Vlieland TP, Van Zeben D, Vos K, Breedveld FC, et al. Long-term outcome in rheumatoid arthritis: a simple algorithm of baseline parameters can predict radiographic damage, disability, and disease course at 12-year followup. *Arthritis and rheumatism* 2002;47(4):383-90.
81. Drossaers-Bakker KW, Kroon HM, Zwinderman AH, Breedveld FC, Hazes JM. Radiographic damage of large joints in long-term rheumatoid arthritis and its relation to function. *Rheumatology (Oxford, England)* 2000;39(9):998-1003.
82. Backhaus M, Kamradt T, Sandrock D, Loreck D, Fritz J, Wolf KJ, et al. Arthritis of the finger joints: a comprehensive approach comparing conventional radiography, scintigraphy, ultrasound, and contrast-enhanced magnetic resonance imaging. *Arthritis and rheumatism* 1999;42(6):1232-45.

83. Benton N, Stewart N, Crabbe J, Robinson E, Yeoman S, McQueen FM. MRI of the wrist in early rheumatoid arthritis can be used to predict functional outcome at 6 years. *Annals of the rheumatic diseases* 2004;63(5):555-61.
84. Eshed I, Althoff CE, Schink T, Scheel AK, Schirmer C, Backhaus M, et al. Low-field MRI for assessing synovitis in patients with rheumatoid arthritis. Impact of Gd-DTPA dose on synovitis scoring. *Scand J Rheumatol* 2006;35(4):277-82.
85. Ostendorf B, Peters R, Dann P, Becker A, Scherer A, Wedekind F, et al. Magnetic resonance imaging and miniarthroscopy of metacarpophalangeal joints: sensitive detection of morphologic changes in rheumatoid arthritis. *Arthritis Rheum* 2001;44(11):2492-502.
86. Ostergaard M, Stoltenberg M, Lovgreen-Nielsen P, Volck B, Jensen CH, Lorenzen I. Magnetic resonance imaging-determined synovial membrane and joint effusion volumes in rheumatoid arthritis and osteoarthritis: comparison with the macroscopic and microscopic appearance of the synovium. *Arthritis and rheumatism* 1997;40(10):1856-67.
87. Brown AK, Conaghan PG, Karim Z, Quinn MA, Ikeda K, Peterfy CG, et al. An explanation for the apparent dissociation between clinical remission and continued structural deterioration in rheumatoid arthritis. *Arthritis and rheumatism* 2008;58(10):2958-67.
88. Boyesen P, Haavardsholm EA, Ostergaard M, van der Heijde D, Sesseng S, Kvien TK. MRI in early rheumatoid arthritis: synovitis and bone marrow oedema are independent predictors of subsequent radiographic progression. *Annals of the rheumatic diseases* 2011;70(3):428-33.
89. Hodgson R, Grainger A, O'Connor P, Barnes T, Connolly S, Moots R. Dynamic contrast enhanced MRI of bone marrow oedema in rheumatoid arthritis. *Annals of the rheumatic diseases* 2008;67(2):270-2.
90. Durez P, Malghem J, Nzeusseu Toukap A, Depresseux G, Lauwerys BR, Westhovens R, et al. Treatment of early rheumatoid arthritis: a randomized magnetic resonance imaging study comparing the effects of methotrexate alone, methotrexate in combination with infliximab, and methotrexate in combination with intravenous pulse methylprednisolone. *Arthritis and rheumatism* 2007;56(12):3919-27.
91. Dohn UM, Ejbjerg BJ, Hasselquist M, Narvestad E, Moller J, Thomsen HS, et al. Detection of bone erosions in rheumatoid arthritis wrist joints with magnetic resonance imaging, computed tomography and radiography. *Arthritis research & therapy* 2008;10(1):R25.
92. Dohn UM, Ejbjerg BJ, Hasselquist M, Narvestad E, Court-Payen M, Szkudlarek M, et al. Rheumatoid arthritis bone erosion volumes on CT and MRI: reliability and correlations with erosion scores on CT, MRI and radiography. *Ann Rheum Dis* 2007;66(10):1388-92.
93. Dohn UM, Ejbjerg B, Boonen A, Hetland ML, Hansen MS, Knudsen LS, et al. No overall progression and occasional repair of erosions despite persistent inflammation in adalimumab-treated rheumatoid arthritis patients: results from a longitudinal comparative MRI, ultrasonography, CT and radiography study. *Annals of the rheumatic diseases* 2011;70(2):252-8.
94. Duer-Jensen A, Vestergaard A, Dohn UM, Ejbjerg B, Hetland ML, Albrecht-Beste E, et al. Detection of rheumatoid arthritis bone erosions by two different dedicated extremity MRI units and conventional radiography. *Annals of the rheumatic diseases* 2008;67(7):998-1003.
95. Bird P, Conaghan P, Ejbjerg B, McQueen F, Lassere M, Peterfy C, et al. The development of the EULAR-OMERACT rheumatoid arthritis MRI reference image atlas. *Annals of the rheumatic diseases* 2005;64 Suppl 1:i8-10.
96. Conaghan P, Bird P, Ejbjerg B, O'Connor P, Peterfy C, McQueen F, et al. The EULAR-OMERACT rheumatoid arthritis MRI reference image atlas: the metacarpophalangeal joints. *Annals of the rheumatic diseases* 2005;64 Suppl 1:i11-21.

97. Haavardsholm EA, Ostergaard M, Ejbjerg BJ, Kvan NP, Uhlig TA, Lilleas FG, et al. Reliability and sensitivity to change of the OMERACT rheumatoid arthritis magnetic resonance imaging score in a multireader, longitudinal setting. *Arthritis and rheumatism* 2005;52(12):3860-7.
98. Ostergaard M, Emery P, Conaghan PG, Fleischmann R, Hsia EC, Xu W, et al. Significant improvement in synovitis, osteitis, and bone erosion following golimumab and methotrexate combination therapy as compared with methotrexate alone: a magnetic resonance imaging study of 318 methotrexate-naive rheumatoid arthritis patients. *Arthritis and rheumatism* 2011;63(12):3712-22.
99. Hetland ML, Stengaard-Pedersen K, Junker P, Ostergaard M, Ejbjerg BJ, Jacobsen S, et al. Radiographic progression and remission rates in early rheumatoid arthritis - MRI bone oedema and anti-CCP predicted radiographic progression in the 5-year extension of the double-blind randomised CIMESTRA trial. *Annals of the rheumatic diseases* 2010;69(10):1789-95.
100. Quinn MA, Conaghan PG, O'Connor PJ, Karim Z, Greenstein A, Brown A, et al. Very early treatment with infliximab in addition to methotrexate in early, poor-prognosis rheumatoid arthritis reduces magnetic resonance imaging evidence of synovitis and damage, with sustained benefit after infliximab withdrawal: results from a twelve-month randomized, double-blind, placebo-controlled trial. *Arthritis and rheumatism* 2005;52(1):27-35.
101. Zikou AK, Argyropoulou MI, Voulgari PV, Xydis VG, Nikas SN, Efremidis SC, et al. Magnetic resonance imaging quantification of hand synovitis in patients with rheumatoid arthritis treated with adalimumab. *The Journal of rheumatology* 2006;33(2):219-23.
102. Freeston JE, Bird P, Conaghan PG. The role of MRI in rheumatoid arthritis: research and clinical issues. *Current opinion in rheumatology* 2009;21(2): 95-101.
103. Lee DN, Georgopoulos AP, Clark MJ, Craig CM, Port NL. Guiding contact by coupling the taus of gaps. *Experimental brain research. Experimentelle Hirnforschung* 2001;139(2):151-9.
104. Ashmead DW, R.; Eaton, S.; Ebinger, K.; Snook, H.; Mary, M., et al. Echolocation reconsidered: Using spatial variations in the ambient sound field to guide locomotion. *Journal of Visual Impairment & Blindness* 1998;92(9): 615.
105. Hughes B. Active artificial echolocation and the nonvisual perception of aperture passability. *Human movement science* 2001;20(4-5):371-400.
106. Ainslie MA. Principles of Sonar Performance Modelling. *Springer* 2010:Page 10.
107. Grassi W, Filippucci E. Ultrasonography and the rheumatologist. *Current opinion in rheumatology* 2007;19(1):55-60.
108. Schmidt WA. Technology Insight: the role of color and power Doppler ultrasonography in rheumatology. *Nat Clin Pract Rheumatol* 2007;3(1):35-42; quiz 59.
109. Quaia E. Microbubble ultrasound contrast agents: an update. *Eur Radiol* 2007;17(8):1995-2008.
110. Rees JD, Pilcher J, Heron C, Kiely PD. A comparison of clinical vs ultrasound determined synovitis in rheumatoid arthritis utilizing gray-scale, power Doppler and the intravenous microbubble contrast agent 'Sono-Vue'. *Rheumatology (Oxford, England)* 2007;46(3):454-9.
111. Szkudlarek M, Court-Payen M, Strandberg C, Klarlund M, Klausen T, Ostergaard M. Power Doppler ultrasonography for assessment of synovitis in the metacarpophalangeal joints of patients with rheumatoid arthritis: a comparison with dynamic magnetic resonance imaging. *Arthritis and rheumatism* 2001;44(9):2018-23.
112. Naredo E, Bonilla G, Gamero F, Uson J, Carmona L, Laffon A. Assessment of inflammatory activity in rheumatoid arthritis: a comparative study of clinical

evaluation with grey scale and power Doppler ultrasonography. *Annals of the rheumatic diseases* 2005;64(3):375-81.
113. Kiris A, Ozgocmen S, Kocakoc E, Ardicoglu O. Power Doppler assessment of overall disease activity in patients with rheumatoid arthritis. *J Clin Ultrasound* 2005;34(1):5-11.
114. Naredo E, Collado P, Cruz A, Palop MJ, Cabero F, Richi P, et al. Longitudinal power Doppler ultrasonographic assessment of joint inflammatory activity in early rheumatoid arthritis: predictive value in disease activity and radiologic progression. *Arthritis and rheumatism* 2007;57(1): 116-24.
115. Szkudlarek M, Court-Payen M, Jacobsen S, Klarlund M, Thomsen HS, Ostergaard M. Interobserver agreement in ultrasonography of the finger and toe joints in rheumatoid arthritis. *Arthritis and rheumatism* 2003;48(4):955-62.
116. Wakefield RJ, Brown AK, O'Connor PJ, Emery P. Power Doppler sonography: improving disease activity assessment in inflammatory musculoskeletal disease. *Arthritis and rheumatism* 2003;48(2):285-8.
117. Wakefield RJ, D'Agostino MA, Iagnocco A, Filippucci E, Backhaus M, Scheel AK, et al. The OMERACT Ultrasound Group: status of current activities and research directions. *The Journal of rheumatology* 2007;34(4):848-51.
118. Hammer HB, Bolton-King P, Bakkeheim V, Berg TH, Sundt E, Kongtorp AK, et al. Examination of intra and interrater reliability with a new ultrasonographic reference atlas for scoring of synovitis in patients with rheumatoid arthritis. *Annals of the rheumatic diseases* 2011;70(11):1995-8.
119. Ejbjerg BJ, Vestergaard A, Jacobsen S, Thomsen HS, Ostergaard M. The smallest detectable difference and sensitivity to change of magnetic resonance imaging and radiographic scoring of structural joint damage in rheumatoid arthritis finger, wrist, and toe joints: a comparison of the OMERACT rheumatoid arthritis magnetic resonance imaging score applied to different joint combinations and the Sharp/van der Heijde radiographic score. *Arthritis and rheumatism* 2005;52(8):2300-6.
120. Filippucci E, Iagnocco A, Salaffi F, Cerioni A, Valesini G, Grassi W. Power Doppler sonography monitoring of synovial perfusion at the wrist joints in patients with rheumatoid arthritis treated with adalimumab. *Annals of the rheumatic diseases* 2006;65(11):1433-7.
121. Brown AK, Quinn MA, Karim Z, Conaghan PG, Peterfy CG, Hensor E, et al. Presence of significant synovitis in rheumatoid arthritis patients with disease-modifying antirheumatic drug-induced clinical remission: evidence from an imaging study may explain structural progression. *Arthritis Rheum* 2006;54(12):3761-73.
122. Backhaus M, Burmester GR, Gerber T, Grassi W, Machold KP, Swen WA, et al. Guidelines for musculoskeletal ultrasound in rheumatology. *Annals of the rheumatic diseases* 2001;60(7):641-9.
123. Albrecht K, Muller-Ladner U, Strunk J. Quantification of the synovial perfusion in rheumatoid arthritis using Doppler ultrasonography. *Clinical and experimental rheumatology* 2007;25(4):630-8.
124. Scire CA, Montecucco C, Codullo V, Epis O, Todoerti M, Caporali R. Ultrasonographic evaluation of joint involvement in early rheumatoid arthritis in clinical remission: power Doppler signal predicts short-term relapse. *Rheumatology (Oxford, England)* 2009;48(9):1092-7.
125. Terslev L, Torp-Pedersen S, Qvistgaard E, Kristoffersen H, Rogind H, Danneskiold-Samsoe B, et al. Effects of treatment with etanercept (Enbrel, TNRF:Fc) on rheumatoid arthritis evaluated by Doppler ultrasonography. *Annals of the rheumatic diseases* 2003;62(2):178-81.
126. Terslev L, Torp-Pedersen S, Savnik A, von der Recke P, Qvistgaard E, Danneskiold-Samsoe B, et al. Doppler ultrasound and magnetic resonance imaging of synovial inflammation of the hand in rheumatoid arthritis: a comparative study. *Arthritis and rheumatism* 2003;48(9):2434-41.

127. Seymour MW, Kelly S, Beals CR, Malice MP, Bolognese JA, Dardzinski BJ, et al. Ultrasound of metacarpophalangeal joints is a sensitive and reliable endpoint for drug therapies in rheumatoid arthritis: results of a randomized, two-center placebo-controlled study. *Arthritis research & therapy* 2012;14(5):R198.
128. Seymour M, Petavy F, Chiesa F, Perry H, Lukey PT, Binks M, et al. Ultrasonographic measures of synovitis in an early phase clinical trial: a double-blind, randomised, placebo and comparator controlled phase IIa trial of GW274150 (a selective inducible nitric oxide synthase inhibitor) in rheumatoid arthritis. *Clinical and experimental rheumatology* 2012;30(2): 254-61.
129. Ellegaard K, Torp-Pedersen S, Terslev L, Danneskiold-Samsoe B, Henriksen M, Bliddal H. Ultrasound colour Doppler measurements in a single joint as measure of disease activity in patients with rheumatoid arthritis--assessment of concurrent validity. *Rheumatology (Oxford, England)* 2009;48(3):254-7.
130. Koski JM, Saarakkala S, Helle M, Hakulinen U, Heikkinen JO, Hermunen H. Power Doppler ultrasonography and synovitis: correlating ultrasound imaging with histopathological findings and evaluating the performance of ultrasound equipments. *Annals of the rheumatic diseases* 2006;65(12):1590-5.
131. Taylor PC, Steuer A, Gruber J, McClinton C, Cosgrove DO, Blomley MJ, et al. Ultrasonographic and radiographic results from a two-year controlled trial of immediate or one-year-delayed addition of infliximab to ongoing methotrexate therapy in patients with erosive early rheumatoid arthritis. *Arthritis and rheumatism* 2006;54(1):47-53.
132. Shio K, Homma F, Kanno Y, Yamadera Y, Ohguchi Y, Nishimaki T, et al. Doppler sonographic comparative study on usefulness of synovial vascularity between knee and metacarpophalangeal joints for evaluation of articular inflammation in patients with rheumatoid arthritis treated by infliximab. *Modern rheumatology / the Japan Rheumatism Association* 2006;16(4):220-5.
133. Terslev L, Torp-Pedersen S, Bang N, Koenig MJ, Nielsen MB, Bliddal H. Doppler ultrasound findings in healthy wrists and finger joints before and after use of two different contrast agents. *Annals of the rheumatic diseases* 2005;64(6):824-7.
134. Naredo E, Moller I, Acebes C, Batlle-Gualda E, Brito E, de Agustin JJ, et al. Three-dimensional volumetric ultrasonography. Does it improve reliabililty of musculoskeletal ultrasound? *Clinical and experimental rheumatology* 2010;28(1):79-82.
135. Naredo E, Acebes C, Brito E, de Agustin JJ, de Miguel E, Mayordomo L, et al. Three-dimensional Volumetric Ultrasound: A Valid Method for Blinded Assessment of Response to Therapy in Rheumatoid Arthritis. *The Journal of rheumatology* 2013;40(3):253-60.
136. Krishnamoorthy VK, Sengupta PP, Gentile F, Khandheria BK. History of echocardiography and its future applications in medicine. *Critical care medicine* 2007;35(8 Suppl):S309-13.
137. Filippucci E, Iagnocco A, Meenagh G, Riente L, Delle Sedie A, Bombardieri S, et al. Ultrasound imaging for the rheumatologist VII. Ultrasound imaging in rheumatoid arthritis. *Clin Exp Rheumatol* 2007;25(1):5-10.
138. Filippucci E, Iagnocco A, Meenagh G, Riente L, Delle Sedie A, Bombardieri S, et al. Ultrasound imaging for the rheumatologist II. Ultrasonography of the hand and wrist. *Clinical and experimental rheumatology* 2006;24(2):118-22.
139. Botar-Jid C, Bolboaca S, Fodor D, Bocsa C, Tamas MM, Micu M, et al. Gray scale and power Doppler ultrasonography in evaluation of early rheumatoid arthritis. *Med Ultrason* 2010;12(4):300-5.
140. Ohashi S, Ohnishi I, Matsumoto T, Bessho M, Matsuyama J, Tobita K, et al. Measurement of articular cartilage thickness using a three-dimensional image reconstructed from B-mode ultrasonography mechanical scans feasibility

study by comparison with MRI-derived data. *Ultrasound in medicine & biology* 2012;38(3):402-11.
141. Delle Sedie A, Riente L, Iagnocco A, Filippucci E, Meenagh G, Grassi W, et al. Ultrasound imaging for the rheumatologist X. Ultrasound imaging in crystal-related arthropathies. *Clinical and experimental rheumatology* 2007;25(4):513-7.
142. Walther M, Harms H, Krenn V, Radke S, Faehndrich TP, Gohlke F. Correlation of power Doppler sonography with vascularity of the synovial tissue of the knee joint in patients with osteoarthritis and rheumatoid arthritis. *Arthritis Rheum* 2001;44(2):331-8.
143. Schmidt WA, Volker L, Zacher J, Schlafke M, Ruhnke M, Gromnica-Ihle E. Colour Doppler ultrasonography to detect pannus in knee joint synovitis. *Clin Exp Rheumatol* 2000;18(4):439-44.
144. Fiocco U, Cozzi L, Rubaltelli L, Rigon C, De Candia A, Tregnaghi A, et al. Long-term sonographic follow-up of rheumatoid and psoriatic proliferative knee joint synovitis. *British journal of rheumatology* 1996;35(2):155-63.
145. Krenn V, Morawietz L, Burmester GR, Kinne RW, Mueller-Ladner U, Muller B, et al. Synovitis score: discrimination between chronic low-grade and high-grade synovitis. *Histopathology* 2006;49(4):358-64.
146. Krenn V, Morawietz L, Haupl T, Neidel J, Petersen I, Konig A. Grading of chronic synovitis--a histopathological grading system for molecular and diagnostic pathology. *Pathol Res Pract* 2002;198(5):317-25.
147. Pontifex EK, Gerlag DM, Gogarty M, Vinkenoog M, Gibbs A, Burgman I, et al. Change in CD3 positive T-cell expression in psoriatic arthritis synovium correlates with change in DAS28 and magnetic resonance imaging synovitis scores following initiation of biologic therapy--a single centre, open-label study. *Arthritis research & therapy* 2011;13(1):R7.
148. Felson DT, Anderson JJ, Boers M, Bombardier C, Furst D, Goldsmith C, et al. American College of Rheumatology. Preliminary definition of improvement in rheumatoid arthritis. *Arthritis and rheumatism* 1995;38(6):727-35.
149. Hanson MT, Keiding S, Lauritzen SL, Manthorpe R, Sorensen SF, Wiik A. Clinical assessment of disease activity in rheumatoid arthritis. *Scand J Rheumatol* 1979;8(2):101-5.
150. van Gestel AM, Haagsma CJ, van Riel PL. Validation of rheumatoid arthritis improvement criteria that include simplified joint counts. *Arthritis and rheumatism* 1998;41(10):1845-50.
151. van Riel PL, van Gestel AM. Clinical outcome measures in rheumatoid arthritis. *Annals of the rheumatic diseases* 2000;59 Suppl 1:i28-31.
152. Hameed B, Pilcher J, Heron C, Kiely PD. The relation between composite ultrasound measures and the DAS28 score, its components and acute phase markers in adult RA. *Rheumatology (Oxford, England)* 2008;47(4):476-80.
153. Salaffi F, Filippucci E, Carotti M, Naredo E, Meenagh G, Ciapetti A, et al. Inter-observer agreement of standard joint counts in early rheumatoid arthritis: a comparison with grey scale ultrasonography--a preliminary study. *Rheumatology (Oxford)* 2008;47(1):54-8.
154. Naredo E, Gamero F, Bonilla G, Uson J, Carmona L, Laffon A. Ultrasonographic assessment of inflammatory activity in rheumatoid arthritis: comparison of extended versus reduced joint evaluation. *Clinical and experimental rheumatology* 2005;23(6):881-4.
155. Kawashiri SY, Kawakami A, Iwamoto N, Fujikawa K, Satoh K, Tamai M, et al. The power Doppler ultrasonography score from 24 synovial sites or 6 simplified synovial sites, including the metacarpophalangeal joints, reflects the clinical disease activity and level of serum biomarkers in patients with rheumatoid arthritis. *Rheumatology (Oxford, England)* 2011;50(5):962-5.
156. Szkudlarek M, Klarlund M, Narvestad E, Court-Payen M, Strandberg C, Jensen KE, et al. Ultrasonography of the metacarpophalangeal and proximal interphalangeal joints in rheumatoid arthritis: a comparison with magnetic

resonance imaging, conventional radiography and clinical examination. *Arthritis research & therapy* 2006;8(2):R52.
157. Kane D, Balint PV, Sturrock RD. Ultrasonography is superior to clinical examination in the detection and localization of knee joint effusion in rheumatoid arthritis. *The Journal of rheumatology* 2003;30(5):966-71.
158. Damjanov N, Radunovic G, Prodanovic S, Vukovic V, Milic V, Simic Pasalic K, et al. Construct validity and reliability of ultrasound disease activity score in assessing joint inflammation in RA: comparison with DAS-28. *Rheumatology (Oxford, England)* 2012;51(1):120-8.
159. Almoallim H, Attar S, Jannoudi N, Al-Nakshabandi N, Eldeek B, Fathaddien O, et al. Sensitivity of standardised musculoskeletal examination of the hand and wrist joints in detecting arthritis in comparison to ultrasound findings in patients attending rheumatology clinics. *Clinical rheumatology* 2012;31(9): 1309-17.
160. Nakagomi D, Ikeda K, Okubo A, Iwamoto T, Sanayama Y, Takahashi K, et al. Ultrasound can improve the accuracy of the 2010 ACR/EULAR classification criteria for rheumatoid arthritis to predict methotrexate requirement. *Arthritis and rheumatism* 2013.
161. Saleem B, Brown AK, Keen H, Nizam S, Freeston J, Wakefield R, et al. Should imaging be a component of rheumatoid arthritis remission criteria? A comparison between traditional and modified composite remission scores and imaging assessments. *Annals of the rheumatic diseases* 2011;70(5): 792-8.
162. Wakefield RJ, D'Agostino MA, Naredo E, Buch MH, Iagnocco A, Terslev L, et al. After treat-to-target: can a targeted ultrasound initiative improve RA outcomes? *Ann Rheum Dis* 2012;71(6):799-803.
163. Saleem B, Nizam S, Emery P. Can remission be maintained with or without further drug therapy in rheumatoid arthritis? *Clinical and experimental rheumatology* 2006;24(6 Suppl 43):S-33-6.
164. Conaghan PG, Ostergaard M, McGonagle D, O'Connor P, Emery P. The validity and predictive value of magnetic resonance imaging erosions in rheumatoid arthritis: comment on the article by Goldbach-Mansky et al. *Arthritis Rheum* 2004;50(3):1009-11.
165. Freeston JE, Conaghan PG, Dass S, Vital E, Hensor EM, Stewart SP, et al. Does extremity-MRI improve erosion detection in severely damaged joints? A study of long-standing rheumatoid arthritis using three imaging modalities. *Annals of the rheumatic diseases* 2007;66(11):1538-40.
166. Quinn MA, Green MJ, Conaghan P, Emery P. How do you diagnose rheumatoid arthritis early? *Best practice & research* 2001;15(1):49-66.
167. Ogishima H, Tsuboi H, Umeda N, Horikoshi M, Kondo Y, Sugihara M, et al. Analysis of subclinical synovitis detected by ultrasonography and low-field magnetic resonance imaging in patients with rheumatoid arthritis. *Modern rheumatology / the Japan Rheumatism Association* 2013.
168. Palosaari K, Vuotila J, Takalo R, Jartti A, Niemela RK, Karjalainen A, et al. Bone oedema predicts erosive progression on wrist MRI in early RA--a 2-yr observational MRI and NC scintigraphy study. *Rheumatology (Oxford, England)* 2006;45(12):1542-8.
169. Ohrndorf S, Hensch A, Naumann L, Hermann KG, Scheurig-Munkler C, Meier S, et al. Contrast-enhanced ultrasonography is more sensitive than grayscale and power Doppler ultrasonography compared to MRI in therapy monitoring of rheumatoid arthritis patients. *Ultraschall Med* 2011;32 Suppl 2:E38-44.
170. Backhaus M BG, Sandrock D, et al. Prospective two year follow up study comparing novel and conventional imaging procedures in patients with arthritic finger joints. . *Ann Rheum* 2002; 61:895-904.
171. Hermann KG, Backhaus M, Schneider U, Labs K, Loreck D, Zuhlsdorf S, et al. Rheumatoid arthritis of the shoulder joint: comparison of conventional

radiography, ultrasound, and dynamic contrast-enhanced magnetic resonance imaging. *Arthritis and rheumatism* 2003;48(12):3338-49.
172. Szkudlarek M, Narvestad E, Klarlund M, Court-Payen M, Thomsen HS, Ostergaard M. Ultrasonography of the metatarsophalangeal joints in rheumatoid arthritis: comparison with magnetic resonance imaging, conventional radiography, and clinical examination. *Arthritis and rheumatism* 2004;50(7):2103-12.
173. Schmidt WA, Schicke B, Ostendorf B, Scherer A, Krause A, Walther M. Low-field MRI versus ultrasound: which is more sensitive in detecting inflammation and bone damage in MCP and MTP joints in mild or moderate rheumatoid arthritis? *Clinical and experimental rheumatology* 2013;31(1):91-6.
174. Amin MF, Ismail FM, El Shereef RR. The role of ultrasonography in early detection and monitoring of shoulder erosions, and disease activity in rheumatoid arthritis patients; comparison with MRI examination. *Acad Radiol* 2012;19(6):693-700.
175. Keen HI, Mease PJ, Bingham CO, 3rd, Giles JT, Kaeley G, Conaghan PG. Systematic review of MRI, ultrasound, and scintigraphy as outcome measures for structural pathology in interventional therapeutic studies of knee arthritis: focus on responsiveness. *J Rheumatol* 2011;38(1):142-54.
176. Grassi W, Filippucci E, Farina A, Cervini C. Sonographic imaging of tendons. *Arthritis and rheumatism* 2000;43(5):969-76.
177. Grassi W, Tittarelli E, Blasetti P, Pirani O, Cervini C. Finger tendon involvement in rheumatoid arthritis. Evaluation with high-frequency sonography. *Arthritis and rheumatism* 1995;38(6):786-94.
178. Grassi W, Tittarelli E, Pirani O, Avaltroni D, Cervini C. Ultrasound examination of metacarpophalangeal joints in rheumatoid arthritis. *Scand J Rheumatol* 1993;22(5):243-7.
179. Leslie BM. Rheumatoid extensor tendon ruptures. *Hand clinics* 1989;5(2): 191-202.
180. Fornage BD, Rifkin MD. Ultrasound examination of the hand and foot. *Radiologic clinics of North America* 1988;26(1):109-29.
181. Wakefield RJ, Balint PV, Szkudlarek M, Filippucci E, Backhaus M, D'Agostino MA, et al. Musculoskeletal ultrasound including definitions for ultrasonographic pathology. *The Journal of rheumatology* 2005;32(12): 2485-7.
182. Symmons DP, Silman AJ. Aspects of early arthritis. What determines the evolution of early undifferentiated arthritis and rheumatoid arthritis? An update from the Norfolk Arthritis Register. *Arthritis research & therapy* 2006;8(4):214.
183. Keen HI, Emery P. How should we manage early rheumatoid arthritis? From imaging to intervention. *Current opinion in rheumatology* 2005;17(3):280-5.
184. Wakefield RJ, Kong KO, Conaghan PG, Brown AK, O'Connor PJ, Emery P. The role of ultrasonography and magnetic resonance imaging in early rheumatoid arthritis. *Clinical and experimental rheumatology* 2003;21(5 Suppl 31):S42-9.
185. Farrant JM, Grainger AJ, O'Connor PJ. Advanced imaging in rheumatoid arthritis: part 2: erosions. *Skeletal Radiol* 2007;36(5):381-9.
186. Funck-Brentano T, Gandjbakhch F, Etchepare F, Jousse-Joulin S, Miquel A, Cyteval C, et al. Sonographic erosions and power-Doppler signal predict radiographic damage in early arthritis: The ESPOIR ultrasonography longitudinal study. *Arthritis Care Res (Hoboken)* 2012.
187. Wakefield RJ, Gibbon WW, Conaghan PG, O'Connor P, McGonagle D, Pease C, et al. The value of sonography in the detection of bone erosions in patients with rheumatoid arthritis: a comparison with conventional radiography. *Arthritis and rheumatism* 2000;43(12):2762-70.
188. Freeston JE, Wakefield RJ, Conaghan PG, Hensor EM, Stewart SP, Emery P. A diagnostic algorithm for persistence of very early inflammatory arthritis:

the utility of power doppler ultrasound when added to conventional assessment tools. *Annals of the rheumatic diseases* 2009.
189. van de Stadt LA, Bos WH, Meursinge Reynders M, Wieringa H, Turkstra F, van der Laken CJ, et al. The value of ultrasonography in predicting arthritis in auto-antibody positive arthralgia patients: a prospective cohort study. *Arthritis research & therapy* 2010;12(3):R98.
190. van den Broek M, Lems WF, Allaart CF. BeSt practice: the success of early-targeted treatment in rheumatoid arthritis. *Clinical and experimental rheumatology* 2012;30(4 Suppl 73):S35-8.
191. Lard LR, Visser H, Speyer I, vander Horst-Bruinsma IE, Zwinderman AH, Breedveld FC, et al. Early versus delayed treatment in patients with recent-onset rheumatoid arthritis: comparison of two cohorts who received different treatment strategies. *Am J Med* 2001;111(6):446-51.
192. van Aken J, van Bilsen JH, Allaart CF, Huizinga TW, Breedveld FC. The Leiden Early Arthritis Clinic. *Clinical and experimental rheumatology* 2003;21(5 Suppl 31):S100-5.
193. Ellegaard K, Christensen R, Torp-Pedersen S, Terslev L, Holm CC, Konig MJ, et al. Ultrasound Doppler measurements predict success of treatment with anti-TNF-α drug in patients with rheumatoid arthritis: a prospective cohort study. *Rheumatology (Oxford, England)* 2011;50(3):506-12.
194. Ostergaard M, Szkudlarek M. Ultrasonography: a valid method for assessing rheumatoid arthritis? *Arthritis and rheumatism* 2005;52(3):681-6.
195. Joshua F, Lassere M, Bruyn GA, Szkudlarek M, Naredo E, Schmidt WA, et al. Summary findings of a systematic review of the ultrasound assessment of synovitis. *The Journal of rheumatology* 2007;34(4):839-47.
196. Algergawy S, Haliem T, Al-Shaer O. Clinical, laboratory, and ultrasound assessment of the knee in juvenile rheumatoid arthritis. *Clin Med Insights Arthritis Musculoskelet Disord* 2011;4:21-7.
197. Backhaus TM, Ohrndorf S, Kellner H, Strunk J, Hartung W, Sattler H, et al. The US7 score is sensitive to change in a large cohort of patients with rheumatoid arthritis over 12 months of therapy. *Annals of the rheumatic diseases* 2012.
198. Taylor PC, Steuer A, Gruber J, Cosgrove DO, Blomley MJ, Marsters PA, et al. Comparison of ultrasonographic assessment of synovitis and joint vascularity with radiographic evaluation in a randomized, placebo-controlled study of infliximab therapy in early rheumatoid arthritis. *Arthritis and rheumatism* 2004;50(4):1107-16.
199. Teh J, Stevens K, Williamson L, Leung J, McNally EG. Power Doppler ultrasound of rheumatoid synovitis: quantification of therapeutic response. *Br J Radiol* 2003;76(912):875-9.
200. Qvistgaard E, Rogind H, Torp-Pedersen S, Terslev L, Danneskiold-Samsoe B, Bliddal H. Quantitative ultrasonography in rheumatoid arthritis: evaluation of inflammation by Doppler technique. *Ann Rheum Dis* 2001;60(7):690-3.
201. Naredo E, Moller I, Moragues C, de Agustin JJ, Scheel AK, Grassi W, et al. Interobserver reliability in musculoskeletal ultrasonography: results from a "Teach the Teachers" rheumatologist course. *Annals of the rheumatic diseases* 2006;65(1):14-9.
202. Szkudlarek M, Court-Payen M, Strandberg C, Klarlund M, Klausen T, Ostergaard M. Contrast-enhanced power Doppler ultrasonography of the metacarpophalangeal joints in rheumatoid arthritis. *European radiology* 2003;13(1):163-8.
203. Qvistgaard E, Torp-Pedersen S, Christensen R, Bliddal H. Reproducibility and inter-reader agreement of a scoring system for ultrasound evaluation of hip osteoarthritis. *Annals of the rheumatic diseases* 2006;65(12):1613-9.
204. Wiell C, Szkudlarek M, Hasselquist M, Moller JM, Vestergaard A, Norregaard J, et al. Ultrasonography, magnetic resonance imaging, radiography, and clinical assessment of inflammatory and destructive

changes in fingers and toes of patients with psoriatic arthritis. *Arthritis research & therapy* 2007;9(6):R119.
205. Naredo E, Rodriguez M, Campos C, Rodriguez-Heredia JM, Medina JA, Giner E, et al. Validity, reproducibility, and responsiveness of a twelve-joint simplified power doppler ultrasonographic assessment of joint inflammation in rheumatoid arthritis. *Arthritis and rheumatism* 2008;59(4):515-22.
206. Luz KR, Furtado R, Mitraud SV, Porglhof J, Nunes C, Fernandes AR, et al. Interobserver reliability in ultrasound assessment of rheumatoid wrist joints. *Acta Reumatol Port* 2011;36(3):245-50.
207. Ohrndorf S, Fischer IU, Kellner H, Strunk J, Hartung W, Reiche B, et al. Reliability of the novel 7-joint ultrasound score: results from an inter- and intraobserver study performed by rheumatologists. *Arthritis Care Res (Hoboken)* 2012;64(8):1238-43.
208. Strunk J, Strube K, Rumbaur C, Lange U, Muller-Ladner U. Interobserver agreement in two- and three-dimensional power Doppler sonographic assessment of synovial vascularity during anti-inflammatory treatment in patients with rheumatoid arthritis. *Ultraschall Med* 2007;28(4):409-15.
209. Koski JM, Saarakkala S, Helle M, Hakulinen U, Heikkinen JO, Hermunen H, et al. Assessing the intra- and inter-reader reliability of dynamic ultrasound images in power Doppler ultrasonography. *Annals of the rheumatic diseases* 2006;65(12):1658-60.
210. Scheel AK, Schmidt WA, Hermann KG, Bruyn GA, D'Agostino MA, Grassi W, et al. Interobserver reliability of rheumatologists performing musculoskeletal ultrasonography: results from a EULAR "Train the trainers" course. *Annals of the rheumatic diseases* 2005;64(7):1043-9.
211. Fink B, Makowiak C, Fuerst M, Berger I, Schafer P, Frommelt L. The value of synovial biopsy, joint aspiration and C-reactive protein in the diagnosis of late peri-prosthetic infection of total knee replacements. *J Bone Joint Surg Br* 2008;90(7):874-8.
212. Munoz-Gomez J, Gomez-Perez R, Sole-Arques M, Llopart-Buisan E. Synovial fluid examination for the diagnosis of synovial amyloidosis in patients with chronic renal failure undergoing haemodialysis. *Annals of the rheumatic diseases* 1987;46(4):324-6.
213. Lurie DP, Musil G. Knee arthropathy in ochronosis: diagnosis by arthroscopy with ultrastructural features. *The Journal of rheumatology* 1984;11(1):101-3.
214. Isaacson C, Bothwell TH. Synovial iron deposits in black subjects with iron overload. *Arch Pathol Lab Med* 1981;105(9):487-9.
215. Archer-Harvey JM, Henderson DW, Papadimitriou JM, Rozenbilds MA. Pigmented villonodular synovitis associated with psoriatic polyarthropathy: and electron microscopic and immunocytochemical study. *J Pathol* 1984;144(1):57-68.
216. Saaibi DL, Schumacher HR, Jr. Percutaneous needle biopsy and synovial histology. *Bailliere's clinical rheumatology* 1996;10(3):535-54.
217. Gerlag D, Tak PP. Synovial biopsy. *Best Pract Res Clin Rheumatol* 2005;19(3):387-400.
218. Kane D, Veale DJ, FitzGerald O, Reece R. Survey of arthroscopy performed by rheumatologists. *Rheumatology (Oxford, England)* 2002;41(2): 210-5.
219. Baeten D, Van den Bosch F, Elewaut D, Stuer A, Veys EM, De Keyser F. Needle arthroscopy of the knee with synovial biopsy sampling: technical experience in 150 patients. *Clinical rheumatology* 1999;18(6):434-41.
220. Collins JJ. Knee-joint arthroscopy--early complications. *The Medical journal of Australia* 1989;150(12):702-3, 06.
221. Bresnihan B, Pontifex E, Thurlings RM, Vinkenoog M, El-Gabalawy H, Fearon U, et al. Synovial tissue sublining CD68 expression is a biomarker of

therapeutic response in rheumatoid arthritis clinical trials: consistency across centers. *The Journal of rheumatology* 2009;36(8):1800-2.
222. Koski JM, Helle M. Ultrasound guided synovial biopsy using portal and forceps. *Ann Rheum Dis* 2005;64(6):926-9.
223. van Vugt RM, van Dalen A, Bijlsma JW. Ultrasound guided synovial biopsy of the wrist. *Scand J Rheumatol* 1997;26(3):212-4.
224. Scire CA, Epis O, Codullo V, Humby F, Morbini P, Manzo A, et al. Immunohistological assessment of the synovial tissue in small joints in rheumatoid arthritis: validation of a minimally invasive ultrasound-guided synovial biopsy procedure. *Arthritis Res Ther* 2007;9(5):R101.
225. Youssef PP, Kraan M, Breedveld F, Bresnihan B, Cassidy N, Cunnane G, et al. Quantitative microscopic analysis of inflammation in rheumatoid arthritis synovial membrane samples selected at arthroscopy compared with samples obtained blindly by needle biopsy. *Arthritis and rheumatism* 1998;41(4): 663-9.
226. Smeets TJ, Kraan MC, Galjaard S, Youssef PP, Smith MD, Tak PP. Analysis of the cell infiltrate and expression of matrix metalloproteinases and granzyme B in paired synovial biopsy specimens from the cartilage-pannus junction in patients with RA. *Ann Rheum Dis* 2001;60(6):561-5.
227. Kane D, Jensen LE, Grehan S, Whitehead AS, Bresnihan B, Fitzgerald O. Quantitation of metalloproteinase gene expression in rheumatoid and psoriatic arthritis synovial tissue distal and proximal to the cartilage-pannus junction. *The Journal of rheumatology* 2004;31(7):1274-80.
228. Smith MD, Barg E, Weedon H, Papengelis V, Smeets T, Tak PP, et al. Microarchitecture and protective mechanisms in synovial tissue from clinically and arthroscopically normal knee joints. *Annals of the rheumatic diseases* 2003;62(4):303-7.
229. Smith MD. The normal synovium. *Open Rheumatol J* 2011;5:100-6.
230. Fava RA, Olsen NJ, Spencer-Green G, Yeo KT, Yeo TK, Berse B, et al. Vascular permeability factor/endothelial growth factor (VPF/VEGF): accumulation and expression in human synovial fluids and rheumatoid synovial tissue. *J Exp Med* 1994;180(1):341-6.
231. van Lent PL, Blom AB, van der Kraan P, Holthuysen AE, Vitters E, van Rooijen N, et al. Crucial role of synovial lining macrophages in the promotion of transforming growth factor beta-mediated osteophyte formation. *Arthritis and rheumatism* 2004;50(1):103-11.
232. Li P, Sanz I, O'Keefe RJ, Schwarz EM. NF-kappa B regulates VCAM-1 expression on fibroblast-like synoviocytes. *J Immunol* 2000;164(11):5990-7.
233. Xu H, Edwards J, Banerji S, Prevo R, Jackson DG, Athanasou NA. Distribution of lymphatic vessels in normal and arthritic human synovial tissues. *Annals of the rheumatic diseases* 2003;62(12):1227-9.
234. Singh JA, Arayssi T, Duray P, Schumacher HR. Immunohistochemistry of normal human knee synovium: a quantitative study. *Annals of the rheumatic diseases* 2004;63(7):785-90.
235. Smith MD. Immunohistochemistry of normal synovium. *Annals of the rheumatic diseases* 2004;63(11):1532-3; author reply 33.
236. Szekanecz Z, Koch AE. Mechanisms of Disease: angiogenesis in inflammatory diseases. *Nature clinical practice* 2007;3(11):635-43.
237. Arend WP, Malyak M, Guthridge CJ, Gabay C. Interleukin-1 receptor antagonist: role in biology. *Annu Rev Immunol* 1998;16:27-55.
238. Takemura S, Braun A, Crowson C, Kurtin PJ, Cofield RH, O'Fallon WM, et al. Lymphoid neogenesis in rheumatoid synovitis. *J Immunol* 2001;167(2): 1072-80.
239. Manzo A, Paoletti S, Carulli M, Blades MC, Barone F, Yanni G, et al. Systematic microanatomical analysis of CXCL13 and CCL21 in situ production and progressive lymphoid organization in rheumatoid synovitis. *Eur J Immunol* 2005;35(5):1347-59.

240. Manzo A, Bombardieri M, Humby F, Pitzalis C. Secondary and ectopic lymphoid tissue responses in rheumatoid arthritis: from inflammation to autoimmunity and tissue damage/remodeling. *Immunol Rev* 2010;233(1): 267-85.
241. Weyand CM, Goronzy JJ. Ectopic germinal center formation in rheumatoid synovitis. *Annals of the New York Academy of Sciences* 2003;987:140-9.
242. Weyand CM, Kang YM, Kurtin PJ, Goronzy JJ. The power of the third dimension: tissue architecture and autoimmunity in rheumatoid arthritis. *Current opinion in rheumatology* 2003;15(3):259-66.
243. Bugatti S, Manzo A, Bombardieri M, Vitolo B, Humby F, Kelly S, et al. Synovial tissue heterogeneity and peripheral blood biomarkers. *Current rheumatology reports* 2011;13(5):440-8.
244. Corsiero E, Bombardieri M, Manzo A, Bugatti S, Uguccioni M, Pitzalis C. Role of lymphoid chemokines in the development of functional ectopic lymphoid structures in rheumatic autoimmune diseases. *Immunol Lett* 2012;145(1-2):62-7.
245. Yanni G, Whelan A, Feighery C, Bresnihan B. Analysis of cell populations in rheumatoid arthritis synovial tissues. *Seminars in arthritis and rheumatism* 1992;21(6):393-9.
246. Yanni G, Whelan A, Feighery C, Quinlan W, Symons J, Duff G, et al. Contrasting levels of in vitro cytokine production by rheumatoid synovial tissues demonstrating different patterns of mononuclear cell infiltration. *Clin Exp Immunol* 1993;93(3):387-95.
247. Singh JA, Pando JA, Tomaszewski J, Schumacher HR. Quantitative analysis of immunohistologic features of very early rheumatoid synovitis in disease modifying antirheumatic drug- and corticosteroid-naive patients. *J Rheumatol* 2004;31(7):1281-5.
248. Baeten D, Houbiers J, Kruithof E, Vandooren B, Van den Bosch F, Boots AM, et al. Synovial inflammation does not change in the absence of effective treatment: implications for the use of synovial histopathology as biomarker in early phase clinical trials in rheumatoid arthritis. *Annals of the rheumatic diseases* 2006;65(8):990-7.
249. Smeets TJ, Barg EC, Kraan MC, Smith MD, Breedveld FC, Tak PP. Analysis of the cell infiltrate and expression of proinflammatory cytokines and matrix metalloproteinases in arthroscopic synovial biopsies: comparison with synovial samples from patients with end stage, destructive rheumatoid arthritis. *Annals of the rheumatic diseases* 2003;62(7):635-8.
250. Klaasen R, Wijbrandts CA, van Kuijk AW, Pots D, Gerlag DM, Tak PP. Synovial synoviolin in relation to response to TNF blockade in patients with rheumatoid arthritis and psoriatic arthritis. *Annals of the rheumatic diseases* 2012;71(7):1260-1.
251. Shi K, Hayashida K, Kaneko M, Hashimoto J, Tomita T, Lipsky PE, et al. Lymphoid chemokine B cell-attracting chemokine-1 (CXCL13) is expressed in germinal center of ectopic lymphoid follicles within the synovium of chronic arthritis patients. *J Immunol* 2001;166(1):650-5.
252. Bombardieri M, Barone F, Lucchesi D, Nayar S, van den Berg WB, Proctor G, et al. Inducible tertiary lymphoid structures, autoimmunity, and exocrine dysfunction in a novel model of salivary gland inflammation in C57BL/6 mice. *J Immunol* 2012;189(7):3767-76.
253. Gatumu MK, Skarstein K, Papandile A, Browning JL, Fava RA, Bolstad AI. Blockade of lymphotoxin-beta receptor signaling reduces aspects of Sjogren's syndrome in salivary glands of non-obese diabetic mice. *Arthritis research & therapy* 2009;11(1):R24.
254. Astorri E, Bombardieri M, Gabba S, Peakman M, Pozzilli P, Pitzalis C. Evolution of ectopic lymphoid neogenesis and in situ autoantibody production in autoimmune nonobese diabetic mice: cellular and molecular

characterization of tertiary lymphoid structures in pancreatic islets. *J Immunol* 2010;185(6):3359-68.
255. Humby F, Bombardieri M, Manzo A, Kelly S, Blades MC, Kirkham B, et al. Ectopic lymphoid structures support ongoing production of class-switched autoantibodies in rheumatoid synovium. *PLoS medicine* 2009;6(1):e1.
256. Pitzalis C, Kelly S, Humby F. New learnings on the pathophysiology of RA from synovial biopsies. *Current opinion in rheumatology* 2013.
257. Kasperkovitz PV, Timmer TC, Smeets TJ, Verbeet NL, Tak PP, van Baarsen LG, et al. Fibroblast-like synoviocytes derived from patients with rheumatoid arthritis show the imprint of synovial tissue heterogeneity: evidence of a link between an increased myofibroblast-like phenotype and high-inflammation synovitis. *Arthritis and rheumatism* 2005;52(2):430-41.
258. Bauer S, Jendro MC, Wadle A, Kleber S, Stenner F, Dinser R, et al. Fibroblast activation protein is expressed by rheumatoid myofibroblast-like synoviocytes. *Arthritis Res Ther* 2006;8(6):R171.
259. Tolboom TC, van der Helm-Van Mil AH, Nelissen RG, Breedveld FC, Toes RE, Huizinga TW. Invasiveness of fibroblast-like synoviocytes is an individual patient characteristic associated with the rate of joint destruction in patients with rheumatoid arthritis. *Arthritis and rheumatism* 2005;52(7):1999-2002.
260. Buckley CD. Why does chronic inflammatory joint disease persist? *Clin Med* 2003;3(4):361-6.
261. Rooney T, Bresnihan B, Andersson U, Gogarty M, Kraan M, Schumacher HR, et al. Microscopic measurement of inflammation in synovial tissue: Inter-observer agreement for manual quantitative, semi-quantitative and computerized digital image analysis. *Annals of the rheumatic diseases* 2007.
262. Tak PP, Smeets TJ, Daha MR, Kluin PM, Meijers KA, Brand R, et al. Analysis of the synovial cell infiltrate in early rheumatoid synovial tissue in relation to local disease activity. *Arthritis and rheumatism* 1997;40(2):217-25.
263. Kraan MC, Haringman JJ, Post WJ, Versendaal J, Breedveld FC, Tak PP. Immunohistological analysis of synovial tissue for differential diagnosis in early arthritis. *Rheumatology (Oxford, England)* 1999;38(11):1074-80.
264. Pettit AR, Weedon H, Ahern M, Zehntner S, Frazer IH, Slavotinek J, et al. Association of clinical, radiological and synovial immunopathological responses to anti-rheumatic treatment in rheumatoid arthritis. *Rheumatology (Oxford)* 2001;40(11):1243-55.
265. Gerlag DM, Haringman JJ, Smeets TJ, Zwinderman AH, Kraan MC, Laud PJ, et al. Effects of oral prednisolone on biomarkers in synovial tissue and clinical improvement in rheumatoid arthritis. *Arthritis Rheum* 2004;50(12): 3783-91.
266. Haringman JJ, Gerlag DM, Zwinderman AH, Smeets TJ, Kraan MC, Baeten D, et al. Synovial tissue macrophages: a sensitive biomarker for response to treatment in patients with rheumatoid arthritis. *Annals of the rheumatic diseases* 2005;64(6):834-8.
267. Klaasen R, Thurlings RM, Wijbrandts CA, van Kuijk AW, Baeten D, Gerlag DM, et al. The relationship between synovial lymphocyte aggregates and the clinical response to infliximab in rheumatoid arthritis: a prospective study. *Arthritis and rheumatism* 2009;60(11):3217-24.
268. Lindberg J, Wijbrandts CA, van Baarsen LG, Nader G, Klareskog L, Catrina A, et al. The gene expression profile in the synovium as a predictor of the clinical response to infliximab treatment in rheumatoid arthritis. *PLoS ONE* 2010;5(6):e11310.
269. Buch MH, Reece RJ, Quinn MA, English A, Cunnane G, Henshaw K, et al. The value of synovial cytokine expression in predicting the clinical response to TNF antagonist therapy (infliximab). *Rheumatology (Oxford)* 2008;47(10): 1469-75.

270. Kanbe K, Chiba J, Nakamura A. Decrease of CD68 and MMP-3 expression in synovium by treatment of adalimumab for rheumatoid arthritis. *Int J Rheum Dis* 2011;14(3):261-6.
271. Buch MH, Smolen JS, Betteridge N, Breedveld FC, Burmester G, Dorner T, et al. Updated consensus statement on the use of rituximab in patients with rheumatoid arthritis. *Annals of the rheumatic diseases* 2011;70(6):909-20.
272. Higashida J, Wun T, Schmidt S, Naguwa SM, Tuscano JM. Safety and efficacy of rituximab in patients with rheumatoid arthritis refractory to disease modifying antirheumatic drugs and anti-tumor necrosis factor-alpha treatment. *The Journal of rheumatology* 2005;32(11):2109-15.
273. Cohen SB. Targeting the B cell in rheumatoid arthritis. *Best practice & research* 2010;24(4):553-63.
274. Thurlings RM, Vos K, Wijbrandts CA, Zwinderman AH, Gerlag DM, Tak PP. Synovial tissue response to rituximab: mechanism of action and identification of biomarkers of response. *Annals of the rheumatic diseases* 2008;67(7): 917-25.
275. Buch MH, Boyle DL, Rosengren S, Saleem B, Reece RJ, Rhodes LA, et al. Mode of action of abatacept in rheumatoid arthritis patients having failed tumour necrosis factor blockade: a histological, gene expression and dynamic magnetic resonance imaging pilot study. *Ann Rheum Dis* 2009;68(7):1220-7.
276. Szekanecz Z, Koch AE. Vascular involvement in rheumatic diseases: 'vascular rheumatology'. *Arthritis research & therapy* 2008;10(5):224.
277. Poole TJ, Finkelstein EB, Cox CM. The role of FGF and VEGF in angioblast induction and migration during vascular development. *Dev Dyn* 2001;220(1): 1-17.
278. Kuwano M, Fukushi J, Okamoto M, Nishie A, Goto H, Ishibashi T, et al. Angiogenesis factors. *Internal medicine (Tokyo, Japan)* 2001;40(7):565-72.
279. Magnusson P, Rolny C, Jakobsson L, Wikner C, Wu Y, Hicklin DJ, et al. Deregulation of Flk-1/vascular endothelial growth factor receptor-2 in fibroblast growth factor receptor-1-deficient vascular stem cell development. *Journal of cell science* 2004;117(Pt 8):1513-23.
280. Ferrara N, Carver-Moore K, Chen H, Dowd M, Lu L, O'Shea KS, et al. Heterozygous embryonic lethality induced by targeted inactivation of the VEGF gene. *Nature* 1996;380(6573):439-42.
281. Burri PH, Djonov V. Intussusceptive angiogenesis--the alternative to capillary sprouting. *Molecular aspects of medicine* 2002;23(6S):S1-27.
282. Risau W, Lemmon V. Changes in the vascular extracellular matrix during embryonic vasculogenesis and angiogenesis. *Developmental biology* 1988;125(2):441-50.
283. Anderson-Berry A, O'Brien EA, Bleyl SB, Lawson A, Gundersen N, Ryssman D, et al. Vasculogenesis drives pulmonary vascular growth in the developing chick embryo. *Dev Dyn* 2005;233(1):145-53.
284. Sato TN, Tozawa Y, Deutsch U, Wolburg-Buchholz K, Fujiwara Y, Gendron-Maguire M, et al. Distinct roles of the receptor tyrosine kinases Tie-1 and Tie-2 in blood vessel formation. *Nature* 1995;376(6535):70-4.
285. Seegar TC, Eller B, Tzvetkova-Robev D, Kolev MV, Henderson SC, Nikolov DB, et al. Tie1-Tie2 interactions mediate functional differences between angiopoietin ligands. *Molecular cell* 2010;37(5):643-55.
286. Stahl A, Connor KM, Sapieha P, Chen J, Dennison RJ, Krah NM, et al. The mouse retina as an angiogenesis model. *Invest Ophthalmol Vis Sci* 2010;51(6):2813-26.
287. Khurana R, Simons M, Martin JF, Zachary IC. Role of angiogenesis in cardiovascular disease: a critical appraisal. *Circulation* 2005;112(12): 1813-24.
288. Amoroso A, Del Porto F, Di Monaco C, Manfredini P, Afeltra A. Vascular endothelial growth factor: a key mediator of neoangiogenesis. A review.

European review for medical and pharmacological sciences 1997;1(1-3): 17-25.
289. Szekanecz Z, Szegedi G, Koch AE. Angiogenesis in rheumatoid arthritis: pathogenic and clinical significance. *J Investig Med* 1998;46(2):27-41.
290. Heissig B, Hattori K, Friedrich M, Rafii S, Werb Z. Angiogenesis: vascular remodeling of the extracellular matrix involves metalloproteinases. *Current opinion in hematology* 2003;10(2):136-41.
291. Mould AW, Tonks ID, Cahill MM, Pettit AR, Thomas R, Hayward NK, et al. Vegfb gene knockout mice display reduced pathology and synovial angiogenesis in both antigen-induced and collagen-induced models of arthritis. *Arthritis and rheumatism* 2003;48(9):2660-9.
292. Lee S, Chen TT, Barber CL, Jordan MC, Murdock J, Desai S, et al. Autocrine VEGF signaling is required for vascular homeostasis. *Cell* 2007;130(4):691-703.
293. Hofmann JJ, Luisa Iruela-Arispe M. Notch expression patterns in the retina: An eye on receptor-ligand distribution during angiogenesis. *Gene Expr Patterns* 2007;7(4):461-70.
294. Taki A, Abe M, Komaki M, Oku K, Iseki S, Mizutani S, et al. Expression of angiogenesis-related factors and inflammatory cytokines in placenta and umbilical vessels in pregnancies with preeclampsia and chorioamnionitis/ funisitis. *Congenit Anom (Kyoto)* 2012;52(2):97-103.
295. Gu JW, Young E, Busby B, Covington J, Johnson JW. Oral administration of pyrrolidine dithiocarbamate (PDTC) inhibits VEGF expression, tumor angiogenesis, and growth of breast cancer in female mice. *Cancer Biol Ther* 2009;8(6):514-21.
296. Hendriksen EM, Span PN, Schuuring J, Peters JP, Sweep FC, van der Kogel AJ, et al. Angiogenesis, hypoxia and VEGF expression during tumour growth in a human xenograft tumour model. *Microvasc Res* 2009;77(2): 96-103.
297. Azizi AA, Haberler C, Czech T, Gupper A, Prayer D, Breitschopf H, et al. Vascular-endothelial-growth-factor (VEGF) expression and possible response to angiogenesis inhibitor bevacizumab in metastatic alveolar soft part sarcoma. *Lancet Oncol* 2006;7(6):521-3.
298. Zheng H, Takahashi H, Murai Y, Cui Z, Nomoto K, Niwa H, et al. Expressions of MMP-2, MMP-9 and VEGF are closely linked to growth, invasion, metastasis and angiogenesis of gastric carcinoma. *Anticancer Res* 2006;26(5A):3579-83.
299. Haigh JJ, Gerber HP, Ferrara N, Wagner EF. Conditional inactivation of VEGF-A in areas of collagen2a1 expression results in embryonic lethality in the heterozygous state. *Development (Cambridge, England)* 2000;127(7): 1445-53.
300. Shamloo A, Xu H, Heilshorn S. Mechanisms of vascular endothelial growth factor-induced pathfinding by endothelial sprouts in biomaterials. *Tissue Eng Part A* 2012;18(3-4):320-30.
301. Senger DR, Connolly DT, Van de Water L, Feder J, Dvorak HF. Purification and NH2-terminal amino acid sequence of guinea pig tumor-secreted vascular permeability factor. *Cancer Res* 1990;50(6):1774-8.
302. Ferrara N, Henzel WJ. Pituitary follicular cells secrete a novel heparin-binding growth factor specific for vascular endothelial cells. *Biochem Biophys Res Commun* 1989;161(2):851-8.
303. Ruggiero D, Dalmasso C, Nutile T, Sorice R, Dionisi L, Aversano M, et al. Genetics of VEGF serum variation in human isolated populations of cilento: importance of VEGF polymorphisms. *PLoS ONE* 2011;6(2):e16982.
304. Fairbrother WJ, Champe MA, Christinger HW, Keyt BA, Starovasnik MA. Solution structure of the heparin-binding domain of vascular endothelial growth factor. *Structure* 1998;6(5):637-48.

305. Woolard J, Wang WY, Bevan HS, Qiu Y, Morbidelli L, Pritchard-Jones RO, et al. VEGF165b, an inhibitory vascular endothelial growth factor splice variant: mechanism of action, in vivo effect on angiogenesis and endogenous protein expression. *Cancer Res* 2004;64(21):7822-35.
306. Kim WU, Kang SS, Yoo SA, Hong KH, Bae DG, Lee MS, et al. Interaction of vascular endothelial growth factor 165 with neuropilin-1 protects rheumatoid synoviocytes from apoptotic death by regulating Bcl-2 expression and Bax translocation. *J Immunol* 2006;177(8):5727-35.
307. Hartenbach EM, Olson TA, Goswitz JJ, Mohanraj D, Twiggs LB, Carson LF, et al. Vascular endothelial growth factor (VEGF) expression and survival in human epithelial ovarian carcinomas. *Cancer Lett* 1997;121(2):169-75.
308. Linderholm BK, Hellborg H, Johansson U, Elmberger G, Skoog L, Lehtio J, et al. Significantly higher levels of vascular endothelial growth factor (VEGF) and shorter survival times for patients with primary operable triple-negative breast cancer. *Ann Oncol* 2009;20(10):1639-46.
309. Linderholm B, Tavelin B, Grankvist K, Henriksson R. Does vascular endothelial growth factor (VEGF) predict local relapse and survival in radiotherapy-treated node-negative breast cancer? *Br J Cancer* 1999;81(4): 727-32.
310. Bachelder RE, Crago A, Chung J, Wendt MA, Shaw LM, Robinson G, et al. Vascular endothelial growth factor is an autocrine survival factor for neuropilin-expressing breast carcinoma cells. *Cancer Res* 2001;61(15): 5736-40.
311. Yuan A, Yu CJ, Chen WJ, Lin FY, Kuo SH, Luh KT, et al. Correlation of total VEGF mRNA and protein expression with histologic type, tumor angiogenesis, patient survival and timing of relapse in non-small-cell lung cancer. *Int J Cancer* 2000;89(6):475-83.
312. Hinton RJ, Serrano M, So S. Differential gene expression in the perichondrium and cartilage of the neonatal mouse temporomandibular joint. *Orthod Craniofac Res* 2009;12(3):168-77.
313. Sun Y, Jin K, Childs JT, Xie L, Mao XO, Greenberg DA. Vascular endothelial growth factor-B (VEGFB) stimulates neurogenesis: evidence from knockout mice and growth factor administration. *Developmental biology* 2006;289(2):329-35.
314. Nag S, Eskandarian MR, Davis J, Eubanks JH. Differential expression of vascular endothelial growth factor-A (VEGF-A) and VEGF-B after brain injury. *J Neuropathol Exp Neurol* 2002;61(9):778-88.
315. Yu DH, Wen YM, Sun JD, Wei SL, Xie HP, Pang FH. [Relationship among expression of vascular endothelial growth factor-C(VEGF-C), angiogenesis, lymphangiogenesis, and lymphatic metastasis in oral cancer]. *Ai Zheng* 2002;21(3):319-22.
316. Jeltsch M, Kaipainen A, Joukov V, Meng X, Lakso M, Rauvala H, et al. Hyperplasia of lymphatic vessels in VEGF-C transgenic mice. *Science (New York, N.Y* 1997;276(5317):1423-5.
317. Cursiefen C, Chen L, Borges LP, Jackson D, Cao J, Radziejewski C, et al. VEGF-A stimulates lymphangiogenesis and hemangiogenesis in inflammatory neovascularization via macrophage recruitment. *J Clin Invest* 2004;113(7): 1040-50.
318. Cha HS, Bae EK, Koh JH, Chai JY, Jeon CH, Ahn KS, et al. Tumor necrosis factor-alpha induces vascular endothelial growth factor-C expression in rheumatoid synoviocytes. *The Journal of rheumatology* 2007;34(1):16-9.
319. Polzer K, Baeten D, Soleiman A, Distler J, Gerlag DM, Tak PP, et al. Tumour necrosis factor blockade increases lymphangiogenesis in murine and human arthritic joints. *Annals of the rheumatic diseases* 2008;67(11):1610-6.
320. Das H, George JC, Joseph M, Das M, Abdulhameed N, Blitz A, et al. Stem cell therapy with overexpressed VEGF and PDGF genes improves cardiac function in a rat infarct model. *PLoS One* 2009;4(10):e7325.

321. Wang JH, Wu QD, Bouchier-Hayes D, Redmond HP. Hypoxia upregulates Bcl-2 expression and suppresses interferon-gamma induced antiangiogenic activity in human tumor derived endothelial cells. *Cancer* 2002;94(10): 2745-55.
322. Li X, Dang X, Sun X. Expression of survivin and VEGF-C in breast cancer tissue and its relation to lymphatic metastasis. *Eur J Gynaecol Oncol* 2012;33(2):178-82.
323. Li S, Chen X, Wu T, Zhang M, Zhang X, Ji Z. Role of heparin on serum VEGF levels and local VEGF contents in reducing the severity of experimental severe acute pancreatitis in rats. *Scandinavian journal of gastroenterology* 2012;47(2):237-44.
324. Sathasivam S. VEGF and ALS. *Neuroscience research* 2008;62(2):71-7.
325. Thanigaimani S, Kichenadasse G, Mangoni AA. The emerging role of vascular endothelial growth factor (VEGF) in vascular homeostasis: lessons from recent trials with anti-VEGF drugs. *Curr Vasc Pharmacol* 2011;9(3): 358-80.
326. Fukumura D, Xu L, Chen Y, Gohongi T, Seed B, Jain RK. Hypoxia and acidosis independently up-regulate vascular endothelial growth factor transcription in brain tumors in vivo. *Cancer Res* 2001;61(16):6020-4.
327. Szekanecz Z, Besenyei T, Szentpetery A, Koch AE. Angiogenesis and vasculogenesis in rheumatoid arthritis. *Current opinion in rheumatology* 2010;22(3):299-306.
328. Kurihara T, Kubota Y, Ozawa Y, Takubo K, Noda K, Simon MC, et al. von Hippel-Lindau protein regulates transition from the fetal to the adult circulatory system in retina. *Development (Cambridge, England)* 2010;137(9): 1563-71.
329. Abaci HE, Truitt R, Luong E, Drazer G, Gerecht S. Adaptation to oxygen deprivation in cultures of human pluripotent stem cells, endothelial progenitor cells, and umbilical vein endothelial cells. *American journal of physiology* 2010;298(6):C1527-37.
330. Murakami M. Signaling required for blood vessel maintenance: molecular basis and pathological manifestations. *Int J Vasc Med* 2012;2012:293641.
331. Hitchon C, Wong K, Ma G, Reed J, Lyttle D, El-Gabalawy H. Hypoxia-induced production of stromal cell-derived factor 1 (CXCL12) and vascular endothelial growth factor by synovial fibroblasts. *Arthritis and rheumatism* 2002;46(10):2587-97.
332. Larsen H, Muz B, Khong TL, Feldmann M, Paleolog EM. Differential effects of Th1 versus Th2 cytokines in combination with hypoxia on HIFs and angiogenesis in RA. *Arthritis research & therapy* 2012;14(4):R180.
333. Patan S. Vasculogenesis and angiogenesis. *Cancer Treat Res* 2004;117:3-32.
334. Kim HR, Park MK, Cho ML, Yoon CH, Lee SH, Park SH, et al. Macrophage migration inhibitory factor upregulates angiogenic factors and correlates with clinical measures in rheumatoid arthritis. *The Journal of rheumatology* 2007;34(5):927-36.
335. Kataru RP, Jung K, Jang C, Yang H, Schwendener RA, Baik JE, et al. Critical role of CD11b+ macrophages and VEGF in inflammatory lymphangiogenesis, antigen clearance, and inflammation resolution. *Blood* 2009;113(22):5650-9.
336. Haigh JJ. Role of VEGF in organogenesis. *Organogenesis* 2008;4(4): 247-56.
337. Nilsson I, Bahram F, Li X, Gualandi L, Koch S, Jarvius M, et al. VEGF receptor 2/-3 heterodimers detected in situ by proximity ligation on angiogenic sprouts. *The EMBO journal* 2010;29(8):1377-88.
338. Nakayama M, Berger P. Coordination of VEGF receptor trafficking and signaling by coreceptors. *Exp Cell Res* 2013.

339. Zhang Z, Neiva KG, Lingen MW, Ellis LM, Nor JE. VEGF-dependent tumor angiogenesis requires inverse and reciprocal regulation of VEGFR1 and VEGFR2. *Cell death and differentiation* 2010;17(3):499-512.
340. Xu Y, Yuan L, Mak J, Pardanaud L, Caunt M, Kasman I, et al. Neuropilin-2 mediates VEGF-C-induced lymphatic sprouting together with VEGFR3. *The Journal of cell biology* 2010;188(1):115-30.
341. Haiko P, Makinen T, Keskitalo S, Taipale J, Karkkainen MJ, Baldwin ME, et al. Deletion of vascular endothelial growth factor C (VEGF-C) and VEGF-D is not equivalent to VEGF receptor 3 deletion in mouse embryos. *Molecular and cellular biology* 2008;28(15):4843-50.
342. Makinen T, Norrmen C, Petrova TV. Molecular mechanisms of lymphatic vascular development. *Cell Mol Life Sci* 2007;64(15):1915-29.
343. Koch M, Dettori D, Van Nuffelen A, Souffreau J, Marconcini L, Wallays G, et al. VEGF-D deficiency in mice does not affect embryonic or postnatal lymphangiogenesis but reduces lymphatic metastasis. *J Pathol* 2009;219(3): 356-64.
344. Qiu X, Yao S, Zhang S. Advances in the research on lymphangiogenesis in carcinoma tissues (Review). *Oncol Lett* 2010;1(4):579-82.
345. Kawamura H, Li X, Goishi K, van Meeteren LA, Jakobsson L, Cebe-Suarez S, et al. Neuropilin-1 in regulation of VEGF-induced activation of p38MAPK and endothelial cell organization. *Blood* 2008;112(9):3638-49.
346. Saban MR, Backer JM, Backer MV, Maier J, Fowler B, Davis CA, et al. VEGF receptors and neuropilins are expressed in the urothelial and neuronal cells in normal mouse urinary bladder and are upregulated in inflammation. *American journal of physiology* 2008;295(1):F60-72.
347. Scott BB, Zaratin PF, Colombo A, Hansbury MJ, Winkler JD, Jackson JR. Constitutive expression of angiopoietin-1 and -2 and modulation of their expression by inflammatory cytokines in rheumatoid arthritis synovial fibroblasts. *The Journal of rheumatology* 2002;29(2):230-9.
348. Zhang J, Fukuhara S, Sako K, Takenouchi T, Kitani H, Kume T, et al. Angiopoietin-1/Tie2 signal augments basal Notch signal controlling vascular quiescence by inducing delta-like 4 expression through AKT-mediated activation of beta-catenin. *J Biol Chem* 2011;286(10):8055-66.
349. Singh H, Hansen TM, Patel N, Brindle NP. The molecular balance between receptor tyrosine kinases Tie1 and Tie2 is dynamically controlled by VEGF and TNFalpha and regulates angiopoietin signalling. *PLoS ONE* 2012;7(1):e29319.
350. Daly C, Eichten A, Castanaro C, Pasnikowski E, Adler A, Lalani AS, et al. Angiopoietin-2 functions as a Tie2 agonist in tumor models, where it limits the effects of VEGF inhibition. *Cancer Res* 2013;73(1):108-18.
351. Thurston G, Daly C. The complex role of angiopoietin-2 in the angiopoietin-tie signaling pathway. *Cold Spring Harb Perspect Med* 2012;2(9):a006550.
352. Qu H, Nagy JA, Senger DR, Dvorak HF, Dvorak AM. Ultrastructural localization of vascular permeability factor/vascular endothelial growth factor (VPF/VEGF) to the abluminal plasma membrane and vesiculovacuolar organelles of tumor microvascular endothelium. *J Histochem Cytochem* 1995;43(4):381-9.
353. Carbajo-Lozoya J, Lutz S, Feng Y, Kroll J, Hammes HP, Wieland T. Angiotensin II modulates VEGF-driven angiogenesis by opposing effects of type 1 and type 2 receptor stimulation in the microvascular endothelium. *Cellular signalling* 2012;24(6):1261-9.
354. Gerhardt H. VEGF and endothelial guidance in angiogenic sprouting. *Organogenesis* 2008;4(4):241-6.
355. Ji RC. Lymphatic endothelial cells, lymphedematous lymphangiogenesis, and molecular control of edema formation. *Lymphatic research and biology* 2008;6(3-4):123-37.

356. Shibuya M, Claesson-Welsh L. Signal transduction by VEGF receptors in regulation of angiogenesis and lymphangiogenesis. *Exp Cell Res* 2006;312(5):549-60.
357. Lohela M, Bry M, Tammela T, Alitalo K. VEGFs and receptors involved in angiogenesis versus lymphangiogenesis. *Curr Opin Cell Biol* 2009;21(2): 154-65.
358. Fagiani E, Lorentz P, Kopfstein L, Christofori G. Angiopoietin-1 and -2 exert antagonistic functions in tumor angiogenesis, yet both induce lymphangiogenesis. *Cancer Res* 2011;71(17):5717-27.
359. Onimaru M, Yonemitsu Y, Fujii T, Tanii M, Nakano T, Nakagawa K, et al. VEGF-C regulates lymphangiogenesis and capillary stability by regulation of PDGF-B. *Am J Physiol Heart Circ Physiol* 2009;297(5):H1685-96.
360. Szekanecz Z, Besenyei T, Paragh G, Koch AE. New insights in synovial angiogenesis. *Joint Bone Spine* 2010;77(1):13-9.
361. Jung SY, Choi JH, Kwon SM, Masuda H, Asahara T, Lee YM. Decursin inhibits vasculogenesis in early tumor progression by suppression of endothelial progenitor cell differentiation and function. *J Cell Biochem* 2012;113(5):1478-87.
362. Kowanetz M, Ferrara N. Vascular endothelial growth factor signaling pathways: therapeutic perspective. *Clin Cancer Res* 2006;12(17):5018-22.
363. Blanco R, Gerhardt H. VEGF and Notch in tip and stalk cell selection. *Cold Spring Harb Perspect Med* 2013;3(1):a006569.
364. Pratheeshkumar P, Kuttan G. Nomilin inhibits tumor-specific angiogenesis by downregulating VEGF, NO and proinflammatory cytokine profile and also by inhibiting the activation of MMP-2 and MMP-9. *Eur J Pharmacol* 2011;668(3):450-8.
365. Taylor PC. Serum vascular markers and vascular imaging in assessment of rheumatoid arthritis disease activity and response to therapy. *Rheumatology (Oxford, England)* 2005;44(6):721-8.
366. Klimiuk PA, Sierakowski S, Latosiewicz R, Cylwik JP, Cylwik B, Skowronski J, et al. Soluble adhesion molecules (ICAM-1, VCAM-1, and E-selectin) and vascular endothelial growth factor (VEGF) in patients with distinct variants of rheumatoid synovitis. *Annals of the rheumatic diseases* 2002;61(9):804-9.
367. Volin MV. Soluble adhesion molecules in the pathogenesis of rheumatoid arthritis. *Curr Pharm Des* 2005;11(5):633-53.
368. Haskard DO. Cell adhesion molecules in rheumatoid arthritis. *Current opinion in rheumatology* 1995;7(3):229-34.
369. Taylor PC, Peters AM, Paleolog E, Chapman PT, Elliott MJ, McCloskey R, et al. Reduction of chemokine levels and leukocyte traffic to joints by tumor necrosis factor alpha blockade in patients with rheumatoid arthritis. *Arthritis and rheumatism* 2000;43(1):38-47.
370. Zhang F, Tang Z, Hou X, Lennartsson J, Li Y, Koch AW, et al. VEGF-B is dispensable for blood vessel growth but critical for their survival, and VEGF-B targeting inhibits pathological angiogenesis. *Proceedings of the National Academy of Sciences of the United States of America* 2009;106(15):6152-7.
371. Etherington PJ, Winlove P, Taylor P, Paleolog E, Miotla JM. VEGF release is associated with reduced oxygen tensions in experimental inflammatory arthritis. *Clinical and experimental rheumatology* 2002;20(6):799-805.
372. Lund-Olesen K, . Oxygen tension in synovial fluids. *Arthritis and rheumatism* 1970;13:769-76.
373. Taylor PC, Sivakumar B. Hypoxia and angiogenesis in rheumatoid arthritis. *Current opinion in rheumatology* 2005;17(3):293-8.
374. Nakahara H, Song J, Sugimoto M, Hagihara K, Kishimoto T, Yoshizaki K, et al. Anti-interleukin-6 receptor antibody therapy reduces vascular endothelial growth factor production in rheumatoid arthritis. *Arthritis and rheumatism* 2003;48(6):1521-9.

375. Pablos JL, Santiago B, Galindo M, Torres C, Brehmer MT, Blanco FJ, et al. Synoviocyte-derived CXCL12 is displayed on endothelium and induces angiogenesis in rheumatoid arthritis. *J Immunol* 2003;170(4):2147-52.
376. Cho ML, Ju JH, Kim HR, Oh HJ, Kang CM, Jhun JY, et al. Toll-like receptor 2 ligand mediates the upregulation of angiogenic factor, vascular endothelial growth factor and interleukin-8/CXCL8 in human rheumatoid synovial fibroblasts. *Immunol Lett* 2007;108(2):121-8.
377. Ji RC. Macrophages are important mediators of either tumor- or inflammation-induced lymphangiogenesis. *Cell Mol Life Sci* 2012;69(6): 897-914.
378. Swenson C, Sward L, Karlsson J. Cryotherapy in sports medicine. *Scand J Med Sci Sports* 1996;6(4):193-200.
379. Bleakley CM, Costello JT. Do thermal agents affect range of movement and mechanical properties in soft tissues? A systematic review. *Archives of physical medicine and rehabilitation* 2013;94(1):149-63.
380. Holm B, Husted H, Kehlet H, Bandholm T. Effect of knee joint icing on knee extension strength and knee pain early after total knee arthroplasty: a randomized cross-over study. *Clinical rehabilitation* 2012;26(8):716-23.
381. Albrecht K, Albert C, Lange U, Muller-Ladner U, Strunk J. Different effects of local cryogel and cold air physical therapy in wrist rheumatoid arthritis visualised by power Doppler ultrasound. *Annals of the rheumatic diseases* 2009;68(7):1234-5.
382. Knobloch K, Grasemann R, Jagodzinski M, Richter M, Zeichen J, Krettek C. Changes of Achilles midportion tendon microcirculation after repetitive simultaneous cryotherapy and compression using a Cryo/Cuff. *The American journal of sports medicine* 2006;34(12):1953-9.
383. Beste KW, Essiger H. [Ultrasound-Doppler analysis of arterial blood flow before and after cryotherapy]. *Zeitschrift fur Rheumatologie* 1984;43(2):66-74.
384. Semerano L, Gutierrez M, Falgarone G, Filippucci E, Guillot X, Boissier MC, et al. Diurnal variation of power Doppler in metacarpophalangeal joints of patients with rheumatoid arthritis: a preliminary study. *Annals of the rheumatic diseases* 2011;70(9):1699-700.
385. Felson DT, Anderson JJ, Lange ML, Wells G, LaValley MP. Should improvement in rheumatoid arthritis clinical trials be defined as fifty percent or seventy percent improvement in core set measures, rather than twenty percent? *Arthritis and rheumatism* 1998;41(9):1564-70.
386. Taylor PC. VEGF and imaging of vessels in rheumatoid arthritis. *Arthritis research* 2002;4 Suppl 3:S99-107.
387. Mitchell KL, Pisetsky DS. Early rheumatoid arthritis. *Current opinion in rheumatology* 2007;19(3):278-83.
388. Iagnocco A, Perella C, Naredo E, Meenagh G, Ceccarelli F, Tripodo E, et al. Etanercept in the treatment of rheumatoid arthritis: clinical follow-up over one year by ultrasonography. *Clinical rheumatology* 2008;27(4):491-6.
389. Felson DT. Choosing a core set of disease activity measures for rheumatoid arthritis clinical trials. *The Journal of rheumatology* 1993;20(3): 531-4.
390. Anderson JJ, Bolognese JA, Felson DT. Comparison of rheumatoid arthritis clinical trial outcome measures: a simulation study. *Arthritis and rheumatism* 2003;48(11):3031-8.
391. Bresnihan B, Baeten D, Firestein GS, Fitzgerald OM, Gerlag DM, Haringman JJ, et al. Synovial tissue analysis in clinical trials. *The Journal of rheumatology* 2005;32(12):2481-4.
392. Tak PP. Analyzing synovial tissue samples. What can we learn about early rheumatoid arthritis, the heterogeneity of the disease, and the effects of treatment? *J Rheumatol Suppl* 2005;72:25-6.
393. Arayssi TK, Schumacher HR, Jr. Evaluation of a modified needle for small joint biopsies. *J Rheumatol* 1998;25(5):876-8.

394. Bresnihan B, Tak PP. Synovial tissue analysis in rheumatoid arthritis. *Baillieres Best Pract Res Clin Rheumatol* 1999;13(4):645-59.
395. van Holten J, Pavelka K, Vencovsky J, Stahl H, Rozman B, Genovese M, et al. A multicentre, randomised, double blind, placebo controlled phase II study of subcutaneous interferon beta-1a in the treatment of patients with active rheumatoid arthritis. *Ann Rheum Dis* 2005;64(1):64-9.
396. Naredo E, Moller I, Cruz A, Carmona L, Garrido J. Power Doppler ultrasonographic monitoring of response to anti-tumor necrosis factor therapy in patients with rheumatoid arthritis. *Arthritis and rheumatism* 2008;58(8): 2248-56.
397. Mal F, Meyrier A, Callard P, Kleinknecht D, Altmann JJ, Beaugrand M. The diagnostic yield of transjugular renal biopsy. Experience in 200 cases. *Kidney Int* 1992;41(2):445-9.
398. Bilbao JI, Idoate F, Joly MA, Vazquez C, Sangro B, Larrea JA, et al. Renal biopsy with forceps through the femoral vein. *J Vasc Interv Radiol* 1995;6(4): 641-5.
399. Sam R, Leehey DJ, Picken MM, Borge MA, Yetter EM, Ing TS, et al. Transjugular renal biopsy in patients with liver disease. *Am J Kidney Dis* 2001;37(6):1144-51.
400. Abbott KC, Musio FM, Chung EM, Lomis NN, Lane JD, Yuan CM. Transjugular renal biopsy in high-risk patients: an American case series. *BMC Nephrol* 2002;3:5.
401. Rychlik I, Petrtyl J, Tesar V, Stejskalova A, Zabka J, Bruha R. Transjugular renal biopsy. Our experience with 67 cases. *Kidney Blood Press Res* 2001;24(3):207-12.
402. McAfee JH, Keeffe EB, Lee RG, Rosch J. Transjugular liver biopsy. *Hepatology* 1992;15(4):726-32.
403. Rasband WS. ImageJ, U. S. National Institutes of Health, Bethesda, Maryland, USA, http://rsb.info.nih.gov/ij/. 1997-2008.
404. Hammer HB, Kvien TK. Comparisons of 7- to 78-joint ultrasonography scores: all different joint combinations show equal response to adalimumab treatment in patients with rheumatoid arthritis. *Arthritis research & therapy* 2011;13(3):R78.
405. Backhaus M, Ohrndorf S, Kellner H, Strunk J, Backhaus TM, Hartung W, et al. Evaluation of a novel 7-joint ultrasound score in daily rheumatologic practice: a pilot project. *Arthritis and rheumatism* 2009;61(9):1194-201.